# The role of auxin and indole glucosinolates in defense against clubroot infection in *Brassica napus*

by

Hui Liu

A thesis submitted in partial fulfillment of the requirements for the degree of

Master of Science

in

Plant Science

Department of Agricultural, Food and Nutritional Science
University of Alberta

© Hui Liu, 2023

## Abstract

Clubroot, caused by the obligate parasite *Plasmodiophora brassicae*, is one of the most damaging diseases of the Brassicaceae. Glucosinolate (GSLs) are a group of defense-related secondary metabolites in cruciferous plants that have been associated with clubroot disease. The breakdown of GSLs results in the generation of isothiocyanates, thiocyanate, and nitriles, which are known to be involved in plant defense mechanisms against numerous herbivores and pathogens. Analysis of a database from Zhou et al. (2020) showed that the resistant rutabaga cultivar ("Whilhelmsburger") had a different gene expression pattern in the indole GSL pathway compared with the susceptible rutabaga cultivar ("Laurentian") in response to *P. brassicae* inoculation. Therefore, quantitation of selected gene targets in the GSL pathway was performed using qRT-PCR in resistant and susceptible rutabaga cultivars that were either non-inoculated or inoculated with *P. brassicae.* The results showed that the transcript abundance of both *BnBGLU30* and *BnNSP5* increased in the roots of both resistant and susceptible cvs. 7 days after inoculation (dai) with *P. brassicae,* suggesting that modulation of expression of specific GSL pathway genes occurs in rutabaga roots likely resulting in elevated nitrile production as a primary infection response to *P. brassicae.* Additionally, the GLS gene expression pattern of the resistant cv. indicated that it may have a greater capacity to produce and maintain the levels of nitriles as a primary infection response to *P. brassicae* than the susceptible cultivar. Future studies involving the quantification of specific GSLs-related compounds including nitriles in the pathway are required to correlate gene expression changes with changes in GSL products produced.

Auxin has been implicated as a key hormone for gall formation induced by *P. brassicae* by promoting cell hyperplasia and hypertrophy. The selective expression of *BnIAGLU* only in

the resistant cv. (a gene that codes for an enzyme that converts the auxin indole-3-acetic acid; IAA) to an inactive glucose ester) suggests that conjugation of free IAA to an inactive IAA-glucose ester may be a defense response to *P. brassicae* at the primary infection stage. In order to determine if modification of auxin response affects clubroot disease progression, two independent transgenic lines expressing the pea auxin receptor *PsAFB6* (this auxin receptor clade does not exist in the Brassicaceae family) in the canola cv. Westar, along with their respective null lines, were phenotypically characterized for their response to clubroot infection using a hydroponic system. Implementation of a hydroponic system during the infection phase of *P. brassciae* with canola as the host plant allowed the characterization of the effect of modulation of auxin response on clubroot disease progression to be completed without interference with the complexities of soil- or peat-based media interactions. The canola *AFB6* transgenic lines showed a notable reduction in their disease index compared to their corresponding transgenic null controls at 30 dai. When characteristic galls were present in both canola *PsAFB6*-expressing lines and the null lines, the *PsAFB6*-expressing lines exhibited significantly reduced surface area at the root-shoot transition zone compared to their corresponding null control lines, indicating that they had milder galling symptoms in response to *P. brassciae* inoculation. Given the mode of action for auxin receptors and the proposed role for auxin facilitating gall development, the reduction in clubroot symptoms in *PsAFB6*-expressing canola lines appears to be the result of reduced auxin response in these lines. Further studies are needed to confirm that a reduction in auxin response is the main mechanism involved in *PsAFB6*-induced reduction in clubroot galling symptoms, and to determine the exact mode of action bringing about the potential reduction in auxin response. Identifying the specific pathways involved in *PsAFB6*-mediated reduction in clubroot galling symptoms, and the role of GSL-related compounds in the defense against

clubroot disease progression, could potentially lead to the development of novel approaches for clubroot disease management in canola.

## Preface

All the experiments in this thesis were conceptualized and designed by Dr. Jocelyn Ozga. Data interpretation was completed with the help of Dr. Jocelyn Ozga for all experiments. I grew plants for all experiments, prepared experimental designs for implementation, prepared and quantified clubroot spore suspensions, performed all clubroot inoculations for experiments, part of team in harvesting all tissues for experiments, received hands-on experience with total RNA extraction, PCR and qPCR techniques, performed all hydroponic experiments and microscopy. For data analysis, I analyzed the Zhou et al. (2020) transcriptomic database for pathways and genes of interest, performed the root surface area measurements using imageJ software, ran the ANOVA analyses, and prepared the figures in Originlab software. Dr Harleen Kaur helped me in refining the experimental design, harvesting of root tissues, performed total RNA extractions, PCR and qRT-PCR assays, developed method for performing hydroponic root growth assays, and standardised method for quantifying root surface area.

**Acknowledgements**

I would like to express my sincere gratitude to my supervisors, Dr. Jocelyn Ozga and Dr. Sheau-Fang Hwang, for giving me an opportunity to do my MSc study with them and their tremendous guidance, encouragement, and support throughout my MSc program. The guidance and mentorship from Dr. Jocelyn Ozga have been invaluable to me, and her belief in my abilities has given me the confidence to pursue my goals. She has always been available to offer guidance and advice, and her constructive feedback has helped me grow both personally and professionally. I would like to devote special appreciation to Dr. Sheau-Fang Hwang and Dr. Stephen Strelkov, who provided great support during my undergraduate studies by allowing me to work and learn as a summer student in the Plant Pathology Laboratory, which also encouraged me to pursue my MSc degree.

I would like to thank all the lab members in Dr. Ozga/Reinecke's lab for creating a professional, supportive, and friendly work environment. I thank Dr. Harleen Kuar for her help in all my experiments and her encouragement. Her willingness to offer her time and expertise has been instrumental in the successful outcome of my experiments. Her enthusiasm for science is infectious, and I feel privileged to be working alongside her. I thank Dr. Bin Shan for her tremendous inspiration throughout my MSc program. Every time I encountered difficulties in conducting the experiments, I would share with her, and her encouragement and inspiration have been crucial in keeping me motivated and focused throughout the project. I thank Ms. Shengjuan Li for being a wonderful and supportive company, sharing and discussing with her has allowed me to have deeper understanding of my experiments and fueled my passion for your work. I would also like to extend my heartfelt gratitude to Duncan Giebelhaus for all the coffee chats and knowledge sharing. Our coffee chats have been a great source of inspiration and motivation, and I have learned so much from our conversations. I consider myself very fortunate to have worked in such a friendly environment, surrounded by smiling faces every day. The positive atmosphere in the workplace has made it a joy to come to work, and I have always felt welcomed and supported by my colleagues.

I would also like to thank the staff from other groups at the University of Alberta for continuous support throughout my MSc program. In particular, many thanks to the Plant Growth Facility Lead/Assist Ms. Kelley Dunfield, Shay Missiaen, and Dr. Andrea Botero for

managing necessary equipment for my experiments. I would also like to extend my heartfelt gratitude to Dr. Victor Manolii for training me to conduct clubroot disease inoculation and providing the necessary inoculum material for my experiments. His expertise and guidance have been invaluable, and his dedication to ensuring that I had the necessary skills and resources to conduct my experiments is greatly appreciated. I thank all the staff in the Department of Agricultural, Food & Nutritional Science and the Faculty of Graduate Studies and Research for organizing workshops, sharing scientific knowledge, and providing support in all aspects.

Finally, I would like to take a moment to express my deep appreciation and gratitude to my friends and family. My parents (Chengming Liu & Xiaohua Hwang) and my brother (Bin Liu) have been there for me through thick and thin, providing a listening ear, words of wisdom, and unwavering support whenever I needed it. Their belief in my abilities has given me the confidence to pursue my dreams and achieve my goals, and I cannot thank them enough for their contributions to my life. My best friends Xiong Sheng Tan, Sangheon Oh, Qinqin Zhou, Xingyu Guan have been a constant source of inspiration for me. They have always been there for me, offering a listening ear, words of encouragement, and a shoulder to lean on when I needed it most. Our shared experiences, inside jokes, and unforgettable memories have enriched my life in so many ways, and I am grateful for each and every moment we have spent together. Also, Xiong Sheng Tan and Sangheon Oh have been the best roommates throughout my MSc program for many years. Living with them has been a joy, and I am grateful for their friendship and camaraderie. Their positive energy, encouragement, and willingness to lend a helping hand have made my life much easier, and I cannot thank them enough for their support. Whether it was listening to me vent about a bad day or celebrating my successes, they have always been there for me, and I am incredibly grateful.

**Table of Contents**

**List of Tables……. x**
**List of Figures……... xii**
**List of Abbreviations……..... xviii**

**Chapter 1: Literature review…….. 1**
1.1 CLUBROOT DISEASE IN BRASSICA CROPS……... 1
1.1.1 Host-pathogen interactions of clubroot pathogen in Brassica crops…… 1
1.1.2 Significance of clubroot disease in Brassica crops……... 3
1.1.3 Management of clubroot in crops……. 4
1.2 THE PLANT GROWTH REGULATOR AUXIN…….. 5
1.2.1 Auxin in plant-pathogen interactions…… 5
1.2.2 Auxin biosynthesis and conjugation……. 6
1.2.3 Auxin signaling……..... 10
1.3 INDOLE GSLs …… 13
1.3.1 GSLs and clubroot disease…… 13
1.3.2 Indole GSL biosynthesis……... 16
1.3.3 Indole GSL modification……... 17
1.3.4 General degradation pathway of GSLs……. 20
1.3.5 PEN2-dependent degradation of indole GSL…… 23
1.3.6 The role of Nitriles in plant-pathogen interaction……. 25
1.3.7 Major GSLs detected in rutabagas and potential degradation products.... 25
1.4 HYPOTHESIS AND OBJECTIVES…… 28

**Chapter 2: Gene expression changes in the indole GSL pathway associated with clubroot pathogen infection in rutabaga (*Brassica napus*)…… 30**
2.1 INTRODUCTION …… 30
2.2 MATERIALS AND METHODS ……. 34
2.2.1 Pathogen material …….. 34
2.2.2 Plant material and inoculation ……... 35
2.2.3 Gene expression analysis …….. 36
2.2.3.1 *Total RNA isolation*……. 36
2.2.3.2 *cDNA Synthesis and PCR Verification*…… 38
2.2.3.3 *Taqman qRT-PCR assay*…….. 39
2.2.3.4 *Preparation of RNA standard curve*…… 42
2.2.3.5 *Amino acid sequence alignments* ……..... 42
2.2.3.6 *Statistical analysis* …….. 43
2.3 RESULTS ……. 43
2.3.1 Differential disease responses of ‘Whilhelmsburger’ and ‘Laurentian’ to *P. brassicae*…….. 43
2.3.2 Differential gene expression patterns in the indole GSL pathway in ‘Wilhelmsburger’ and ‘Laurentian’ cultivars at 7 dai against *P. brassicae.* 46
2.3.3 Gene expression quantification using qRT-PCR assays with Taqman probes in roots of rutabaga cultivars at early stage of clubroot pathogen inoculations……. 53

2.4 DISCUSSION……. 70
2.4.1 'Wilhelmsburger' cultivar exhibits greater resistance to clubroot compared with 'Laurentian'……. 70
2.4.2 Differential expression of GSL biosynthesis genes during clubroot primary infection based on transcriptomic analysis……. 70
2.4.3 Expression of genes in the indole GSL modification pathway…… 71
2.4.4 Expression of genes in the indole GSL degradation pathway…….. 73
2.4.5 Summary……... 75

**Chapter 3: Phenotypic characterization of clubroot disease progression in canola plants with modified auxin response……. 78**
3.1 INTRODUCTION……... 78
3.2 MATERIALS AND METHODS…… 80
3.2.1 Pathogen material……. 80
3.2.2 Plant inoculation and harvesting…….. 81
3.2.3 Digitized clubroot disease scoring……... 83
3.2.4 Root surface area quantification……... 85
3.2.5 Statistical analysis……..... 85
3.3 RESULTS…… 86
3.3.1 A 7 dai hydroponic root assay system for digitized clubroot disease scoring …….. 86
3.3.2 The canola cv. Westar transgenic *AFB6* PCR+ plants developed less severe clubroot symptoms compared to their *AFB6* Null plants……... 91
3.4 DISCUSSION……... 101
3.4.1 The hydroponic system supported successful *P. brassciae* infection of canola seedings ……..... 101
3.4.2 The canola cv. Westar *AFB6* transgenic showed less severe clubroot symptoms than their respective transgenic null controls……... 102
3.4.3 Summary……..... 105

**Chapter 4: Conclusions and future directions……... 106**
4.1 INTRODUCTION…… 106
4.2 GENERAL CONCLUSIONS……... 107
4.3 FUTURE DIRECTIONS……..... 107

**References**……..... 110
**Appendix-A**…… 133
**Appendix-B**…… 164

## List of Tables


| Tables | | Page |
|---|---|---|
| **1.1** | GSL classes present in rutabaga roots their derived hydrolysis products: isothiocyanates (ITC) and derivates, nitriles, and epithionitriles…….. | 27 |
| **2.1** | Taqman primers and probes used for quantification of gene expression in root tissues of non-inoculated control and 7d-*P. brassicae*-inoculated rutabaga resistant 'Wilhelmsburger' and susceptible 'Laurentian' cultivars by qRT-PCR assays and their PCR efficiencies and r2 values…… | 40 |
| **2.2** | Differentially expressed genes belonging to indole GSL biosynthesis pathway in root tissues of rutabaga (*Brassica napus* subsp. *rapifera* Metzg) resistant 'Wilhelmsburger' and susceptible 'Laurentian' cultivars at 7, 14, and 21 days after clubroot (*P. brassicae*) inoculation (dai)……. | 47 |
| **2.3** | Differentially expressed genes belonging to indole GSL modification pathways in root tissues of rutabaga (*Brassica napus* subsp. *rapifera* Metzg) resistant 'Wilhelmsburger' and susceptible 'Laurentian' cultivars at 7, 14, and 21 days after clubroot (*P. brassicae*) inoculation (dai)…….. | 49 |
| **2.4** | Differentially expressed genes belonging to indole GSL degradation and auxin conjugation pathways in root tissues of rutabaga (*Brassica napus* subsp. *rapifera* Metzg) resistant 'Wilhelmsburger' and susceptible 'Laurentian' cultivars at 7, 14, and 21 days after clubroot (*P. brassicae*) inoculation (dai)…… | 51 |
| **A1** | PCR primer sequences used for amplification of gene of interest in root tissues of non-inoculated control and 7d-*P. brassicae*-inoculated rutabaga resistant 'Wilhelmsburger' cultivar……... | 161 |
| **A2** | Two-way ANOVA analysis followed by mean separation using Tukey HSD post-hoc test was performed on the relative transcript abundance of genes in the root tissues of non-inoculated control and 7d-*P. brassicae*-inoculated rutabaga resistant 'Wilhelmsburger' and susceptible 'Laurentian' cultivars, degrees of freedom, F value, and probability for treatments (non-inoculated vs. 7d-*P. brassicae*-inoculated), cultivars, and treatments x cultivars interaction presented in Figures 3-9…….. | 163 |
| **B1** | Two-way ANOVA analysis followed by mean separation using Tukey HSD | |

post-hoc test was performed on the root surface area of non-inoculated and 30d-*P. brassicae*-inoculated canola cv. Westar *AFB6-9* PCR+ and *AFB6-9* Null, degrees of freedom, F value, and probability for treatments (non-inoculated vs. 30d-*P. brassicae*-inoculated), lines (*AFB6-9* PCR+ vs. *AFB6-9* Null), and treatments x lines interaction presented in Figure 3.10……..... 166

**B2** Two-way ANOVA analysis followed by mean separation using Tukey HSD post-hoc test was performed on the root surface area of non-inoculated and 30d-*P. brassicae*-inoculated canola cv. Westar *AFB6-52* PCR+ and *AFB6-52* Null, degrees of freedom, F value, and probability for treatments (non-inoculated vs. 30d-*P. brassicae*-inoculated), lines (*AFB6-52* PCR+ vs. *AFB6-52* Null), and treatments x lines interaction presented in Figure 3.13……. 167

## List of Figures


| Figure | | Page |
|---|---|---|
| **1.1** | The life cycle of *P. brassicae* in *Arabidopsis thaliana* and other Brassica hosts……..... | 2 |
| **1.2** | Trp-dependent IAA biosynthesis and conjugation pathway in Arabidopsis……. | 9 |
| **1.3** | Mechanism of auxin signaling through the TIR1/AFB-mediated pathway…….. | 12 |
| **1.4** | The core structure of GSLs and examples of aromatic, aliphatic, and indole GSLs……... | 15 |
| **1.5** | Indole GSL biosynthesis and modification pathway……. | 18 |
| **1.6** | General GSL degradation pathway…… | 22 |
| **1.7** | PEN-catalyzed 3-indolylmethy GSL breakdown……... | 24 |
| **2.1** | Indole GSL biosynthesis and metabolism pathways……..... | 33 |
| **2.2** | Representative clubroot symptom development in roots of rutabaga (*Brassica napus* subsp. *rapifera* Metzg) susceptible 'Laurentian' and resistant 'Wilhelmsburger' cultivars at 45 days after inoculation with resting spores of 3A pathotype of *P. brassicae* at a density of 1 x 107 spores/mL..... | 44 |
| **2.3** | Clubroot disease severity index in the roots of rutabaga resistant 'Wilhelmsburger' and susceptible 'Laurentian' cultivars caused by 3A pathotype of *P. brassicae* collected from a field population……. | 45 |
| **2.4** | Agarose gels showing PCR amplicons of indole GSL modification genes in root tissues of non-inoculated control (NR) and 7d-*P. brassicae*-inoculated (IR) clubroot resistant 'Wilhelmsburger' cultivar. Genes with observed expected amplicons sizes are: [A]: *BnCYP81F2*; [B]: *BnCPY81F4*; [C]: *BnIGMT1/2*; [D]: *BnIGMT5*. …… | 54 |
| **2.5** | Agarose gels showing PCR amplicons of indole GSL degradation pathway genes in root tissues of non-inoculated control (NR) and 7d-*P. brassicae*-inoculated (IR) clubroot resistant 'Wilhelmsburger' cultivar. Genes with observed expected amplicons sizes are: [A]: *BnBGLU30*; [B]: *BnNSP5*…… | 55 |
| **2.6** | Agarose gels showing PCR amplicons of indole GSL degradation pathway genes in root tissues of non-inoculated control (NR) and 7d- | |

*P. brassicae*-inoculated (IR) clubroot resistant 'Wilhelmsburger' cultivar. Genes with observed expected amplicons sizes are: [A]: *BnNIT2*; [B]: *BnNIT4*.. 56

**2.7** Agarose gels showing PCR amplicons of indole GSL degradation and auxin conjugation pathways genes in root tissues of non-inoculated control (NR) and 7d-*P. brassicae*-inoculated (IR) clubroot resistant 'Wilhelmsburger' cultivar. Genes with observed expected amplicons sizes are: [A]: *BnGSTU13*; [B]: *BnIAGLU*…….. 57

**2.8** Transcript abundance of genes encoding cytochrome P450 monooxygenase, family 81, subfamily F polypeptide (A, *BnCYP81F2* and B, *BnCYP81F4*) in root tissues of control and 7d-*P. brassicae*-inoculated rutabaga resistant 'Wilhelmsburger' and susceptible 'Laurentian' cultivars……. 59

**2.9** Transcript abundance of gene encoding indole glucosinolate O-methyltransferase 5 (*BnIGMT5*) in root tissues of control and 7d-*P. brassicae*-inoculated rutabaga resistant 'Wilhelmsburger' and susceptible 'Laurentian' cultivars……. 60

**2.10** Transcript abundance of gene encoding *β*-glucosidase 30 (*BnBGLU30*) in root tissues of control and 7d-*P. brassicae*-inoculated rutabaga resistant 'Wilhelmsburger' and susceptible 'Laurentian' cultivars……. 62

**2.11** Transcript abundance of gene encoding nitrile specifier protein 5 (*BnNSP5*) in root tissues of control and 7d-*P. brassicae*-inoculated rutabaga resistant 'Wilhelmsburger' and susceptible 'Laurentian' cultivars……. 63

**2.12** Transcript abundance of genes encoding nitrilase 2 and 4 (A, *BnNIT2* and B, *BnNIT4*) in root tissues of control and 7d-*P. brassicae*-inoculated rutabaga resistant 'Wilhelmsburger' and susceptible 'Laurentian' cultivars……... 65

**2.13** Transcript abundance of gene encoding Glutathione S-transferase Tau type 13 (*BnGSTU13*) in root tissues of control and 7d-*P. brassicae*-inoculated rutabaga resistant 'Wilhelmsburger' and susceptible 'Laurentian' cultivars……... 67

**2.14** Transcript abundance of gene encoding indole-3-acetate *β*-D-glucosyltransferase (*BnIAGLU*) in root tissues of control and 7d-*P. brassicae*-inoculated rutabaga resistant 'Wilhelmsburger' and susceptible 'Laurentian' cultivars…….. 69

**2.15** A working model of a potential early host defence response involving the indole and general GSL pathway in *Brassica napus* against *P. brassicae*…….. 77

**3.1** Disease rating scale range of clubroot symptoms on digitized microscopic images of the root-shoot transition zone of canola cv. Westar at 30 days after *P. brassicae* inoculations…….. 84

**3.2** Representative image of clubroot inoculated (A, $1 \times 10^7$ spores/mL) and non-inoculated (B) seedlings of canola cv. Westar *AFB6-9* transgenic line (*AFB6-9* PCR+) and its *AFB6-9* Null after 7 days of growth in the hydroponic assay system……... 87

**3.3** Representative images of roots of canola cv. Westar *AFB6-9* transgenic (*AFB6-9* PCR+: +) and its respective null (*AFB6-9* Null: -) non-inoculated control (A and C) and clubroot-inoculated (B and D) seedlings grown hydroponically in bags for 7 days after inoculation……..... 88

**3.4** Representative image of non-inoculated (A) and clubroot inoculated (B, $1 \times 10^7$ spores/mL) seedlings of canola cv. Westar *AFB6-52* transgenic line (*AFB6-52* PCR+) and its *AFB6-52* Null after 7 days of growth in the hydroponic assay system…….. 89

**3.5** Representative images of roots of canola cv. Westar *AFB6-52* transgenic (*AFB6-52* PCR+: +) and its respective null (*AFB6-52* Null: -) non-inoculated control (A and C) and clubroot-inoculated (B and D) seedlings grown hydroponically in bags for 7 days after inoculation……..... 90

**3.6** Representative microscopic images of roots of canola cv. Westar *AFB6-9* transgenic (*AFB6-9* PCR+) and its respective null non-inoculated (A and B) and clubroot-inoculated (C to H) seedlings at 30 dai (7 days grown hydroponically followed by 23 days of growth in the peat based medium)…… 93

**3.7** Representative microscopic images of roots of canola cv. Westar *AFB6-52* transgenic (*AFB6-52* PCR+) and its respective null non-inoculated (A and B) and clubroot-inoculated (C to H) seedlings at 30 dai (7 days grown hydroponically followed by 23 days of growth in the peat based medium)…….... 94

**3.8** The frequency distribution of *P. brassicae*-inoculated canola cv. Westar

*AFB6-9* transgenic (*AFB6-9* PCR+; n = 123) and its respective *AFB6-9* Null (n = 124) seedlings categorised according to the digitized clubroot disease scoring on 0-9 scale at 30 dai (7 days grown hydroponically followed by 2 3 days of growth in the peat based medium)…….. 95

**3.9** Clubroot disease severity index of the roots of canola cv. Westar *AFB6-9* Null and *AFB6-9* PCR+ plants caused by 3H pathotype single spore isolate of *P. brassicae*……. 96

**3.10** The surface area of the root-shoot transition zone of canola cv. Westar *AFB6-9* Null and *AFB6-9* PCR+ non-inoculated and *P. brassicae*-inoculated plants at 30 dai ……..... 97

**3.11** The frequency distribution of *P. brassicae*-inoculated canola cv. Westar *AFB6-52* transgenic (*AFB6-52* PCR+; n = 40) and its respective *AFB6-52* Null (n = 41) seedlings categorised according to the digitized clubroot disease scoring on 0-9 scale at 30 dai (7 days grown hydroponically followed by 23 days of growth in the peat based medium)…… 98

**3.12** Clubroot disease severity index of the roots of canola cv. Westar *AFB6-52* Null and *AFB6-52* PCR+ plants caused by 3H pathotype single spore isolate of *P. brassicae*…… 99

**3.13** The surface area of root-shoot transition zone of canola cv. Westar *AFB6-52* Null and *AFB6-52* PCR+ non-inoculated and *P. brassicae*-inoculated plants at 30 dai. …….. 100

**3.14** Two potential working models of *PsAFB6*-mediated reduction in clubroot galling symptoms in canola ……..... 104

**A1** Schematic representation of the improved Neubauer counting chamber of the hemocytometer used for estimating the clubroot resting spore concentration..... 133

**A2** The procedure followed for growing rutabaga seedlings and harvesting root samples for PCR and Taqman qRT-PCR studies……..... 135

**A3** The complete coding sequence of gene encoding cytochrome P450 monooxygenase, family 81, subfamily F, polypeptide 2 (*BnCYP81F2*: BnaA10g11280D) retrieved from *Brassica napus* genome (AST_PRJEB5043_v1; http://plants.ensembl.org/Brassica_napus/Info/Index).. 137

**A4** The complete coding sequence of gene encoding cytochrome P450 monooxygenase, family 81, subfamily F, polypeptide 4 (*BnCYP81F4*: BnaCnng68210D) retrieved from *Brassica napus* genome (AST_PRJEB5043_v1; http://plants.ensembl.org/Brassica_napus/Info/Index). 138

**A5** The complete coding sequence of gene encoding indole glucosinolate *O*-methyltransferase 5 (*BnIGMT5a*: BnaC06g37610D, Top; *BnIGMT5b*: BnaA07g33060D, Bottom) retrieved from *Brassica napus* genome (AST_PRJEB5043_v1; http://plants.ensembl.org/Brassica_napus/Info/Index). 139

**A6** The complete coding sequence of gene encoding *β*-Glucosidase 30 (*BnBGLU30a*: BnaC04g22390D, Top; *BnBGLU30b*: BnaA04g01360D, Bottom) retrieved from *Brassica napus* genome (AST_PRJEB5043_v1; http://plants.ensembl.org/Brassica_napus/Info/Index)..... 141

**A7** The complete coding sequence of gene encoding nitrile specifier protein 5 (*BnNSP5*: BnaA02g29990D) retrieved from *Brassica napus* genome (AST_PRJEB5043_v1; http://plants.ensembl.org/Brassica_napus/Info/Index). 142

**A8** The complete coding sequence of gene encoding nitrilase 2 (*BnNIT2a*: BnaC03g13560D, Top; *BnNIT2b*: BnaA03g10890D, Bottom) retrieved from *Brassica napus* genome (AST_PRJEB5043_v1; http://plants.ensembl.org/Brassica_napus/Info/Index)..... 143

**A9** The complete coding sequence of gene encoding nitrilase 4 (*BnNIT4a*: BnaA02g05560D, Top; *BnNIT4b*: BnaC02g09450D, Bottom) retrieved from *Brassica napus* genome (AST_PRJEB5043_v1; http://plants.ensembl.org/Brassica_napus/Info/Index)..... 144

**A10** The complete coding sequence of gene encoding glutathione S-transferase TAU type 13 (*BnGSTU13*: BnaA07g09120D) retrieved from *Brassica napus* genome (AST_PRJEB5043_v1; http://plants.ensembl.org/Brassica_napus/Info/Index)..... 145

**A11** The complete coding sequence of gene encoding indole-3-acetate *β*-D glucosyltransferase (*BnIAGLU*: BnaA03g41970D) retrieved from *Brassica napus* genome (AST_PRJEB5043_v1; http://plants.ensembl.org/Brassica_napus/Info/Index)..... 146

**A12** The complete coding sequence of tubulin gene (*BnTubulin*: BnaA03g41970D) retrieved from *Brassica napus* genome (AST_PRJEB5043_v1;http://plants.ensembl.org/Brassica_napus/Info/Index).. 147

**A13** Amino acid sequence alignment of cytochrome P450 monooxygenase, family 81, subfamily F polypeptide 2 and 4, the enzymes that participate in indole GSL modification…… 151

**A14** Amino acid sequence alignment of indole GSL *O*-Methyltransferase, the enzyme that participates in indole GSL side-chain modification…… 155

**A15** Amino acid sequence alignment of *β*-glucosidase 30, the enzymes that participate in indole GSL degradation pathway……. 157

**A16** Amino acid sequence alignment of Nitrilases, the enzymes that participate in indole GSL degradation pathways……. 160

**B1** Plastic bag used for hydroponic root assay system…… 164

## List of Abbreviations

| Abbreviations | Definition |
|---|---|
| ABC | ATP-binding Cassette |
| ANOVA | Analysis of Variance |
| Asp | Aspartic Acid |
| AUX/IAA | Auxin/Indole-3-acetic Acid |
| ARF | Auxin Response Factor |
| AMI1 | Amidase 1 |
| Ala | Alanie |
| ASK1 | ARABIDOPSIS SKP-LIKE1 CUL1 |
| AREs | Auxin Response Elements |
| BGLUs | β-glucosidases |
| CYP83B1 | Cytochrome P450, Family 83, Subfamily B, Polypeptide 1 |
| CYP79B2 | Cytochrome P450, Family 79, Subfamily B, Polypeptide 2 |
| CYP79B3 | Cytochrome P450, Family 79, Subfamily B, Polypeptide 3 |
| CYP71A13 | Cytochrome P450, Family 71, Subfamily A, Polypeptide 13 |
| CYP81Fs | Cytochrome P450, Family 8q, Subfamily F, Polypeptides |
| CUL1 | CULLIN 1 |
| NR | non-inoculated resistant |
| NS | non-inoculated susceptible |
| CCD | Canadian Clubroot Differential |
| DI | Disease Index |
| dai | Day After Inoculation |
| DAMPs | Damage-Associated Molecular Patterns |
| ET | Ethylene |
| ESPs | Epithiospecifiers |
| ESM | Epithiospecifier Modifier |
| GSL | Glucosinolate |
| Glu | Glutamic Acid |
| GSH | Glutathione |

| | |
|---|---|
| GSTF 9 | GLUTATHIONE S-TRANSFERASE PHI 9 |
| GSTF 10 | GLUTATHIONE S-TRANSFERASE PHI 10 |
| GSTU13 | GLUTATHIONE S-TRANSFERASE TAU 13 |
| GGPs | $\gamma$-Glutamyl peptidases |
| IAA | Indole-3-acetic acid |
| IAM | Indole-3-acetamide |
| IPyA | Indole-3-pyruvic acid |
| IAOx | Indole-3-acetaldoxime |
| IAN | Indole-3-acetonitrile |
| I3C | Indole-3-carbinol |
| I3M | 3-indolylmethyl GSL; Glucobrassicin |
| IGMTs | Indole glucosinolate-*O*-methyltrasferases |
| I3A | Indol-3-ylmethylamine |
| IR | inoculated resistant |
| IS | inoculated susceptible |
| IBFQ | Black Fluorescent Quencher |
| ITCs | Isothiocyanates |
| JA | Jasmonic Acid |
| LiCl | Lithium Chloride |
| Leu | Leucine |
| MGBS | Methoxyglucobrassicins |
| MeJA | Methyl JA |
| NIT | Nitrilase |
| NIL | Near Isogenic Lines |
| NSPs | Nitrile-specifier Proteins |
| NO | Nitric Oxide |
| Phe | Phenylalanine |
| PEN2 | Penetration 2 |
| PCS1 | Phytochelatin synthase 1 |
| PCR | Polymerase Chain Reaction |
| ppm | Parts Per Million |

| | |
|---|---|
| QTL | Quantitative Trait Loci |
| qRT-PCR | Quantitative reverse transcription polymerase chain reaction |
| RBX1 | RING-BOX 1 |
| ROS | Reactive Oxygen Species |
| RNA | Ribonucleic acid |
| RNA-Seq | RNA sequencing |
| RA | Raphanusamic Acid |
| rpm | Revolutions per minute |
| SKP1 | S PHASE KINASE-ASSOCIATED PROTEIN 1 |
| SOT16 | SULFOTRANSFERASE 16 |
| SOT18 | SULFOTRANSFERASE 18 |
| SUR1 | SUPERROOT 1 |
| SAM | S-adenosyl-L-methionine |
| SAH | S-adenosyl-L-homocysteine |
| SSI | Single Spore Isolates |
| SE | Standard Error |
| SIN | sinigrin |
| Tukey’s HSD | Tukey's Honest Significant Difference |
| Trp | Tryptophan |
| TAA1 | Tryptophan Aminotransferase of Arabidopsis1 |
| TARs | TAA1-Related Proteins |
| TIR1/AFB | Transport Inhibitor Response 1/ Auxin Signaling F-box |
| TGG | β-thioglucoside glucohydrolase |
| TFPs | Thiocyanate-forming Proteins |
| UGT74B1 | UDP-GLUCOSYL TRANSFERASE 74B1 |
| XTH | Xyloglucan endo Transglucosylase/hydrolase |
| YUC | YUCCA |
| Y2H | Yeast Two-hybrid Assays |
| ZEN | N, N-diethyl-4-(4-nitronaphthalen-1-ylazo)-phenylamine |
| 1OHI3M | 1-hydroxy-3-indolylmethyl GSL |
| 4OHI3M | 4-hydroxy-3-indolylmethyl GSL |

| | |
|---|---|
| 1MOI3M | 1-methoxy-3-indolylmethyl GSL |
| 4MOI3M | 4-methoxy-3-indolylmethyl GSL |
| $\mu E\ m^2\ s^{-2}$ | microeinsteins per second per square meter |
| 3BN | 3-butenenitrile |
| 2,4-D | 2,4-dichlorophenoxyacetic acid |
| 6-FAM | 6-carboxyfluorescein |

# Chapter 1: Literature review

## 1.1 CLUBROOT DISEASE IN BRASSICA CROPS

### 1.1.1 Host-pathogen interactions of clubroot pathogen in Brassica crops

Clubroot disease caused by the obligate parasite *Plasmodiophora brassicae* Woronin is one of the most damaging soilborne diseases in the Brassica family. Disease development is characterized by the formation of galls in host roots, which interfere with the acquisition of nutrients and water from the soil. This impaired uptake causes yellowing, wilting, premature ripening, and stunning in host plants, leading to losses in both yield and quality of Brassica crops (Strelkov et al., 2006). The causal agent *P. brassicae* is a obligate parasite that remains viable in soil for more than 15 years (Wallenhammar, 1996) as hardy resting spores, and grows and reproduces actively once inside the roots of host plants.

The life cycle of *P. brassicae* can be divided into two main phases (Figure 1.1). The first phase is characterized by the germination of resting spores in response to host root exudates and the subsequent infection of root hairs by motile zoospores released from the resting spores. Once in the root hair, the pathogen produces primary plasmodia, which upon maturity, form and release secondary zoospores. The second phase is characterized by the infection of the root cortex by secondary zoospores (Ingram and Tommerup, 1972). The infection of secondary zoospores leads to the formation of secondary plasmodia, which stimulate the cortical cells to swell and form the characteristic club-like phenotype of roots. The mature secondary plasmodia produce and release resting spores into the soil when host plants die and decay, thus, the disease cycle repeats.

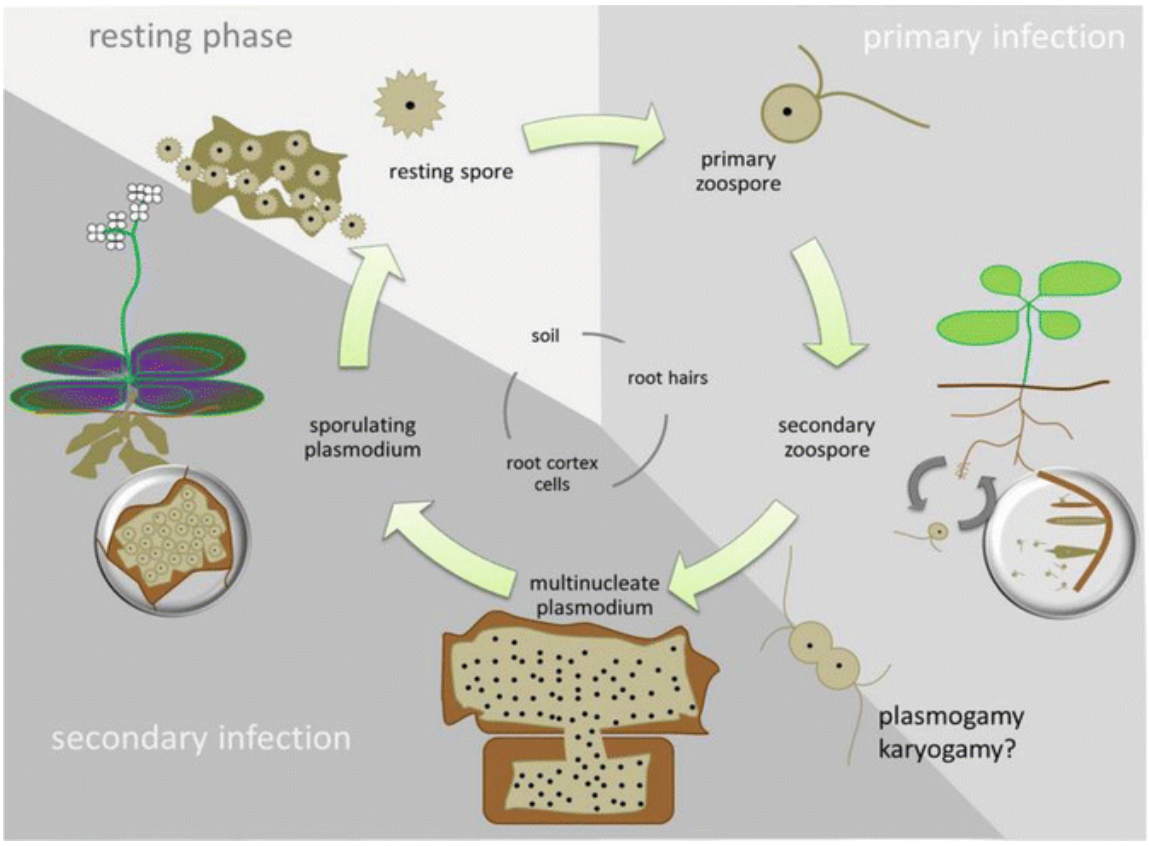


**Figure 1.1 The life cycle of *P. brassicae* in *Arabidopsis thaliana* and other Brassica hosts.** The pathogen remains in the soil as hardy resting spores during the resting phase. In response to host root exudates, they germinate and release primary zoospores, which multiply in root hairs of the host plant producing multinucleate primary plasmodium. Upon maturity, the primary plasmodia form and release secondary zoospores. The secondary zoospores can reinfect root hairs or enter the root cortex tissue leading to the formation of secondary multinucleate plasmodia, which can alter the host metabolism and stimulate the cortical cells to swell and form the characteristic clubbing of roots. The mature secondary plasmodia produce and release resting spores into the soil when host plants die and decay, thus, the disease cycle repeats. Figure from Ludwig-Müller et al. (2017), with permission.

### 1.1.2 Significance of clubroot disease in Brassica crops

The devastating effects of clubroot can be judged throughout its geographical distribution and the resulting yield losses including compromised quality. Clubroot, noticed for the first time in 1736 in Europe, has now become a disease of worldwide importance in the Brassica family, with global yield losses estimated to be 10 - 15% (Dixon, 2009). In Germany, clubroot has been reported to be widely spread in all regions of the country (Diederichsen, et al., 2014). Between 2012 and 2015, 49 new *P. brassicae*-infected fields were detected in 12 German federal states, with clubroot incidence varying from 22% to 25% (Zamani-Noor, 2017). In Poland, the application of DNA-based screening detected the presence of the *P. brassicae* DNA in as much as 62% (267) of the fields, within which, 26% was found consisting of *P. brassicae* DNA at the level corresponding to a risk of crop losses of more than 10% in susceptible crops (Czubatka-Bieńkowska, 2020). Japan was the first Asian country that reported the presence of clubroot in the 1890s (Ikegami et al., 1981), and this disease has now become a major threat in cabbage and Chinese cabbage production in Japan and Korea (Hirai, 2006). In China, the area affected by clubroot disease accounts for 1/3 of the total area of Brassica crops, resulting in 20 -30% yield losses, with more than 60% yield loss in the most seriously damaged regions (Wang et al., 2011).

In Canada, documented research on clubroot dates to 1916, suggesting that this disease was probably well established in Canada by the late 19th or early 20th centuries (Estey, 1994). Since then, clubroot disease has been a major threat to the production of Brassica vegetables in traditional vegetable growing regions such as Ontario, Quebec, British Columbia, and Atlantic Provinces, but rarely reported in the Prairie provinces (Alberta, Saskatchewan and Manitoba (Howard et al. 2010). Canadian canola (*Brassica napus* L.) is economically one of the most important crops in Canada, contributing an estimated $29.9 billion yearly to the national economy (calculated for 2016-17 to 2018-19; Canola Council of Canada, 2022). Clubroot was first identified on canola in 1997 in Quebec (Morasse et al., 1997). In 2003, clubroot was first reported in the Prairie Provinces, where more than 98% of the harvested hectares of Canadian canola are grown (Tewari et al., 2005). By 2020, clubroot had spread to a total of 3353 canola fields distributed throughout most parts of Alberta (Strelkov et al., 2020). In Saskatchewan, the visible symptoms of clubroot have been confirmed in 75 commercial canola fields since 2017, including 24 fields in 2020. The 2020 Manitoba canola survey reported positive clubroot symptoms in 10 rural municipalities, bringing the total to 44 clubroot-infected canola fields since

symptomatic fields records began in 2013 (Canola Council of Canada, 2021). Given the significant economic value of canola, there has been an increasing research effort aiming at understanding and managing clubroot disease in this crop.

### 1.1.3 Management of clubroot in crops

Through the years, various strategies have been proposed or assessed for the management of clubroot disease in infected fields including liming the soil to increase soil pH as disease development is often favored by acidic soil conditions (Murakami et al., 2002; Myers, 1985), sanitization of farm machinery to slow or eliminate the spread of the pathogen (Howard et al., 2010), and crop rotation with cruciferous bait crops (Chinese cabbage), non-cruciferous host crops (red clover, perennial ryegrass, orchardgrass, bentgrass), or non-host crops (barley, wheat), to lower the spore population (Ahmed et al., 2011; Friberg et al., 2006). Although these strategies show good performance for disease management of short-season Brassica vegetables, most of them are not economically feasible for the large-scale canola production in western Canada, hence, not widely adopted by western Canadian farmers (Hwang et al., 2014). In comparison, cropping with resistant cultivars is more cost effective and has been the major option for clubroot management in western Canada. Since the release of the first clubroot-resistant canola cultivar in 2009, the number of available cultivars with clubroot resistance has reached 28 by 2019 (Canola Council of Canada, 2019). While the genetic mechanism of resistance is largely unknown, it was found that the resistance to *P. brassicae* present in Canada is mostly conferred by a single dominant gene present in the winter canola cultivar 'Mendel' and in specific rutabaga cultivars (Rahman et al., 2014). The large-scale production of canola cultivars with single gene resistance to clubroot has imposed a significant selection pressure on the *P. brassicae* population, leading to the shifting of the major *P. brassicae* pathotypes with the population, and a rapid decline in the level of resistance (Strelkov et al., 2016, Strelkov et al., 2018, Fredua-Agyeman et al., 2018, Cao et al, 2020). Therefore, the identification of new sources of resistance is urgently needed for canola production in western Canada.

Rutabaga (*Brassica napus* ssp. napobrassica (L.) Hanelt) is cultivated as a table vegetable and as fodder for animals (Gowers, 2010). In Canada, commercial cultivation of rutabaga as a vegetable crop began in the 1950s and 1960s (Spaner, 2002). Rutabaga is also known as an excellent source of clubroot-resistance genes (Rahman et al., 2014; Fredua-Agyeman et al.,

2020; Hasan and Rahman, 2016). As early as the 1960s, it was observed that certain rutabaga lines showed clubroot resistance under controlled environmental or field conditions (Karling, 1968; Lammerink, 1967). Consequently, rutabaga can serve as a valuable resource for the development of clubroot-resistant canola varieties through breeding. Although rutabaga is a root vegetable, and canola is an oilseed, they belong to the same species, *B. napus*, with identical ploidy level and genome (2n = 38, AACC). As a result, the transfer of clubroot resistance genes from rutabaga to canola is not impeded by many of the pre- and post-zygotic barriers encountered in crosses with more distantly related species (Fredua-Agyeman et al., 2020). In recent years, several large-scale screening projects have identified resistance in rutabaga to a range of *P. brassicae* pathotypes (Fredua-Agyeman et al., 2019; Hasan et al. 2012). The rutabaga cultivars 'Wilhemsburger' and 'Laurentian' were included in multiple clubroot differential sets due to their variation in resistance to different isolates of *P. brassicae* (Williams, 1966, Buczacki et al., 1975; Somé et al., 1996; Strelkov et al., 2018). Broad-spectrum resistance was reported in 'Wilhemsburger' to 17 *P. brassicae* pathotypes identified from Canada on the (Canadian Clubroot Differential) CCD set, while 'Laurentian' was resistant to seven of these pathotypes (Strelkov et al. 2018). Ayers and Lelacheur (1972) reported that 'Wilhemsburger' is resistant to pathotypes 2 and 3 of *P. brassicae* (as defined on the differentials of Williams 1966). 'Laurentian', on the other hand, is susceptible to pathotype 3A, the predominant resistance-breaking pathotype in western Canada (Strelkov et al., 2018).

## 1.2 THE PLANT GROWTH REGULATOR AUXIN

### 1.2.1 Auxin in plant-pathogen interactions

Auxin is a well-known phytohormone that has an important role in regulating plant growth and development (Davies, 2010). On the cellular level, auxins contribute to cell division, expansion, differentiation and polarity. On the whole plant level, organ development including the formation of roots, shoots, leaves, as well as flowers and fruits, is achieved with the presence of auxin. In addition to plant developmental processes, auxin has been implicated in plant-pathogen interactions (Fu and Wang, 2011). In some cases, auxin contributes directly to resistance, and activation of auxin signaling inhibits microbial activity, presumably through activation of Jasmonic acid (JA)-mediated defense (Fu and Wang, 2011, Zhang et al., 2017; Zhang et al., 2019; Qi et al., 2012). In other instances, auxin can promote disease symptoms,

hence enhancing disease susceptibility in host plants. There has been a growing number of reports of pathogens that use auxin machinery to promote pathogenesis; some by suppression of auxin-mediated defense responses (Zhang et al., 2019; Zhang et al., 2020), others by synthesis of auxin and manipulation of host auxin physiology (e.g., biosynthesis, signaling, and transport) to directly promote disease development (Duca et al., 2014; Patten et al., 2013; Ma and Ma, 2016; Mashiguchi et al., 2019; Kyndt et al., 2016). The causal agent of clubroot disease, *P. brassicae,* is one of the pathogens that forms large galls on the roots, and manipulation of the host auxin levels is proposed to be part of mechanism by which the pathogen creates the galls (Ludwig-Müller et al., 2009). There are a number of studies that investigated the role of auxins in the development of clubroot disease (Raa, 1971; Devos et al., 2005; Mousdale, 1981). It appears that cell division, cell elongation, and the production of hypertrophied cells during the formation of the galls are associated with higher auxin availability and biosynthesis (Ludwig-Müller et al., 2017; Grsic-Rausch et al., 2000; Devos et al., 2006). Thus, further understanding of the role of auxin in the *P. brassicae-Brassicaceae spp.* interaction is crucial for understanding clubroot symptom development.

### 1.2.2 Auxin biosynthesis and conjugation

Indole-3-acetic acid (IAA) is the most abundant naturally occurring auxin in plants. IAA biosynthesis is known to be synthesized *de novo* using tryptophan (Trp) as a precursor (Trp-dependent pathway) or by a Trp-independent pathway (Zhao, 2012, 2014). IAA is mainly synthesized by the plant through the tryptophan (Trp)-dependent pathway (Zhao, 2012, 2014; Figure 1.2). Synthesis of IAA through indole-3-pyruvic acid (IPA pathway) is the main contributor to Trp-dependent IAA synthesis (Zhao, 2012), and is the only plant IAA biosynthesis route that has been completely described to date. In the IPA pathway, TRYPTOPHAN AMINOTRANSFERASE OF ARABIDOPSIS1 (TAA1) and TAA1-RELATED proteins (TARs) catalyze the conversion of Trp to IPA. Subsequently, IPA is converted to IAA by the YUCCA (YUC) family of flavin-containing monooxygenases (Zhao, 2012). The Trp-dependent indole-3-acetaldoxime (IAOx) pathway for production of IAA is likely restricted to the Brassicaceae family (Sugawara et al., 2009; Figure 1.2). In Arabidopsis, Trp is converted to IAOx by the cytochrome P450 monooxygenases CYP79B2 and CYP79B3 (Hull e al., 2000; Mikkelsen et al., 2000; Zhao et al., 2002). IAOx contributes largely to the production of indole glucosinolate

(GSL) defense compounds, while the role of IAOx in IAA biosynthesis is rather minor because the *cyp79b2/cyp79b3* double mutant had little effect on IAA levels in Arabidopsis (Sugawara et al., 2009). *In vitro* enzymatic assays indicated that indole acetaldoxime dehydratase (coded by *CYP71A13*) catalyzes the conversion of IAOx to indole-3-acetonitrile (IAN) in the biosynthesis of the plant defense compound camalexin in Arabidopsis (Nafisi et al., 2007). IAN appears to not be a major product synthesized via indole GSL metabolism, as IAN levels were not significantly reduced in the SUPERROOT (*sur1–1*) null mutant (does not produce indole GSLs; Mikkelsen et al., 2004) in comparison to that in wild type (WT) plants under normal growth conditions. IAN was shown to be converted to both IAM and IAA *in vitro* by plant nitrilases (NITs) (Pollmann et al., 2002; Bartel and Fink, 1994). The IAM pathway is well known in auxin-synthesizing bacteria, involving two enzymes, tryptophan monooxygenase (iaaM) and indole-3-acetamide hydrolase (iaaH). The iaaM is responsible for the conversion of Trp to IAM whereas the iaaH is responsible for the conversion of IAM to IAA (Patten and Glick, 1996). Endogenous IAM has also been reported in many plant species as an IAA precursor (Korasick et al., 2013). In Arabidopsis, it was suggested that IAM is produced from IAOx (Sugawara et al., 2009). However, Korasick and colleagues (2013) found that IAM was present in many species in which IAOx was not detected, which suggests that IAM can be produced from precursors other than IAOx (Sugawara et al., 2009). IAM is converted to IAA by AMIDASE1 (AMI1) in plants (Pollmann et al., 2003).

Nitrilases (nitrile aminohydrolase, E.C. 3.5.1.x) are enzymes that catalyze the hydrolytic cleavage of nitriles into their corresponding carboxylic acids and ammonia (Piotrowski, 2008). In Arabidopsis, there are four nitrilase genes (*NIT1-4*), and *NIT2* and *NIT3* are homologs of NIT1. NIT1 and NIT4 enzymes have different substrate preferences (Piotrowski, 2008). Recombinant proteins (from *Brassica rapa* expressed in *E. coli*) of NIT1 and NIT2, but not NIT4, were able to convert IAN to IAA (Ishikawa et al., 2007). However, IAN was a poor substrate for these NIT enzymes compared with various aliphatic and aromatic nitriles. The *B. rapa* NIT4 recombinant enzyme specifically converted β-cyano-L-alanine to aspartic acid and asparagine, consistent with the proposal that NIT4 is involved in the cyanide detoxification pathway (Ishikawa et al., 2007). As mentioned above, nitrilases can convert IAN to IAA, but nitrilase mutants or nitrilase over-expressors lack severe phenotypes that should be observed when auxin biosynthesis is significantly disturbed (Normanly et al., 1997). With respect to infection of Brassicaceae species

with *P. brassicae*, alterations of nitrilase gene expression and enzyme activity are closely associated with host cells containing pathogen plasmodium. Increased gene expression of certain plant host nitrilase genes was observed during *P. brassicae* infection of Arabidopsis (*NIT1*, *NIT2*) and *B. rapa* (*NIT1*) (Grsic-Rausch et al., 2000; Ishikawa et al., 2007). In Arabidopsis, the nitrilase mutant *nit1* (Grsic-Rausch et al., 2000; Ishikawa et al., 2007), and transgenic lines that down-regulate the expression of *NIT1* or *NIT2*, were observed to have reduced or delayed clubroot development (Neuhaus et al., 2000). As hypothesized by Piotrowski (2008), nitrilase activity induction in the host could have a two-fold effect for the pathogen: the first is the induction of IAA synthesis, and the second is the alteration of the defense metabolites in the host.

Free auxin (IAA) is the biologically active auxin form, and levels are tightly controlled throughout the plant life cycle by the processes of synthesis, inactivation, and transport (Korasick et al., 2013). Conjugated auxins are considered storage forms that can be converted to free auxins or to intermediates destined for degradation (Woodward and Bartel, 2005). Naturally occurring auxin conjugates in plants include ester conjugates, amide conjugates, and protein conjugates (Ludwig-Müller, 2011, Figure 1.2). Ester conjugates can be synthesized via auxin glycosyltransferases, usually through catalyzing the transfer of activated sugars to auxin, and thereby they regulate auxin levels in plants by removing them from the biologically active free auxin pool (Szerszen et al., 1994). IAA-esters such as IAA-glucose can be hydrolysed back to free IAA by IAA-glucose hydrolases (Jakubowska et al., 1993; Ludwig-Müller et al., 1996; Kowalczyk and Bandurski, 1990). IAA can also be conjugated to single amino acids via amide bonds. It was suggested that only a fraction of amide conjugates such as IAA-Ala, IAA-Leu, and IAA-Phe are hydrolysed back to free IAA via IAA-amide hydrolases, whereas amino acid conjugates with IAA-Asp and IAA-Glu are thought to be precursors for degradation pathway. Finally, there are protein conjugates with IAA, however, their functions and biosynthesis pathways remain largely unknown (Park et al, 2010).

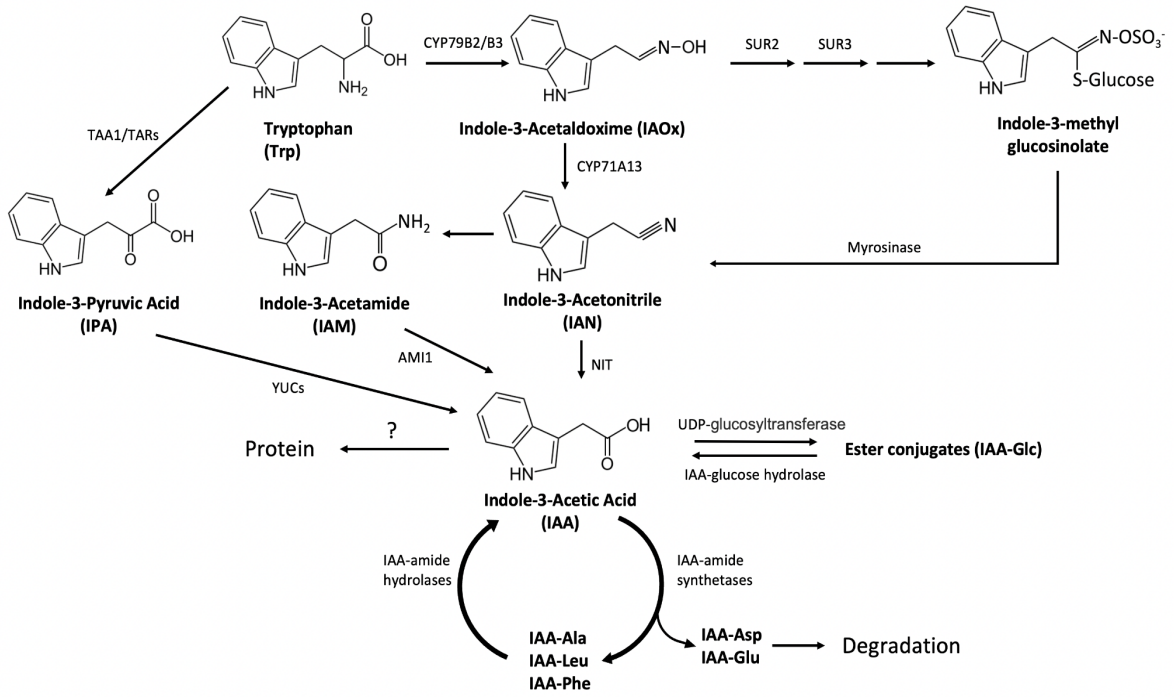


**Figure 1.2 Trp-dependent IAA biosynthesis and conjugation pathway in Arabidopsis.** Tryptophan-dependent IAA biosynthesis involves multiple enzymatic reactions that convert tryptophan into IAA. The IPA pathway, which is primarily responsible for Trp-dependent IAA synthesis, involves TAA1 and TARs catalyzing the conversion of Trp to IPA, followed by YUC family enzymes converting IPA to IAA. In the Trp-dependent IAOx pathway, CYP79B2 and CYP79B3 convert Trp to IAOx, which is mainly involved in producing indole GSL that can be further hydrolyzed by myrosinase to form IAN Subsequently, IAN can be converted to IAA by plant nitrilases, while AMI1 converts IAM to IAA. The main categories of IAA conjugates include sugar conjugates (IAA-glucose), amino acid conjugates (IAA-Ala, IAA-Leu, IAA-Phe, IAA-Asp, IAA-Glu), and protein conjugates. The Upper section shows different pathways of auxin biosynthesis from Trp. The lower section illustrates various auxin conjugation pathways. Pathway intermediates are bolded, and the enzyme names are in smaller font. The figure was developed based on Zhao (2014), Malka and Cheng (2017), and Bajguz and Piotrowska (2009).

### 1.2.3 Auxin signaling

Auxins are perceived, and their signal are transduced through a signaling cascade that includes three protein families, the auxin receptor or TRANSPORT INHIBITOR RESPONSE 1/ AUXIN SIGNALING F-BOX (TIR1/AFB) proteins, the AUXIN/INDOLE-3-ACETIC ACID (AUX/IAA) proteins, and the AUXIN RESPONSE FACTOR (ARF) proteins (Figure 1.3). The TIR1/AFB protein families are grouped into four phylogenetic clades TIR1, AFB2, AFB4, and AFB6 (Parry et al., 2009). Arabidopsis has six auxin receptors which fall into three phylogenetic clades, the TIR1 clade (TIR1 and AFB1), AFB2 clade (AFB2 and AFB3) and the AFB4 clade (AFB4 and AFB5; Dharmasiri et al., 2005b; Parry et al., 2009). Aux/IAA proteins are repressors of auxin-regulated transcriptional activation, they repress transcription of the ARF genes (Overvoorde et al., 2005). There are 29 Aux/IAA proteins in Arabidopsis, most of which have similar domain structures (Overvoorde et al., 2005).

Auxin does not bind to a TIR1/AFB receptor without an Aux/IAA; therefore, Aux/IAAs and TIR1/AFBs are also referred to as co-receptors (Calderón-Villalobos et al., 2012). When the concentration of auxin is low, the Aux/IAA proteins bind to the ARF transcription factors inhibiting transcription (Kim et al., 1997; Ulmasov et al., 1997). The TIR1/AFB family of TIR1/AFB proteins forms a ubiquitination ligase (E3) complex with S PHASE KINASE-ASSOCIATED PROTEIN 1 [SKP1; or ARABIDOPSIS SKP-LIKE1 (ASK1)], CULLIN 1 (CUL1), and RING-BOX 1 (RBX1) known as SCFTIR1/AFB complex (Wang and Estelle, 2014). When auxin is present, it acts as a 'molecular glue' binding the SCF-TIR1/ AFB complex with Aux/IAA at domain II, leading to ubiquitination and degradation of the Aux/IAA proteins. Then the *ARF* genes are released from repression allowing subsequent transcriptional activation. In addition, the expression of *Aux/IAA* genes themselves is auxin-inducible (Quint and Gray, 2006). As auxin levels decrease, increased Aux/IAA transcription leads to increased levels of Aux/IAA proteins that diminish the signaling pathway by restoring repression of the ARF transcription factors (Paciorek and Friml, 2006; Quint and Gray, 2006)

Interestingly, evidence suggests that the indole GSL degradation product indole-3-carbinol (I3C) has the ability to directly alter auxin perception by interacting with the TIR1 auxin receptor (Katz et al., 2015). As mentioned above, auxin promotes interaction between the auxin receptors TIR1/AFBs and Aux/IAA family proteins; the I3C interaction with the auxin binding site of TIR1 appears to perturb the docking of the Aux/IAA proteins facilitated by auxin, leading

to an inhibition in auxin responses. In this study, the authors first modeled the potential interaction of I3C with TIR1 based on crystal structure of auxin binding with TIR1 (Tan et al., 2007), and it was predicted that I3C associates with the auxin binding site of the TIR1 auxin receptor. Additionally, with the use of a reporter for auxin responses, the authors found that exogenous treatment of I3C reduced auxin responses. Thirdly, at the physiological level, it was showed that I3C partially antagonizes the effect of auxin on several root phenotypes. Previously, Villalobos et al. (2012) showed that auxin promotes interaction between the auxin receptors TIR1/AFBs and Aux/IAA (IAA) family proteins in yeast two-hybrid assays (Y2H). With the same system, Katz et al. (2015) showed that I3C perturbed the auxin-dependent interaction of TIR1 with IAA proteins using Y2H assays, and this result was further confirmed with an *in vitro* pull-down assay. Taken together, the results from these experiments suggest that I3C modulates auxin action in an antagonistic manner.

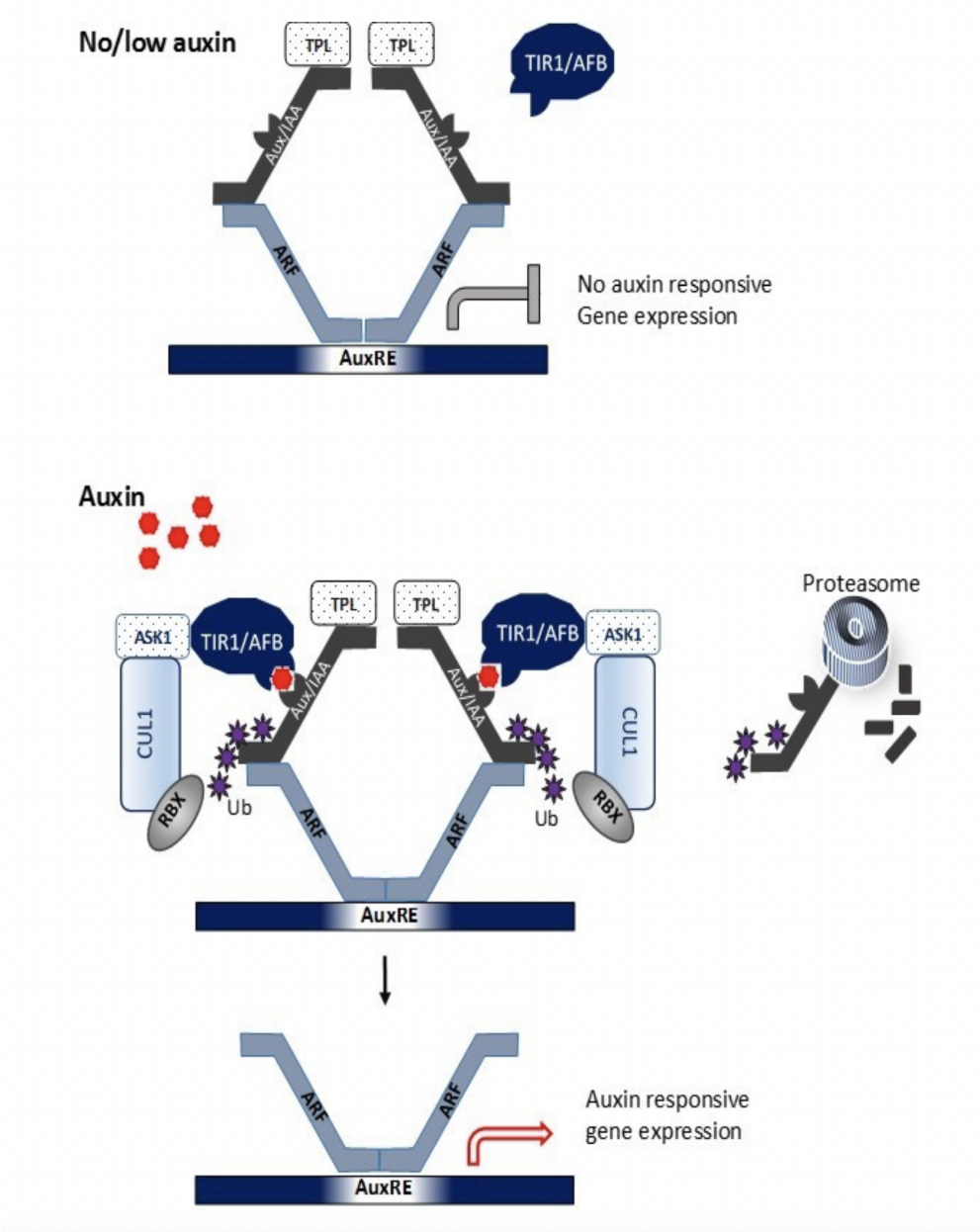


**Figure 1.3 Mechanism of auxin signaling through the TIR1/AFB-mediated pathway.** In the absence of auxin, Aux/IAA repressors bind with ARF transcription factors and repress the auxin responsive gene expression. Aux/IAAs recruit TPL co-repressors in this repression process. Auxin acting like a molecular glue brings the TIR1/AFB and Aux/IAA proteins together. This association causes SCFTIR1/AFB mediated ubiquitination of Aux/IAAs. Degradation of ubiquitinated Aux/IAAs by 26S proteasome releases ARF transcription factors initiating auxin-responsive gene expression. Ub: Ubiquitin. Figure from Jayasinghege (2017) by permission, based on Wang and Estelle (2014) and Salehin et al. (2015).

## 1.3 INDOLE GSLs

### 1.3.1 GSLs and clubroot disease

GSLs are a well-defined group of secondary plant metabolites involved in plant defense against herbivores and pathogens. They are commonly found in the plants in the Brassicaceae family. GSLs are synthesized from certain amino acids and their biological roles depend largely on the structure of their side chains. All GSLs can be classified into three categories, according to the amino acid from which they are derived: aliphatic (predominately from methionine), aromatic (from phenylalanine or tyrosine) or indolic (from tryptophan). The chain elongation of amino acid leads to the formation of the core structure of GSLs, which consists of a β-D-glucopyranose residue linked via a sulfur atom to a (Z)-N-hydroximinosulfate ester (Figure 1.4; Harun et al., 2020; Ishida et al., 2014). After enzymatic hydrolysis of the GSL by myrosinase, the sulfated aglucone can undergo rearrangement to compounds including isothiocyanate, thiocyanate, and nitriles, which are recognized as plant defense compounds (Halkier and Gershenzon, 2006; Chhajed et al., 2020, Harun et al., 2020). In Arabidopsis, aliphatic GSLs predominate in most organs, while indole GSLs were found to made up nearly half of the total GSL pool in roots (Brown et al., 2003). The metabolism of indole GSLs are linked to auxin homeostasis in a complex manner. It was hypothesized that indole GSLs play a role as a precursor of IAA during clubroot disease development (Butcher et al., 1974). More specifically, the indole GSL pathway contributes to auxin biosynthesis via two metabolic intermediates IAOx and IAN. IAOx is proposed as a metabolic branch point for the biosynthesis of IAA, camalexin, and indole GSLs, while IAN is one of the hydrolysis products of indole GSL that could be metabolized to IAA by nitrilases (Hansen and Halkier, 2005; Bartel and Fink, 1994). The different classes of GSLs were differentially induced during the development of the clubroot disease in Chinese cabbage (Ludwig-Müller et al., 1997). In the study by Ludwig-Müller et al. (1997), infection with *P. brassicae* led to an increased level of indole GSLs (only aliphatic aromatic, and indolic GSL classes were quantified) in roots of two clubroot-susceptible cultivars ‘Granat’ and ‘Osiris’ 14 and 20 days after inoculation whereas there was no difference between infected and control roots of two resistant cultivars ‘Parkin’ and ‘Yuki’. Also, lower indole GSL biosynthesis was indicated in five-day-old seedlings of the tolerant varieties as they were observed to have lower tryptophan oxidizing enzyme activity. From these data, the authors concluded that indole GSLs may play a role in the initial infection process, as well as in later

stages of infection for clubroot symptom development in Chinese cabbage. On the other hand, Mullin et al. (1980) found no relationship between the indole GSLs content (as measured by thiocyanate ion content) and clubroot resistance in 43 clubroot-resistant versus susceptible cultivars of rutabaga and turnip. Plant stress responses to pathogens include constitutive and induced metabolic changes, producing specialized metabolites for plant defense. Metabolic profiling of near isogenic lines (NILs) showing contrasting resistance and susceptibility to a given pathogen allows the identification of candidate compounds involved in plant defense, and in the meantime, minimizes the genetic background effects and can explain the resistance mechanisms governed by a specific locus (Sade et al., 2015; Yogendra et al., 2014; Gunnaiah et al., 2012). However, in a given interaction, plant cellular responses are often controlled by the combined influence of sets of quantitative trait loci (QTLs) (St. Clair, 2010). In this regard, Wagner and colleagues (2019) combined metabolomics and quantitative genetics in identifying the roles of specific metabolites and their associated QTLs in plant-pathogen interaction between two *Brassica napus* NILs (Darmor-bzh and Yudal) with different degrees of clubroot resistance/susceptibility to *P. brassicae*. This work suggested that the partial resistance to *P. brassicae* is genetically related to the accumulation of citric acid, gluconasturtiin and potentially its degradation products, and two unknown metabolites. Consistently, Zamani-Noor et al., (2021) reported that the more aggressive *P. brassicae* isolate might be able to suppress gluconasturtiin synthesis in a more pronounced manner as a trend for lower levels of gluconasturtiin in roots at 35 dai was observed in susceptible cultivars (Bender, Ladoga, Visby) inoculated with pathotype 1 (P1) and the average levels were even lower in plants inoculated with the more aggressive isolated P1 (+) compared to resistant cultivars (Aristoteles, Creed, Mendel). However, these trends were not statistically significant. Therefore, it appears that many factors are involved in clubroot resistance, and there is no simple relationship between clubroot disease and GSL content.

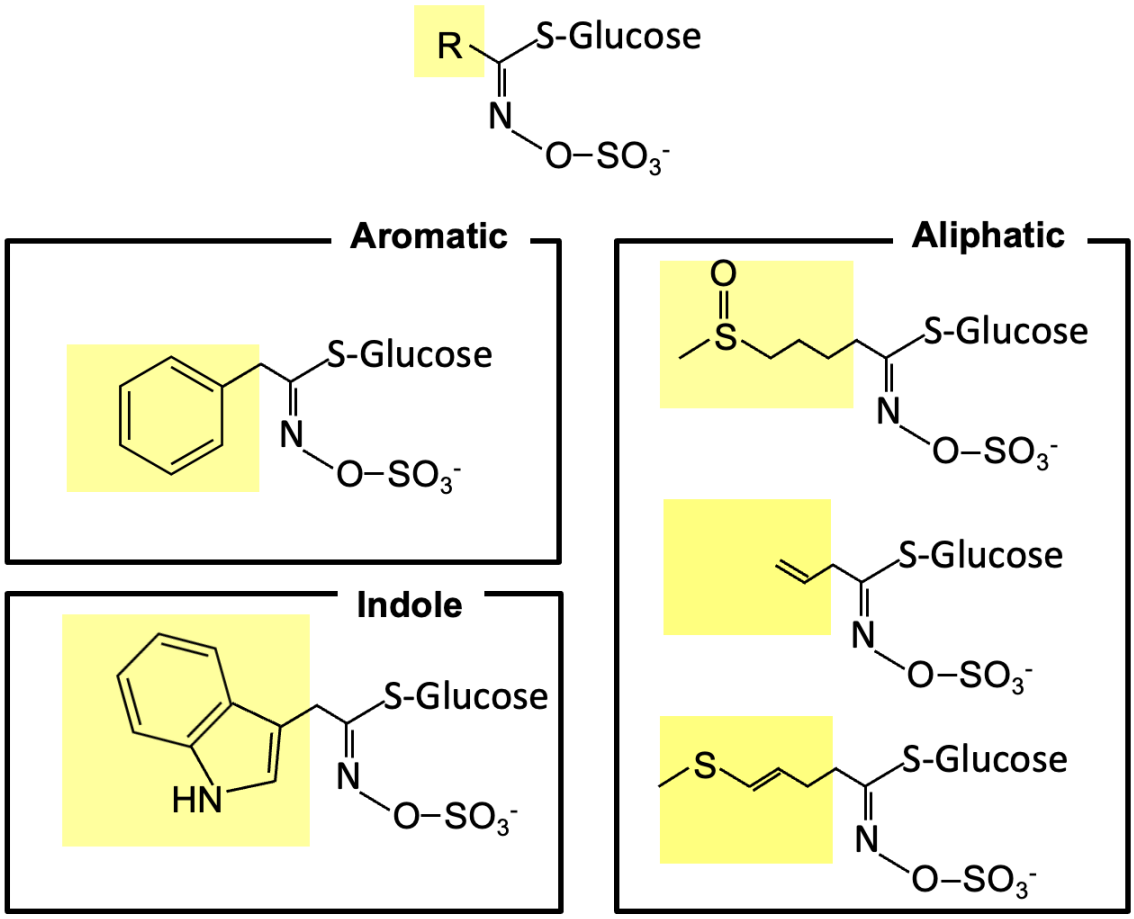


**Figure 1.4 The core structure of GSLs and examples of aromatic, aliphatic, and indole GSLs.** GSLs can be categorized into three types based on the amino acid source: aliphatic (mostly derived from methionine), aromatic (from phenylalanine or tyrosine), or indolic (from tryptophan). The core structure of GSLs is formed by the elongation of the amino acid chain, resulting in a (Z)-N-hydroximinosulfate ester linked to a β-D-glucopyranose residue through a sulfur atom. The figure was developed based on Ishida et al. (2014).

### 1.3.2 Indole GSL biosynthesis

Biosynthesis of GSLs can be divided into three stages: 1) amino acid chain elongation, 2) core structure synthesis and 3) secondary side-chain modifications. It was found that genes encoding enzymes of the indole GSL biosynthetic pathway, and Trp biosynthetic genes are co-expressed in response to a wide range of stress conditions such as cold, heat, drought, osmotic, saline, oxidative, UV, wounding, and pathogen infection, suggesting the involvement of Trp biosynthesis in the indole GSL biosynthesis pathway (Gachon et al., 2005). Synthesis of indole GSL starts with conversion of Trp to aldoxime via the cytochrome P450 enzymes, CYP79B2/CYP79B3, forming IAOx (Figure 1. 5; Hull et al., 2000; Mikkelsen et al., 2000). IAOx can subsequently serve as a substrate for the cytochrome P450 family B enzyme CYP83B1 that oxidizes aldoximes into nitrile oxide compounds forming indole-3-acetonitrile oxide (Naur et al., 2003). Next, the nitrile oxide compounds can be converted to a glutathione (GSH) conjugate by glutathione S-transferases (GSTF9 and GSTF 10), resulting in the formation of indole-3-acetohydroxymoyl GSH (Wentzell et al., 2007). $\gamma$-Glutamyl peptidases (GGP1 and GGP3) are then responsible for metabolization of GSH conjugate into Cys-Gly conjugate, producing indole-3-acetohyfroxymoyl Cys-Gly (Geu-Flores et al., 2011). C-S cleavage (SUR1) participates in the next step of reaction, converting indole-3-acetohyfroxymoyl Cys-Gly into indolylmethyl-thiohydroximate (Mikkelsen et al., 2004). During the glycosylation process, the glucotransferase of the UDP-glycosyltransferase 74 (UGT74) family, UGT74B1, converts thiohydroximates into desulfoglucosinolates (Douglas et al., 2004). The final step of GSL core structure synthesis is the sulfation of desulfo-GSLs to form intact GSLs, catalyzed by sulfotransferases (SOT 16, SOT18) to form 3-indolylmethyl GSL (I3M; glucobrassicin) (Klein and Papenbrock, 2009).

The Arabidopsis double mutant *cyp79b2 / b3* had reduced indole GSL levels (almost to zero (Zhao et al., 2002), and mutant and wild-type Arabidopsis roots were analysed for gall formation, free IAA levels and camalexin content in *P. brassicae*-inoculated and non-inoculated seedlings (Siemens et al., 2008). The *cyp79b2 / b3* mutant had no detectable camalexin content, but free IAA levels were similar to that of the WT roots. Both WT and the *cyp79b2 / b3* mutant seedlings were susceptible to *P. brassicae* producing similar-sized galls as assessed in the Siemens et al. (2008) study. These data suggest that the absence of camalexin and indole GSLs does not affect the *P. brassicae* infection or proliferation processes in Arabidopsis host; but the

present of these compounds still may function as deterrents to the *P. brassicae* infection and/or proliferation processes. For example, Lemarié and colleagues (2015) reported that at 10, 14, 17 days after inoculation (dai), the accumulation of camalexin was four-seven times higher in partially resistant (Bur-0) than susceptible (Col-0) Arabidopsis, which is defective in camalexin biosynthesis (*pad3 mutant*) and showed clear enhancement in clubroot symptoms. This suggests that clubroot-triggered camalexin biosynthesis might play a role in the quantitative control of partial resistance of Arabidopsis to clubroot. Consistently, Siemens et al., (2008) reported camalexin accumulation in wild-type Arabidopsis Col-0 in response to *P. brassicae* (isolate e3) infection at 28 dai. Furthermore, Zamani-Noor et al., (2021) investigated the changes of GSLs content in root and leaves of different clubroot-resistant and -susceptible oilseed rape cultivars upon inoculation of various *P. brassicae* isolates and found that indole GSL contents in roots were lower in susceptible cultivars compared with resistant cultivars at 35 dai. It was hypothesized by the authors that higher content of indole GSL in the resistant cultivars may lead to a greater formation of I3C, which may inhibit root growth by blocking auxin signaling (Katz et al., 2015), thus inhibiting root-gall growth.

### 1.3.3 Indole GSL modification

The modification of indole GSL starts with the catalysis by the cytochrome P450 monooxygenases of the CYP81F subfamily, converting 3-indolylmethyl GSL (I3M; glucobrassicin) to hydroxyl GSLs, either 1-hydroxy-3-indolylmethyl GSL (1OHI3M) or 4-hydroxy-3-indolylmethyl GSL (4OHI3M) (Figure 1.5; Pfalz et al., 2011; Harun et al., 2020). CYP81F1-3 can participate in the hydroxylation reactions at positions 1and 4 of the indole rings, leading to the production of 1OHI3M and 4OHI4M, whereas CYP81F4 can only hydroxylate the indole ring at position 1, producing 1OHI3M (Pfalz et al., 2011). The next step in indole GSL modification is the conversion of 1OHI3M to 1-methoxy-3-indolylmethyl GSL (1MOI3M) and 4OHI4M to 4-methoxy-3-indolylmethyl GSL (4MOI3M), by indole glucosinolate-*O*-methyltrasferases (IGMTs), in which the hydroxyl group is converted to a methoxy group (Pfalz et al., 2011). It is reported that IGMT1 and IGMT2 can produce both 1MOI3M and 4MOI3M, whereas IGMT5 only converts 1OHI3M to 1MOI3M (Pfalz et al., 2016).

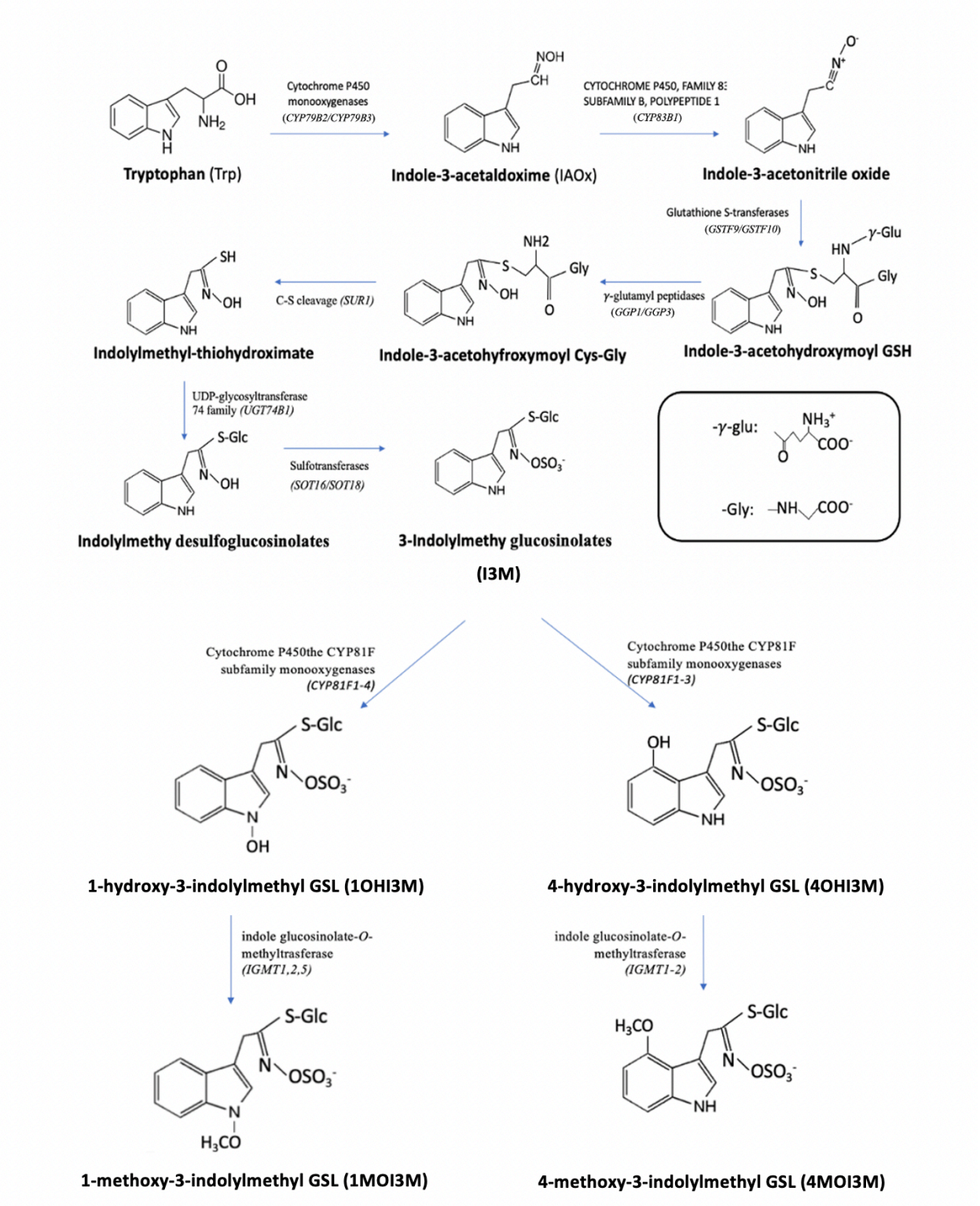


**Figure 1.5 Indole GSL biosynthesis and modification pathway.** The synthesis of indole GSL starts with the conversion of Trp to aldoxime by CYP79B2/CYP79B3, forming IAOx. CYP83B1 oxidizes IAOx into nitrile oxide compounds, which can be converted to a GSH conjugate by

GSTF9 and GSTF10. GGP1 and GGP3 metabolize the GSH conjugate into Cys-Gly conjugate, which was then converted into indolylmethyl-thiohydroximate by SUR1. UGT74B1 converts the thiohydroximates into desulfoglucosinolates during glycosylation, and SOT16/SOT18 sulfates desulfo-GSLs to form I3M. Indole GSL modification begins with cytochrome P450 enzymes, CYP81F1-4, hydroxylating I3M to form 1OHI3M and 4OHI3M. CYP81F1-3 can catalyze hydroxylation at positions 1 and 4, while CYP81F4 only at position 1. IGMTs then convert 1OHI3M and 4OHI3M to 1MOI3M and 4MOI3M, respectively, by converting the hydroxyl group to a methoxy group. IGMT1 and IGMT2 catalyze the formation of both 1MOI3M and 4MOI3M, while IGMT5 only catalyze the modification of 1OHI3M to 1MOI3M.The Upper section shows the indole GSL core structure synthesis from Trp. The lower section illustrates indole modification. Pathway intermediates are bolded, and the enzyme names and the genes that encode these enzymes are in smaller font. Structures of -$\gamma$-glu and -Gly are shown as insert. The figure was developed based on Harun et al., (2020).

### 1.3.4 General degradation pathway of GSLs

GSLs are well-known second metabolites almost exclusively found in Brassicaceae as defense compounds. When plant tissue is damaged, the GSLs stored in the vacuole come in contact with myrosinase enzymes (β-thioglucosidases), leading to the hydrolysis of GSLs and subsequent production of degradation products such as epithiontriles, nitriles, isothiocyanate, thiocyanates, and oxazolidine-2-thiones, some of which can be toxic and pungent (Figure 1.6; Wittstock and Halkier, 2002). In GSL degradation, all GSLs (aliphatic-, indolic-, and aromatic GSLs) can form isothiocyanates and nitriles, but only aliphatic GSLs are degraded into epithionitriles (Blažević et al., 2020). This characteristic reaction of cruciferous plants is often referred to as the "mustard oil bomb". There are two types of myrosinases: classic and atypical. Classic myrosinases use ascorbate as a cofactor, have two amino acid catalytic residues glutamine and glutamate, and take GSLs as the only substrates. On the other hand, atypical myrosinases do not need ascorbate as a cofactor, have two glutamates as the catalytic amino acid residues, and take GSLs as well as O-glucosides as substrates (Burmeister et al., 1997; Wittstock and Burow, 2010). In Arabidopsis, β-thioglucoside glucohydrolase (TGG) 1-6 are classic myrosinases, while Penetration 2 (PEN2), PYK10, and other β-glucosidases (BGLUs) are atypical myrosinases (Chhajed et al., 2019; Bhat and Vyas, 2019; Sugiyama and Hirai, 2019). In Arabidopsis, *TGG1 and TGG2* are expressed in shoots (Barth and Jander, 2006), *TGG4* and *TGG5* are expressed in roots (Toufighi et la., 2005). On the other hand, *TGG3* and *TGG6* were found to be expressed in specific flower tissues in Arabidopsis (Zhang et al., 2002). PEN2 and PYK10 were found to catalyze the hydrolysis of indole GSL, while another two atypical myrosinases, BGLU28 and BGLU30 also play important roles in GSL degradation under plant sulfur deficiency (Bednarek et al., 2009; Nakano et al., 2017; Zhang et al., 2020). The basic structure of all the GSLs consists of a β-D-thioglucose residue linked to a sulfonated aldoxime moiety and a side chain (R group) derived from an amino acid (either methionine, phenylalanine or tryptophan; Figure 1.6; Yan and Chan, 2007; Blažević et al. 2020). Upon contact of GSLs with myrosinases, an unstable aglycone, thiohydroximate-O-sulfate is generated, and it rapidly undergoes the elimination of the sulfate group, resulting in the formation of defensive compounds against pathogens and herbivores (Chhajed et al., 2019). Hydrolysis of GSLs would typically result in the formation of isothiocyanates, which are potent toxins against many plant pests including bacteria, nematodes, and insects (Fahey et al., 2001; Halkier and Gershenzon,

2006; Rask et al., 2000). Interestingly, if a hydroxyl group is present at C-2 of the GSLs side chain, the isothiocyanate formation would be unstable and would rapidly catalyze to oxazolidine-2-thiones (Radojčić Redovniković et al., 2008). It was found that epithiospecifiers (ESPs) and epithiospecifier modifier (ESM) enzymes can control the production of nitriles from multiple indole GSLs (Burow et al., 2008). Nitrile-specifier protein (NSPs) enzymes, on the other hand, can also promote the formation of simple nitriles at physiological pH values (7.35-7.45), but do not catalyze epithionitrile or thiocyanate formation (Burow et al., 2009; Kissen and Bones, 2009). Interestingly, this simple nitrile formation by NSPs is increased by $Fe2^{+}$ (Burow et al., 2009; Kissen and Bones, 2009). Epithionitrile formation is catalyzed by ESPs as well as the related thiocyanate-forming proteins (TFPs) (Wittstock and Burow, 2007). Thiocyanate formation, on the other hand, only happens in the presence of TFPs (Burow et al., 2007; Wittstock and Burow, 2007), and this reaction has only been reported for three GSLs, namely benzylglucosinolate, allylglucosinolate and 4-methylthiobutylglucosinolate (Wittstock and Burow, 2007).

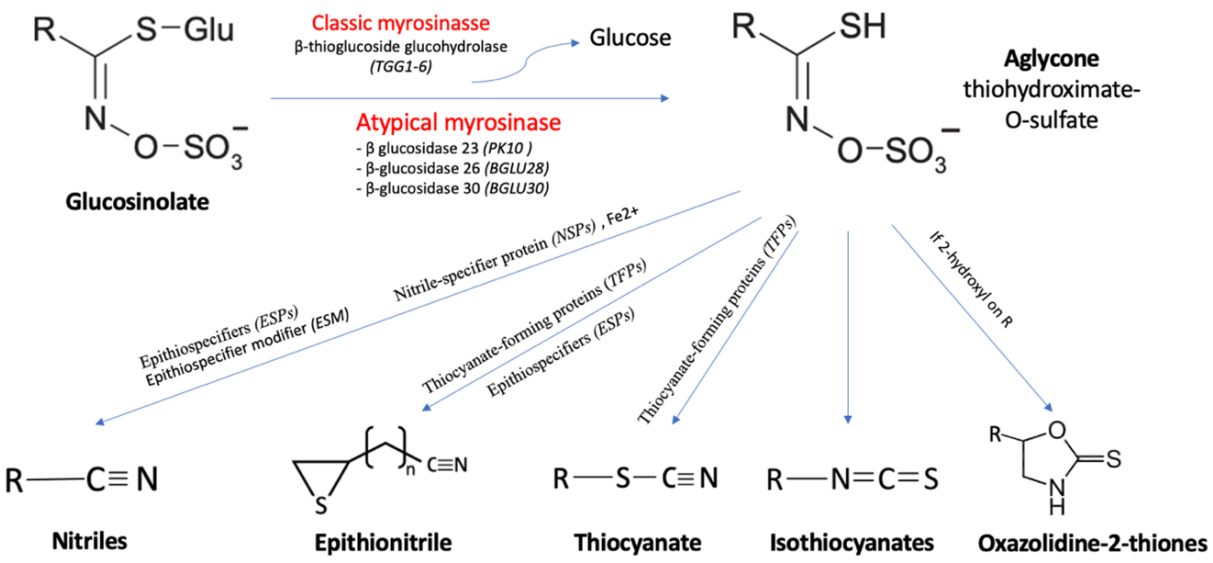


**Figure 1.6 General GSL degradation pathway.** When glucosinolates (GSLs) come into contact with myrosinases, an unstable compound called thiohydroximate-O-sulfate is produced, which quickly undergoes the elimination of the sulfate group to create compounds that help protect the plant against pathogens and herbivores. This hydrolysis process typically results in the formation of isothiocyanates, which are toxic to many plant pests including bacteria, nematodes, and insects. However, if a hydroxyl group is present at C-2 of the GSLs side chain, the isothiocyanate formation is unstable and rapidly converts to oxazolidine-2-thiones. The production of nitriles from multiple indole GSLs can be controlled by enzymes called epithiospecifiers (ESPs) and epithiospecifier modifier (ESM), while nitrile-specifier protein (NSP) enzymes can promote the formation of simple nitriles. Epithionitrile formation is catalyzed by ESPs and related thiocyanate-forming proteins (TFPs), while thiocyanate formation only occurs in the presence of TFPs. Pathway intermediates are bolded, and the enzyme names and the genes that encode these enzymes are in smaller font. The side chain R represents indolic, aromatic, or aliphatic structures. The figure was developed based on Harun et al., (2020) and Radojčić Redovniković et al., (2008).

### 1.3.5 PEN2-dependent degradation of indole GSL

Penetration 2 (PEN2) is an atypical myrosinase that can catalyze the hydrolysis of indole GSLs but not aliphatic GSLs (Bednarek et al., 2009). Evidence has showed that PEN2 is involved in defense against pathogens rather than in GSL turnover (Wittstock et al., 2016). PEN2 can catalyze the breakdown of I3M and 4MOI3M (Bednarek et al., 2009). Products of PEN2-dependent 4MOI3M hydrolysis have not yet been identified; however, the products from PEN2-catalyzed I3M breakdown are repeatedly found (Wittstock et al., 2016; Czerniawski and Bednarek, 2018, Figure 1.7). The hydrolysis of I3M by PEN2 leads to the production of an unstable thiohydroximate-*O*-sulfonate intermediate that subsequently forms indol-3-ylmethyl isothiocyanate and indole-3-acetonitrile (IAN) (Bednarek et al., 2009; Radojčić Redovniković et al., 2008). In the next step, indol-3-ylmethyl isothiocyanate can rapidly degrade to indole-3-carbinol (I3C) (Kim et al., 2008), which can form ascorbigen in the presence of free ascorbate (Agerbirk et al., 1998; Chevolleau et al., 1997). In addition, indol-3-ylmethyl isothiocyanate can be conjugated to GHS by the glutathione-S-transferase GSTU13 (Piślewska-Bednarek et al., 2018). On the other hand, the NITs could convert IAN to IAA (Wittstock et al., 2016). It was revealed that phytochelatin synthase (PCS1) can catalyze the conversion of the GSH-conjugate (indol-3-ylmethyl isothiocyanate-GSH) to indol-3-ylmethyl isothiocyanate- [$\gamma$-glu-cys] (Clemens, 2006). Further reactions downstream of this pathway can lead to the accumulation of indol-3-ylmethylamine (I3A) and raphanusamic acid (RA) (Bednarek et al., 2009). Penetration 3 (PEN3), on the other hand, is a membrane bound ATP-binding cassette (ABC) transporter that is believed to translocate the toxic PEN2 hydrolysis products into the apoplast, poisoning the fungal penetration peg as it attempts to cross the cell wall (Stein et al., 2006; Kobae et al., 2006). Removal of either PEN2 or PEN3 results in loss of penetration resistance in Arabidopsis towards non-adapted pathogens (Johansson et al., 2014; Lipka et al., 2010).

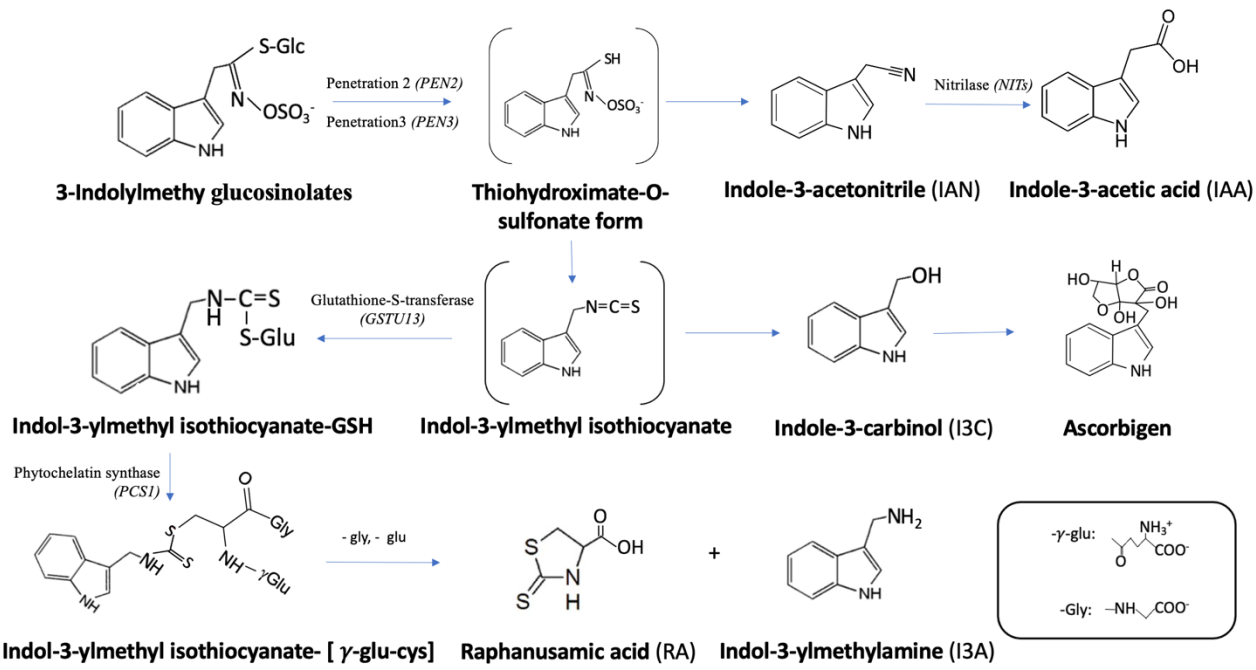


**Figure 1.7 PEN-catalyzed 3-indolylmethy GSL breakdown**. The breakdown of I3M by PEN2 generates an unstable thiohydroximate-O-sulfonate intermediate, which subsequently forms indol-3-ylmethyl isothiocyanate and IAN. Nitralises can also convert IAN to IAA. Indol-3-ylmethyl isothiocyanate can rapidly degrade to indole-3-carbinol (I3C), which can form ascorbigen in the presence of free ascorbate. Moreover, indol-3-ylmethyl isothiocyanate can be conjugated to GHS by GSTU13. PCS1 can catalyze the conversion of the GSH-conjugate (indol-3-ylmethyl isothiocyanate-GSH) to indol-3-ylmethyl isothiocyanate-[γ-glu-cys], which can lead to the accumulation of indol-3-ylmethylamine (I3A) and raphanusamic acid (RA) through downstream reactions. The related compounds are bolded, and the enzyme names and the genes that encode these enzymes are in smaller font. The bracket indicates unstable intermediates and enzymes that are not characterised are not listed in the figure. Structures of γ-glutamyl group (-γ-glu) and -glycine (-Gly) are shown as insert. The figure was developed based on Harun et al., (2020) and Radojčić Redovniković et al., (2008).

### 1.3.6 The role of Nitriles in plant-pathogen interaction

Nitriles (organic cyanides) are one of the products generated through the hydrolysis of GSLs by myrosinases upon pathogen attack or mechanical damage that causes disruption of plant tissues. In plants, it has been known that nitriles are synthesized from GSLs by NSPs and ESPs as mentioned above (Burow et al., 2008; Kissen and Bones, 2009), and they are found to be less toxic compared to their corresponding isothiocyanates (Wittstock et al., 2003). Miao and Zentgraf (2007) revealed that an *ESP* overexpressing transgenic Arabidopsis showed increased level of nitriles and enhanced resistance against the bacterial pathogen *Pseudomonas syringae pv. tomato* DC3000 and the fungal pathogen *Alternaria brassicicola*, suggesting that the GSL-derived nitriles may be involved in disease resistance. Recent studies suggested that nitriles may trigger signaling pathways that are involved in innate immune responses in Arabidopsis. Hossain et al. (2013) found that 3-butenenitrile, one of the GSL-derived nitriles, can induce reactive oxygen species (ROS) accumulation, nitric oxide (NO) production, and stomatal closure in guard cells of Arabidopsis, which are characterized as damage-associated molecular patterns (DAMPs)-triggered by immune response during pathogen attack. More recently, it was demonstrated that exogenous application of 3-butenenitrile (nitrile-counterpart of GSL sinigrin-derived allyl-isothiocyanate) triggered lesion formation resulting from the accumulation of NO, which is known as an important signal molecule in plant defense against pathogens (Ting et al., 2020). Interestingly, when the nitrile concentration was low, an enhanced disease tolerance against necrotrophic pathogens such as *Pectobacterium carotovorum ssp*. *Carotovorum* and *Botrytis cinerea* were observed with no lesions formed. Additionally, 3-butenenitrile treatment also triggered an elevated synthesis of SA and JA, which is well known in triggering defense responses against necrotrophic pathogens and biotrophs/hemi-biotrophs, respectively (Mei et al., 2006; Sticher et al., 1997). Therefore, it was concluded by Ting et al. (2020) that 3-butenenitrile may function as a DAMP in Brassicaceae. The toxicity of most nitriles was found to originate from the cyanide released during degradation by cytochrome P450 instead of the nitriles themselves (Grogan et al., 1992).

### 1.3.7 Major GSLs detected in rutabagas and potential degradation products

The major GSL classes detected in mature rutabaga roots (outer epidermis and adjacent tissue removed) of 13 cultivars were 2-hydroxy-3-butenyl-GSL, 4-(methylthio) butyl-GSL, 2-

phenylethyl-GSL, and 3-indolylmethyl-GSL (Carlson et al., 1981). Depending on several factors such as GSL structure, pH, and protein, the degradation of these GSLs by myrosinase can lead to a variety of products (Kissen and Bones, 2009). As their formation only requires myrosinase activity, the most common products of enzymic degradation of GSLs are isothiocyanates (ITCs; Kissen and Bones, 2009). The production of epithionitriles from alkenyl-GSLs requires cooperative action of myrosinase and ESP (Tookey, 1973). NSPs are able to redirect the hydrolysis of GSLs towards nitriles (Kissen and Bones, 2009). Acidic conditions generally favour nitrile formation while higher pH favors ITC formation (Vaughn & Berhow, 2005). The corresponding isothiocyanate, nitrile and epithionitrile degradation products for the GSL classes present in rutabaga roots as identified by Carlson et al. (1981) are given in Table 1.1.

GSLs extracted from rutabaga roots were hydrolyzed using myrosinase, and the volatile GSL products identified included four ITCs (3-butenyl-, 4-pentenyl-, 4-methylthiobutyl-, and 2-phenylethyl-ITCs), and benzene propanenitrile (cv. Laurentian; Ju et al., 1982). These are derived from 3-butenyl-, 4-pentenyl-, 4-(methylthio) butyl-, and 2-phenylethyl-GSL. It is also possible to have degradation products from progoitrin (2-hydroxy-3-butenyl-GSL) and 3-indolylmethyl-GSLs. In the analysis of GSLs breakdown products in seeds of broccoli varieties, it was found that in addition to ITCs, 2-hydroxy-3-butenyl-GSL (progoitrin) and 4-(methylthio) butyl-GSL (glucoerucin) were converted to their corresponding nitriles (3-hydroxy-4-pentenylnitrile and 5-(methylthio) pentylnitrile) upon myrosinase-catalysed hydrolysis (Wang et al., 2019). Moreover, progoitrin could also be degraded by myrosinases to 3-hydroxy-4-pentenylnitrile at acidic pH in the presence of iron but in the absence of ESP (Frandsen et al., 2019; Macleod and Rossiter, 1987). The presence of both iron and ESP on the other hand could direct progoitrin hydrolysis into the production of both 3-hydroxy-4-pentenylnitrile and epithonitriles at acidic conditions (Galletti et al., 2001; Matusheski et al., 2006). Degradation of 3-indolylmethyl-GSL (glucobrassicin) and its corresponding modified indole GSLs in the presence of NSP or ESP yield IAN which can be converted to auxin IAA (discussed above).

**Table 1.1 GSL classes present in rutabaga roots their derived hydrolysis products: isothiocyanates (ITC) and derivates, nitriles, and epithionitriles**. Information derived from Kissen and Bones, 2009 and Chroston et al. (2022).

| Glucosinolate class | Name of glucosinolate | R group | Name of isothiocyanate | Name of nitrile | Name of epithionitrile |
|---|---|---|---|---|---|
| aliphatic glucosinolate | 2-hydroxy-3-butenyl-GSL | | 5-vinyl-2-oxazolidine thione | 3-hydroxy-4-pentenylnitrile | 1-cyano-2-hydroxy-3,4-epithiobutane |
| methylthioalkyl glucosinolate | 4-(methylthio)-butyl-GSL | 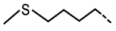 | 4-(methylthio)-butyl-ITC | 5-(methylthio)-pentylnitrile | n.a |
| aromatic glucosinolate | 2-phenylethyl-GSL | | 2-phenylethyl-ITC | benzene propanenitrile | n.a |
| indolic glucosinolate | 3-indolylmethyl-GSL | | 3-indolylmethyl-ITC | indole-3-acetonitrile | n.a |
| | 4-methoxy-3-indolylmethyl-GSL | | 4-methoxy-indole-3-carbinol | 4-methoxy-indole-3-acetonitrile | n.a |
| | 1-methoxy-3-indolylmethyl-GSL | | 1-methoxy-indole-3-carbinol | 1-methoxy-indole-3-acetonitrile | n.a |
| alkenyl glucosinolate | 3-butenyl-GSL | | 3-butenyl-ITC | 4-pentenylnitrile | 4,5-epithiopentylnitrile |
| | 4-pentenyl-GSL | | 4-pentenyl-ITC | 5-hexenylnitrile | 5,6-epithiohexylnitrile |

## 1.4 HYPOTHESIS AND OBJECTIVES

I will test the hypothesis that the plant hormone auxin and the indole GSL pathway (which can synthesize IAA as well as defense-related secondary metabolites) are linked in the plant-pathogen interaction between *Brassica napus* and *P. brassicae*.

There are two main objectives that my research will address to test this hypothesis. The first objective will focus on determining if the indole GSL pathway plays a role in inducing enhanced plant defense against the clubroot pathogen in *Brassica napus.* The second objective will focus on determining if reduced production of or response to the auxin IAA is a strategy to aid the plant host defense response to the clubroot pathogen.

*Specific Objectives:*

*Objective 1: Determining if the indole GSL pathway plays a role in inducing enhanced plant defense against the clubroot pathogen in Brassica napus*

For this objective, rutabaga (*Brassica napus* subsp*. rapifera*) will be used as the experimental model species. In a recently published study (Zhou et al., 2020), the authors compared transcriptomic profiles of two rutabaga (*Brassica napus* subsp*. rapifera*) cultivars which showed resistant ('Wilhelmsburger') and susceptible ('Laurentian') responses to *P. brassicae* inoculation. I will determine if gene expression patterns in the indole GSL pathway differ in the resistant compared to the susceptible cultivar that could potentially lead to an increase in the production in GSL-related defense compounds. If the transcriptomic database search reveals that gene expression changes in the GSL pathway are specific to the resistant cultivar and they indicate that modification of the GSL-related defense compounds likely occurs, qPCR will be performed on selected gene targets to confirm transcript abundance differences. I will also determine if expression changes occur in genes involved in the production of IAA via the GSL pathway in the resistant rutabaga cultivar compared to the susceptible cultivar that could indicate a potential for modification in auxin production.

*Objective 2: Determining if reduced response to the auxin IAA is a potential strategy to facilitate the plants' defense response to the clubroot pathogen in Canola.*

Phenotypically characterize canola plants that express the auxin receptor *PsAFB6* from pea to confirm previous results that expression of this receptor (that does not occur in

Brassicaceae) reduces clubroot symptoms, potentially by reducing auxin response by native receptors.

# Chapter 2: Gene expression changes in the indole GSL pathway associated with clubroot pathogen infection in rutabaga (*Brassica napus*)

## 2.1 INTRODUCTION

The clubroot pathogen upon infection influences the plant host's physiology, and primary and secondary metabolic and regulatory networks (including plant hormone homeostasis) (Malinowski et la., 2019; Ludwig-Müller and Schuller, 2007). These changes in the plant host are directly connected to the life cycle of the protist. The life cycle of *P. brassicae* can be divided into two main phases. The primary phase is characterized by the infection of root hair by motile zoospores released from the resting spores. Once in the root hair, the pathogen produces primary plasmodia, which upon maturity, form and release secondary zoospores. The second phase is characterized by the infection of the root cortex by secondary zoospores, which leads to the production of secondary plasmodia and subsequent formation of the characteristic clubbing roots (Ingram and Tommerup, 1972).

Collective evidence has shown that clubroot disease correlates with the presence indole GSL (Butcher et al., 1974; Ockendon and Buczacki, 1979; Chong et al., 1981), which also can be a precursor for auxin biosynthesis. Specifically, indole GSL contributes to auxin biosynthesis via two metabolic intermediates IAOx and IAN. IAOx is proposed as a metabolic branch point for the biosynthesis of IAA, camalexin, and indole GSL while IAN is one of the hydrolysis products of indole GSL that could be metabolized to IAA by nitrilases.

In the past decades, an increasing research effort has focused on understanding indole GSL metabolism (Figure 2.1). The biosynthesis of indole GSL results in the formation of glucobrassicin (I3M). Subsequently, I3M can be modified at position 1 or 4 of the indole ring. During the modification, the cytochrome P450 monooxygenases of the CYP81F subfamily (CYP81Fs) introduce hydroxy groups at specific positions of the indole ring of I3M, leading to the formation of 4-hydroxyindol-3-ylmethyl (4OHI3M) and 1-hydroxyindol-3-ylmethyl (1OHI3M) while the indole glucosinolate O-methyltransferases (IGMTs) convert hydroxyl to methoxy groups, further modifying 4OHI3M and 1OHI3M to 4MOI3M and 1MOI3M respectively (Pfalz et al., 2011). The first necessary enzyme for the formation of IAN through hydrolysis of indole GSLs is myrosinase. There are two types of myrosinases: classic and atypical. In Arabidopsis, β-thioglucoside glucohydrolase (TGG) 1-6 are classic myrosinases,

while Penetration 2 (PEN2), PYK10, and other β-glucosidases (BGLUs) are atypical myrosinases (Chhajed et al., 2019; Bhat and Vyas, 2019; Sugiyama and Hirai, 2019). Generally, upon the contact of GSLs with myrosinases, an unstable aglycone, thiohydroximate-O-sulfate is generated, and it rapidly undergoes the elimination of the sulfate group, resulting in the formation of various defensive compounds against pathogens and herbivores (Chhajed et al., 2019). Nitrile-specifier protein (NSPs) enzymes were found to be able to redirect the hydrolysis of GSLs toward nitriles (Kissen and Bones, 2009), therefore promoting the formation of IAN and subsequent IAA during indole GSL hydrolysis. PEN2 shows clear myrosinase activity against I3M and its 4-methoxy analog (Bednarek et al., 2009). The hydrolysis of I3M by PEN2 leads to the production of the unstable thiohydroximate-O-sulfonate intermediate and the subsequent formation of indol-3-ylmethyl isothiocyanate and IAN (Bednarek et al., 2009; Radojčić Redovniković et al., 2008). In the next step, indol-3-ylmethyl isothiocyanate could rapidly degrade to I3C (Kim et al., 2008), and IAN could be converted to IAA by the NITs (Wittstock et al., 2016). Additionally, indol-3-ylmethyl isothiocyanate could be conjugated to GHS by Glutathione-S-Transferase class-tau member 13 (GSTU13) (Piślewska-Bednarek et al., 2018), and subsequently to indol-3-ylmethyl isothiocyanate- [ $\gamma$-glu-cys] by phytochelatin synthase (PCS1) (Clemens, 2006). Interestingly, GSTU13 has been discussed as an indispensable component of the PEN2-dependent pathway for indole GSL metabolism (Piślewska-Bednarek et al., 2018).

In addition to indole GSLs, three others major GSL classes were detected in mature rutabaga roots, 2-hydroxy-3-butenyl-GSL, 4-(methylthio) butyl-GSL, and 2-phenylethyl-GSL, (Carlson et al., 1981). During myrosinase-catalyzed hydrolysis, 2-hydroxy-3-butenyl-GSL and 4-(methylthio) butyl-GSL, known as progoitrin and glucoerucin respectively, were mainly converted to their corresponding isothiocyanates (ITCs) (5-vinyl-2-oxazolidine thione and 4-(methylthio)-butyl-ITC). Additionally, progoitrin- and glucoerucin-derived nitriles (3-hydroxy-4-pentenylnitrile and 5-(methylthio)- pentylnitrile) were also detected in several studies of GSL hydrolysis (Hanschen and Schreiner, 2017; Wang et al., 2019; Klopsch et al., 2017). On hydrolysis of progoitrin in the presence of Fe2+/ESP, the corresponding nitrile (3-hydroxy-4-pentenylnitrile) and epithionitrile (1-cyano-2-hydroxy-3,4-epithiobutane) were formed while in the absence of Fe2+/ESP, the corresponding 5-vinyl-2-oxazolidine thione was mainly formed (Foo et al., 2000). 2-phenylethyl-ITC and benzene propanenitrile on the other hand are the

corresponding ITC and nitrile of 2-phenylethyl-GSL (gluconasturtiin) upon the myrosinase-catalyzed degradation. They were all detected as the GSL hydrolysis product in root of rutabaga (Laurentian cv.; Ju et al., 1982).

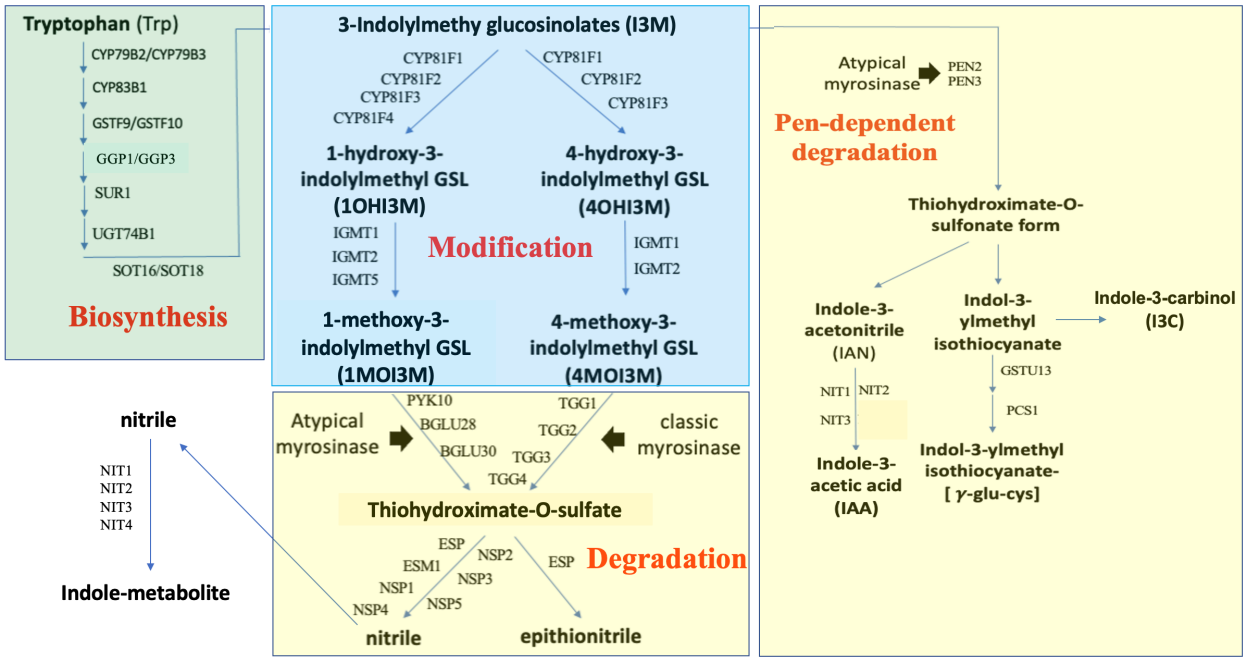


**Figure 2.1 Indole GSL biosynthesis and metabolism pathways**. modified from Harun et al., 2020. Abbreviations:

**Biosynthesis:** CYP79B2, cytochrome P450 monooxygenase family 79 subfamily B polypeptide 2; CYP79B3, CYP family 79 subfamily B polypeptide 3; CYP83B1, CYP family 83 subfamily B polypeptide 1; GSTF9, glutathione S-transferase F9; GSTF10, glutathione S-transferase F10; GGP1, gamma-glutamyl peptidase 1; GGP3, gamma-glutamyl peptidase 3; SUR1, super root 1; UGT74B1, UDP-glucosyl transferase 74B1; SOT16, sulfotransferase 5a; SOT18, sulfotransferase 5b.

**Modification:**
CYP81F1, CYP family 81 subfamily F polypeptide 1; CYP81F2, CYP81 subfamily F polypeptide 2; CYP81F3, CYP81 subfamily F polypeptide 3; CYP81F4, CYP81 subfamily F polypeptide 4; IGMT1, indole glucosinolate *O*-methyltransferase 1; IGMT2, indole glucosinolate *O*-methyltransferase 2; IGMT5, indole glucosinolate *O*-methyltransferase 5.

**Degradation:**
PYK10, *β*-glucosidase 23; BGLU28, *β*-glucosidase 28; BGLU30, *β*-glucosidase 30; TGG1, Thioglucoside glucohydrolase 1; TGG2, Thioglucoside glucohydrolase 2; TGG3, Thioglucoside glucohydrolase 3; TGG4, Thioglucoside glucohydrolase 4; ESP, Epithiospecifier protein; ESM1, Epithiospecifier modifier 1; NSP1, Nitrile specifier protein 1; NSP2, Nitrile specifier protein 2; NSP3, Nitrile specifier protein 3; NSP4, Nitrile specifier protein 4; NSP5, Nitrile specifier protein 5; PEN2, Penetration 2; PEN3, Penetration 3; NIT1, Nitrilase 1; NIT2, Nitrilase 2; NIT3, Nitrilase 3; NIT4, Nitrilase 4; GSTU13, Glutathione S-transferase TAU type 13; PCS1, Phytochelatin synthase 1.

Despite a large amount of published research on the GSL-clubroot linkage, little information is available on the regulation of GSL metabolism during early clubroot infection. In a recently published study by Zhou et al. (2020), the authors compared transcriptomic profiles of two rutabaga (*Brassicae napus* subsp. *rapifera*) cultivars, which showed resistant ('Wilhelmsburger') and susceptible ('Laurentian') responses to *P. brassicae* inoculation. Numerous transcripts with significant changes ($p \leq 0.05$; $\log_2$ fold change $\geq 1$ or $\leq -1$) in expression were identified in each host at 7, 14, and 21 dai in inoculated vs. non-inoculated plants, and it was highlighted that the activation of genes associated with SA- and ET-mediated responses might be associated with the resistance observed in the 'Wilhelmsburger' cultivar. However, the expression differences in the indole GSL and general GSL degradation pathways were not investigated. In the current study, we analysed the transcriptomic data from Zhou et al. (2020) and determined if gene expression patterns in the GSL pathways differ in the resistance compared to the susceptible cultivar that could potentially lead to an increase in the production in GSL-related defense compounds. Following analysis of this transcriptomic data, further studies were performed focusing on the early stage of pathogen infection (7 dai) to confirm if gene expression changes in the indole GSL and general GSL degradation pathway are associated with the resistance observed in the 'Wilhelmsburger' cultivar by qRT-PCR for validating gene expression profile changes.

## 2.2 MATERIALS AND METHODS

### 2.2.1 Pathogen material

*P. brassicae* field spore isolate F3-14 was used as the inoculum for the current study. This isolate was originally collected from the (clubroot resistant) CR canola 'L135C' and classified as pathotype 3A on the Canadian Clubroot Differential set (Strelkov et al., 2018). The resting spores inoculum suspension was prepared from frozen (-20 °C) root galls as adapted from Strelkov et al. (2006). In short, 2.5 g galls per 100 mL distilled water were weighed and homogenized in a blender for 2 min. The resulting homogenate was then filtered through eight layers of cheesecloth to remove the debris. The estimation of the clubroot resting spore concentration was done using an improved Neubauer counting chamber of the hemocytometer (for detailed description see Appendix Figure A1). Distilled water was added to adjust the

clubroot spore concentration to 1 x $10^{7,}$ spores/mL. The prepared inoculum suspension was stored at 4 °C and was used within 24 hours of its preparation.

### 2.2.2 Plant material and inoculation

The experiments were conducted with two rutabaga (*Brassicae napus* subsp. *rapifera*) cultivars that showed resistance ('Wilhelmsburger') and susceptible ('Laurentian') responses to 3A pathotype of *P. brassicae* (Strelkov et al., 2018; Zhou et al., 2020). The plant seedlings were germinated in Petri dishes (TC Dish 100, Sarstedt, Nümbrecht, Germany) on moistened Whatman filter paper #1 (Whatman International Ltd., Maidstone, UK) for eight days and then inoculated by the root dip method following Strelkov et al. 2006 (Appendix Figure A2). Briefly, the seedlings were first dipped in the resting spore suspension for 10 sec and then transferred to 72 cell insert-trays (insert size is 3.8 x 3.8 x 5.7 cm) filled with water-saturated peat-based medium (Sunshine #4 mix; SunGro Horticulture, Vancouver, BC, Canada). An additional 1 mL spore suspension was then added to each seedling with a micropipette to ensure enough disease pressure. The non-inoculated seedlings were directly transferred from Petri plates to water-saturated peat-based medium, keeping them separate from the inoculated plants. Later, water was added into the insert-trays if needed to ensure enough moisture in the planting medium. The roots of the plants were harvested after 7 days of growth under long day conditions (16 h light) at an average daily temperature of 25°C in the greenhouse. Seedlings were washed and cleaned with a fine-tipped painting brush three times in tap water followed by three washes in Petri dishes containing Milli-Q water, seedlings were pat dried using paper towels, roots were dissected from the seedling using a scalpel and collected into 20 mL plastic scintillation vials and placed onto dry ice. The details on the harvesting of the root samples of the non-inoculated control and 7-d clubroot-inoculated seedlings of each cultivar are described Appendix Figure A2.

For clubroot disease severity scoring, the experiment was planted on two consecutive days and consisted of a total of 5 trays, a tray of non-inoculated controls of resistant and susceptible cultivars and 2 trays of clubroot-inoculated plants for each cultivar. Four independent biological replicates, with 36 plants per replicate, were used for assessing clubroot symptom severity as described by Zhang et al. (2015) at 45 days after inoculation (dai) on a 0–9 scale, where 0 = no visible galls (no infection or symptoms), 1-3= a few small galls, 4-6 = moderate galling, and 7-9 = severe galling (heavily infected). The resulting severity scores was then used

to calculated disease index (DI) following the formula developed by Horiuchi & Hori (1980) and modified by Strelkov et al. (2006): DI (%) = [(n 1× 1 + n 2× 2 + n 3× 3 + n 4× 4 + n 5× 5 + n 6× 6 + n 7× 7 + n 8× 8 + n 9× 9)/(N × 9)] × 100, where n 1, to n 9 refer to the number of plants in each symptom severity class and N refers to the total number of plants tested. Independent Student's t-test (two-tailed) was used to compare differences between means of the clubroot-inoculated clubroot-resistant Wilhelmsburger cv. and clubroot-susceptible Laurentian cv. for clubroot disease index.

### 2.2.3 Gene expression analysis

#### 2.2.3.1 *Total RNA isolation*

Total RNA was extracted from frozen rutabaga root tissue using a modified Trizol-based method as described in Ozga et al. (2003). The frozen root tissues were ground to a fine powder with a combination of manual grinding with a pre-cooled mortar and pestle in liquid $N_2$ and bead-beating using a Mini-BeadBeater (Biospec Products). Approximately 200 mg of ground-frozen root tissue was transferred to a pre-cooled 2 mL microcentrifuge tube with 5 3-mm glass beads and further homogenized using a Mini-BeadBeater for 30 sec. One mL of Trizol reagent (Ambion, USA) was then added to the ground tissue samples followed by thorough vortexing. The samples were incubated at room temperature for 30 min and then centrifuged at 4 °C for 15 min at 14,800 rpm to remove cellular debris. The aqueous phase was transferred to a new 2 mL microfuge tube, followed by phase separation with chloroform to separate RNA from protein and DNA. After adding 200 µL chloroform, tubes were shaken vigorously and incubated at room temperature for 5 min followed by centrifugation at 4 °C for 15 min at 14,800 rpm. The supernatant containing total RNA was transferred to a 1.5 mL microfuge tube. Total RNA was then precipitated with 400 µL isopropanol and high salt solutions of 250 µL 0.8 M sodium citrate (EMD Millipore, USA) and 250 µL 1 M sodium chloride (Promega, USA) to remove polysaccharides and proteoglycans. Samples were then mixed thoroughly, incubated at room temperature for 15 min, and centrifuged at 4 °C for 15 min at 14,800 rpm. After removal of the supernatant, the RNA pellet was washed with 200 µL 75% ethanol to dissolve organic impurities, centrifuged at 4 °C for 5 min at 14,800 rpm, and the supernatant was discarded. The RNA pellet was then resuspended in 600 µL of nuclease-free water (Invitrogen, USA). To purify and selectively precipitate RNA, total RNA was further precipitated with 200 µL 8 M lithium

chloride (LiCl) and incubated overnight at 4 °C. Subsequently, the solution was centrifuged at 4 °C for 30 min at 14,800 rpm, and the supernatant was discarded. The RNA pellet was resuspended with 400 µL nuclease-free water and reprecipitated with 40 µL 3 M sodium acetate (Sigma Aldrich) and 800 µL 100% ethanol. After overnight incubation at -20 °C, the solution was centrifuged at 4 °C for 10 min at 14,800 rpm, and the supernatant was discarded. Pelleted RNA was washed with 200 µL 75 % aqueous ethanol, centrifuged at 4 °C for 5 min at 14,800 rpm and then the supernatant was removed. The resulting RNA pellet was air-dried at room temperature for 10 min to remove remaining ethanol and dissolved in 20 µL of nuclease-free water. The concentration of total RNA was quantified with a NanoDrop (ND-1000 spectrophotometer, Thermo Fisher Scientific) and purity was assessed using absorbance ratios at 260/280 nm and 260/230 nm for each sample. A ratio of approximately 2.0 or greater for both metrics was obtained for all samples, indicating highly pure RNA. The total RNA samples were stored at -80 °C until DNase treatment was performed.

The high-quality total RNA samples were treated with DNase (DNA-free kit, Ambion, USA) following the manufacturer's instructions to remove any residual DNA contamination. An aliquot of 25 µg of total RNA was diluted with nuclease-free water to make an 88 µL sample in a new 1.5 mL microfuge tube and treated with 10 µL of 10x DNase reaction buffer and 2 µL of DNase I. The sample was vortexed, centrifuged briefly, and incubated at 37 °C for 30 min. After DNase digestion, 10 µL DNase inactivating reagent was added to effectively remove all traces of DNase and divalent cations from the reaction mixture and vortexed continuously for 5 min at room temperature followed by a quick centrifugation at 4 °C for 5 min at 14,800 rpm. The supernatant containing DNase-treated total RNA (85 µL) was carefully transferred to a new 1.5 mL microfuge tube and re-extracted with 85 µL mixture of phenol:choroform:isoaml alcohol (Sigma Aldrich) [25:24:1 pH 8]. The sample was then vortexed and centrifuged at 4 °C at 14,800 rpm for 10 min. A 60 µL aliquot of the upper phase was reprecipitated with 10 µL 3M sodium acetate [pH 5.2] and 300 µL 100% ethanol, vortexed, and then incubated overnight at -20 °C. After incubation, the sample was centrifuged at 4 °C for 30 min at 14,800 rpm and the supernatant was discarded. The DNA-free total RNA pellet was then washed with 200 µL 75% aqueous ethanol by rolling the tubes and centrifuged at 4 °C for 10 min at 14,800 rpm. Following the removal of the supernatant, the RNA pellet was air-dried before being resuspended in nuclease-free water. The total RNA concentration and purity was determined using a Nanodrop

spectrophotometer as described above. DNase-treated total RNA samples were stored at -80 ºC until the gene expression analyses were performed.

2.2.3.2 *cDNA Synthesis and PCR Verification*

Aliquots of 1 µg DNase-treated total RNA of root tissues from non-inoculated and 7d-*P. brassicae*-inoculated resistant 'Wilhelmsburger' cultivar served as the template for cDNA using the iScript Select cDNA Synthesis Kit (Biorad, USA), following the manufacturer's instructions. The cDNA synthesis was carried out in a 20 µL reaction volume in a 200 µL PCR tube (Thermo Fisher) consisting of 1 µg of total RNA in 15 µL of nuclease-free water, 4 µL of 5x iScript buffer, and 1 µL of iScript reverse transcriptase. The tubes were vortexed, spun down, and incubated at 46 ºC for 90 min for first-strand synthesis in a GeneAmp PCR system 9700 thermocycler (Applied Biosystems, USA) followed by heat-inactivation of the reverse transcriptase at 95 ºC for 5 min and cDNA samples were stored at -80 ºC until amplified using PCR.

Gene-specific PCR primers were designed using the PrimerQuest tool from Integrated DNA Technologies (see Appendix Table A1). For specific highly homologous genes within a gene family, a common set of PCR primers was designed using the conserved regions. A total 25 µL volume of PCR reaction was used and consisted of 13 µL nuclease-free water, 2.5 µL of 10x PCR buffer ($Mg^{2+}$ plus), 1.5 µL each of 5 µM forward and reverse primers (Appendix Table A1), 1 µL of dNTP mix (2.5 mM each), 0.5 µL of Taq polymerase (2.5 U per reaction: Taq Master Mix from Frogga Bio, Canada), and 5 µL of cDNA template (250 ng/µL). The PCR amplification was performed with initial denaturation at 94 ºC for 5 min followed by 35 cycles of denaturation at 94 ºC for 30 sec, annealing at 56 ºC for 30 sec, and extension at 72 ºC for 60 sec. The final extension step was carried out at 72 ºC for 7 min. Subsequently, 25 µL of PCR products and 8 µL of 6x loading buffer (Frogga Bio) were mixed, loaded into the wells of a 1.2 % (w/v) agarose gel (prepared using 1x TAE buffer pH = 8 consisted of 40 mM Trizma baseUSA; 1 mM EDTA and 20 mM glacial acetate) with 8 µL SYBR Safe DNA gel stain (Invitrogen). The gel was subjected to electrophoresis in a 1x TAE buffer at 150 V for approximately 15 min with 12 µL of 100 bp DNA ladder (Invitrogen) molecular size marker to accurately estimate the size of PCR products. Amplicon bands were visualized using a Chemidoc Imaging System (Biorad).

2.2.3.3 *Taqman qRT-PCR assay*

TaqMan One-Step RT-PCR Master Mix Reagents Kit (Applied Biosystems) was used to quantify the relative transcript abundance of candidate genes on a StepOnePlus Real-Time PCR System Instrument (Applied Biosystems) as described by Kaur et al. (2021). Gene-specific qRT-PCR primers and Taqman probes were designed with the PrimerQuest tool from IDT using double-quenched probes with an Iowa Black Fluorescent Quencher (IBFQ) at the 3′ end, and a ZEN (N, N-diethyl-4-(4-nitronaphthalen-1-ylazo)-phenylamine) quencher positioned 9 bp from the 6-FAM (6-carboxyfluorescein) fluorescent dye-containing 5′ end (see Table 2.1). DNase-treated total RNA samples were diluted with nuclease-free water to 40 ng/µL concentration and were quantified using a nanodrop spectrophotometer for performing Taqman qRT-PCR assays. Each Taqman PCR amplification reaction contained 5 µL of 40 ng/µL total RNA, 1.2 µL each of 5 µM forward and reverse primers (Table 2.1 for primer and probe sequences), 0.5 µL of 5 µM Taqman probe, 0.5 µL of 40x TaqMan arrayScript™ UP Reverse Transcriptase and RNase inhibitor, 10 µL of 2x TaqMan qRT-PCR mix (contains Ultra-Pure AmpliTaq Gold DNA Polymerase, Uracil-DNA glycosylase, dNTPs and dUTP, ROX passive reference dye, and optimized buffer components) and 1.6 µL of nuclease-free water. Relative transcript abundance for each sample was quantified in duplicate (2 technical replicates) in an Optical 96-well reaction plate (Applied Biosystems) covered with MicroAmp Optical Adhesive Film (Applied Biosystems) on a StepOnePlus Real-Time PCR System Instrument. On each plate a no-template control using nuclease-free water instead of total RNA as template and a no reverse-transcriptase control was run. The thermocycler program consisted of reverse transcription at 48 ºC for 30 min, followed by enzyme activation at 95 ºC for 10 min, 40 cycles of amplification and detection with denaturation at 95 ºC for 15 sec and annealing/extension at 60 ºC for 1 min. The cycle threshold was set to 0.05.

**Table 2.1 Taqman primers and probes used for quantification of gene expression in root tissues of non-inoculated control and 7d-*P. brassicae*-inoculated rutabaga resistant 'Wilhelmsburger' and susceptible 'Laurentian' cultivars by qRT-PCR assays and their PCR efficiencies and $r^2$ values.**

| Gene name | *Brassica napus* Gene Accession ID | qRT-PCR Primers/Probe Sequences | PCR Efficiency (%), $r^2$ |
|---|---|---|---|
| Indole glucosinolate modification genes[a] | | | |
| *BnCYP81F2* | BnaA10g11280D | F: 5'-GCTCTTATTGCCACTCGTATTG-3'<br>R: 5'-GACGATGGGAAAGGGAGTT-3'<br>P: 5'-CATCTAAGAGTTTCAATCTTCCACCAGG-3' | 100.84, 0.9969 |
| *BnCYP81F4* | BnaCnng68210D | F: 5'-AATTGATGAGAAAATCGGACAAGGC-3'<br>R: 5'-CGTTTCGGACACTACGTTTTGA-3'<br>P: 5'-AGGTAGGTTTGGTATGTCTGTTTCCTCAATC-3' | 99.44, 0.9992 |
| *BnIGMT5*[b] | ***BnIGMT5a*:** BnaC06g37610D<br>***BnIGMT5b*:** BnaA07g33060D | F: 5'-CACACAACTCTCTGGAGGAAA-3'<br>R: 5'-TGATATGCAGGGCACACAA-3'<br>P: 5'-TGGCTGCTAATTCAGGTTTTGCAAGTTGC-3' | 97.10, 0.9916 |
| Indole glucosinolate degradation genes[a] | | | |
| *BnBULU30*[b] | ***BnBULU30a:*** BnaC04g22390D<br>***BnBULU30b:*** BnaA04g01360D | F: 5'-GTATCAGTACGAAGGAGCAACA-3'<br>R: 5'-CTTCGTCCGTTCTGGGTAAG-3'<br>P: 5'-AGCTGGAGACTTGCCACCTTCATC-3' | 103.59, 0.9913 |
| *BnNSP5* | BnaA02g29990D | F: 5'-CTGGACCAAGAAGCTCACAT-3'<br>R: 5'-GAAGACGTAGAGATCGTTGTCG-3'<br>P: 5'-CACTTACCGTCGTGGGCAACAAAGTC-3' | 92.14, 0.9966 |
| *BnNIT2*[b] | ***BnNIT2a:*** BnaC03g13560D<br>***BnNIT2b:*** BnaA03g10890D | F: 5'-GACGGATCAACCATCCCTGTTTAC-3'<br>R: 5'-CGTACAGGGCAGTTCTGTAGAGG-3'<br>P: 5'-CACCCATTGGCAAACTCGGTGCTGC-3' | 92.33, 0.9954 |
| *BnNIT4*[b] | ***BnNIT4a:*** BnaA02g05560D | F: 5'-CAGGCATGCACCATCTTCTAC-3' | 90.42, 0.9967 |

| | | | |
|---|---|---|---|
| | ***BnNIT4b:*** BnaC02g09450D | R: 5'-ACGAGCTGTGACCCGTTAT-3'<br>P: 5'-ACAAGGCTGAGAGGTTACTTGCCG-3' | |
| *BnGSTU13* | BnaA07g09120D | F: 5'-CAGGTCAAAGAGTGAACTCCTTC-3'<br>R: 5'-TGTACTGAACAATGTTGAGTGACTCAC-3'<br>P: 5'-CATCTTCAAGAAAGTCCCAGTTCTCATCCATGGT-3' | 89.84, 0.9953 |
| Auxin conjugation gene[a] | | | |
| *BnIAGLU* | BnaA03g41970D | F: 5'-GCTCGTGGAGATACCAGAAAG-3'<br>R: 5'-GAACTCTCAAACAGACCGAAGA-3'<br>P: 5'-ACGCAGCGTCTTGGATTAGTGATCC-3' | 110.16, 0.9991 |
| Loading control[a] | | | |
| *BnTubulin* | BnaC09g37930D | F: 5'-GTTGATCTGGAGCCTACTGTTATC-3'<br>R: 5'-TGTTAGCAGCGTCCTCTTTC-3'<br>P: 5'-AAAGCTGACGGTACGTTCCGGTAC-3' | 90.00, 0.9976 |

[a] 5' end fluorescent reporter dye, FAM, 6-carboxyfluorescein; middle quencher, ZEN, N,N-diethyl-4-(4-nitronaphthalen-1-ylazo)-phenylamine; and 3' end quencher, IBFQ, Iowa Black Fluorescent Quencher from Integrated DNA technologies)

[b] Due to very high homology at the nucleotide sequence level, primers and probes were designed to homologous sequences within the gene class to produce a common amplicon across the genes.

F: Forward primer, R: Reverse primer, and P: Probe

2.2.3.4 *Preparation of RNA standard curve*

The qRT-PCR efficiency for each gene was calculated using a standard curve of a 10-fold serially diluted series consisting of four or five concentrations (1165.9-0.1166 ng/µL) of a pooled total RNA sample obtained from root tissues of non-inoculated and 7d-*P. brassicae*-inoculated rutabaga resistant 'Wilhelmsburger' and susceptible 'Laurentian' cultivars. Linear regression curves and the correlation coefficient ($r^2$) were obtained by plotting the Ct values against the log transformed RNA concentrations for each gene. The qRT-PCR efficiencies were calculated for genes with $r^2 > 0.9910$ using the slope of the linear regression line with equation 1. Relative transcript abundance for each sample was calculated using a modified ΔCt method (Livak and Schmittgen, 2001; Nadeau et al., 2011; Jayasinghege et al., 2017) with equation 2, where X is an arbitrary value equal to or greater than the highest assayed Ct value. The arbitrary Ct value was set at 33 for all target genes.

**Equation 1:** qRT-PCR Efficiency

$$Efficiency = \left(10^{\left[-\frac{1}{slope}\right]} - 1\right) \times 100$$

**Equation 2:** Relative Transcript Abundance

$$Transcript\ abundance = (1 + Efficiency)^{X - AVE\ Ct}$$

The tubulin (*BnTubulin*) gene from *Brassica napus* was used as a loading control for each sample when performing Taqman qPCR assays. For *BnTubulin* transcript quantitation, 5 µL of 40 ng/µL total RNA was used for each sample reaction and assays were performed as for the target genes of interest. The coefficient of variation of the Ct value of all the samples for the *BnTubulin* gene was less than 0.5 %; therefore, normalizing the target amplicon mRNA values to the reference tubulin signal was not performed (Nadeau et al., 2011).

2.2.3.5 *Amino acid sequence alignments*

Full-length protein sequences were obtained from The Arabidopsis Information Resource (TAIR) and full-length protein sequences of *B. napus* were retrieved from *B. napus* genome (AST_PRJEB5043_v1; http://plants.ensembl.org/Brassica_napus/Info/Index). Protein sequences were aligned for comparison using the PSI-PRALINE multiple sequence alignment tool (https://www.ibi.vu.nl/programs/pralinewww/) under default parameters for comparison.

2.2.3.6 *Statistical analysis*

Statistical analysis was performed using R studio software version 1.2.5001. (RStudio Team (2020). RStudio: Integrated Development for R. RStudio, PBC, Boston, MA URL http://www.rstudio.com/.) Transcript abundance of genes was transformed into log2 scale prior to performing the statistical analysis. In detail, the data were checked for normality with Shapiro-Wilk test and homogeneity of variances with Levene's test. The Experimental design was 2 (cultivars: clubroot-resistant Wilhelmsburger cv. and clubroot-susceptible Laurentian cv.) x 2 (treatments: non-inoculated and 7d-*P. brassicae*-inoculated) factorial. A two-way analysis of variance (ANOVA) was performed on the transcript abundance data. Mean separation was performed using Tukey's Honest Significant Difference (Tukey's HSD) post-hoc test. Statistical significance was declared at $p \leq 0.05$ (see Appendix Table A2 for ANOVA details).

## 2.3 RESULTS

### 2.3.1 Differential disease responses of 'Whilhelmsburger' and 'Laurentian' to *P. brassicae*

To examine the differential disease response of clubroot pathogen *P. brassicae* field isolate F3-14 (pathotype 3A) in rutabaga (*B. napus* subsp. *rapifera* Metzg) resistant 'Wilhelmsburger' and susceptible 'Laurentian' cultivars (cvs.), we examined the disease symptoms at 45 days after inoculation (dai). As expected, the susceptible cv. 'Laurentian' showed stunted growth with purplish foliage and exhibited the typical clubroot symptoms at 45 dai, which included formation of enlarged, deformed, club-shaped root system with a few lateral roots. Of 144 clubroot-inoculated susceptible cv. plants, 121 seedlings developed severely clubbed roots as shown in Figure 2.2. In contrast, the resistant cv. 'Whilhelmsburger', either exhibited no disease symptoms or showed formation of very small bulbous galls only on the main root while lateral roots showed no clubroot symptoms. At 45 dai, the clubroot disease index (DI) of 'Laurentian' cv. was 76.23 ± 1.87 %, which was 4 times higher than that of 'Wilhelmsburger' cv. (20.37 ± 3.40 %; Figure 2.3), indicating that the disease development in 'Wilhelmsburger' cv. was considerably less severe than 'Laurentian' when inoculated with the *P. brassicae* pathotype 3A.

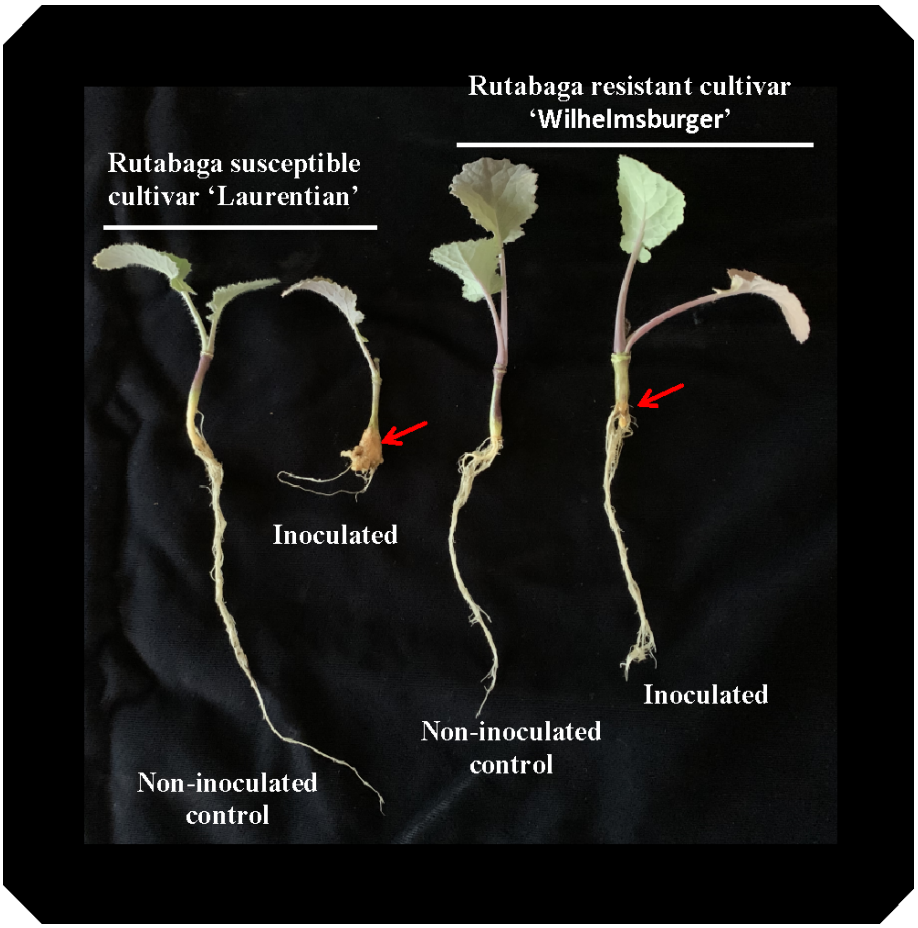


**Figure 2.2 Representative clubroot symptom development in roots of rutabaga (*Brassica napus* subsp. *rapifera* Metzg) susceptible 'Laurentian' and resistant 'Wilhelmsburger' cultivars at 45 days after inoculation with resting spores of 3A pathotype of *P. brassicae* at a density of 1 x $10^7$ spores/mL.** No clubbing of roots was observed in non-inoculated control plants of both cultivars. *P. brassicae*-inoculated plants of 'Laurentian' exhibited severe root galling; however, those of 'Whilhelmsburger' exhibited minimal to no root galling (red arrows denotes galls).

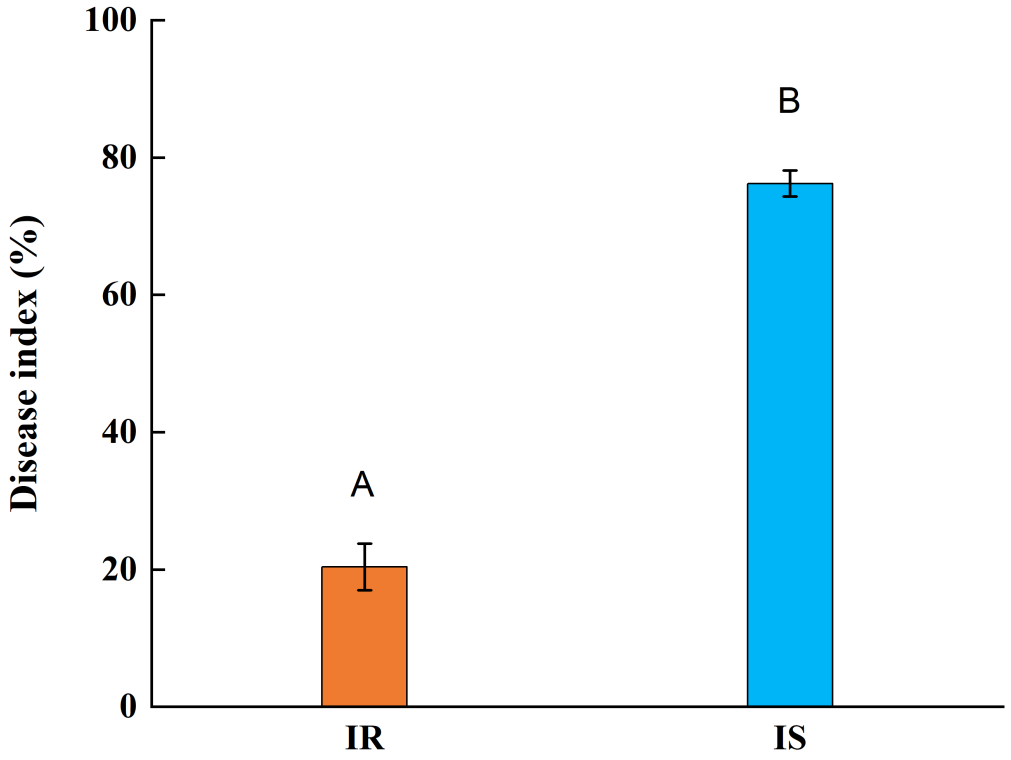


**Figure 2.3 Clubroot disease severity index in the roots of rutabaga resistant 'Wilhelmsburger' and susceptible 'Laurentian' cultivars caused by 3A pathotype of *P. brassicae* collected from a field population.** All the roots of non-inoculated control plants of both cultivars were clubroot-symptom free. The scoring was performed at 45 days after *P. brassicae* inoculation (dai). Data are the means ± standard error of the mean (SE) from four independent experiments (n=4), each experiment was performed with 36 plants per cultivar. Different letters indicate statistically significant differences between the treatments (Student's T-test, P≤0.05). IR = *P. brassicae*–inoculated roots of clubroot resistant rutabaga cultivar and IS = *P. brassicae*–inoculated roots of clubroot susceptible rutabaga cultivar.

### 2.3.2 Differential gene expression patterns in the indole GSL pathway in 'Wilhelmsburger' and 'Laurentian' cultivars at 7 dai against *P. brassicae*

Using the root transcriptome dataset from Zhou et al (2020), we analysed the expression profiles of genes involved in the indole GSL biosynthesis, modification, and degradation pathways in rutabaga resistant and susceptible cvs. in response to clubroot pathogen *P. brassicae* 3A pathotype at 7, 14, and 21 days after inoculation. In general, a majority of genes involved in the indole GSL biosynthesis, modification, and degradation pathways showed contrasting expression profiles in roots of resistant and susceptible cvs. at an early stage of clubroot infection (7 dai; Tables 2.2-2.4), indicating potential involvement of the GSL pathway in clubroot resistance and/or pathogenesis mechanisms in the rutabaga cvs. at this time. In the resistant cv., the indole GSL biosynthesis genes, *CYP79B2, GGP1, UGT74B1, SOT16, and SOT18* were either down-regulated or not changed in 7dai-*P. brassicae* inoculated roots compared to the non-inoculated roots (Table 2.2; Figure 2.1). Among them, *CYP79B2* encodes the enzyme that converts Trp to Aldoxime, while *GGP1* is responsible for the metabolization of indole-3-acetohyfroxymoyl Cys-Gly into indole-3-acetohydroxymoyl GSH. *UGT74B1* encodes a glucotransferase that coverts indolylmethyl-thiohydroximate into indolylmethy desulfo-GSLs, which are then sulfated by sulfotransferases encoded by *SOT16* and *SOT18*. In contrast, the expression of these genes in the susceptible cv. was either up-regulated (*CYP79B2 & GPP1*) or not changed (*UGT74B1 and SOT16*) in the *P. brassicae* inoculated roots at 7 dai compared to the non-inoculated roots.

**Table 2.2 Differentially expressed genes belonging to indole GSL biosynthesis pathway in root tissues of rutabaga (*Brassica napus* subsp. *rapifera* Metzg) resistant 'Wilhelmsburger' and susceptible 'Laurentian' cultivars at 7, 14, and 21 days after clubroot (*P. brassicae*) inoculation (dai).** A $\log_2$ fold change value represents the changes in *P. brassicae* -inoculated root compared to the non-inoculated roots. The $\log_2$ fold change values that are statistically significant at $p \leq 0.05$ are shown in bold font with an asterisk with upregulated genes ($\log_2$ fold change $\geq 1$) highlighted in red and down- regulated genes ($\log_2$ fold change $\leq -1$) highlighted in blue.

| Enzyme (encoded by gene) | *Arabidopsis thaliana* gene accession ID | *Brassica napus* gene accession ID | $\log_2$ fold change in *P. brassicae* inoculated roots relative to the non-inoculated control roots | | | | | |
|---|---|---|---|---|---|---|---|---|
| | | | 7-dai | | 14-dai | | 21-dai | |
| | | | resistant 'Wilhelmsburger' cv. | susceptible 'Laurentian' cv. | resistant 'Wilhelmsburger' cv. | susceptible 'Laurentian' cv. | resistant 'Wilhelmsburger' cv. | susceptible 'Laurentian' cv. |
| **Indole glucosinolate biosynthesis genes** | | | | | | | | |
| Tryptophan N-monooxygenase (*CYP79B2*) | AT4G39950 | BnaC01g00800D | **-1.12 *** | -0.60 | 0.12 | -0.56 | **-1.60 *** | -0.33 |
| | | BnaA08g16100D | -0.26 | **1.45 *** | -0.05 | **-1.08 *** | -0.81 | **-1.25** |
| | | BnaC07g51280D | **-1.31 *** | -0.55 | -0.30 | -0.92 | -0.72 | -0.17 |
| | | BnaC03g60820D | -0.78 | **1.30 *** | 0.05 | -0.65 | -0.14 | -0.84 |
| | | BnaA01g34610D | **-1.10 *** | -0.42 | -0.36 | -0.50 | -0.82 | -0.24 |
| | | BnaC07g51280D | **-2.04 *** | -0.46 | -0.09 | -0.88 | -0.92 | 0.12 |
| Tryptophan N-monooxygenase (*CYP79B3*) | AT2G22330 | BnaA04g12790D | -0.09 | -0.89 | -0.61 | **-1.09 *** | -0.21 | 0.24 |
| | | BnaA04g12790D | -0.59 | **-2.23 *** | -0.59 | **-1.38 *** | -0.84 | -0.28 |
| | | BnaA04g12790D | -0.16 | **-1.66 *** | -0.46 | **-1.73 *** | **-1.65 *** | **-1.07** |
| Glutathione S-transferase F9 (*GSTF9*) | AT2G30860 | BnaC03g17110D | **-1.07 *** | **-1.06 *** | -0.45 | -0.84 | -0.62 | 0.12 |
| | | BnaC04g41510D | -0.91 | -0.48 | -0.61 | **-1.07 *** | **-1.85 *** | **-1.23** |
| | | BnaC03g17110D | -0.97 | **-1.21 *** | -0.32 | -0.92 | -0.44 | 0.39 |
| | | BnaA04g17910D | -0.44 | -0.08 | -0.45 | -0.71 | **-1.60 *** | -0.84 |
| Glutathione S-transferase F10 (*GSTF10*) | AT2G30870 | BnaA03g14150D | -0.86 | -0.85 | -0.32 | **-1.01 *** | -0.67 | -0.40 |
| Gamma-glutamyl peptidase 1 (*GGP1*) | AT4G30530 | BnaA08g13020D | -0.41 | **1.17 *** | -0.07 | -0.39 | -0.50 | -0.65 |
| | | BnaA01g06540D | **-1.48 *** | 0.64 | -0.50 | **-1.30 *** | **-1.06 *** | **-1.78 *** |
| | | BnaA03g50240D | **-1.26 *** | 0.49 | -0.58 | **-1.52 *** | **-1.44 *** | **-2.01 *** |
| | | BnaC01g07810D | **-1.54 *** | 0.62 | -0.54 | **-1.39 *** | **-1.19 *** | **-1.87 *** |
| | | BnaC07g42720D | -0.53 | 0.48 | -0.62 | **-1.30 *** | -0.96 | **-1.52 *** |
| UDP-glucosyl transferase 74B1 (*UGT74B1*) | AT1G24100 | BnaA09g29790D | **-1.00 *** | -0.52 | -0.35 | **-1.20 *** | **-1.36 *** | -0.90 |
| | | BnaC05g50780D | **-1.16 *** | -0.49 | -0.29 | **-1.53 *** | **-1.86 *** | **-1.63 *** |
| Sulfotransferase 5a (*SOT16*) | AT1G74100 | BnaAnng27200D | **-1.03 *** | 0.32 | -0.09 | **-1.05 *** | **-1.22 *** | **-1.15 *** |
| | | BnaC06g35000D | **-1.21 *** | 0.00 | -0.28 | **-1.28 *** | **-1.25 *** | -0.87 |
| | | BnaA07g31260D | **-1.53 *** | -0.10 | -0.72 | **-1.99 *** | **-1.62 *** | **-1.47 *** |
| Sulfotransferase 5b (*SOT18*) | AT1G74090 | BnaC09g15510D | 0.41 | 0.81 | 0.70 | **1.52 *** | **1.23 *** | **2.22 *** |
| | | BnaC09g15460D | 0.10 | -0.78 | 0.27 | -0.16 | -0.53 | -1.09 ***** |
| | | BnaA09g14900D | 0.52 | 0.38 | 0.43 | **1.20 *** | **1.05 *** | **2.70 *** |
| | | BnaCnng14860D | -0.26 | 0.82 | 0.10 | -0.07 | -0.68 | **-1.28 *** |
| | | BnaC06g24250D | -0.18 | -0.26 | -0.74 | -0.78 | **-1.21 *** | **-1.30 *** |
| | | BnaCnng61560D | -0.51 | -0.06 | -0.98 | -0.50 | -0.84 | **-1.09 *** |
| | | BnaA09g10820D | -0.88 | 0.25 | **-1.09 *** | **-1.44 *** | **-1.42 *** | **-2.32 *** |
| | | BnaC06g34930D | **-2.63 *** | 0.75 | -0.61 | **-1.88 *** | **-2.64 *** | **-4.17 *** |
| | | BnaA07g31230D | **-1.41 *** | **-1.32 *** | 0.87 | **-2.18 *** | **-1.38** | **-2.48 *** |
| | | BnaA07g31250D | -0.19 | -0.45 | -0.10 | -0.70 | -0.54 | **-1.25 *** |

The expression patterns of genes in the GSL modification and degradation pathways also showed differential regulation in the roots of rutabaga cvs. at 7 dai. The most notable changes were the gene expression changes of the *CYP81F4* and *IGMT5* genes that are involved in the hydroxylation and methylation of I3M at position 1 of the indole ring yielding neo-glucobrassicin (Figure 2.1). *CYP81F4* and *IGMT5* expression was downregulated in the resistant cv. compared to its non-inoculated control, but no changes in expression were observed in the susceptible cv. compared to its non-inoculated control at 7 dai (Table 2.3). A minor up-regulation trend was observed for *CYP81F2* and *IGMT1* genes that code for enzymes involved in the hydroxylation and methylation of I3M at position 4 of the indole ring producing 4-methoxyglucobrassicin in the susceptible cv. compared to its non-inoculated control (Table 2.3). At a later stage of the clubroot infection (21 dai), both resistant and susceptible cvs. showed significant upregulation of *CYP81F2* and *IGMT1* genes with a markedly higher $\log_2$ fold values in the roots of the susceptible cv. compared to its non-inoculated control.

**Table 2.3 Differentially expressed genes belonging to indole GSL modification pathways in root tissues of rutabaga (*Brassica napus* subsp. *rapifera* Metzg) resistant 'Wilhelmsburger' and susceptible 'Laurentian' cultivars at 7, 14, and 21 days after clubroot (*P. brassicae*) inoculation (dai).** A $\log_2$ fold change value represents the fold changes in *P. brassicae* - inoculated root compared to the non-inoculated root tissues. The $\log_2$ fold change values that are statistically significant at $p \leq 0.05$ are shown in bold font with an asterisk with upregulated genes ($\log_2$ fold change $\geq 1$) highlighted in red and down- regulated genes ($\log_2$ fold change $\leq -1$) highlighted in blue.

| Enzyme (encoded by gene) | *Arabidopsis thaliana gene accession ID* | *Brassica napus gene accession ID* | log2 fold change in *P. brassicae* inoculated roots relative to the non-inoculated control roots | | | | | |
|---|---|---|---|---|---|---|---|---|
| | | | 7-dai | | 14-dai | | 21-dai | |
| | | | resistant 'Wilhelmsburger' cv. | susceptible 'Laurentian' cv. | resistant 'Wilhelmsburger' cv. | susceptible 'Laurentian' cv. | resistant 'Wilhelmsburger' cv. | susceptible 'Laurentian' cv. |
| **Indole glucosinolate modification pathways genes** | | | | | | | | |
| **Cytochrome P450 81F1 (*CYP81F1*)** | AT4G37430 | BnaC01g01490D | -0.37 | **-1.21 *** | 0.50 | -0.40 | 0.12 | -0.13 |
| | | BnaA01g00520D | 0.59 | 0.28 | 0.43 | -0.38 | -0.48 | **-1.18 *** |
| **Cytochrome P450 81F2 (*CYP81F2*)** | AT5G57220 | BnaA02g08270D | 0.90 | **1.02 *** | **1.02 *** | **1.26 *** | **1.70 *** | **4.01 *** |
| | | BnaA10g11280D | 0.58 | -0.01 | 0.77 | **1.66 *** | **2.23 *** | **3.76 *** |
| | | BnaC02g11750D | 0.47 | -0.18 | 0.58 | **1.23 *** | 0.79 | **2.48 *** |
| | | BnaC02g11750D | 0.03 | 0.72 | -0.35 | -0.75 | **-1.05 *** | **-1.40 *** |
| | | BnaA02g08270D | -0.05 | -0.95 | -0.23 | 0.25 | **-1.18 *** | 0.22 |
| **Cytochrome P450 81F3 (*CYP81F3*)** | AT4G37400 | BnaC03g61440D | 0.12 | -0.34 | -0.12 | -0.77 | -0.95 | **-1.42 *** |
| **Cytochrome P450 81F4 (*CYP81F4*)** | AT4G37410 | BnaA08g15660D | **-2.44 *** | 0.63 | **-1.05 *** | **-1.58 *** | **-1.07 *** | **-1.48 *** |
| | | BnaCnng68210D | **-2.29 *** | -0.32 | **-1.06 *** | -0.80 | **-1.25 *** | **-2.07 *** |
| | | BnaC03g61420D | **-1.48 *** | -0.65 | -0.25 | **-1.38 *** | -0.01 | 0.25 |
| | | BnaC01g01530D | **-2.50 *** | -0.51 | -0.77 | **-1.44 *** | **-2.08 *** | **-2.86 *** |
| | | BnaC03g61420D | **-1.35 *** | -0.55 | -0.43 | **-1.09 *** | **1.02 *** | **1.32 *** |
| **Indole glucosinolate *O*-methyltransferase 1 (*IGMT1*)** | AT1G21100 | BnaA07g11060D | -0.13 | -0.23 | -0.13 | 0.55 | 0.75 | **2.68 *** |
| | | BnaA07g11070D | 0.46 | 0.19 | 0.72 | 0.50 | -0.05 | **1.71 *** |
| | | BnaC08g19680D | 0.56 | **1.18 *** | 0.98 | **2.38 *** | **1.08 *** | **2.90 *** |
| | | BnaC07g14650D | -0.47 | -0.98 | -0.03 | 0.09 | **1.03 *** | **2.07 *** |
| | | BnaC07g14640D | 0.18 | -0.13 | 0.32 | 0.35 | 0.25 | **1.47 *** |
| | | BnaC07g14620D | -0.07 | 0.58 | 0.54 | -0.09 | 0.50 | **1.35 *** |
| **Indole glucosinolate *O*-methyltransferase 5 (*IGMT5*)** | AT1G76790 | BnaA07g21250D | -0.84 | 0.23 | **-1.48 *** | -0.76 | **-1.00 *** | **-1.11 *** |
| | | BnaA07g33060D | **-1.52 *** | -0.36 | **-1.27 *** | -0.97 | **-1.53 *** | -0.73 |
| | | BnaC06g37610D | **-1.70 *** | -0.27 | -0.65 | -0.91 | -0.79 | -0.30 |

In the GSL degradation pathway, the *BGLU30* and *NSP5* genes, which encode an atypical myrosinase β-glucosidases that hydrolyzes GSLs and a NSP that directs myrosinase-catalyzed GSL breakdown towards the formation of nitriles, were more highly expressed in the inoculated compared to the non-inoculated controls in both cvs., but more so in the resistant cv. compared to its non-inoculated control than the susceptible cv. compared to its non-inoculated control at 7 dai, and these differences generally diminished at 21dai as the disease advanced (Table 2.4). In addition, the genes that code for NIT enzymes (*NIT2* and *NIT4*) that catalyze the hydrolytic cleavage of nitriles (such as indole-3-acetonitrile) into their corresponding carboxylic acids (such as indole-3-acetic acid, IAA) and ammonia were also upregulated in the resistant cv. compared to its non-inoculated control, but no changes in expression were observed in the susceptible cv. compared to its non-inoculated control at 7 dai (Table 2.4).

In the PEN-dependent GSL degradation pathway (Figure 2.1), the expression of *GSTU13,* which codes for an enzyme that is involved in the conjugation of indol-3-ylmethyl isothiocyanate to GHS, was significantly downregulated in the resistant cv. compared to its non-inoculated control, while no changes in expression were not observed in the susceptible cv. compared to its non-inoculated control at 7 dai (Table 2.4). At later stages of the infection, inoculated roots of both cvs. exhibited reduced *GSTU13* expression. The auxin conjugation gene *IAGLU* that codes for an enzyme that conjugates free IAA to a bio-inactive IAA conjugate was upregulated in the resistant cv. compared to its non-inoculated control, but no expression changes were observed in the susceptible cv. compared to its non-inoculated control at 7 dai (Table 2.4).

**Table 2.4 Differentially expressed genes belonging to indole GSL degradation and auxin conjugation pathways in root tissues of rutabaga (*Brassica napus* subsp. *rapifera* Metzg) resistant 'Wilhelmsburger' and susceptible 'Laurentian' cultivars at 7, 14, and 21 days after clubroot (*P. brassicae*) inoculation (dai).** A $\log_2$ fold change value represents the fold changes in *P. brassicae* -inoculated root compared to the non-inoculated root tissues. The $\log_2$ fold change values that are statistically significant at $p \leq 0.05$ are shown in bold font with an asterisk with upregulated genes ($\log_2$ fold change $\geq 1$) highlighted in red and down- regulated genes ($\log_2$ fold change $\leq -1$) highlighted in blue.

| Enzyme (encoded by gene) | *Arabidopsis thaliana* gene accession ID | *Brassica napus* gene accession ID | log2 fold change in *P. brassicae* inoculated roots relative to the non-inoculated control roots | | | | | |
|---|---|---|---|---|---|---|---|---|
| | | | 7-dai | | 14-dai | | 21-dai | |
| | | | resistant 'Wilhelmsburger' cv. | susceptible 'Laurentian' cv. | resistant 'Wilhelmsburger' cv. | susceptible 'Laurentian' cv. | resistant 'Wilhelmsburger' cv. | susceptible 'Laurentian' cv. |
| **Indole glucosinolate degradation genes** | | | | | | | | |
| **β-glucosidase 23 (*PYK10*)** | AT3G09260 | BnaCnng39140D | -0.80 | 0.36 | -0.70 | -0.93 | **-1.21 *** | **-2.23 *** |
| | | BnaC03g36110D | -0.77 | -0.27 | -0.69 | -0.43 | **-1.26 *** | **-2.12 *** |
| | | BnaC05g43610D | -0.39 | 0.51 | **-1.26 *** | -0.61 | **-1.11 *** | **-1.74 *** |
| | | BnaC05g43620D | -0.93 | 0.97 | **-1.40 *** | -0.10 | 0.12 | -0.19 |
| | | BnaA05g29150D | -0.45 | 0.51 | -0.87 | -1.04 | **-1.37 *** | **-1.69 *** |
| | | BnaA05g29140D | -0.48 | 0.22 | **-1.03 *** | -0.89 | -0.68 | **-1.63 *** |
| **β-glucosidase 30 (*BGLU30*)** | AT3G60140 | BnaA04g01360D | **3.87 *** | **1.69 *** | **1.57 *** | **1.90 *** | 0.35 | **1.50 *** |
| | | BnaA04g01360D | **3.58 *** | **2.76 *** | **1.43 *** | **1.63 *** | **1.01 *** | **1.20 *** |
| | | BnaA04g01360D | **3.44 *** | **1.74 *** | **2.08 *** | **1.53 *** | 0.76 | **1.10 *** |
| | | BnaA04g01360D | **1.17 *** | 0.41 | 0.50 | 0.42 | 0.27 | 0.38 |
| | | BnaC04g22390D | **2.84 *** | **1.16 *** | **1.25 *** | **1.57 *** | 0.55 | 0.97 |
| **Thioglucoside glucohydrolase 1 (*TGG1*)** | AT5G26000 | BnaC02g40130D | -0.35 | -0.04 | -0.06 | **-1.28 *** | **-1.94 *** | **-1.46 *** |
| | | BnaCnng22330D | -0.28 | -0.32 | 0.44 | 0.15 | **-1.34 *** | -0.43 |
| **Thioglucoside glucohydrolase 2 (*TGG2*)** | AT5G25980 | BnaCnng53320D | 0.02 | -0.11 | 0.06 | -0.26 | -0.64 | **-1.20 *** |
| | | BnaC08g09960D | -0.61 | 0.57 | -0.03 | **1.16 *** | **1.42 *** | **2.02 *** |
| **Thioglucoside glucohydrolase 4 (*TGG4*)** | AT1G47600 | BnaA07g24400D | **1.25 *** | -0.04 | -0.60 | **1.53 *** | 0.89 | **2.59 *** |
| | | BnaA05g15660D | -0.18 | 0.39 | **-1.32 *** | -0.07 | -0.37 | -0.12 |
| | | | -0.50 | 1.33 | -0.80 | **1.27 *** | 0.33 | 0.28 |
| **Epithiospecifier protein (*ESP*)** | AT1G54040 | BnaC06g06840D | -0.39 | -0.42 | -0.02 | -0.49 | -0.86 | **-1.10 *** |
| | | BnaC06g06830D | 0.59 | 1.04 | -0.19 | **-1.12 *** | -0.70 | -0.83 |
| | | BnaAnng10080D | -0.39 | -0.41 | 0.69 | 0.57 | -0.68 | **1.95 *** |
| | | BnaA06g01390D | -0.56 | -0.17 | 0.22 | 0.65 | **1.30 *** | **2.78 *** |
| | | BnaC02g31070D | -0.76 | 0.01 | -0.64 | **-1.07 *** | **-1.23 *** | **-2.01 *** |
| | | BnaA06g00610D | -0.03 | 0.85 | **-1.04 *** | **-1.00 *** | **-1.07 *** | **-1.88 *** |
| **Nitrile specifier protein 1 (*NSP1*)** | AT3G16400 | BnaAnng40010D | **-1.01 *** | 0.09 | **-1.41 *** | -0.74 | **-1.00 *** | -0.91 |
| | | BnaC07g11830D | -0.04 | 0.41 | -0.75 | -0.86 | **-1.77 *** | **-2.53 *** |
| | | BnaA01g28080D | **-1.31 *** | -0.07 | **-1.08 *** | **-1.40 *** | **-1.46 *** | **-2.88 *** |
| | | BnaC01g35360D | -0.46 | 0.09 | -0.66 | **-1.06 *** | **-1.00 *** | **-1.66 *** |
| | | BnaA05g36920D | **-1.01 *** | -0.17 | **-1.37 *** | **-1.83 *** | **-2.20 *** | **-3.18 *** |
| **Nitrile specifier protein 2 (*NSP2*)** | AT2G33070 | BnaCnng21640D | 0.06 | -0.08 | 0.24 | -0.18 | **-1.29 *** | -0.77 |
| | | BnaA05g36920D | **-1.33 *** | -0.05 | **-1.37 *** | **-2.42 *** | **-1.90 *** | **-4.82 *** |
| **Nitrile specifier protein 4 (*NSP4*)** | AT3G16410 | BnaA06g01970D | -0.13 | 0.32 | **1.33 *** | -0.92 | 0.68 | **-1.42 *** |
| | | BnaA08g01700D | -0.03 | 0.03 | 0.01 | -0.55 | -0.26 | **-1.22 *** |
| | | BnaA08g01710D | -0.75 | 0.27 | -0.78 | **-1.06 *** | -0.89 | 0.86 |
| | | BnaC06g05180D | **-1.38 *** | 0.83 | 0.65 | **-1.11 *** | -0.59 | **-2.59 *** |
| | | BnaC03g68970D | -0.10 | 0.11 | -0.68 | -0.64 | -0.64 | **-1.50 *** |
| **Nitrile specifier protein 5 (*NSP5*)** | AT5G48180 | BnaA02g29990D | **3.08 *** | 0.97 | 0.41 | -0.36 | -0.73 | **-1.20 *** |
| | | BnaC07g26280D | **2.23 *** | **2.07 *** | 0.04 | 0.10 | -0.57 | -0.85 |
| | | BnaA06g30390D | **2.34 *** | **1.49 *** | 0.01 | 0.29 | -0.34 | -0.09 |
| | | BnaC02g38400D | **2.61 *** | 0.85 | 0.54 | -0.04 | -0.59 | **-1.15 *** |

| Enzyme (encoded by gene) | *Arabidopsis thaliana gene accession ID* | *Brassica napus gene accession ID* | log2 fold change in *P. brassicae* inoculated roots relative to the non-inoculated control roots | | | | | |
|---|---|---|---|---|---|---|---|---|
| | | | 7-dai | | 14-dai | | 21-dai | |
| | | | resistant 'Wilhelmsburger' cv. | susceptible 'Laurentian' cv. | resistant 'Wilhelmsburger' cv. | susceptible 'Laurentian' cv. | resistant 'Wilhelmsburger' cv. | susceptible 'Laurentian' cv. |
| **Indole glucosinolate degradation genes** | | | | | | | | |
| **Penetration 3 (*PEN3*)** | AT1G59870 | BnaA07g19610D | -0.12 | 0.79 | 0.20 | 0.55 | 1.53 * | **1.09** * |
| **Epithiospecifier modifier 1 (*ESM1*)** | AT3G14210 | BnaA05g25240D | -0.15 | -0.52 | -0.17 | **-1.88** * | -0.64 | **-3.49** * |
| | | BnaA05g25230D | **-1.28** * | **-1.44** * | 0.57 | -0.02 | **-2.16** * | **-2.04** * |
| | | BnaC05g39470D | **-1.29** * | **-1.34** * | 0.61 | -0.08 | **-1.95** * | **-2.09** * |
| | | BnaA05g25240D | -0.43 | -0.95 | -0.03 | **-2.29** * | -0.86 * | **-3.48** * |
| **Nitrilase 2 (*NIT2*)** | AT3G44300 | BnaA03g10890D | **1.49** * | 0.99 | **1.01** * | **1.44** * | 0.32 | 0.51 |
| | | BnaA06g38980D | 0.06 | -0.36 | 0.05 | 0.46 | **1.07** * | **1.61** * |
| | | BnaC02g07040D | -0.54 | -0.23 | -0.83 | 0.02 | **1.29** * | **2.42** * |
| | | BnaC03g13560D | **1.77** * | 0.78 | 0.82 | 0.72 | 0.20 | 0.15 |
| **Nitrilase 3 (*NIT3*)** | AT3G44320 | BnaCnng75490D | -0.21 | 0.19 | **-1.06** * | **-1.28** * | **-1.45** * | **-1.33** * |
| **Nitrilase 4 (*NIT4*)** | | BnaA02g05560D | **2.22** * | 0.81 | 0.19 | 0.60 | -0.65 | -0.03 |
| | | BnaC02g09450D | **1.89** * | 0.87 | 0.11 | 0.52 | -0.93 | -0.67 |
| **Glutathione S-transferase TAU type 13 (*GSTU13*)** | AT1G27130 | BnaC07g12800D | **-2.18** * | 0.31 | **-1.03** * | **-1.83** * | **-1.64** * | **-2.25** * |
| | | BnaA07g09120D | **-2.34** * | 0.39 | -0.78 | **-1.75** * | **-1.39** * | **-2.55** * |
| | | BnaC05g19610D | -0.98 | 0.16 | -0.34 | **-1.44** * | **-1.49** * | **-2.11** * |
| | | BnaA09g29540D | **-1.06** * | 0.44 | -0.16 | **-1.20** * | **-1.28** * | **-2.25** * |
| | | BnaA07g09580D | **-2.44** * | 0.41 | -0.02 | **-1.76** * | -0.31 | **-2.76** * |
| **Auxin conjugation gene** | | | | | | | | |
| **Indole-3-acetate *β*-D-glucosyltransferase (*IAGLU*)** | AT4G15550 | BnaA03g41970D | **1.44** * | 0.62 | 0.00 | 0.48 | **1.68** * | **2.36** * |
| | | BnaC07g33070D | **1.05** * | -0.02 | -0.04 | 0.39 | 0.77 | **1.51** * |
| | | BnaC01g41850D | 0.25 | -0.86 | -0.81 | -0.16 | -1.04 * | -0.36 |

### 2.3.3 Gene expression quantification using qRT-PCR assays with Taqman probes in roots of rutabaga cultivars at early stage of clubroot pathogen inoculations

As greater $\log_2$ fold differences in the expression profile of genes involved in GSL modification and degradation pathways was noticed amongst the clubroot-inoculated resistant and susceptible cvs. at 7 dai in the transcriptome study by Zhou et al. (2020), further validation of the expression profile of selected genes belonging to GSL modification and degradation pathways was performed in non-inoculated and 7d-*P. brassicae* inoculated roots of both resistant and susceptible rutabaga cvs. by qRT-PCR (for Taqman primers and probe see Table 2.1; for complete coding sequences see Appendix Figure A3-A12; for amino acid sequence alignments including conserved domains, see Appendix Figure A13-A16). Prior to designing Taqman primers and probes and performing qRT-PCR assays for gene expression quantification, gene specific-PCR primers were designed, and amplifications were performed on the selected genes using roots of non-inoculated control and 7-d clubroot-inoculated seedlings of the resistant cv. as a template (Appendix Table A1, Appendix Figure A3-A12). For indole GSL modification genes *BnIGMT1* and *BnIGMT5* (Appendix Figure A5) and indole GSL degradation genes *BnNIT2*, and *BnNIT4* (Appendix Figure A9), sequences within a gene family were highly homologous; therefore, a common set of PCR primers was designed using the conserved regions (Appendix Table A1).

Agarose gel electrophoresis of PCR products for each of the 10 selected genes produced one amplicon of expected size in two independent PCR reaction using cDNA as template for each of the roots of non-inoculated control and 7-d clubroot-inoculated resistant cv. as shown in Figures 2.4-2.7. The primers and taqman probe of *BnIGMT1* gene did not show proper amplification with the standard 10-fold dilution series consisting of five concentrations (1165.9-0.1166 ng/µL) obtained from pooled total RNA sample obtained from root tissues of non-inoculated and 7d-*P. brassicae*-inoculated rutabaga resistant 'Wilhelmsburger' and susceptible 'Laurentian' cvs.; therefore, this gene was not used in further qRT-PCR validation studies, and the expression of a total of nine genes was quantified by qRT-PCR.

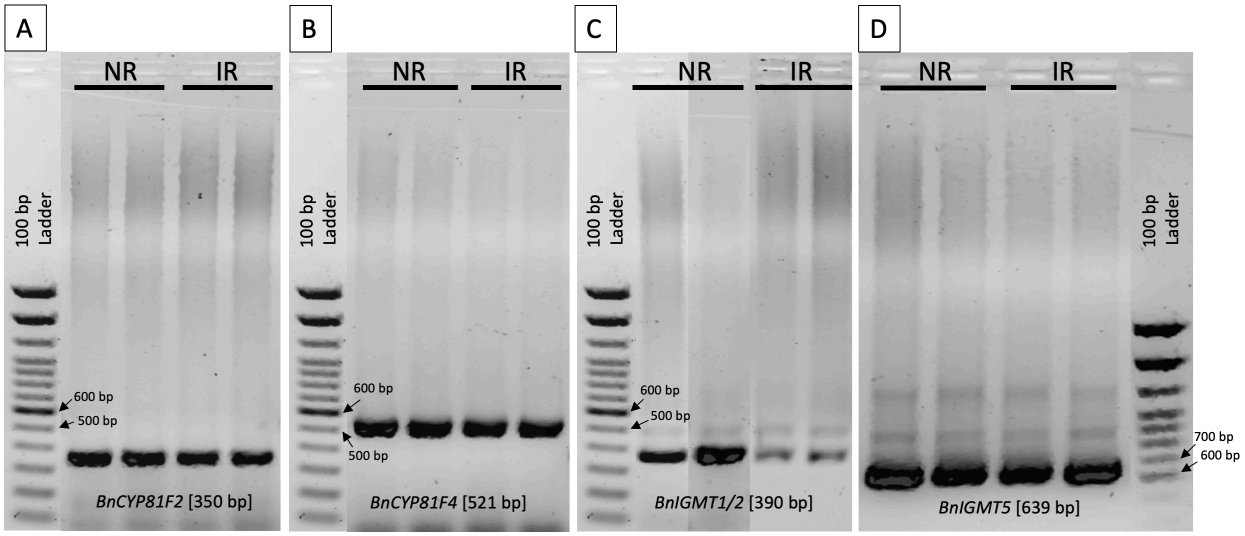


**Figure 2.4 Agarose gels showing PCR amplicons of indole GSL modification genes in root tissues of non-inoculated control (NR) and 7d-*P. brassicae*-inoculated (IR) clubroot resistant 'Wilhelmsburger' cultivar. Genes with observed expected amplicons sizes are: [A]: *BnCYP81F2*; [B]: *BnCPY81F4*; [C]: *BnIGMT1/2*; [D]: *BnIGMT5.*** These genes were amplified using PCR with primer sets described in Appendix Table A1.

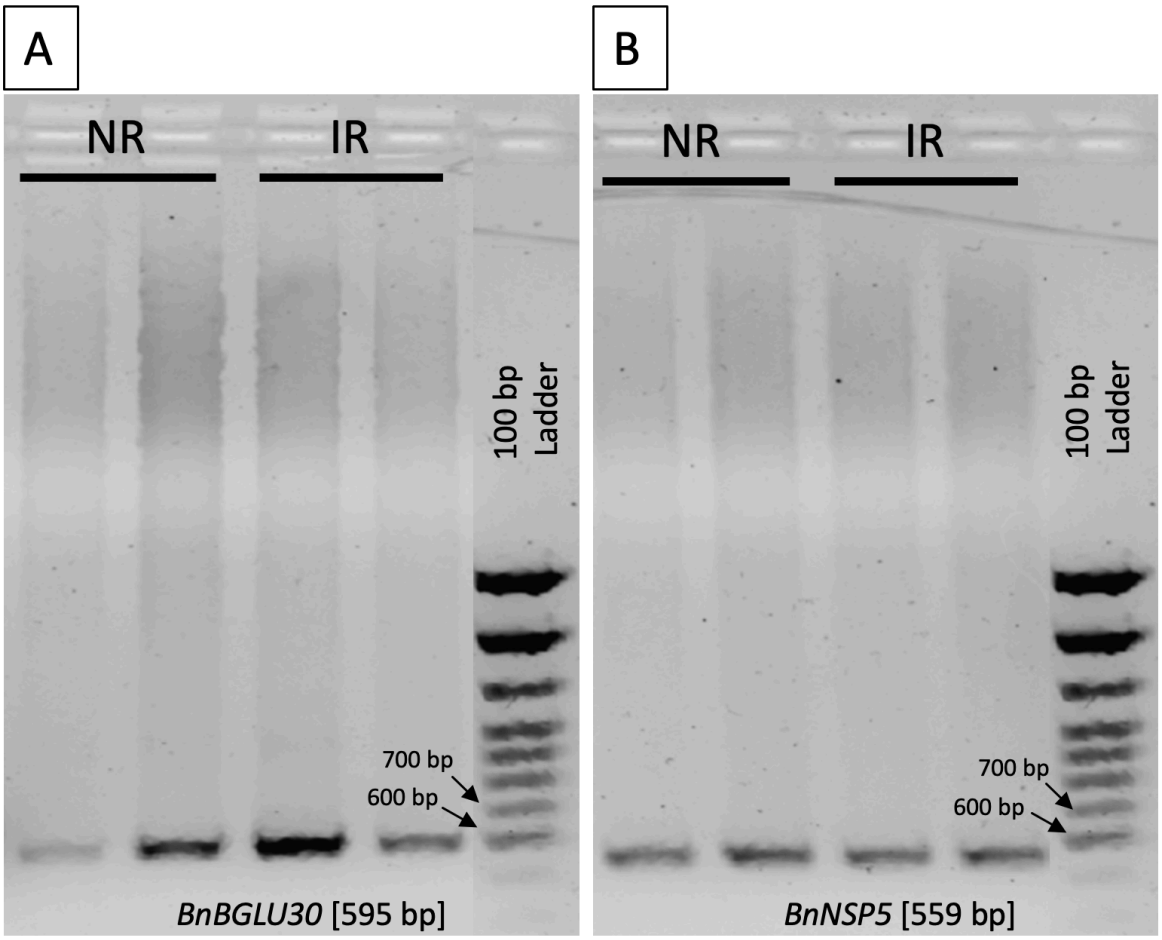


**Figure 2.5 Agarose gels showing PCR amplicons of indole GSL degradation pathway genes in root tissues of non-inoculated control (NR) and 7d-*P. brassicae*-inoculated (IR) clubroot resistant 'Wilhelmsburger' cultivar. Genes with observed expected amplicons sizes are: [A]: *BnBGLU30*; [B]: *BnNSP5.*** These genes were amplified using PCR with primer sets described in Appendix Table A1.

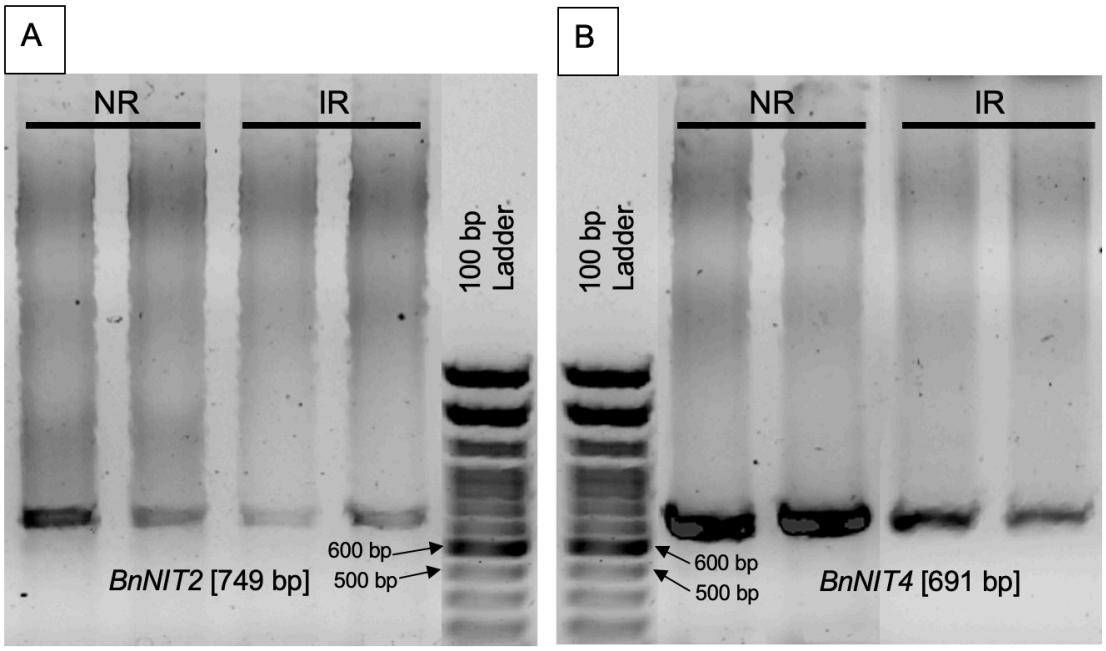


**Figure 2.6 Agarose gels showing PCR amplicons of indole GSL degradation pathway genes in root tissues of non-inoculated control (NR) and 7d-*P. brassicae*-inoculated (IR) clubroot resistant 'Wilhelmsburger' cultivar. Genes with observed expected amplicons sizes are: [A]: *BnNIT2*; [B]: *BnNIT4.*** These genes were amplified using PCR with primer sets described in Appendix Table A1.

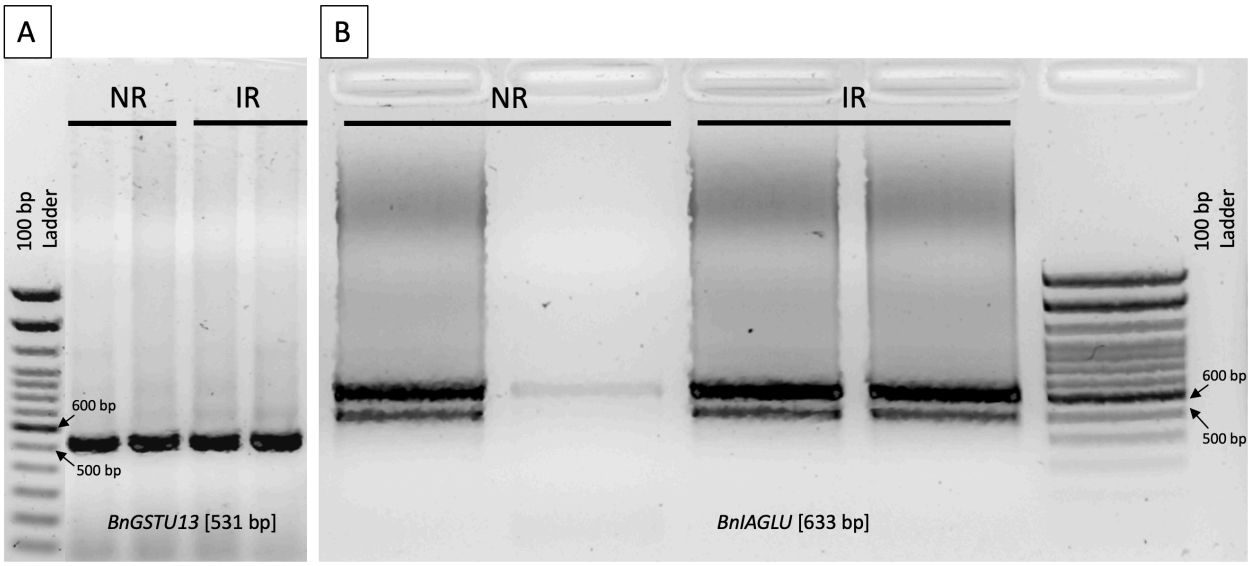


**Figure 2.7 Agarose gels showing PCR amplicons of indole GSL degradation and auxin conjugation pathways genes in root tissues of non-inoculated control (NR) and 7d-*P. brassicae*-inoculated (IR) clubroot resistant 'Wilhelmsburger' cultivar. Genes with observed expected amplicons sizes are: [A]: *BnGSTU13*; [B]: *BnIAGLU.*** These genes were amplified using PCR with primer sets described in Appendix Table A1.

In the indole GSL modification pathway, a significant upregulation in the expression of the *CYP81F2* gene (encodes for enzyme that hydroxylates I3M at position 4 of the indole ring) was observed in both the resistant (~2.0-fold relative to non-inoculated control) and susceptible (2.5-fold relative to non-inoculated control) cvs. (Figure 2.8A). This qRT-PCR-derived expression profile confirms up-regulation of *CYP81F2* expression in both resistant and susceptible cvs. 7 dai with *P. brassicae*, a trend alluded to, but not significant in both cultivars in the transcriptomic database (Table 2.3). Transcript abundance of *BnCYP81F4* (encodes for enzyme involved in the hydroxylation of I3M at position 1 of the indole ring) was higher (9-fold) in the roots of inoculated and non-inoculated seedlings of the resistant cv. compared to the susceptible cv. (Figure 2.8B). Inoculation with *P. brassicae* did not affect the transcript abundance of *BnCYP81F4* in the resistant cv. at 7 dai, but it reduced it in the susceptible cv. by ~2.0-fold. The transcript abundance of *BnIGMT5* (encodes for enzyme involved in the methylation of I3M at position 1 of the indole ring) was similar in non-inoculated control and 7d-*P. brassicae*-inoculated roots of resistant and susceptible cvs. (Figure 2.9). The qRT-PCR expression profiles of *BnCYP81F4* and *BnIGMT5* substantially differ from that observed in the transcriptomic database in the non-inoculated control and 7d-*P. brassicae*-inoculated roots of the resistant and susceptible cvs..

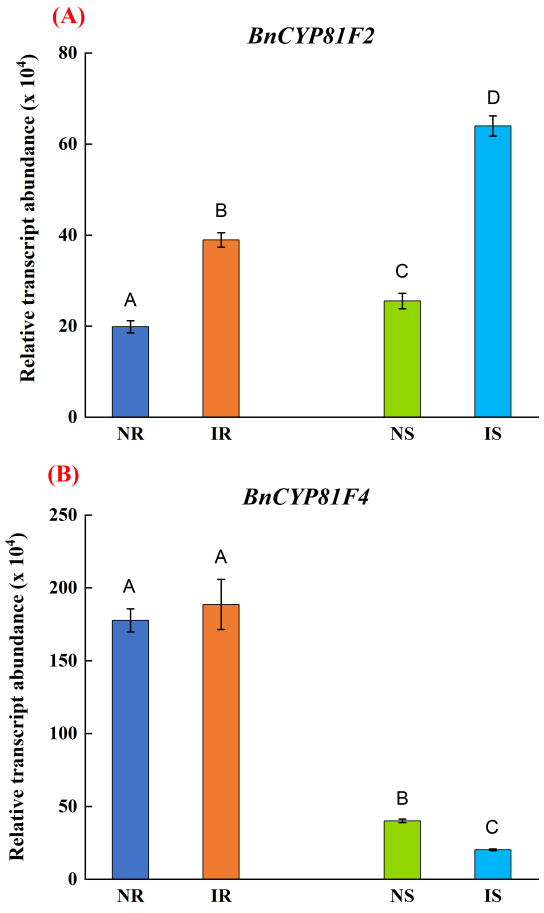


**Figure 2.8 Transcript abundance of genes encoding cytochrome P450 monooxygenase, family 81, subfamily F polypeptide (A, *BnCYP81F2* and B, *BnCYP81F4*) in root tissues of control and 7d-*P. brassicae*-inoculated rutabaga resistant 'Wilhelmsburger' and susceptible 'Laurentian' cultivars.** The resting spores of *P. brassicae* pathotype 3A field isolate F3-14 were used at 1 x $10^7$ spores/mL. Data are means ± standard error (SE), n=4, each biological replicate is a pool of roots obtained from 75 seedlings for non-inoculated susceptible cultivar, 77 seedlings for non-inoculated resistant cultivar, and 78 seedlings for inoculated susceptible and resistant cultivars. Different letters indicate statistically significant differences between the treatments and cultivars (Two-way-ANOVA, Tukey HSD post-hoc test, P≤0.05; **Appendix Table A2**). NR = non-inoculated roots of clubroot resistant rutabaga cultivar; IR = 7d-*P. brassicae*–inoculated roots of clubroot resistant rutabaga cultivar; NS = non-inoculated roots of clubroot susceptible rutabaga cultivar; and IS = 7d-*P. brassicae*–inoculated roots of clubroot susceptible rutabaga cultivar.

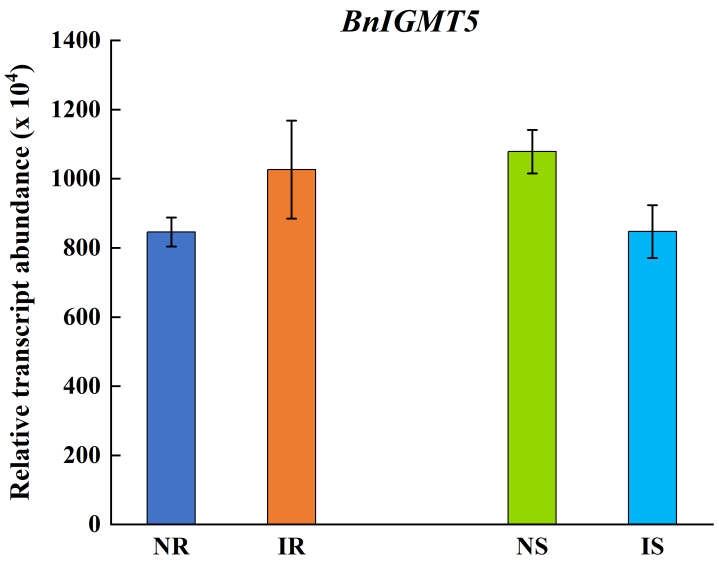


**Figure 2.9 Transcript abundance of gene encoding indole glucosinolate O-methyltransferase 5 (*BnIGMT5*) in root tissues of control and 7d-*P. brassicae*-inoculated rutabaga resistant 'Wilhelmsburger' and susceptible 'Laurentian' cultivars.** The resting spores of *P. brassicae* pathotype 3A field isolate F3-14 were used at 1 x $10^7$ spores/mL. Data are means ± standard error (SE), n=4, each biological replicate is a pool of roots obtained from 75 seedlings for non-inoculated susceptible cultivar, 77 seedlings for non-inoculated resistant cultivar, and 78 seedlings for inoculated susceptible and resistant cultivars. No statistically significant differences were observed between the treatments and cultivars (Two-way-ANOVA, Tukey HSD post-hoc test, P≥0.05; **Appendix Table A2**). NR = non-inoculated roots of clubroot resistant rutabaga cultivar; IR = 7d-*P. brassicae*–inoculated roots of clubroot resistant rutabaga cultivar; NS = non-inoculated roots of clubroot susceptible rutabaga cultivar; and IS = 7d-*P. brassicae*–inoculated roots of clubroot susceptible rutabaga cultivar.

The transcript abundance of *BnBGLU30*, which encodes for a myrosinase for indole GSL hydrolysis, increased in roots of both resistant (~14-fold relative to non-inoculated control) and susceptible (~33-fold relative to non-inoculated control) cvs. 7 dai with *P. brassicae* (Figure 2.10). Increased expression of *BnBGLU30* at 7 dai with *P. brassicae* was also observed in both cvs. in the transcriptome database (Table 2.4). *BnNSP5* (gene product directs the indole GSL hydrolysis into the production of nitriles) transcript abundance increased in both resistant (~1.7-fold relative to non-inoculated control) and susceptible (~1.7-fold relative to non-inoculated control) cvs. in response to clubroot inoculation at 7 dai (Figure 2.11). *BnNSP5* abundance was higher in the roots of non-inoculated (~1.9-fold) and inoculated (~1.9-fold) resistant cv. compared to the susceptible cv. (Figure 2.11). Increased expression of *BnNSP5* at 7 dai with *P. brassicae* was also observed in both cvs. in the transcriptome database (Table 2.4).

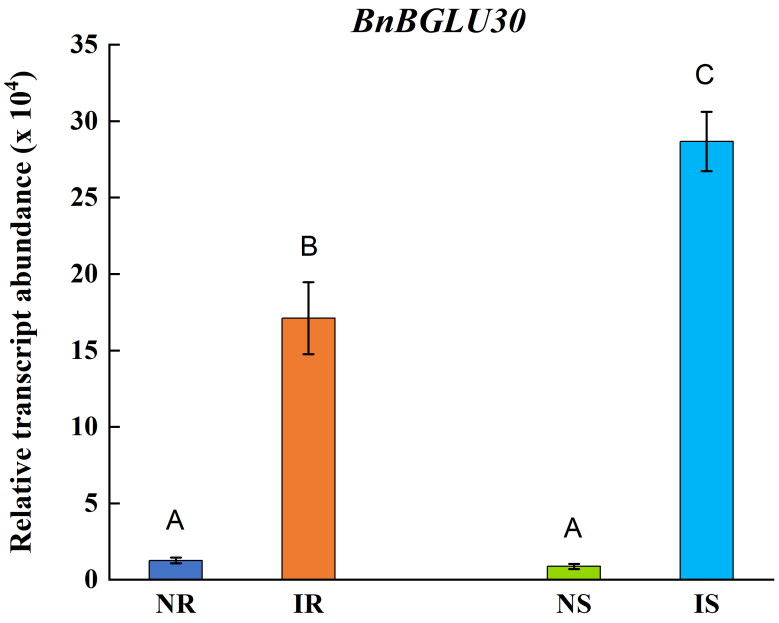


**Figure 2.10 Transcript abundance of gene encoding *β*-glucosidase 30 (*BnBGLU30*) in root tissues of control and 7d-*P. brassicae*-inoculated rutabaga resistant 'Wilhelmsburger' and susceptible 'Laurentian' cultivars.** The resting spores of *P. brassicae* pathotype 3A field isolate F3-14 were used at 1 x $10^7$ spores/mL. Data are means ± standard error (SE), n=4, each biological replicate is a pool of roots obtained from 75 seedlings for non-inoculated susceptible cultivar, 77 seedlings for non-inoculated resistant cultivar, and 78 seedlings for inoculated susceptible and resistant cultivars. Different letters indicate statistically significant differences between the treatments and cultivars (Two-way-ANOVA, Tukey HSD post-hoc test, $P \leq 0.05$; **Appendix Table A2**). NR = non-inoculated roots of clubroot resistant rutabaga cultivar; IR = 7d-*P. brassicae*–inoculated roots of clubroot resistant rutabaga cultivar; NS = non-inoculated roots of clubroot susceptible rutabaga cultivar; and IS = 7d-*P. brassicae*–inoculated roots of clubroot susceptible rutabaga cultivar.

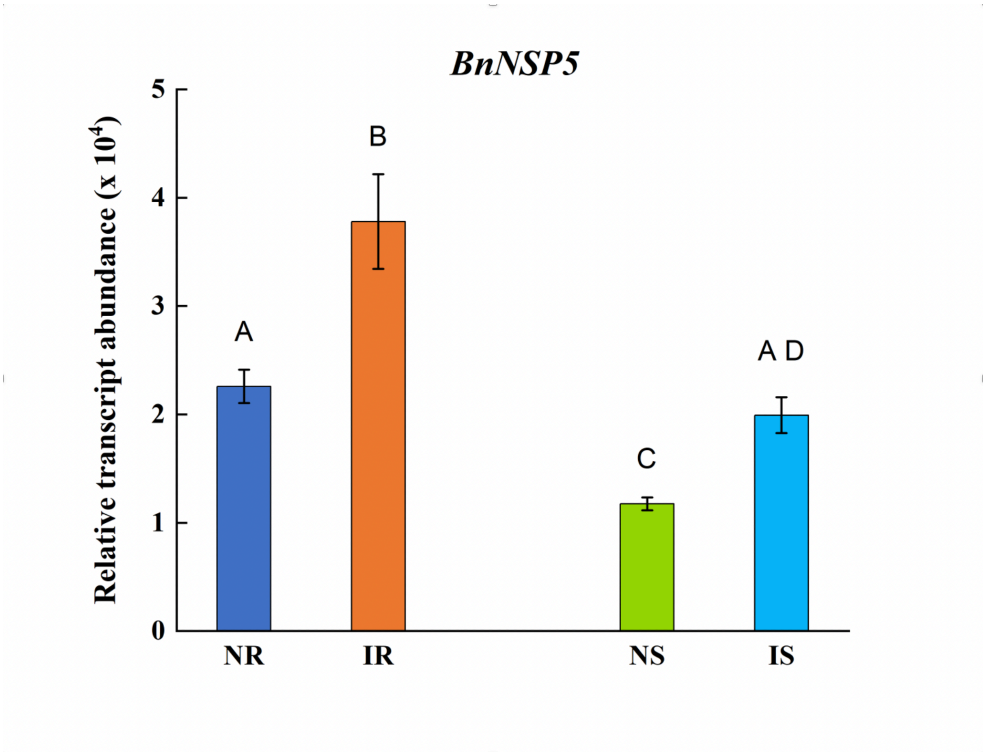


**Figure 2.11 Transcript abundance of gene encoding nitrile specifier protein 5 (*BnNSP5*) in root tissues of control and** 7d-***P. brassicae*-inoculated rutabaga resistant 'Wilhelmsburger' and susceptible 'Laurentian' cultivars.** The resting spores of *P. brassicae* pathotype 3A field isolate F3-14 were used at 1 x $10^7$ spores/mL. Data are means ± standard error (SE), n=4, each biological replicate is a pool of roots obtained from 75 seedlings for non-inoculated susceptible cultivar, 77 seedlings for non-inoculated resistant cultivar, and 78 seedlings for inoculated susceptible and resistant cultivars. Different letters indicate statistically significant differences between the treatments and cultivars (Two-way-ANOVA, Tukey HSD post-hoc test, P≤0.05; **Appendix Table A2**). NR = non-inoculated roots of clubroot resistant rutabaga cultivar; IR = 7d-*P. brassicae*–inoculated roots of clubroot resistant rutabaga cultivar; NS = non-inoculated roots of clubroot susceptible rutabaga cultivar; and IS = 7d-*P. brassicae*–inoculated roots of clubroot susceptible rutabaga cultivar.

Clubroot inoculation increased *BnNIT2* transcript abundance (encodes for a nitrilase that catalyzes the hydrolytic cleavage of nitriles) in the roots of the resistant cv. (~1.4-fold relative to non-inoculated control), but not the susceptible cv. at 7 dai (Figure 2.12A), similar expression patterns were observed in the transcriptome database. The transcript abundance of *BnNIT2* was higher in the resistant cv. compared to the susceptible cv. under non-inoculated (~2.3-fold) or pathogen-inoculated (~2.4-fold) conditions. The transcript abundance *BnNIT4,* which encodes for a β-cyano-L-alanine-hydratase/nitrilase involved in cyanide detoxification, was higher in the pathogen-inoculated roots of both resistant (~1.8-fold relative to non-inoculated control) and susceptible (~2.5-fold relative to non-inoculated control) cvs. at 7 dai (Figure 2.12B). However, *BnNIT4* transcripts were more predominant in the susceptible cv. (~1.7-fold) relative to 7d- *P. brassicae* inoculated resistant cv. (Figure 2.12B). This qRT-PCR-derived expression profile confirms up-regulation of *BnNIT4* expression in both resistant and susceptible cvs. 7 dai with *P. brassicae*, a trend observed, but only significant in the resistant cv. in the transcriptomic database (Table 2.4).

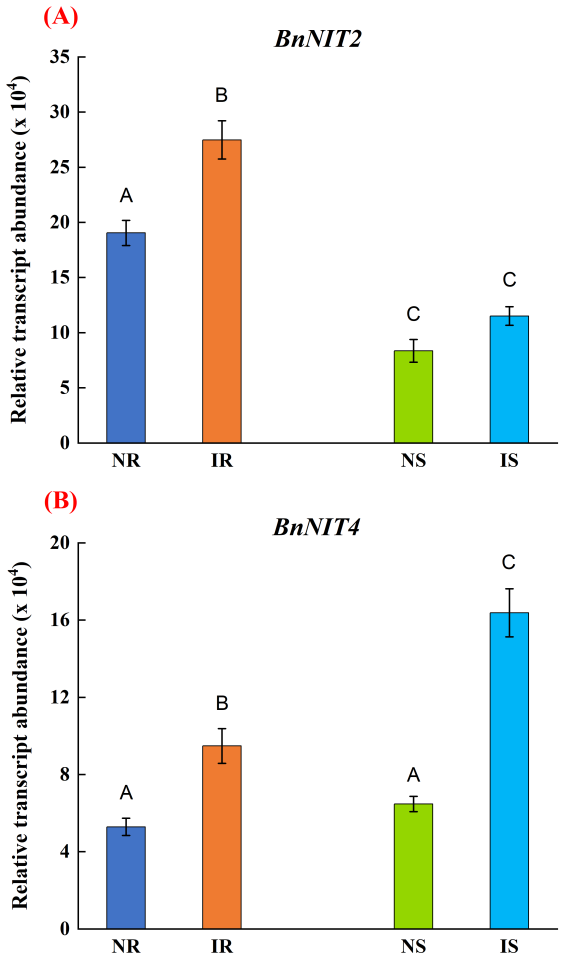


**Figure 2.12 Transcript abundance of genes encoding nitrilase 2 and 4 (A, *BnNIT2* and B, *BnNIT4*) in root tissues of control and 7d-*P. brassicae*-inoculated rutabaga resistant 'Wilhelmsburger' and susceptible 'Laurentian' cultivars.** The resting spores of *P. brassicae* pathotype 3A field isolate F3-14 were used at 1 x $10^7$ spores/mL. Data are means ± standard error (SE), n=4, each biological replicate is a pool of roots obtained from 75 seedlings for non-inoculated susceptible cultivar, 77 seedlings for non-inoculated resistant cultivar, and 78 seedlings for inoculated susceptible and resistant cultivars. Different letters indicate statistically significant differences between the treatments and cultivars (Two-way-ANOVA, Tukey HSD post-hoc test, P≤0.05; **Appendix Table A2**). NR = non-inoculated roots of clubroot resistant rutabaga cultivar; IR = 7d-*P. brassicae*–inoculated roots of clubroot resistant rutabaga cultivar; NS = non-inoculated roots of clubroot susceptible rutabaga cultivar; and IS = 7d-*P. brassicae*–inoculated roots of clubroot susceptible rutabaga cultivar.

*BnGSTU13* transcript abundance (gene products involve in the GHS conjugation of unstable indol-3-ylmethyl isothiocyanates that are formed via PEN2-mediated hydrolysis of indole GSL) was higher in the non-inoculated (~1.4-fold) roots of the susceptible cv. compared to the resistant cv. (Figure 2.13). *P. brassicae* inoculation increased *BnGSTU13* transcript abundance in the susceptible cv. (~1.5-fold relative to non-inoculated control), but not in the resistant cv. at 7 dai. This differs from the pattern observed in the transcriptomic database, where *BnGSTU13* expression was downregulated in the resistant cv. compared to its non-inoculated control, while no changes in expression were observed in the susceptible cv. compared to its non-inoculated control at 7 dai (Table 2.4).

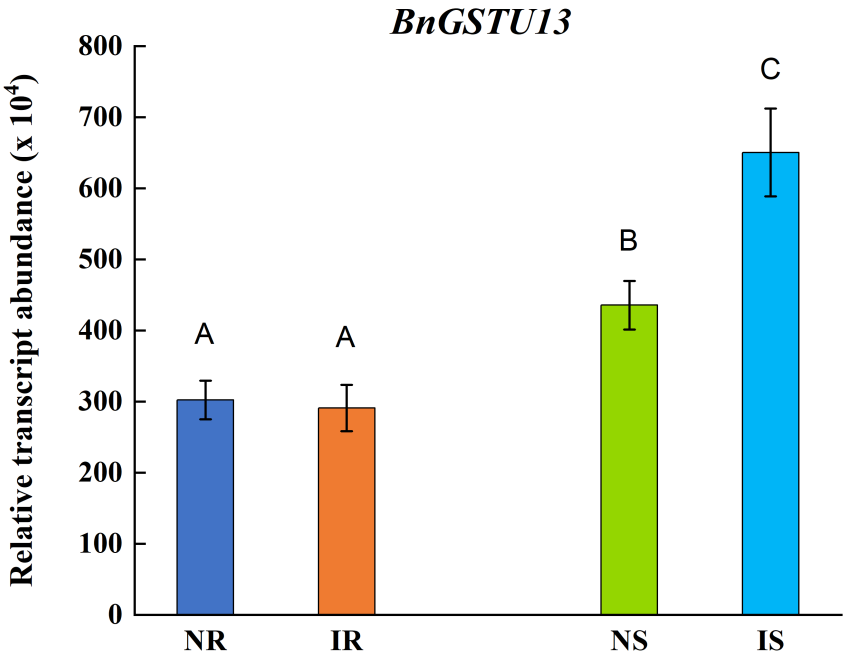


**Figure 2.13 Transcript abundance of gene encoding Glutathione S-transferase Tau type 13 (*BnGSTU13*) in root tissues of control and 7d-*P. brassicae*-inoculated rutabaga resistant 'Wilhelmsburger' and susceptible 'Laurentian' cultivars.** The resting spores of *P. brassicae* pathotype 3A field isolate F3-14 were used at 1 x $10^7$ spores/mL. Data are means ± standard error (SE), n=4, each biological replicate is a pool of roots obtained from 75 seedlings for non-inoculated susceptible cultivar, 77 seedlings for non-inoculated resistant cultivar, and 78 seedlings for inoculated susceptible and resistant cultivars. Different letters indicate statistically significant differences between the treatments and cultivars (Two-way-ANOVA, Tukey HSD post-hoc test, P≤0.05; **Appendix Table A2**). NR = non-inoculated roots of clubroot resistant rutabaga cultivar; IR = 7d-*P. brassicae*–inoculated roots of clubroot resistant rutabaga cultivar; NS = non-inoculated roots of clubroot susceptible rutabaga cultivar; and IS = 7d-*P. brassicae*–inoculated roots of clubroot susceptible rutabaga cultivar.

The transcript abundance of *BnIAGLU,* which codes for an enzyme that converts free IAA auxin to an inactive glucose ester conjugate, was detected only in the roots of the resistant cv., and it was ~1.9-fold higher in the roots of *P. brassicae* inoculated seedlings relative to that of the non-inoculated control seedlings (Figure 2.14). Increased expression of *BnIAGLU* at 7 dai with *P. brassicae* was also observed in resistant cv. but not the susceptible cv. in the transcriptomic database (Table 2.4).

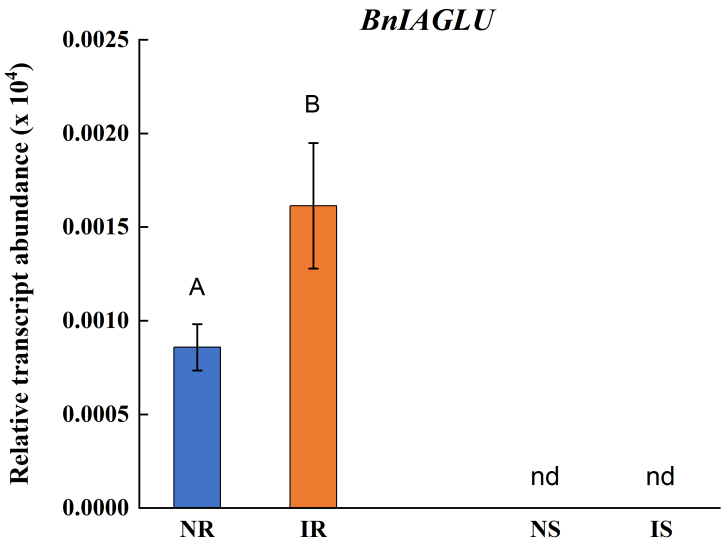


**Figure 2.14 Transcript abundance of gene encoding indole-3-acetate *β*-D-glucosyltransferase (*BnIAGLU*) in root tissues of control and 7d-*P. brassicae*-inoculated rutabaga resistant 'Wilhelmsburger' and susceptible 'Laurentian' cultivars.** The resting spores of *P. brassicae* pathotype 3A field isolate F3-14 were used at 1 x $10^7$ spores/mL. Data are means ± standard error (SE), n=4, nd=not detected, each biological replicate is a pool of roots obtained from 75 seedlings for non-inoculated susceptible cultivar, 77 seedlings for non-inoculated resistant cultivar, and 78 seedlings for inoculated susceptible and resistant cultivars. Different letters indicate statistically significant differences between the treatments and cultivars (Two-way-ANOVA, Tukey HSD post-hoc test, P≤0.05; **Appendix Table A2**). NR = non-inoculated roots of clubroot resistant rutabaga cultivar; IR = 7d-*P. brassicae*–inoculated roots of clubroot resistant rutabaga cultivar; NS = non-inoculated roots of clubroot susceptible rutabaga cultivar; and IS = 7d-*P. brassicae*–inoculated roots of clubroot susceptible rutabaga cultivar.

## 2.4 DISCUSSION

### 2.4.1 'Wilhelmsburger' cultivar exhibits greater resistance to clubroot compared with 'Laurentian'

The rutabaga cvs. 'Wilhelmsburger' and 'Laurentia' were included in multiple clubroot differential sets due to their differing resistance to various of isolates of *P. brassicae* (Williams, 1966; Somé et al., 1996; Strelkov et al., 2018). In this study, the severity of root galling was used to evaluate the development of clubroot in both cvs. after inoculation. At 45 dai, the DI of 'Laurentian' was ~4 times higher than that of 'Wilhelmsburger' (Figure 2.3), indicating a higher susceptibility of 'Laurentian' to *P. brassicae* pathotype 3A field isolate F3-14. The current findings are in line with those of Zhou et al. (2020) and Strelkov et al. (2018), who respectively reported a DI of 99% and 93.1 ± 2.9% for 'Laurentian' and a DI of 48% and 19.8 ± 2.9% for 'Wilhelmsburger' in response to pathotype 3A field isolate F3-14.

### 2.4.2 Differential expression of GSL biosynthesis genes during clubroot primary infection based on transcriptomic analysis

The association of clubroot disease with indole GSLs and auxin has been studied by a number of researchers (Ludwig-Müller et al.,1999; Ludwig-Müller et al., 2009; Zamani-Noor et al., 2021). Despite the existence of a substantial amount of published research on the relationship between GSL and clubroot, there is a lack of information regarding the regulation of GSL metabolism during the early stage of clubroot infection. In order to more fully understand the GSL-clubroot linkage at the primary infection stage of *P. brassicae* with brassica plant hosts, the transcriptomic profiles published by Zhou et al. (2020) that compared resistant and susceptible rutabaga cvs. responses to *P. brassicae* inoculation were studied. Transcriptomic analysis indicated that the gene expression patterns in the indole GSL pathways in the clubroot-resistant and -susceptible rutabaga cvs. differed at 7 dai. Specifically, in the resistant cv. several indole GSL biosynthesis genes were either down-regulated or not changed in 7dai-*P. brassicae* inoculated roots compared to the non-inoculated roots, which might result in a reduced indole GSLs level in the inoculated roots of resistant cv. compared to the non-inoculated roots. However, in the susceptible cv., these genes were found to be either up-regulated or not changed in the *P. brassicae* inoculated roots at 7 dai relative to its non-inoculated roots, indicating differential regulation of these GSL biosynthesis genes during primary infection depending on

the cultivar susceptibility to clubroot. Several studies in both Brassicaceae (Butcher et al., 1974; Ockendon and Buczacki 1979) and cabbage (Chong et al., 1981, 1985) found that clubroot resistance was associated with low indole GSL content at later stages of infection. In Chinese cabbage, the indole GSLs content increased in two susceptible cvs. 'Granat' and 'Osiris' at 14 and 20 days after germinating on soil containing *P. brassicae* spores, whereas no changes were observed in two resistant cvs. 'Yuki' and 'Parkin' (Ludwig-Müller et al., 1997). Nonetheless, the relationship between GSLs levels and clubroot susceptibility/resistance in different plant species is a topic of debate. While high levels of indole GSLs have been linked to susceptibility in some Brassica and non-host species (Butcher et al., 1974; Ludwig-Müller et al., 1999), resistant varieties have been found to produce more aromatic GSLs (Ludwig-Müller, 2009). Ludwig-Müller (2009) suggested that this relationship might be explained by a dual role of GSLs in the clubroot pathosystem as some GSLs function as defensive compounds, while others are precursors for auxin and auxin-like molecules.

### 2.4.3 Expression of genes in the indole GSL modification pathway

Due to the advancements in next-generation sequencing technology, RNA sequencing (RNA-Seq) has become a widely used technique for studying transcriptomes of different organisms for various purposes (Wang et al., 2009; Stone and Storchova, 2014). Compared to microarrays, RNA-seq offers several benefits such as the ability to identify novel transcripts, measure expression across a wider dynamic range, and lower expenses (Wang et al., 2009; Zhao et al., 2014). Identifying differentially expressed genes is the primary outcome of RNA-Seq data analysis. Currently, there is a growing interest in using RNA-seq methodologies to investigate the defense mechanisms of Brassica species against *P. brassicae* infection. (Chu et al., 2014; Chen et al., 2016a, 2016b; Zhang et al., 2016). Analyzing transcriptomic data is crucial in understanding the molecular mechanisms underlying the host's response to *P. brassicae* infection and can aid in determining the functions of important genes. However, not all differentially expressed genes can be considered as putative candidates or key players in the defense response, as post-translational regulation and the intricate nature of regulatory networks can also affect gene expression. A potential method for identifying strong candidate genes involved in resistance is by examining consistent gene expression patterns across various host-pathotype combinations. The RNA-seq workflow can be quite complex and may introduce biases that can

compromise the quality of the dataset, potentially leading to misinterpretation of sequencing results (Li et al., 2015; Shi et al., 2021). Meanwhile, qRT-PCR is frequently utilized to confirm transcriptomic data and determine the expression levels of specific genes (Andersen et al., 2004; Caldana et al., 2007) as qRT-PCR can offer a more precise and accurate measurement of gene expression for a limited set of genes, which can complement the transcriptome-wide expression analysis provided by RNA-seq. Furthermore, qRT- PCR assays incorporating species-specific primers and TaqMan probes are considered highly accurate due to the specificity provided by both the primers and the specially-designed TaqMan probe. This approach significantly improves the reliability of the assay, allowing for more precise detection of the target species (Köppel et al., 2011; Sakai et al., 2011).

Obtaining a single band of the expected size after running the PCR products on agarose gels for 9 of the 10 selected genes (Figures 2.4-2.7), we conducted qRT-PCR validation on the expression changes on these 9 genes in the GSL pathway including *BnCYP81F2, BnCYP81F4, BnIGMT5, BnBGLU30, BnNSP5, BnNIT2, BnNIT4, BnIAGLU, BnGSTU13* in the roots of *P. brassicae*-inoculated (7 dai) and non-inoculated controls of the two cvs. of interest. In contrast to the transcriptomic data, the qRT-PCR results showed that in the indole GSL modification pathway, a significant upregulation in the expression of the *BnCYP81F2* gene was observed in both the resistant and susceptible cvs. (Figure 2.8A), suggesting that increased hydroxylation of I3M either at the 1 or 4 position of the indole ring may occur during the primary infection stage. *BnCYP81F4* transcript abundance was higher in the resistant cv. than the susceptible cv., with either no or minor changes observed with *P. brassicae* inoculation at 7 dai, suggesting that a greater capacity for hydroxylation of I3M at the 1 position of the indole ring exists in the resistant cv. during the primary infection stage. Although the transcriptomic data revealed a difference in gene expression of *IGMT5* (encodes for enzyme involved in the methylation of I3M at position 1 of the indole ring) between the resistant and susceptible cvs. at 7 dai with *P. brassicae*, this finding was not confirmed by qRT-PCR as the transcript abundance of *BnIGMT5* was similar in non-inoculated control and 7d-*P. brassicae*-inoculated roots of resistant and susceptible cvs (Figure 2.9). In a previous study, Robin et al. (2017) showed that *CYP81F2* and *CYP81F4* expression was upregulated in the *Leptosphaeria maculans*-resistant cabbage (*Brassica oleracea var. capitata*) cv. as compared to the susceptible cabbage cv. at 4 dai with pathogen. Additionally, these gene expression patterns were associated with increased

methoxyglucobrassicins (MGBS; 1MOI3M and 4MOI3M) measured in the study in the resistant cv. but not the susceptible cvs., suggesting a role for MGBS in the resistance response in this particular host-pathogen interaction. Similarly, MGBS levels were reported to increase by 30–47% in response to *L. maculans* infection in *Brassica napus* after 5–8 dai (Wretblad and Dixelius, 2000). In an *in vitro* study, Mithen et al. (1986) found that MGBS, along with sinigrin (SIN) and I3M, exhibited anti-fungal properties. Jasmonic acid (JA) signalling plays a central role in plant defences against necrotrophic pathogens and herbivorous insects, and experimental evidence has suggested that resistance against necrotrophic pathogens could be modulated by the JA/ethylene (ET) signaling pathway (Yang et al., 2009). In a previous study, methyl JA (MeJA) treatment increased the expression of *CYP81F4* by 2400-fold in broccoli and 10-fold in cabbage (Yi et al., 2016), suggesting that the resistance against pathogen might be associated with the metabolism of indole GSLs. Taken together, the accumulation of particular GSLs at early stage of clubroot infection might be associated with the resistant response.

### 2.4.4 Expression of genes in the indole GSL degradation pathway

The qRT-PCR results indicated that the transcript abundance of both *BnBGLU30* and *BnNSP5* (encode for enzymes that hydrolyze glucose from GSL and direct product into nitrile production, respectively) increased in roots of both resistant and susceptible cvs. 7 dai with *P. brassicae* (Figures 2.10 and 2.11). This confirms the upregulation of both *BnBULU30* and *BnNSP5* expression in both cvs. 7 dai with *P. brassicae*, a trend identified in the transcriptomic database. These data suggest that increased expression of these genes in both cvs. at the primary infection stage is likely a defense response to elevate production of nitriles to impede the infection process. Additionally, *BnNSP5* transcript abundance was higher in the roots of the non-inoculated and inoculated resistant cv. compared to the susceptible cv., which may suggest that the resistant cv. generally has a greater ability to produce nitriles than the susceptible cv. (Figure 2.11). The type of nitriles identified in rutabaga roots are listed in Table 1.1. The potential of nitriles as defence compounds against pathogens in Brassicaceae plants was demonstrated in a study conducted by Ting and colleagues (2020), where it was observed that treating Arabidopsis Col-0 plants with a 2.0 mM solution of 3BN, a nitrile derived from GSL, prior to exposure to the pathogen *Pectobacterium carotovorum* ssp., effectively alleviated the leaf lesion symptoms. In accordance with this observation, Miao and Zentgraf (2007) demonstrated that transgenic

Arabidopsis plants overexpressing epithiospecifier proteins (ESPs) exhibited a significant increase in the production of nitriles, derived from GSLs, which act as defensive compounds, resulting in increased resistance to the bacterial pathogen *Pseudomonas syringae pv*. tomato DC3000 and the fungal pathogen *Alternaria brassicicola*.

Nitrilases are enzymes that facilitate the breakdown of nitriles into carboxylic acids and ammonia through hydrolytic cleavage (Piotrowski, 2008). Increased nitrilase gene expression (Arabidopsis, *NIT1* at 21 dai and *NIT2* at 32 dai*; B. rapa, NIT1* at 21-31 dai) was observed during *P. brassicae* infection in the plant host (Grsic-Rausch et al., 2000; Ishikawa et al., 2007). *BnNIT2* transcript abundance increased in the roots of resistant cv. but not the susceptible cv. at 7 dai (Figure 2.12A), indicating a resistant cultivar-specific response to primary infection. *BnNIT4* expression was induced in the pathogen-inoculated roots of both resistant and susceptible cvs.; however, the increase in *BnNIT4* transcript abundance was greater in the susceptible cv. than the resistant cv. (Figure 2.12 B). Previous evidence showed that NIT4 encodes β-cyano-L-alanine-hydratases/nitrilases involved in cyanide detoxification (Piotrowski et al. 2001; Ishikawa et al., 2007). The *BnNIT4* expression patterns may indicate that cyanide levels may be greater, or cyanide has a greater half-life in the resistant cv. where it can potentially inhibit the pathogen infection process.

The hydrolysis of I3M by PEN2 leads to the production of an unstable thiohydroximate-*O*-sulfonate intermediate that subsequently forms indol-3-ylmethyl isothiocyanate and indole-3-acetonitrile (IAN) (Bednarek et al., 2009; Radojčić Redovniković et al., 2008). The indol-3-ylmethyl isothiocyanate can be conjugated to GHS by the glutathione-S-transferase GSTU13 (Piślewska-Bednarek et al., 2018). The qRT-PCR gene expression results showed that *GSTU13* was upregulation in the susceptible cv. but not the resistant cv. (Figure 2.13), suggesting that indol-3-ylmethyl isothiocyanate levels may be greater or have a greater half-life in the resistant cv. where they can potentially inhibit the pathogen infection process.

Both the transcriptomic dataset and qRT-PCR results indicated that *BnIAGLU,* codes for an enzyme that transforms free IAA auxin to inactive glucose ester conjugate, was only significantly upregulated in the resistant cv. compared to the susceptible cv., suggesting that more bioactive IAA might be conjugated in the resistant cv. removing it from the bioactive free IAA pool. In studying the early response of *Brassica napus* L. to *P. brassicae*, Xu et al. (2016) reported that a significant increase in endogenous free IAA level occurred 3-7 days after

inoculation, but then the IAA content decreased to nearly that of the control at 10 dai. A similar pattern was also reported in several other studies (Ishikawa et al., 2007; Grsic et al., 1999; Ugajin et al., 2003; Ludwig-Müller et al., 1993), where at the beginning of the measured period (20 days after germination (dag), 14 dai, 20 days after sowing, and 10 days after incubation, respectively), the free IAA level in the infected root was significantly higher than that in the non-infected root, and subsequently, the free IAA content in infected root decreased significantly to a similar level as that of non-inoculated roots. Devos et al. (2005) on the other hand found that the free IAA content of control and infected roots did not differ at 6 and 13 dai; however, the conjugated IAA content of roots of infected plants was much greater than that of the controls at 6 dai. Ding et al. (2008) demonstrated that overexpression of *GH3-8,* which encodes an IAA–amido synthetase that maintains auxin homeostasis by conjugating excess IAA to amino acids, resulted in enhanced disease resistance in rice to the pathogen *Xanthomonas oryzae pv. oryzae.* This prevents the accumulation of free IAA and can be at least partly attributed to the suppression of a group of auxin-responsive genes encoding expansins, proteins that control cell wall loosening and expansion (Ding et al., 2008). As higher free IAA levels can also induce IAA-conjugation as a mechanism to modulate free IAA pools (Ludwig-Müller, 2011), one cannot speculate if higher expression of *BnIAGLU* expression will be associated with lower IAA levels in this study. It can be stated that auxin-homeostasis mechanisms were triggered (in this case increase in *BnIAGLU* transcript abundance) in the roots of the resistant cv. at 7 dai.

### 2.4.5 Summary

In conclusion, the results of this research suggest that modulation of expression of specific GSL pathway genes occurs in rutabaga roots likely resulting in elevated nitrile production as a primary infection response to *P. brassicae* (Figure 2.15). Nitriles are known to be toxic to many herbivores and fungal pathogens and may therefore play an important role in the plant's defense mechanism. Furthermore, the GLS gene expression pattern of the resistant cv. indicates that it may have a greater capacity to produce and maintain the levels of nitriles as a primary infection response to *P. brassicae* than the susceptible cv. Additionally, the selective expression of *BnIAGLU* only in the resistant cv. suggests that increased conjugation of free IAA to an inactive IAA-glucose ester is associated with *P. brassicae* resistance at the primary infection stage. Overall, these findings suggest that the resistant cv. may have a more robust

defense response against clubroot infection at the primary infection stage. Further studies are needed to fully elucidate the mechanisms underlying this defense response and to quantitate specific indole GSLs-related compounds including nitriles in the pathway to correlate gene expression changes with changes in GSL products produced.

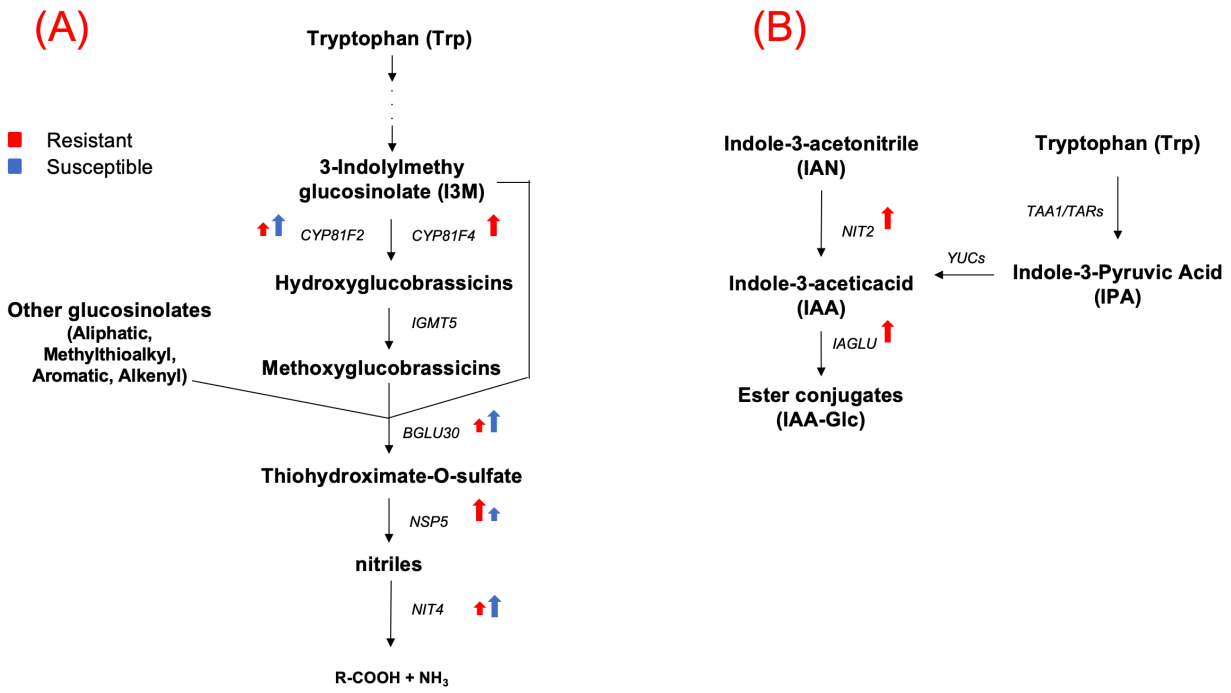


**Figure 2.15 A working model of a potential early host defence response involving the indole and general GSL pathway in *Brassica napus* against *P. brassicae*.** (A): Production of nitriles from GSL pathways. Overall, at 7 dai upon *P. brassicae,* the resistant cv. exhibited a greater capacity for conversion of I3M to hydroxy-I3Ms (greater expression of CYP81F genes monitored) than the susceptible cultivar. The transcript abundance of *BGLU30* increased with *P. brassicae* inoculation in both cvs. 7 dai; however, greater transcript levels of *NSP5* and lower transcript levels of *NIT4* in the resistant cv. suggests that a greater capacity for nitrile production, and lower metabolism of nitriles in this cultivar may be an early defense response to *P. brassicae* infection. (B) IAA synthesis and conjugation. The *P. brassicae*-induced increase in *BnIAGLU* transcript abundance exhibited in the resistant cv. at 7 dai suggests that conjugation of free IAA to an inactive IAA-glucose ester may be a defense response to *P. brassicae* at the primary infection stage. Red arrows represent higher gene expression upon inoculation with *P. brassicae* in the resistant cv. 'Wilhelmsburger', or higher expression in the resistant cv. compared to the susceptible cv. regardless of inoculation. Blue arrows represent higher gene expression upon inoculation with *P. brassicae* in the susceptible cv. 'Laurentian'.

# Chapter 3: Phenotypic characterization of clubroot disease progression in canola plants with modified auxin response.

## 3.1 INTRODUCTION

Clubroot disease, caused by the obligate biotrophic protist *P. brassicae* is an infectious disease of plants of the Brassicaceae family. The life cycle of *P. brassicae* can be divided into two phases: a primary phase in which infections are confined to the root hairs and a secondary phase that occurs in the cortex and the stele of roots and hypocotyl of the infected plants, where abnormal tissue proliferation takes place, leading to the formation of galls. Galls are formed as a result of increased cell division, followed by the elongation of the newly formed cells. (Ingram and Tommerup, 1972). Morphological changes associated with increased cell expansion were observed in the roots of Chinese cabbage (*Brassica rapa s*pp. *Pekinensis*) during the early stages of *P. brassicae* infection (Devos et al., 2005). For cell expansion to occur, the cell wall must undergo a remodeling process, allowing cellulose microfibrils to separate and/or shift past one another and ultimately leading to an expansion in the cell's volume. Xyloglucan endo Transglucosylase/hydrolase (XTH) and expansins are major enzymes facilitating the remodelling of the cell wall during cell elongation (Devos et al., 2005). Upon clubroot infection (4 dai), an increase in XTH action in the epidermal layer of infected roots was associated with the primary infection stage in the root hairs (Devos et al., 2005). Additionally, the upregulation of expansin-encoding genes was also reported from clubroot tissue in several transcriptomic studies at a later infectious stage characterized by clearly visible clubs (Siemens et al., 2006; Irani et al., 2018; Ciaghi et al., 2019). Auxins act in concert with other plant hormones to promote cell division and elongation (Yang et al., 1996; Kou et al., 2021; Chapman and Estelle, 2009), and auxins can induce gene expression of expansins (Cho and Cosgrove, 2004). The free IAA level in clubroot-infected roots was significantly higher than that in the non-infected roots in a number of studies (Ishikawa et al., 2007; Grsic et al., 1999; Ugajin et al., 2003; Ludwig-Müller et al. 1993) around the secondary infection phase (20 days after germination (dag), 14 dai, 20 days after sowing, and 10 days after incubation, respectively), and subsequently, the free IAA content in infected root decreased significantly to a similar level as that of non-inoculated roots. In another study, the steady-state levels of bioactive free IAA did not change in the clubroot infected root tissues at 13 dai; however, IAA-conjugate levels increased suggesting that increased biosynthesis of IAA

leading to increased conjugation may have occurred (Devos et al., 2005). These data along with many other studies have noted a role for auxin in clubroot infection and disease progression, but little is known about how auxin signaling mechanisms are involved.

In order for the plant to elicit an auxin response, the auxin molecule must be perceived. Auxin perception occurs via interactions between the Transport Inhibitor1/Auxin-Signaling (TIR1/AFB) receptor and the auxin co-receptors Auxin/Indole-3-Acetic Acid (Aux/IAA) repressor proteins and the auxin molecule (Dharmasiri et al., 2005 a, b; Kepinski and Leyser, 2005; Tan et al., 2007). As a result, the Aux/IAA repressors are polyubiquitinated and degraded through the action of the 26S-mediated proteasome (dos Santos Maraschin, 2009). The degradation of the repressors leads to the activation of auxin response transcriptional factors (ARFs), resulting in the transcriptional modulation of auxin-responsive genes. The auxin-dependent interactions of the TIR1/AFB and Aux/IAA proteins appear to depend on the specific combination of TIR1/AFB and Aux/IAA proteins that form the co-receptor with distinct auxin-binding affinities (Calderón Villalobos et al., 2012). Since there are 6 TIR1/AFBs and 29 Aux/IAA proteins in Arabidopsis many combinations are possible, leading to specific auxin responses (Calderón Villalobos et al., 2012). The TIR1/AFB auxin-receptor protein family is conserved across land plants, and it is divided into four distinct phylogenetic clades TIR1, AFB2 (AFB2/AFB3), AFB4 (AFB4/AFB5) and AFB6 (Parry et al., 2009). Phylogenetic analysis revealed three pairs of paralogues in *A. thaliana*, TIR1/AFB1, AFB2/AFB3 and AFB4/AFB5, which are grouped into three separate clades. However, a fourth clade, AFB6, is not present and is presumed to have been lost early in the evolution of Brassicaceae and Poaceae families (Parry et al., 2009). Pea (*Pisum sativum*) on the other hand contains members of all four auxin TIR1/AFB receptor clades (TIR1a and TIR1b; AFB2; AFB4; AFB6; Jayasinghege et al., 2019; Ozga et al., 2010; Ligerot et al., 2017).

Due to the absence of AFB6 homologs in Arabidopsis, less is known about this auxin receptor clade. Data in tomato (*Solanum lycopersicum*) indicate that SlTIR1 and SlAFB6 play a role in the auxin-signalling network controlling simplified leaf architecture formation (Ben-Gera et al., 2012). In pea, the work by Ozga et al. (2022) suggests that a functional AFB6 auxin receptor works in conjunction with auxin receptors from the TIR1, AFB2, and AFB4 clades to regulate auxin responses during plant growth and development, and specifically during reproductive growth in this species. In *Lotus japonicus*, the examination of two *Ljafb6* knock-out

LORE1 mutants showed a substantial improvement in the tolerance of primary and lateral root growth in plants exposed to 2,4-D and IAA for 10 days, compared to wild type plants (Rogato et la., 2021). Additionally, etiolated mutant seedlings showed a notable decrease in hypocotyl length when compared to seedlings of the wild type. These results indicate that *LjAFB6* might be involved in the auxin-dependent signaling pathways governing both primary and lateral root elongation and hypocotyl elongation processes (Rogato et la., 2021). In the context where AFB6 clade is absent in Brassicaceae while present in pea, transgenic canola (*Brassica napus*) plants were created in the Ozga lab that express the auxin receptor *PsAFB6* from pea. Preliminary data (Unpublished data in the Ozga lab) suggests that the *PsAFB6* expressing canola plants developed less severe clubbing symptoms when infected with clubroot and that it modifies auxin response in a manner that increases stress tolerance and lateral bud break.

Clubroot inoculation of plants is typically carried out using a soil- or peat-based rooting medium in which an aqueous solution containing resting spores of clubroot is applied to the stem base of the seedlings. However, soil- and peat-based media are complex substrates that include an extensive ecosystem of microorganisms, minerals, and a heterogenous mixture of other inorganic and organic materials (Torsvik and Øvreås, 2002). Using a hydroponic root growth system can offer the advantage of providing a simplified root growth environment to directly assess the host-pathogen interaction with less potentially interfering factors. The Hoagland nutrient solution has been widely used in most of the previous hydroponic studies. In a hydroponic study on *P. brassicae* inoculations in Chinese cabbage, ½ strength Hoagland solution was found to be optimal for the growth of the Chinese cabbage (Ji et al., 2014); however, the strength of the Hoagland solution utilized in other research have varied depending on the plant species and purpose of cultivation (Li et al., 2007; Zhao et al., 2007).

In the current study, in order to determine if modification of auxin response affects clubroot disease progression, two independent transgenic lines expressing the pea auxin receptor *PsAFB6* in the canola cv. Westar (*AFB6-9* and *AFB6-52*), along with their respective null lines, were phenotypically characterized for their response to clubroot infection using a hydroponic system.

## 3.2 MATERIALS AND METHODS

### 3.2.1 Pathogen material

*P. brassicae* single spore isolate (P3-SACAN-SS1) was used as the inoculum for the current study. The resting spore suspension used for inoculations was prepared from frozen (-20°C) root galls in 1/3-strength sterile Hoagland solution, quantified using a haemocytometer (as described previously in Appendix Figure A1), and adjusted to 1 x $10^7$ spores/mL using 1/3-strength Hoagland solution. The prepared inoculum suspension was stored at 4 °C and was used within 24 hours of its preparation.

### 3.2.2 Plant inoculation and harvesting

In this experiment, T3 generation seeds of two independent transgenic lines of Canola (cv. Westar) expressing *PsAFB6* driven by the constitutive promoter CaMV-35S created via Agrobacterium-mediated transformation (AFB6-9 and AFB6-52; both lines confirmed to express *PsAFB6* at significant levels), and their associated null lines (transgene segregated out at the T2 generation), were chosen for characterization from the Ozga lab. Seeds were germinated on moistened Whatman filter paper #1 (Whatman International Ltd., Maidstone, UK) in Petri dishes (50 seeds per Petri dish; TC Dish 100, Sarstedt, Nümbrecht, Germany) at room temperature.

Eight-day-old seedlings were then transferred to pre-labelled Ziploc medium-sized plastic bags (17.7 x 18.8 cm, S.C. Johnson & Son Inc., USA). Each plastic bag was lined with a sterile heavy weight seed germination paper #76 (17 x 18 cm; Anchor Paper Company, USA) soaked in 50 mL of 1/3-strength sterile Hoagland solution (Hoagland′s No. 2 Basal Salt Mixture, Sigma-Aldrich, USA). An additional 150 mL of Hoagland solution was added to the bag to provide nutrients to the growing seedlings. Plastic bags were covered with aluminum foil (Fisherbrand; Fisher Scientific, USA) to provide a dark environment for root growth. The non-inoculated control seedlings were directly transferred from the Petri dishes to the plastic bags (3 seedlings per bag in combinations of 2 Null and a PCR+ or a Null and 2 PCR+ seedlings; Appendix Figure B1). For clubroot pathogen-inoculated seedlings, the roots were dipped in the clubroot resting spore suspension (1 x $10^7$spores/mL concentration) and transferred to bags. To ensure enough disease pressure, an additional 1 mL spore suspension (*P. brassicae* at 1 × $10^7$ spores/mL) was added onto the roots of each seedling with a micropipette. In each bag, three seedlings were held in place between two layers of Hoagland-moistened paper (a 17 x 18 cm germination paper that fits the bag and an additional short strip of 17 x 4 cm germination paper that covers the root shoot transition region) using paper clips. The bags were then sealed to minimize the risk of

contamination. Bags containing non-inoculated control and clubroot-inoculated seedlings were then placed upright in trays and transferred to an environmentally controlled growth chamber maintained at 22/18 °C (day/night) with a 16h-light/8h-dark photoperiod under cool-white fluorescent lights at 269.59 ± 15.78 μE $m^2$ $s^{-2}$ measured with a LI-188 photometer (Li-Cor Biosciences, Lincoln, Nebraska, USA).

After 7 days of growth in the hydroponic bag system, seedlings were carefully transferred to trays with 32 cell inserts (insert size 5.89 x 4.54 x 7.04 cm) filled with moistened Sunshine #4 peat-based medium (SunGro Horticulture, Vancouver, BC, Canada) for continued development of disease symptoms (one seedling per cell). Plants continued to grow in the peat-based medium for 23 days in the same growth chamber until harvested and were watered at an interval of three days. One week after transfer to the peat-based medium, plants were fertilized once per week with 20:20:20 (N: P: K) fertilizer solution at 100 ppm until harvested. At 30 days after *P. brassicae* inoculations (dai), plant roots were washed two times to remove the rooting medium and handled gently to prevent the loss of lateral roots, after washing, plants were transferred to pre-labelled glass tubes filled with water. Seedlings were pat dried using paper towels and images of the root-shoot transition zone were captured at 30 dai (7 days grown hydroponically followed by 23 days of growth in the peat-based medium) using a Zeiss Axiocam ERc 5s Rev. 2.0 (Carl Zeiss Microscopy GmbH, Göttingen, Germany) digital camera mounted on a Zeiss Discovery V8 dissecting stereoscope (Objective lens: Zeiss 0.5x Achromat S lens and plane eyepiece: widefield 10x/23mm). The root-shoot transition region was assessed manually by the human eye for clubroot disease severity and was further verified with the microscopic images of the roots for accuracy.

The two transgenic lines and their respective nulls were assessed in separate experiments over time. The experimental design for each transgenic line consisted of one *AFB6* transgenic line and its respective null line (2 lines) x (2) applications (inoculated and non-inoculated) for a total of 4 treatments. The same growth chamber was used for all experiments, and replications within each experiment were sequenced over time to obtain sufficient replication for each experiment. For estimating clubroot symptom severity and calculating the clubroot disease index, four independent biological replications with 28 to 32 inoculated plants per replication of *AFB6-9* transgenic (PCR+) and *AFB6-9* Null lines were assessed. In addition, four independent biological replications with 8 non-inoculated plants per replication of *AFB6-9* transgenic (PCR+) and *AFB6-9* Null lines were grown as controls at the same time. For the experiment with the

*AFB6-52* transgenic line, three independent biological replications consisting of 12 to 16 inoculated plants per replication of *AFB6-52* transgenic (PCR+) and *AFB6-52* Null lines were assessed. Four independent biological replications with 8 non-inoculated plants per replication of *AFB6-52* transgenic (PCR+) and *AFB6-52* Null lines were assessed for clubroot symptom severity and clubroot disease index. Plants that grew very poorly and developed minimal roots were excluded from the analysis.

### 3.2.3 Digitized clubroot disease scoring

Clubroot disease scoring was performed on the plants at the time of harvest at 30 dai, and these disease scores were further verified using the digitized microscopic images of the root-shoot transition zone taken at harvest. For disease scoring, a 0–9 scale using a modified method developed by Zhang et al. (2015) was employed, where 0 = no galling (no symptoms or infection), 1-3 = small galls on less than 1/3 of the root, 4-6 = moderate galling (small to medium-sized galls on 1/3 ~ 2/3 of the root, and 7-9 = severe galling (medium to large-sized galls on more than 2/3 of root) with 9 being heavily infected seedlings with severe galling and virtually 100% of root tissue being affected (Figure 3.1). The resulting severity scores were then used to calculate the disease index (DI) following the formula developed by Horiuchi & Hori (1980) and modified by Strelkov et al. (2006): DI (%) = [(n 1× 1 + n 2× 2 + …+n 9× 9)/(N ×9)] × 100, where n1, n2, …n9 refer to the number of plants in each symptom severity class and N refers to the total number of plants tested.

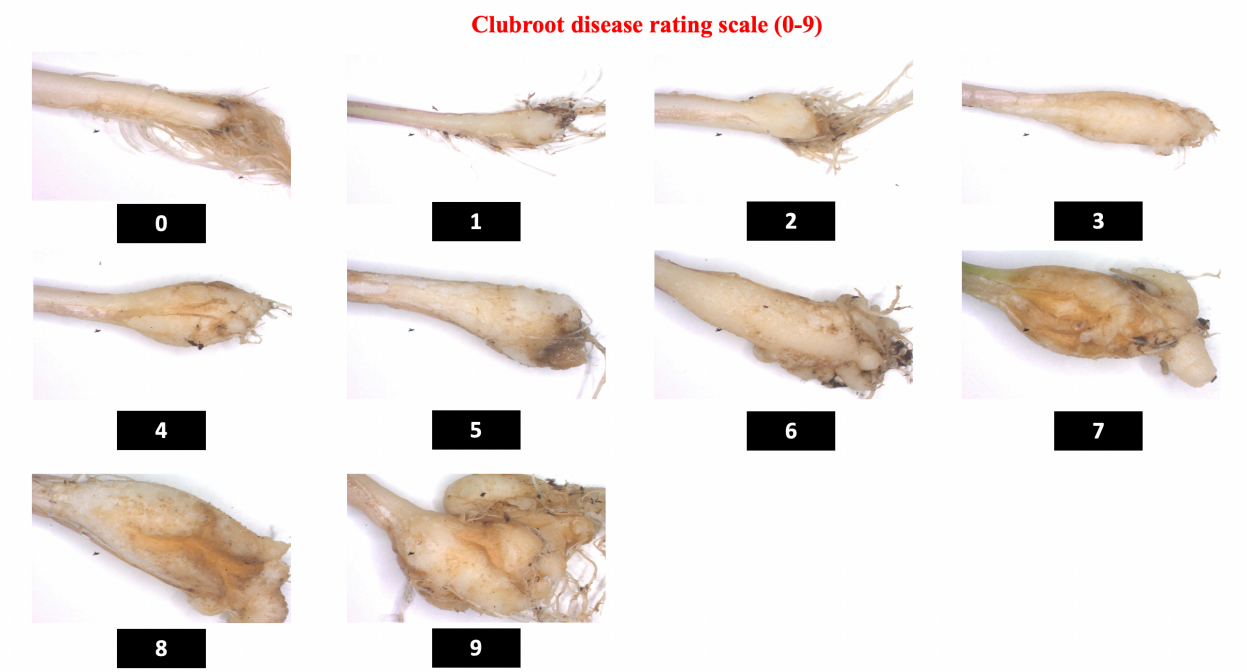


**Figure 3.1 Representative images of the disease rating scale range of clubroot symptoms on digitized microscopic images of the root-shoot transition zone of canola cv. Westar at 30 days after *P. brassicae* inoculation**. The disease rating scores range from 0 to 9, with 0 representing a plant with no galling symptoms and 9 representing a severely infected plant with extensive root swelling.

### 3.2.4 Root surface area quantification

First the digitalized quantification of the root surface area was performed on the digitized microscopic images of the root-shoot transition zone using freely accessible ImageJ software. All the images were processed with Python (Van Rossum and Drake, 2009) to the same pixel width (294), height (244), size (1 x 1 pixel squares), and bits per pixel (32 RGB). Then the actual root surface area was obtained from the digitalized root surface area using a Canadian dime (10-cent coin, diameter = 18.03 mm) as a reference.

### 3.2.5 Statistical analysis

Statistical analysis was performed using R studio software version 1.2.5001. (RStudio Team (2020). RStudio: Integrated Development for R. RStudio, PBC, Boston, MA URL http://www.rstudio.com/.) In detail, the data were checked for normality with Shapiro-Wilk test and homogeneity of variances with Levene's test. Independent Student's t-test (two-tailed) was used to compare differences between means of the clubroot-inoculated canola cv. Westar expressing pea auxin receptor transgenic *AFB6* PCR+ line and its respective *AFB6* Null line for clubroot disease index.

For root surface area, the experimental design was 2 (canola cv. Westar pea auxin receptor expressing *AFB6* line: transgenic *AFB6-9* PCR+ and its respective *AFB6-9* Null or transgenic *AFB6-52* PCR+ and its respective *AFB6-52* Null) x 2 (applications: non-inoculated and 30 d-*P. brassicae*-inoculated plants) factorial, where each plant was treated as a replicate. For the *AFB6-9* transgenics, non-inoculated *AFB6-9* Null, n = 26; non-inoculated *AFB6-9* PCR+, n = 23; clubroot-inoculated *AFB6-9* Null, n = 123; and non-inoculated *AFB6-9* PCR+, n = 121. For the *AFB6-52* transgenics, non-inoculated *AFB6-52* Null, n = 16; non-inoculated *AFB6-52* PCR+, n = 15; clubroot-inoculated *AFB6-52* Null, n = 41; non-inoculated *AFB6-52* PCR+, n = 40. A two-way analysis of variance (ANOVA) was performed on the root surface area quantification data. Mean separation was performed using Tukey's Honest Significant Difference (Tukey’s HSD) post-hoc test. Statistical significance for all statistical testes was declared at $P \leq 0.05$ (see Appendix Tables B1 and B2 for ANOVA details).

## 3.3 RESULTS

### 3.3.1 A 7 dai hydroponic root assay system for digitized clubroot disease scoring

A hydroponic system for the clubroot primary infection stage (0-7 dai) was established as a technique for inoculating canola seedlings in a soil-less medium with a single spore isolate suspension of *P. brassicae* which eliminates interference from soil and peat-based media on the host-pathogen interactions during this process. At 7 dai, the clubroot-inoculated canola transgenic *AFB6-9* PCR+ and its respective *AFB6-9* Null seedlings were visually distinct from their non-inoculated control seedlings in terms of the size of the cotyledonary leaves and the root morphology (Figures 3.2 & 3.3). Fifteen-day-old seedlings (8 days of growth in Petri dishes followed by 7 days of growth in the hydroponic system) non-inoculated canola transgenic *AFB6-9* PCR+ and its respective *AFB6-9* Null had normal cotyledonary leaves (Figure 3.2 B, top view of the seedlings in the bag) with well-developed tap root system (Figure 3.3 A & C). In contrast, at an early stage of clubroot disease (7dai), the inoculated seedlings developed smaller cotyledonary leaves (Figure 3.2 A, top view of the seedlings in the bag) with an overall less extensive root system (Figure 3.3 B & D). Similar changes in plant phenotype were observed in clubroot-inoculated and non-inoculated canola transgenic *AFB6-52* PCR+ and *AFB6-52* Null seedlings at 7dai (Figures 3.4 & 3.5).

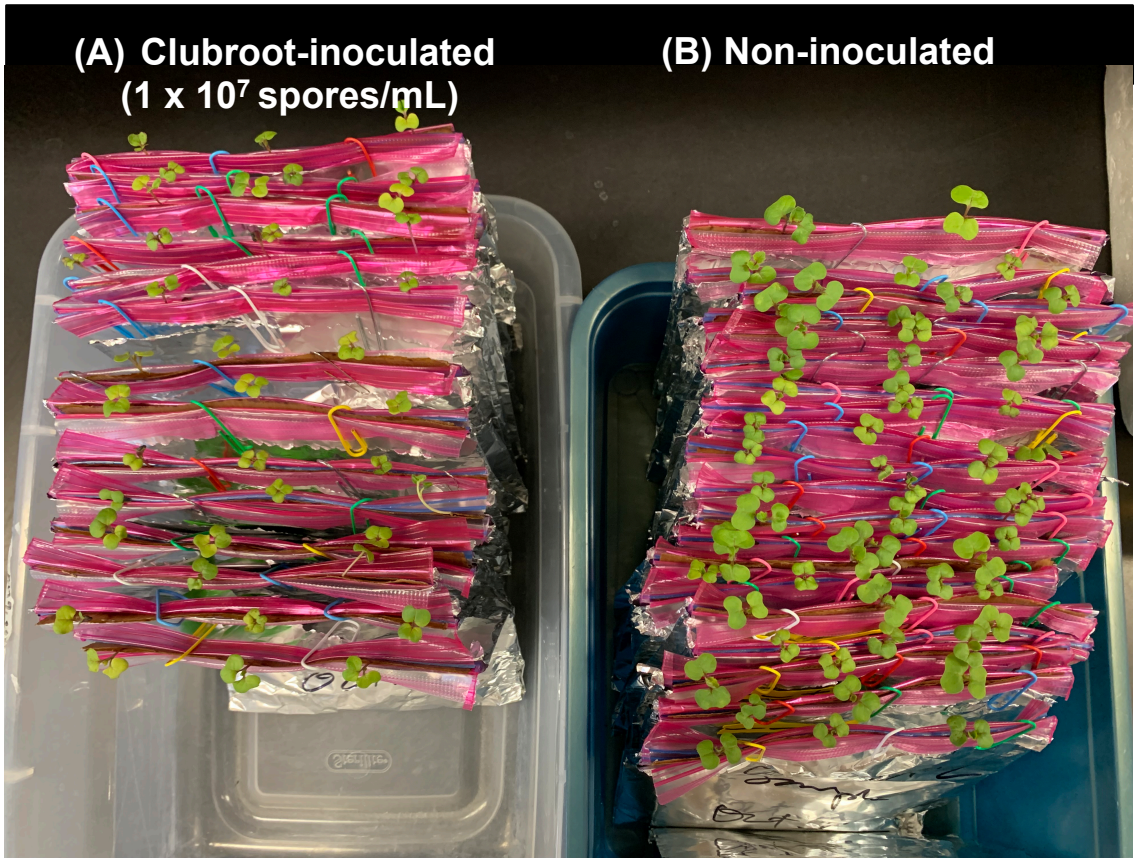


**Figure 3.2 Representative image of clubroot inoculated (A, 1 × $10^7$ spores/mL) and non-inoculated (B) seedlings of canola cv. Westar *AFB6-9* transgenic line (*AFB6-9* PCR+) and its *AFB6-9* Null lines after 7 days of growth in the hydroponic assay system (15 day-old seedlings).** At 7 dai, the cotyledonary leaves of the canola transgenic AFB6-9 PCR+ and AFB6-9 Null seedlings that were inoculated with clubroot were visibly smaller in size compared to their non-inoculated control seedlings.

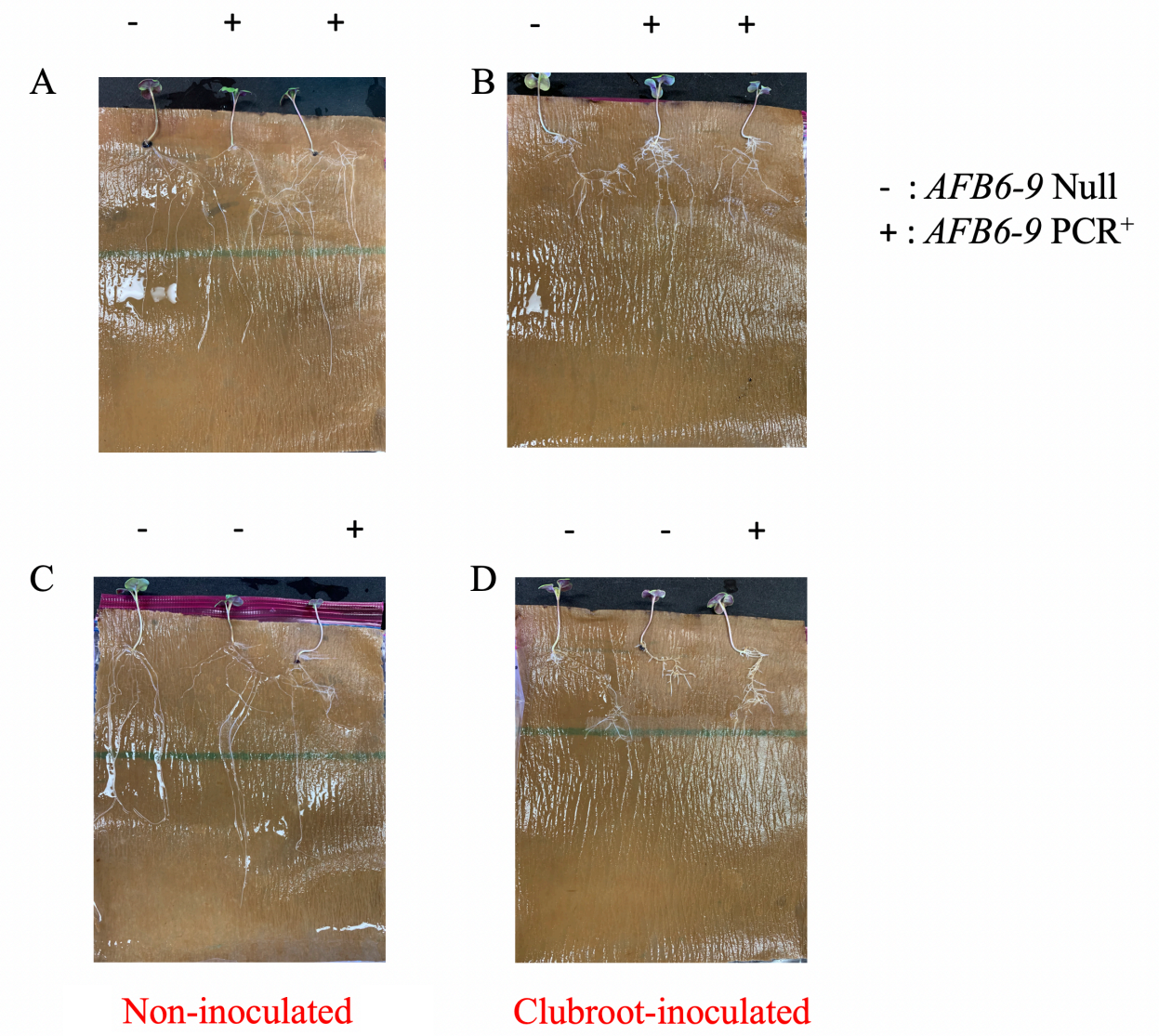


**Figure 3.3 Representative images of roots of canola cv. Westar *AFB6-9* transgenic (*AFB6-9* PCR+: +) and its respective null (*AFB6-9* Null: -) non-inoculated control (A and C) and clubroot-inoculated (B and D) seedlings grown hydroponically in bags for 7 days after inoculation (15 day-old seedlings).** At 7 dai, root length of the canola transgenic AFB6-9 PCR+ and AFB6-9 Null seedlings that were inoculated with clubroot were significantly shorter compared to their non-inoculated control seedlings.

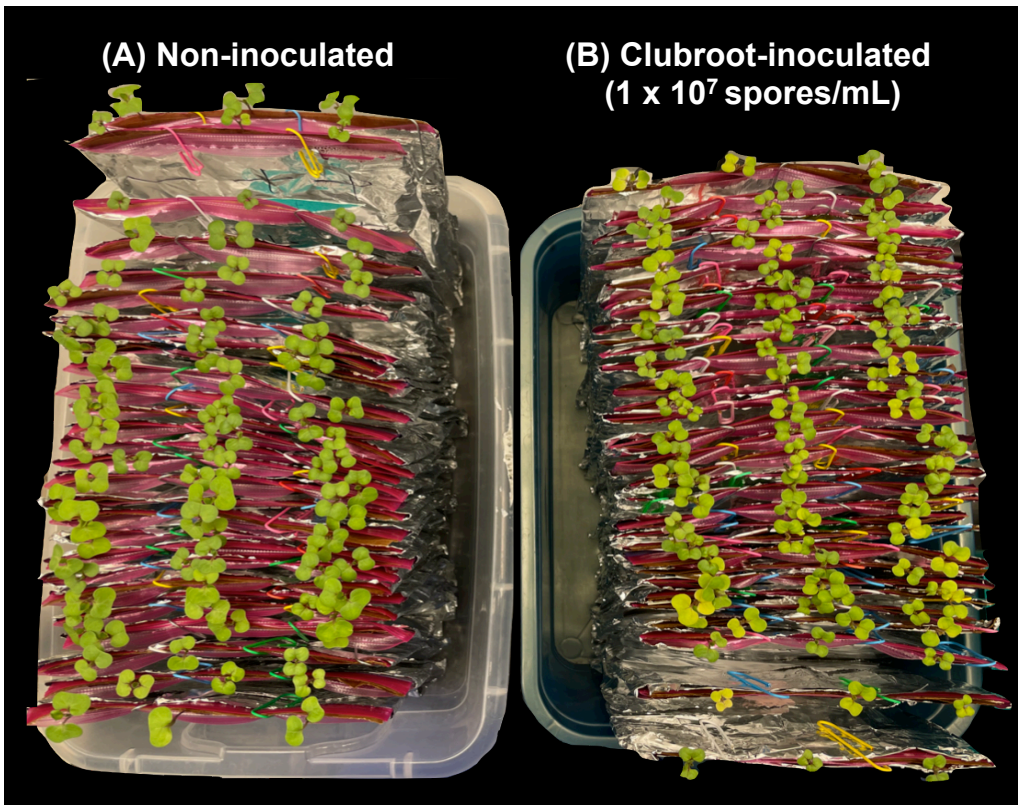


**Figure 3.4 Representative image of non-inoculated (A) and clubroot inoculated (B, 1 × $10^7$ spores/mL) seedlings of canola cv. Westar *AFB6-52* transgenic line (*AFB6-52* PCR+) and its *AFB6-52* Null line after 7 days of growth in the hydroponic assay system (15 day-old seedlings).** At 7 dai, the cotyledonary leaves of the canola transgenic AFB6-52 PCR+ and AFB6-52 Null seedlings that were inoculated with clubroot were visibly smaller in size compared to their non-inoculated control seedlings.

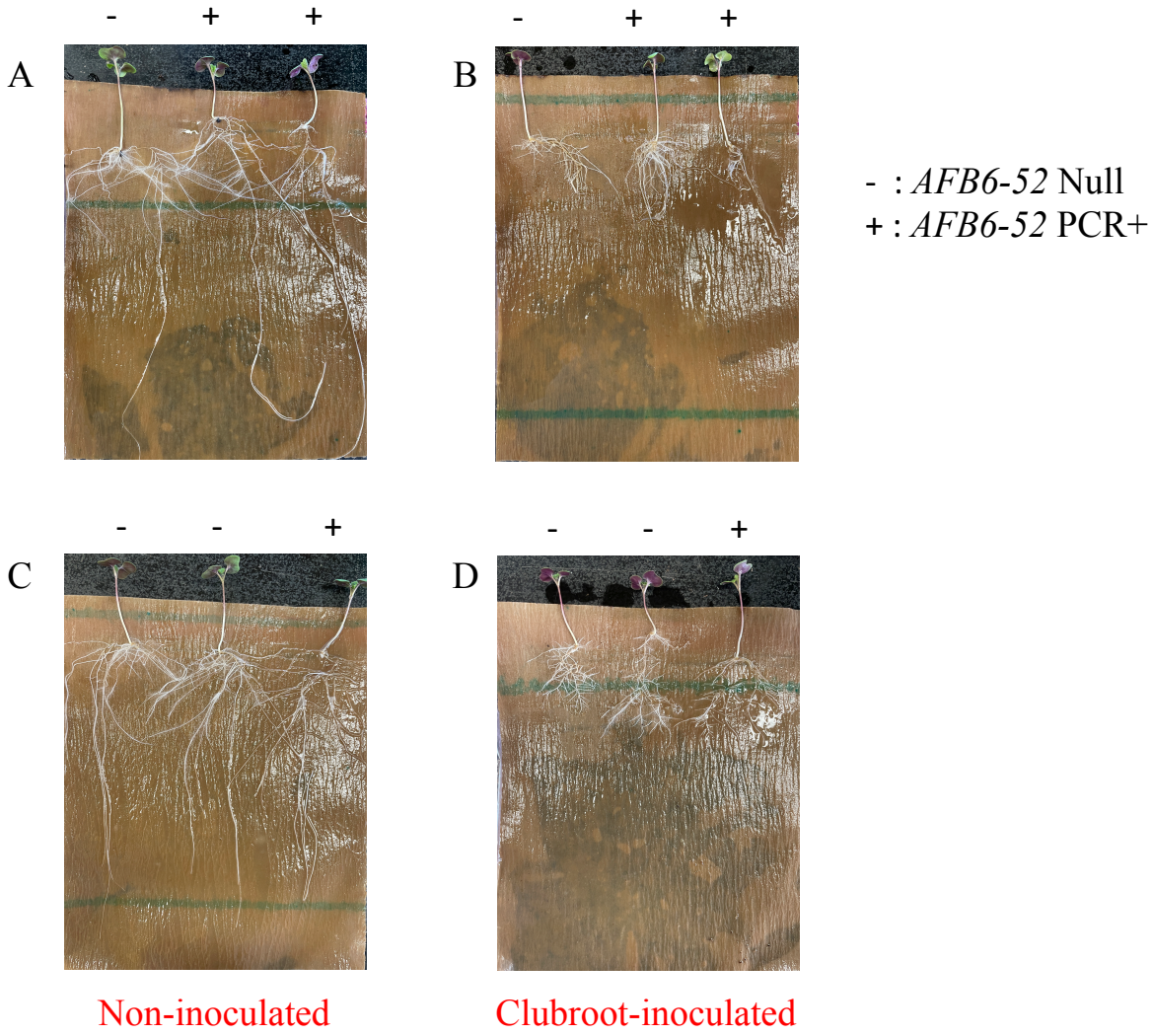


**Figure 3.5 Representative images of roots of canola cv. Westar *AFB6-52* transgenic (*AFB6-52* PCR+: +) and its respective null (*AFB6-52* Null: -) non-inoculated control (A and C) and clubroot-inoculated (B and D) seedlings grown hydroponically in bags for 7 days after inoculation (15 day-old seedlings).** At 7 dai, root length of the canola transgenic AFB6-52 PCR+ and AFB6-52 Null seedlings that were inoculated with clubroot were significantly shorter compared to their non-inoculated control seedlings.

### 3.3.2 The canola cv. Westar transgenic *AFB6* PCR+ plants developed less severe clubroot symptoms compared to their *AFB6* Null plants

To investigate the disease response of a single spore isolate of 3H pathotype of the clubroot pathogen in canola cv. Westar *AFB6* transgenics and their respective null seedlings were harvested at 30 dai (7 days grown hydroponically followed by 23 days of growth in the peat based medium). In general, at the later stages of clubroot disease development (30 dai), the canola *AFB6* transgenic (*AFB6-9* PCR+ and *AFB6-52* PCR+) and their respective *AFB6* Null (*AFB6-9* Null and *AFB6-52* Null) plants showed a range of clubroot symptoms (from no visible symptoms with a disease scale of 0 to large sized galls with disease scale of 7-9; Figures 3.6 & 3.7). At 30 dai, approximately 50 % of *P. brassicae*-inoculated canola cv. Westar *AFB6-9* transgenic (*AFB6-9* PCR+, 64 out of 124 plants) developed milder clubroot disease symptoms and showed higher distribution in the clubroot disease scale range of 0-5 than its respective *P. brassicae*-inoculated *AFB6-9* Null seedlings (~22 %, 27 out of 123 plants). In contrast to the clubroot inoculated *AFB6-9* PCR+ plants (~47 %, 58 out of 124 plants) at 30 dai, the *AFB6-9* Nulls (~76 %, 93 out of 123 plants) developed moderate to severe galling on more than 1/3 of the root with higher abundance in the clubroot disease scale range of 6-8 (Figure 3.8). Altogether, these contrasting differences in the frequency distribution in the scores of clubroot disease of *P. brassicae* inoculated canola *AFB6-9* transgenic (*AFB6-9* PCR+) and its respective null contributed to significant differences in the clubroot disease index (DI) with higher values for *AFB6-9* Null (72.50 ± 3.00 %), which was ~15 % higher than canola *AFB6-9* PCR+ (DI = 57.56 ± 3.23; Figure 3.9). Consistently, the clubroot-inoculated canola *AFB6-9* PCR+ plants also showed approximately 20 % reduction in the root surface area than the clubroot-inoculated canola *AFB6-9* Null plants at 30 dai (Figure 3.10). No difference in the surface area of the primary root was observed in the non-inoculated *AFB6-9* PCR+ and *AFB6-9* Null plants when the experiment was terminated at 38 days (8 days of growth in Petri dishes followed by 7 days in hydroponic root assay system and 23 days in the peat-based medium; Figure 3.10).

In general, at 30 dai, the clubroot-inoculated *AFB6-52* transgenic and null plants developed milder symptoms than the *AFB6-9* transgenic and null plants, which resulted in a shift in the distribution pattern of the clubroot disease scoring. Weak (very poorly growing) plants that developed poor roots were excluded from the analysis. At 30 dai, approximately 68 % of *P. brassicae*-inoculated canola cv. Westar *AFB6-52* transgenic (*AFB6-52* PCR+, 27 out of 40

plants) developed milder clubroot disease symptoms and showed higher distribution in the clubroot disease scale range of 0-3 than its respective *P. brassicae*-inoculated *AFB6-52* Null seedlings (~42 %, 17 out of 41 plants; Figure 3.11). In contrast to the clubroot-inoculated *AFB6-52* PCR+ plants (~33 %, 13 out of 40 plants) at 30 dai, the *AFB6-52* Nulls (~59 %, 24 out of 41 plants) developed medium to large sized galls on more than 1/3 of the root with higher abundance in the clubroot disease scale range of 4-8 (Figure 3.11). Altogether, this differential frequency distribution in the scores of clubroot disease of *P. brassicae*-inoculated canola *AFB6-52* transgenic (*AFB6-52* PCR+) and its respective null contributed to significant differences in the clubroot disease index (DI) with higher values for *AFB6-52* Null (45.23 ± 3.24 %), which was ~9 % higher than canola *AFB6-52* $PCR^+$ (DI = 36.16 ± 0.44; Figure 3.12). Consistently, the clubroot-inoculated canola *AFB6-52* PCR+ plants showed ~19 % reduction in the root surface area than the clubroot-inoculated canola *AFB6-52* Null plants at 30 dai (Figure 3.13). No difference in the surface area of the primary root was observed in the non-inoculated *AFB6-52* PCR+ and *AFB6-52* Null plants when the experiment was terminated at 38 days (8 days of growth in Petri dishes followed by 7 days in hydroponic root assay system and 23 days in the peat-based medium; Figure 3.13). Overall, both independently transformed canola transgenic lines expressing pea auxin receptor *AFB6* transgenic lines showed reduced clubroot disease symptoms compared to their respective null lines in this study.

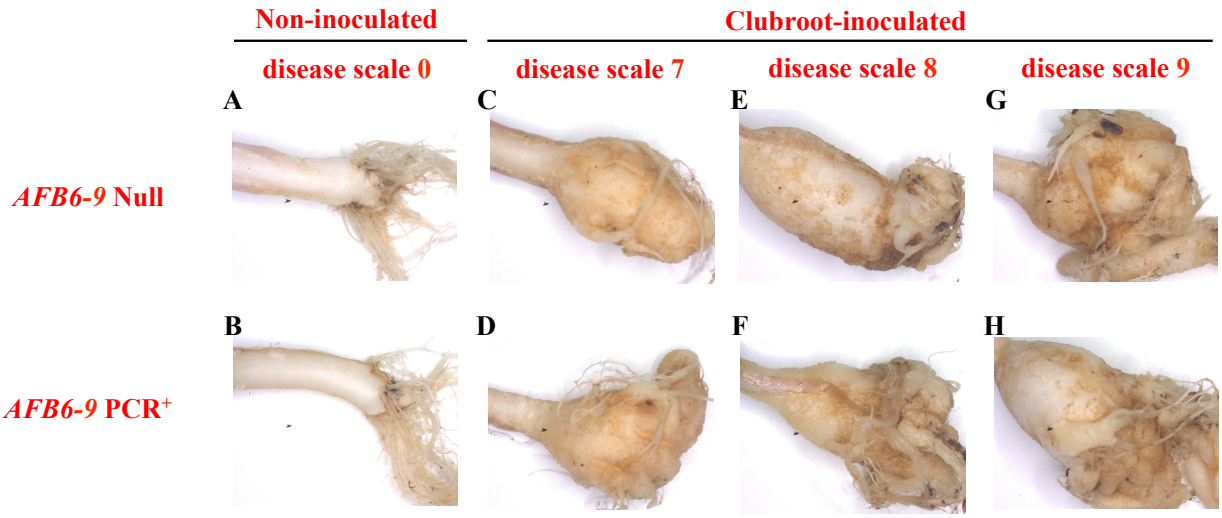


**Figure 3.6 Representative microscopic images of roots of canola cv. Westar *AFB6-9* transgenic (*AFB6-9* PCR+) and its respective null non-inoculated (A and B) and clubroot-inoculated (C to H) seedlings at 30 dai (7 days grown hydroponically followed by 23 days of growth in the peat-based medium).** Disease severity scoring was done as described by Zhang et al. (2016) on a 0-9 scale, where 0 = no visible galls (no infection or symptoms) and 7-9 = medium to large-sized galls on more than 2/3 of root with 9 being the heavily infected seedling with severe galling.

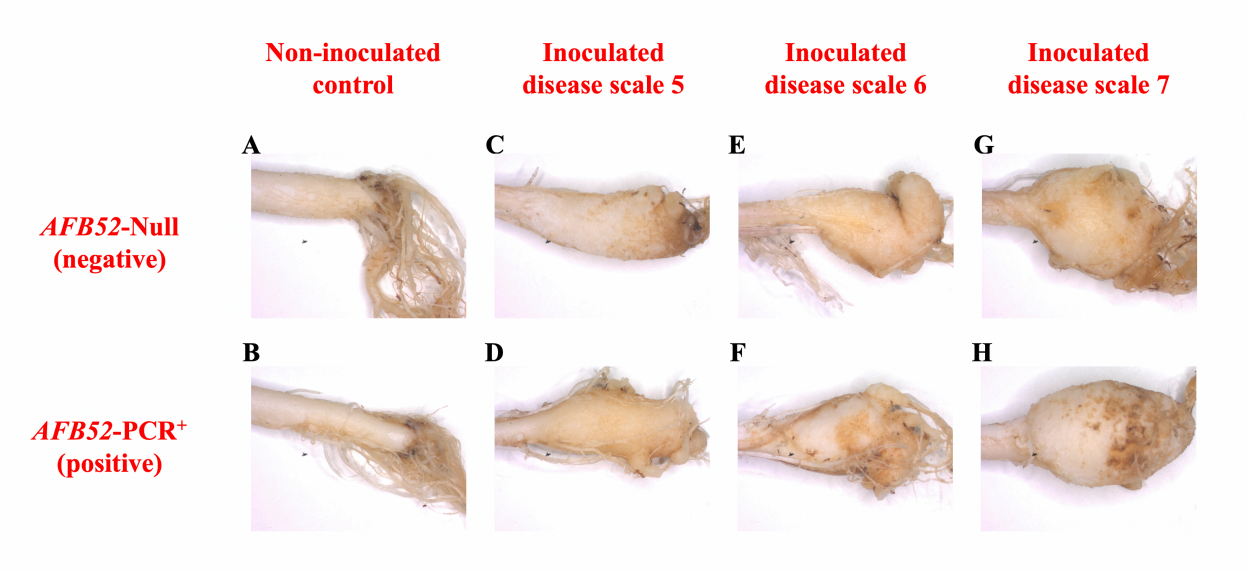


**Figure 3.7 Representative microscopic images of roots of canola cv. Westar *AFB6-52* transgenic (*AFB6-52* PCR+) and its respective null non-inoculated (A and B) and clubroot-inoculated (C to H) seedlings at 30 dai (7 days grown hydroponically followed by 23 days of growth in the peat-based medium).** Disease severity scoring was done as described by Zhang et al. (2016) on a 0-9 scale, where 0 = no visible galls (no infection or symptoms) and 7-9 = medium to large-sized galls on more than 2/3 of root with 9 being the heavily infected seedling with severe galling.

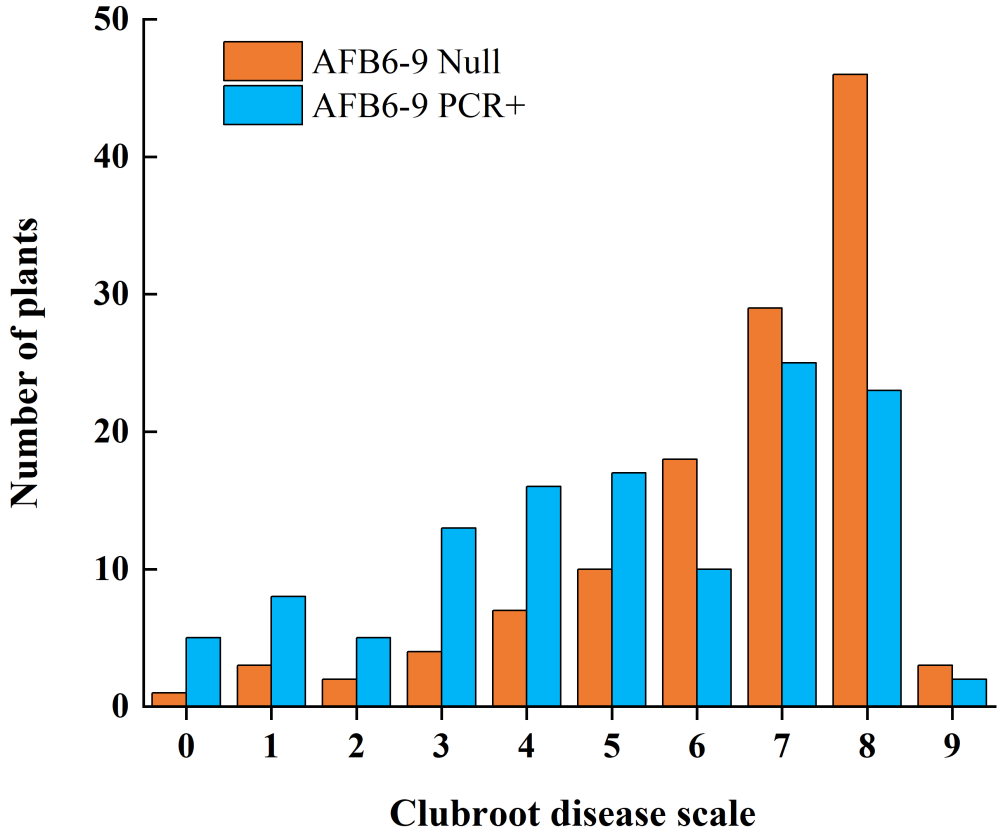


**Figure 3.8 The frequency distribution of *P. brassicae*-inoculated canola cv. Westar *AFB6-9* transgenic (*AFB6-9* PCR+; n = 123) and its respective *AFB6-9* Null (n = 124) seedlings categorised according to the digitized clubroot disease scoring on 0-9 scale at 30 dai (7 days grown hydroponically followed by 23 days of growth in the peat-based medium).** Disease severity scoring was done as described by Zhang et al. (2016) on a 0-9 scale, where 0 = no visible galls (no infection or symptoms) and 9 being the heavily infected seedling with severe galling.

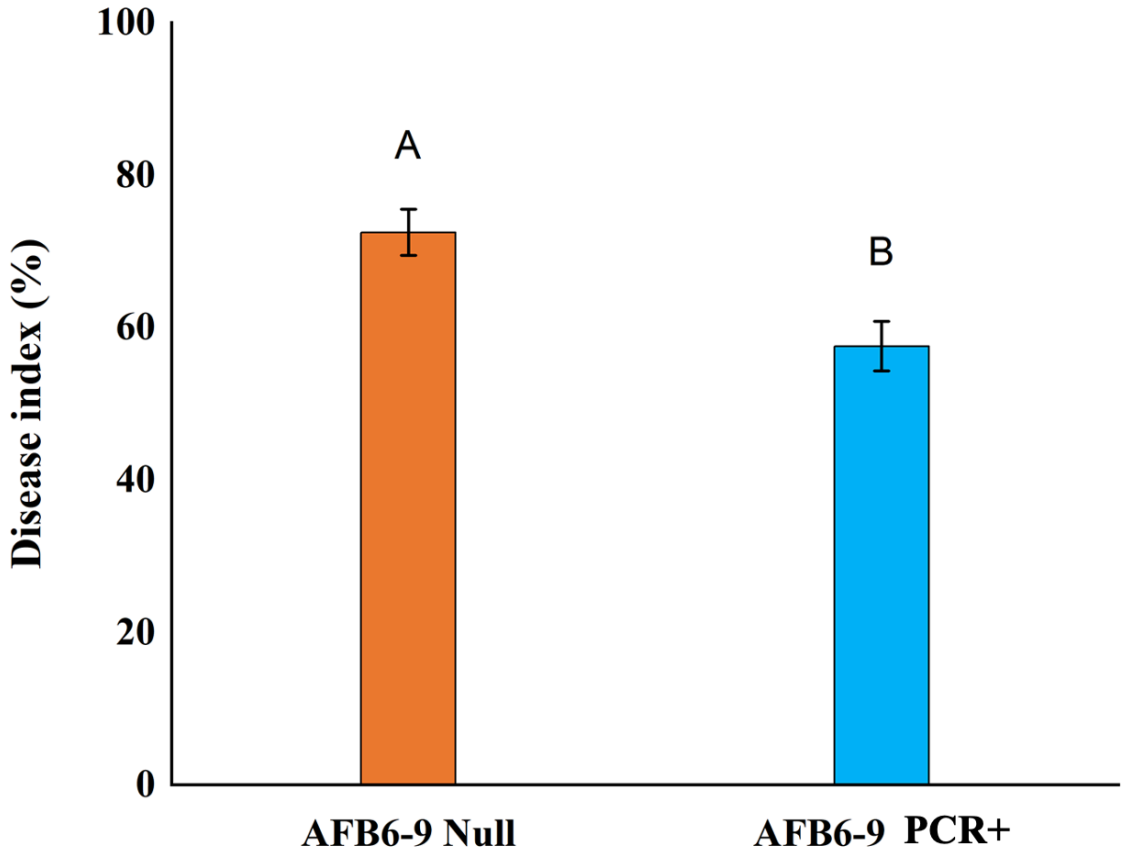


**Figure 3.9 Clubroot disease severity index of the roots of canola cv. Westar *AFB6-9* Null and *AFB6-9* PCR+ plants caused by 3H pathotype single spore isolate of *P. brassicae*.** All the roots of non-inoculated plants were clubroot-symptom free. The scoring was performed at 30 days after *P. brassicae* inoculation (7 days grown hydroponically followed by 23 days of growth in the peat-based medium). Data are the means ± standard error of the mean (SE) from four independent replications (n=4) with 28 to 32 inoculated plants per replication of *AFB6-9* Null and PCR+. Different letters indicate significantly different means between the treatments (Student's T test, $P \leq 0.05$).

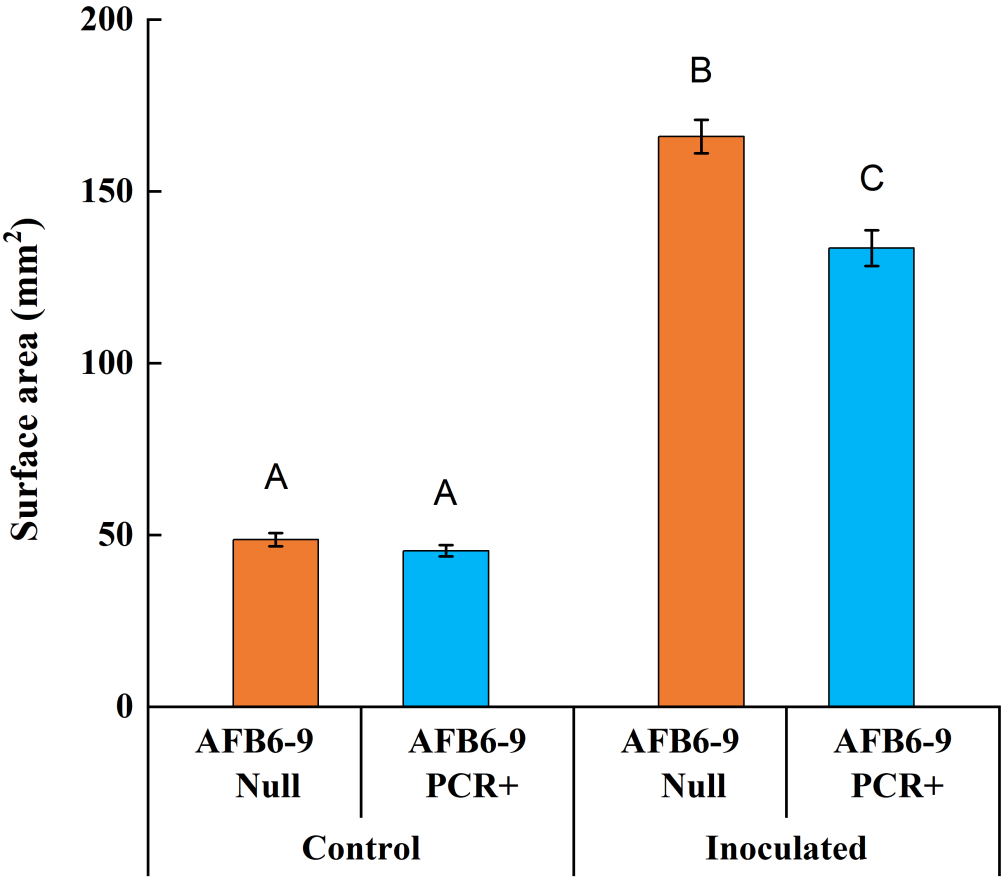


**Figure 3.10 The surface area of the root-shoot transition zone of canola cv. Westar *AFB6-9* Null and *AFB6-9* PCR+ non-inoculated and *P. brassicae*-inoculated plants at 30 dai.** All the roots of non-inoculated plants were clubroot-symptom free. The scoring was performed at 30 days after *P. brassicae* inoculation (7 days grown hydroponically followed by 23 days of growth in the peat based medium). Data are the means ± standard error of the mean (SE). Each plant was treated as a replicate for this analysis (non-inoculated *AFB6-9* Null: n = 26; non-inoculated *AFB6-9* PCR+: n = 23; clubroot-inoculated *AFB6-9* Null: n = 123; non-inoculated *AFB6-9* PCR+: n = 121). Different letters indicate significantly different means between lines within application (non-inoculated or inoculated) by Two-way-ANOVA, Tukey HSD post-hoc test, at $P \leq 0.05$; **Appendix Table B1**).

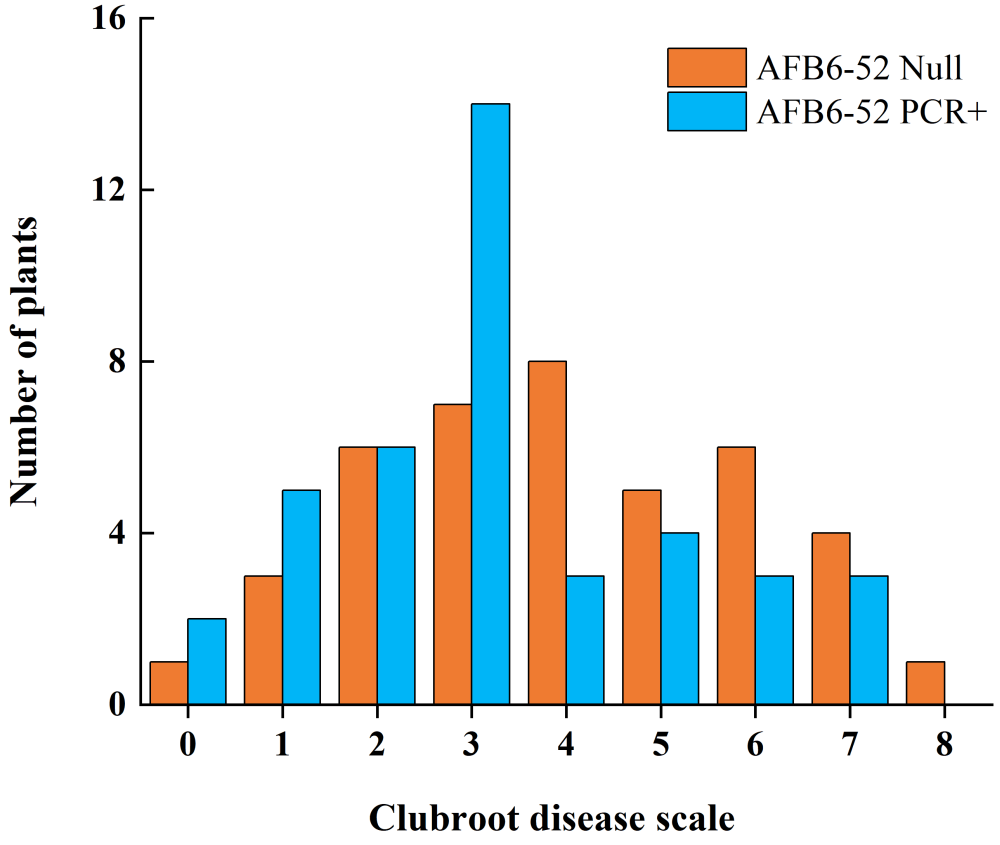


**Figure 3.11 The frequency distribution of *P. brassicae*-inoculated canola cv. Westar *AFB6-52* transgenic (*AFB6-52* PCR+; n = 40) and its respective *AFB6-52* Null (n = 41) seedlings categorised according to the digitized clubroot disease scoring on 0-9 scale at 30 dai (7 days grown hydroponically followed by 23 days of growth in the peat-based medium).** Disease severity scoring was done as described by Zhang et al. (2016) on a 0-9 scale, where 0 = no visible galls (no infection or symptoms) and 9 being the heavily infected seedling with severe galling.

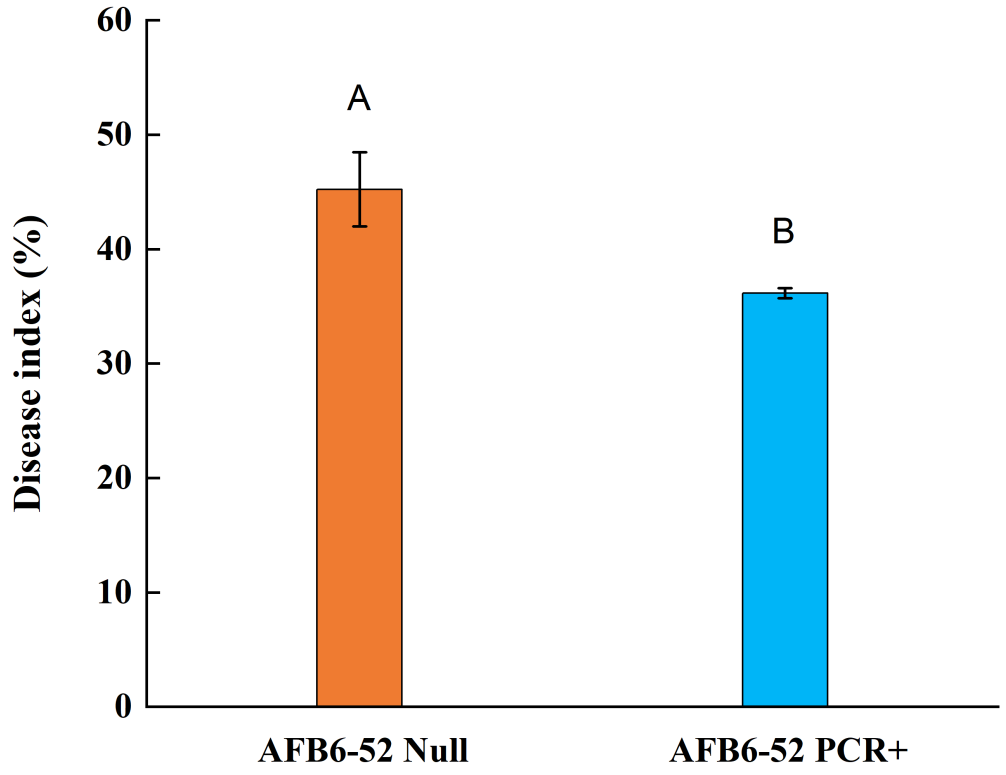


**Figure 3.12 Clubroot disease severity index of the roots of canola cv. Westar *AFB6-52* Null and *AFB6-52* PCR+ plants caused by 3H pathotype single spore isolate of *P. brassicae*.** All the roots of non-inoculated plants were clubroot-symptom free. The scoring was performed at 30 days after *P. brassicae* inoculation (7 days grown hydroponically followed by 23 days of growth in the peat-based medium). Data are the means ± standard error of the mean (SE) from three independent replications (n=3) with 12 to 16 inoculated plants per replication of *AFB6-52* Null and PCR+. Different letters indicate significantly different means between the treatments (Student's T test, $P \leq 0.05$).

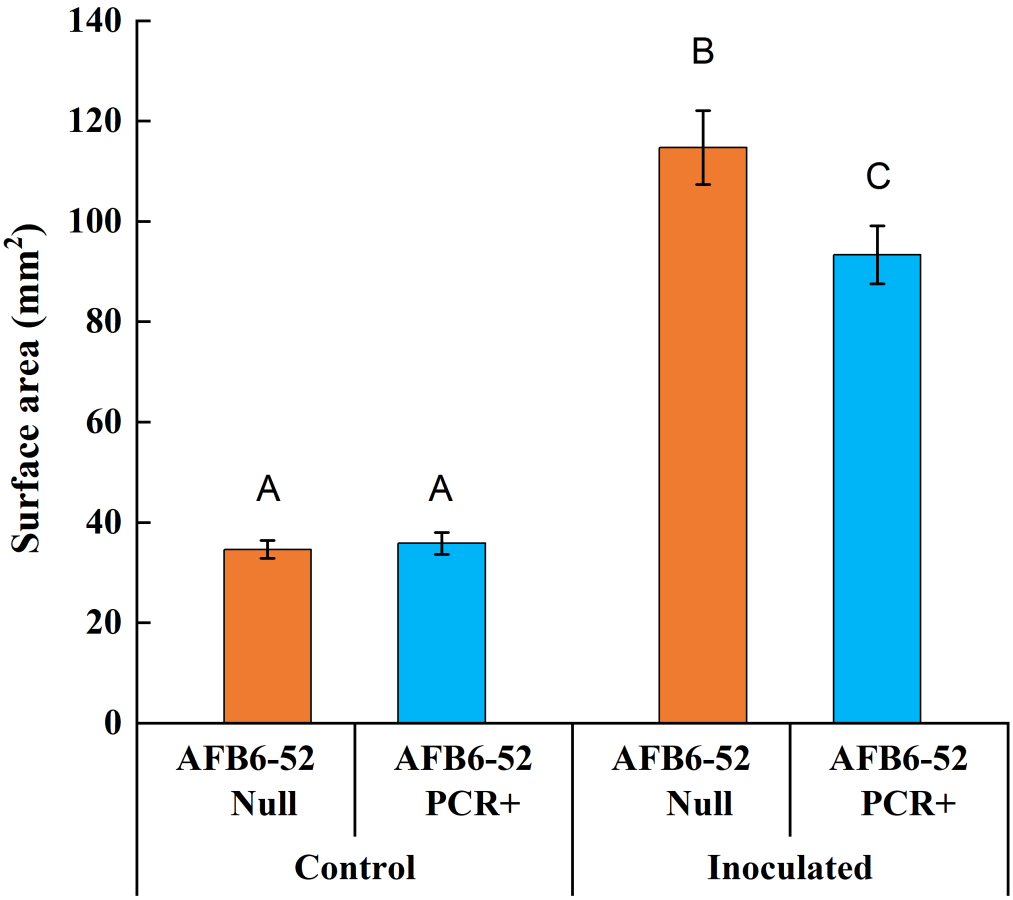


**Figure 3.13 The surface area of root-shoot transition zone of canola cv. Westar *AFB6-52* Null and *AFB6-52* PCR+ non-inoculated and *P. brassicae*-inoculated plants at 30 dai.** All the roots of non-inoculated plants were clubroot-symptom free. The scoring was performed at 30 days after *P. brassicae* inoculation (7 days grown hydroponically followed by 23 days of growth in the peat based medium). Data are the means ± standard error of the mean (SE). Each plant was treated as a replicate for this analysis (non-inoculated *AFB6-52* Null: n = 16; non-inoculated *AFB6-52* PCR+: n = 15; clubroot-inoculated *AFB6-52* Null: n = 41; non-inoculated *AFB6-52* PCR+: n = 40). Different letters indicate significantly different means between lines within application (non-inoculated or inoculated) by Two-way-ANOVA, Tukey HSD post-hoc test, $P \leq 0.05$; **Appendix Table B2**).

## 3.4 DISCUSSION

### 3.4.1 The hydroponic system supported successful *P. brassciae* infection of canola seedings

In order to avoid complex interactions between soil- or peat-based media with host-pathogen interactions at the infection stage, a hydroponic system was developed for the growth of the seedling the first 7 day after pathogen inoculation. In this study, the root morphology of the canola *AFB6* transgenics and their respective transgenic null controls were noticeably different with and without *P. brassicae* inoculation at both 7 dai (Figures 3.3 and 3.5) and 30 dai (Figures 3.6 and 3.7). In general, *P. brassciae*-inoculated canola had shorter roots than non-inoculated canola at 7 dai, and at 30 dai, characteristic galls were present in the inoculated canola, but non-inoculated plants developed a normal root system with fine lateral roots and showed no sign of clubroot disease symptoms at time of harvest. Additionally, the estimates of the surface area of root-shoot transition zone of inoculated canola seedlings were significantly higher than that of the non-inoculated seedlings regardless of the lines (Figures 3.10 and 3.13). These data indicate that *P. brassicae* was able to successfully inoculate the root hairs of the canola seedlings in the hydroponic system Successful inoculation of the clubroot pathogen in Brassica-hosts using a hydroponic system was also reported in previous studies (Ji et al., 2014; Wa, 2009; Badi, 2013; Xie et al., 2022). The primary phase of clubroot infection is characterized by the infection of root hair by motile zoospores released from the resting spores and the production of primary plasmodia, which upon maturity, form and release secondary zoospores. After 7 days of hydroponic inoculation with the clubroot pathogen, Ji and colleagues (2014) did not observe any external clubroot symptoms in susceptible Chinese cabbage lines, but microscopic examination revealed that the primary plasmodia within the root hair had started to replicate and gradually increase. Similarly, a large number of zoospores were also observed in the susceptible broccoli roots under microscopic observation after hydroponic inoculation conditions, indicating that *P. brassicae* could infect the root hairs in hydroponic systems (Xie et al., 2022). With the extension of infection time, the root hair infection rate at 14 dai was found to be significantly higher than that at 7 dai (Xie et al., 2022). These results are consistent with those in the current study as we did not observe clubroot symptoms in *P. brassciae*-inoculated canola at 7 dai; however, we observed that the *P. brassciae*-inoculated canola roots were in general shorter than the non-inoculated roots. At 30 dai, Ji et al. (2014) found that both infected and neighboring uninfected cells undergo extreme hyperplasia (cell division) and hypertrophy (cell

expansion) under microscopic observation, leading to the formation of the characteristic root galls. These results are consistent with morphological differences that were observed between the non-inoculated and inoculated canola plants, suggesting that the hydroponic system could be successfully used for clubroot inoculation. Furthermore, it was observed that the hydroponic system facilitated abundant growth of root tissues without disrupting clubroot infection (Wa, 2009). This growth led to the ability to harvest greater root tissue mass and obtain significantly higher total RNA yields from seedlings grown hydroponically than those harvested from the soil-based system.

### 3.4.2 The canola cv. Westar *AFB6* transgenic lines showed less severe clubroot symptoms than their respective transgenic null controls

At 7 dai, no difference was observed in external morphology between *P. brassciae*-inoculated canola *AFB6* transgenic and their respective transgenic null controls. However, canola *AFB6* transgenic lines showed a notable reduction in their DI compared to their corresponding transgenic null controls at 30 dai. Furthermore, at 30 dai when characteristic galls were present in both canola *PsAFB6* expressing lines (*AFB6* PCR+) and canola *AFB6* Null lines, both *P. brassciae*-inoculated canola *AFB6-9* $PCR^+$ and canola *AFB6-52* $PCR^+$ exhibited significantly reduced surface area at the root-shoot transition zone compared to their corresponding transgenic null controls, indicating that canola *AFB6* PCR+ plants had milder galling symptoms than their respective transgenic null controls in response to *P. brassciae*. Previous research suggested that the AFB6 auxin receptor, along with auxin receptors belonging to the TIR1, AFB2, and AFB4 clades, regulate plant growth and development via the auxin-dependent signaling pathways, potentially governing the elongation of primary and lateral roots (Ozga et al., 2022; Rogato et la., 2021). Auxin facilitates the physical interaction between TIR1/AFB receptors and Aux/IAA repressor proteins, resulting in the breakdown of the repressors and subsequent activation of auxin response transcription factors (ARFs), which bind to specific AREs and modulate the transcription of genes responsive to auxin. Given this mode of action for auxin receptors and the proposed role for auxin facilitating gall development, the reduction in clubroot symptoms in *PsAFB6*-expressing canola lines appears to be the result of reduced auxin response in these lines. We propose two potential ways reduced auxin response could occur in the *PsAFB6*-expressing canola lines (Figure 3.14). The first option is that the pea AFB6 auxin receptor, produced

through the expression of *PsAFB6*, competes for auxin binding with the endogenous auxin receptors such TIR1 and AFB2, but it does not initiate the auxin signaling cascade. In such a scenario, the PsAFB6 auxin receptor functions as an auxin sink, thereby reducing the auxin levels in the roots of the transgenic plants and subsequently decreasing the signaling and response to auxin, resulting in milder galling symptoms in *P. brassciae* inoculated plants. The second option is that the PsAFB6 auxin receptor binds auxin, but it initiates auxin signaling pathways (by facilitating degradation of specific Aux/IAA proteins) in a manner that leads to reduced clubroot galling symptoms.

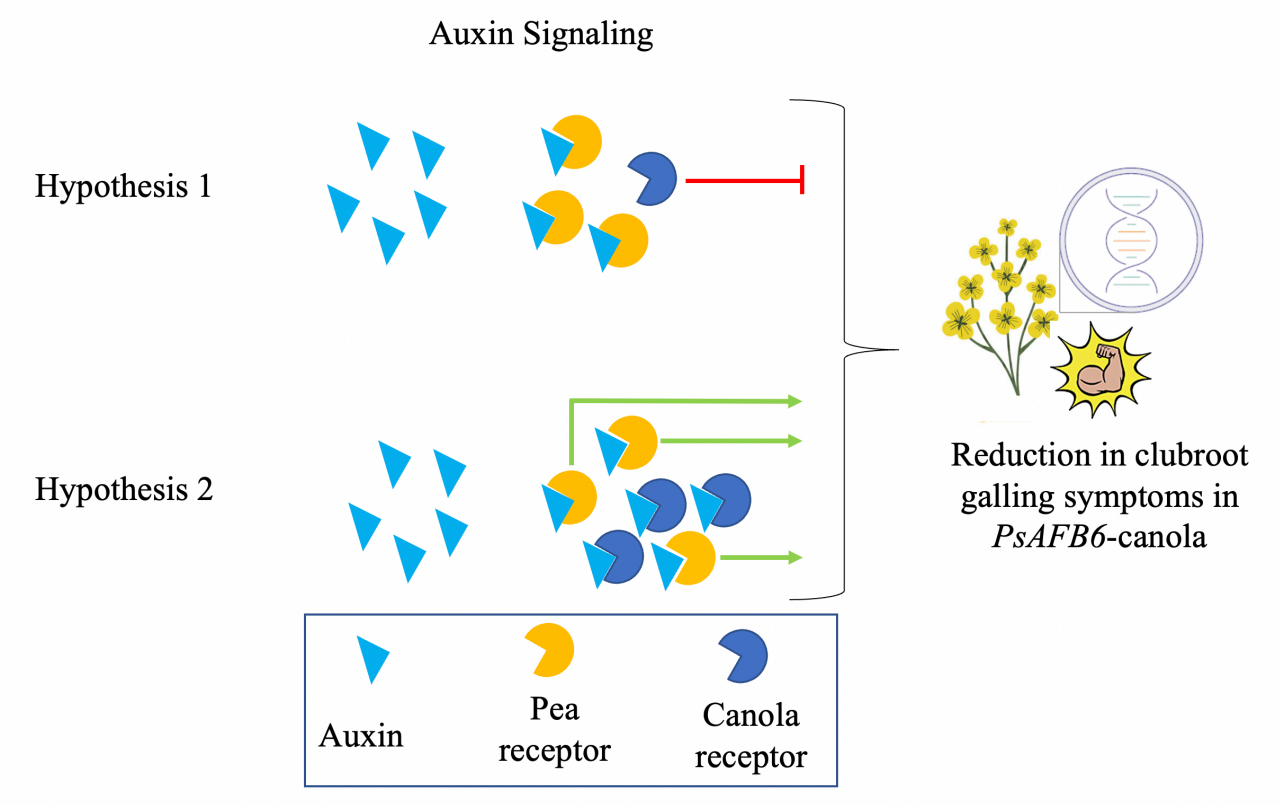


**Figure 3.14 Two potential working models of *PsAFB6*-mediated reduction in clubroot galling symptoms in canola.** Hypothesis 1: reduced clubroot galling symptoms in PsAFB6-expressing canola lines results from competition for auxin binding between PsAFB6 and the endogenous auxin receptors, which reduces auxin signalling and response in the transgenic plants. Hypothesis 2: PsAFB6 binds auxin and modifies the resulting auxin signal transduction pathway in a manner that leads to reduced clubroot galling symptoms.

### 3.4.3 Summary

In conclusion, the successful implementation of a hydroponic system during the infection phase of *P. brassciae* with canola as the host plant allowed the characterization of the effect of modulation of auxin response on clubroot disease progression to be completed without interference with the complexities of soil- or peat-based media interactions. The observed milder clubroot symptoms in the canola *AFB6* transgenic lines compared to their transgenic null controls suggest that the expression of the pea AFB6 auxin receptor in canola reduced the auxin response in the roots and thereby lead to the reduction of galling symptoms during a later infection stage. Further studies are needed to confirm that a reduction in auxin response is the main mechanism involved in *PsAFB6*-induced reduction in clubroot galling symptoms, and to determine the exact mode of action bringing about the potential reduction in auxin response. Identifying the specific pathways involved in *PsAFB6*-mediated reduction in clubroot galling symptoms could potentially lead to the development of novel approaches for disease management in canola.

# Chapter 4: Conclusions and future directions

## 4.1 INTRODUCTION

Clubroot pathogen infection leads to alterations in the host plant's physiology, including changes to primary and secondary metabolic and regulatory networks, such as plant hormone homeostasis (Malinowski et la., 2019; Ludwig-Müller and Schuller, 2007). Cumulative evidence suggests that indole GSL, which can serve as a precursor for auxin biosynthesis, correlates with clubroot disease (Butcher et al., 1974; Ockendon and Buczacki, 1979; Chong et al., 1981). The analysis of a database from Zhou et al. (2020) revealed that in response to *P. brassicae* inoculation, the resistant rutabaga cultivar "Whilhelmsburger" exhibited a distinct gene expression pattern in the indole GSL pathway when compared to the susceptible rutabaga cultivar "Laurentian". Following the transcriptomic data analysis, qRT-PCR was conducted on the early stage of pathogen infection (7 dai) to validate gene expression profile changes in the indole GSL and general GSL degradation pathway and to confirm their association with the observed resistance in the 'Wilhelmsburger' cultivar (as described in chapter 2).

The hormone auxin has been implicated in the formation of galls induced by *P. brassicae*, which promotes cell hyperplasia and hypertrophy. The absence of the AFB6 clade of auxin receptors in Brassicaceae and Poaceae families has been inferred from phylogenetic analysis (Parry et al., 2009). In the absence of the auxin receptor AFB6 clade in Brassicaceae, transgenic canola (*Brassica napus*) plants expressing the auxin receptor AFB6 from pea were created in the Ozga lab. Analysis of the transgenic canola plants has shown that they exhibit less severe clubbing symptoms when infected with clubroot and that the expression of *PsAFB6* modifies auxin response, increasing stress tolerance and lateral bud break. To gain insight into the function of the pea auxin receptor AFB6 in the development of clubroot disease in canola, a new hydroponic system was developed to characterize disease progression in two independently transformed canola (cv. Westar) lines expressing the pea auxin receptor AFB6 (*AFB6-9* PCR+ and *AFB6-52* PCR+) and their respective transgenic null controls (as described in chapter 3).

Understanding regulation of GSL metabolism during early clubroot infection and the function of the pea auxin receptor AFB6 in the development of clubroot disease in canola may be

informative and important for the development of canola cultivars with resistance to clubroot disease.

## 4.2 GENERAL CONCLUSIONS

In chapter 2, we conducted qRT-PCR validation on the expression changes of 9 genes in the GSL pathway including *BnCYP81F2, BnCYP81F4, BnIGMT5, BnBGLU30, BnNSP5, BnNIT2, BnNIT4, BnIAGLU, BnGSTU13* in the roots of *P. brassicae*-inoculated (7 dai) and non-inoculated controls of the two cvs. of interest, respectively the clubroot resistant cultivar "Wilhelmsburger" and the clubroot susceptible cultivar "Laurentian". Our study indicates that when rutabaga roots are infected with *P. brassicae*, certain genes involved in the production of nitriles are upregulated, resulting in increased nitrile production as a primary response to the infection. Nitriles are known for their toxicity to herbivores and fungal pathogens, which implies that they may contribute significantly to the plant's defense mechanism. Moreover, the gene expression pattern of the resistant cv. suggests that it has a higher potential to produce and maintain nitrile levels as a primary response to *P. brassicae* compared to the susceptible cv. Interestingly, the expression of *BnIAGLU*, which conjugates free IAA to an inactive IAA-glucose ester, is exclusively observed in the resistant cv. This suggests that *P. brassicae* resistance at the primary infection stage may be associated with increased IAA conjugation. In summary, our findings suggest that the resistant cv. may exhibit a stronger defense response against clubroot infection at the primary infection stage.

In Chapter 3, we developed a novel hydroponic system to evaluate two canola (cv. Westar) lines that were independently transformed to express the pea auxin receptor AFB6 (*AFB6-9* PCR+ and *AFB6-52* PCR+) along with their corresponding transgenic null controls. Our analysis, based on both DI and digital measurement of gall surface area, revealed that the canola *AFB6* PCR+ plants had milder clubroot symptoms compared to their respective transgenic null controls when infected with *P. brassicae*. This observation implies that the expression of the pea AFB6 auxin receptor in canola reduced the auxin response in the roots and thereby lead to the reduction of galling symptoms during a later infection stage.

## 4.3 FUTURE DIRECTIONS

My thesis findings could provide a basis for further investigation into the interaction between *P. brassicae* and B. napus. This will not only include the elucidation of the mechanisms underlying the defense response in "Wilhelmsburger" and the quantification of specific GSLs-related compounds including nitriles in the pathway to correlate gene expression changes with changes in GSL products produced but also the identification of the underlying mechanism involved in *PsAFB6*-mediated clubroot resistance. I elaborate on the specifics of these potential avenues for research in the following discussion.

In chapter 2, I discussed that the gene expression pattern of the clubroot resistant cultivar indicated that it has a higher potential to produce and maintain nitrile levels as a primary response to *P. brassicae* compared to the susceptible cv. However, the changes in GSLs and GSL products produced at 7 dai remained unknown in both cvs. Therefore, to establish a correlation between gene expression changes and alterations in GSLs and GSL-related compounds, future studies could employ High-pressure liquid chromatography-diode array detection (HPLC-DAD) to quantify the levels of these specific compounds in the pathway. For GSL quantitation, the HPLC-DAD procedure of Grosser and van Dam (2017) could be used. The GSL compounds of interest that could be quantitated might include glucobrassicin, 1-methoxyglucobrassicin, and 4-methoxyglucobrassicin. Moreover, this should also include the changes of content of the main GSLs in rutabaga including 2-hydroxy-3-butenyl-GSL, 4-(methylthio) butyl-GSL, and 2-phenylethyl-GSL (Carlson et al., 1981) upon *P. brassicae*-inoculation in both cvs. at 7 dai. For GSL products quantitation, the UPLC-MS/MS/MS procedures described in Tivendale et al (2012), Lam et al (2015), and Revelou et al. (2020) could be used. The nitriles of interest that could be quantitated should include the nitriles listed in (Table 1.1) that are derived from the main GSLs in rutabaga. Additionally, as discussed in chapter 2, the exclusive expression of *BnIAGLU*, responsible for conjugating free IAA to an inactive IAA-glucose ester, in the resistant cultivar suggests a potential association between increased IAA conjugation and *P. brassicae* resistance during the primary infection stage. To verify or provide additional evidence to support this finding, future studies could involve quantifying several compounds including IAN, 4-methoxy-IAN, 1-methoxy-IAN, IAA, and the IAA-glucose ester. Ideally, this correlation between gene expression changes and alterations in GSLs and GSL-related compounds will further advance understanding of the host reaction to clubroot in rutabaga.

In chapter 3, a hydroponic system was established as novel technique in disease characterization of two independently transformed canola (cv. Westar) lines that express pea auxin receptor AFB6 (*AFB6-9* PCR+ and *AFB6-52* PCR+) and their respective transgenic null controls. The results imply that the expression of *AFB6* may confer a protective effect against clubroot disease in canola. To identify the underlying mechanism involved in *PsAFB6*-mediated clubroot resistance, several approaches can be employed in the future. Specifically, to test the hypothesis 1 presented in Figure 3.14, which proposes a potential role for AFB6 receptor as an auxin sink in *PsAFB6*-mediated clubroot resistance, it may be beneficial to quantify the levels of auxin in both *PsAFB6*-expressing and non-expressing plants following clubroot infection. To test hypothesis 2, which proposes that *PsAFB6* may bind auxin and modify the resulting auxin signal transduction pathway in a manner that leads to increased clubroot resistance, transcriptomic analysis could be employed to compare the gene expression patterns in auxin signalling pathway between *PsAFB6*-expressing and non-expressing plants following infection with clubroot, which could lead to the identification of genes and pathways that are differentially regulated in response to clubroot infection in the presence or absence of *PsAFB6*. Furthermore, the hydroponic system was chosen for its notable benefits, which include the use of a mineral nutrient solution for plant growth, facilitating the observation of symptoms during infection stage more easily than with soil-based systems. The system also reduces the challenges associated with soil, such as the growth of potentially contaminating microorganisms that could affect disease development. Other benefits include the ability to maintain a uniform clubroot spore concentration, requiring less space than pot-based systems, facilitating tissue collection, and providing optimal growth conditions, such as consistent temperature and high moisture levels for infection and disease progression. However, the hydroponic system used our study could be further improved as it still involves the use of the peat based medium. Although the current system provides several advantages over traditional soil-based growing methods, the use of peat-based medium can potentially introduce variables that may affect disease progression. Future studies may seek to enhance the hydroponic system used in this research by eliminating the use of peat-based medium and transitioning to a fully hydroponic setup.

## References


**Andersen CL, Jensen JL, Ørntoft TF. 2004.** Normalization of real-time quantitative reverse transcription-PCR DATA: A model-based variance estimation approach to identify genes suited for normalization, applied to bladder and colon cancer data sets. Cancer Research **64**, 5245–5250. doi: 10.1158/0008-5472.can-04-0496

**Ahmed HU, Hwang SF, Strelkov SE, Gossen BD, Peng G, Howard RJ, Turnbull GD**. 2011. Assessment of bait crops to reduce inoculum of clubroot (*Plasmodiophora brassicae*) of canola. Canadian Journal of Plant Science **91**, 545–551. doi: 10.4141/cjps10200

**Agerbirk N, Olsen CE, Sørensen H**. 1998. Initial and final products, nitriles, and ascorbigens produced in Myrosinase-catalyzed hydrolysis of indole glucosinolates. Journal of Agricultural and Food Chemistry **46**, 1563–1571. doi: 10.1021/jf9708498

**Ayers GW, Lelacheur KE**. 1972. Genetics of resistance in rutabaga to two races of *Plasmodiophora brassicae*. Canadian Journal of Plant Science **52**, 897–900. doi: 10.4141/cjps72-155

**Buczacki ST, Toxopeus H, Mattusch P, Johnston TD, Dixon GR, Hobolth LA**. 1975. Study of physiologic specialization in *Plasmodiophora brassicae*: Proposals for attempted rationalization through an international approach. Transactions of the British Mycological Society **65**, 295–303. doi: 10.1016/s0007-1536(75)80013-1

**Bajguz A, Piotrowska A**. 2009. Conjugates of auxin and cytokinin. Phytochemistry **70**, 957–969. doi: 10.1016/j.phytochem.2009.05.006

**Bartel B, Fink GR**. 1994. Differential regulation of an auxin-producing nitrilase gene family in *Arabidopsis thaliana*. Proceedings of the National Academy of Sciences **91**, 6649–6653. doi: 10.1073/pnas.91.14.6649

**Barth C, Jander G**. 2006. Arabidopsis myrosinases TGG1 and TGG2 have redundant function in glucosinolate breakdown and insect defense. The Plant Journal **46**, 549–562. doi: 10.1111/j.1365-313x.2006.02716.x

**Bednarek P, Piślewska-Bednarek Mariola, Svatoš Aleš, *et al.***. 2009. A glucosinolate metabolism pathway in living plant cells mediates broad-spectrum antifungal defense. Science **323**, 101–106. doi: 10.1126/science.1163732

**Blažević I, Montaut S, Burčul F, Olsen CE, Burow M, Rollin P, Agerbirk N**. 2020. Glucosinolate structural diversity, identification, chemical synthesis and metabolism in plants. Phytochemistry **169**, 112100. doi: 10.1016/j.phytochem.2019.112100

**Burmeister WP, Cottaz S, Driguez H, Iori R, Palmieri S, Henrissat B**. 1997. The crystal structures of Sinapis Alba Myrosinase and a covalent glycosyl–enzyme intermediate

provides insights into the substrate recognition and active-site machinery of an S-glycosidase. Structure **5**, 663–676. doi: 10.1016/s0969-2126(97)00221-9

**Burow M, Losansky A, Müller René, Plock A, Kliebenstein DJ, Wittstock U**. 2009. The genetic basis of constitutive and herbivore-induced ESP-independent nitrile formation in Arabidopsis. Plant Physiology **149**, 561–574. doi: 10.1104/pp.108.130732

**Burow M, Zhang ZY, Ober JA, Lambrix VM, Wittstock U, Gershenzon J, Kliebenstein DJ**. 2008. ESP and ESM1 mediate indol-3-acetonitrile production from indol-3-ylmethyl glucosinolate in Arabidopsis. Phytochemistry **69**, 663–671. doi: 10.1016/j.phytochem.2007.08.027

**Burow M, Bergner A, Gershenzon J, Wittstock U**. 2007. Glucosinolate hydrolysis in *Lepidium sativum*—identification of the thiocyanate-forming protein. Plant Molecular Biology **63**, 49–61. 10.1007/s11103-006-9071-5

**Brown PD, Tokuhisa JG, Reichelt M, Gershenzon J**. 2003. Variation of glucosinolate accumulation among different organs and developmental stages of *Arabidopsis thaliana*. Phytochemistry **62**, 471–481. doi: 10.1016/s0031-9422(02)00549-6

**Bhat R, Vyas D**. 2019. Myrosinase: Insights on structural, catalytic, regulatory, and environmental interactions. Critical Reviews in Biotechnology **39**, 508–523. doi:10.1080/07388551.2019.1576024

**Butcher DN, El-Tigani S, Ingram DS**. 1974. The role of indole glucosinolates in the club root disease of the Cruciferae. Physiological Plant Pathology **4**, 127–140. doi: 10.1016/0048-4059(74)90052-6

**Ben-Gera H, Shwartz I, Shao M-R, Shani E, Estelle M, Ori N**. 2012. Entire and goblet promote leaflet development in tomato by modulating auxin response. The Plant Journal **70**, 903–915. doi: 10.1111/j.1365-313x.2012.04939.x

**Badi A. 2013.** Morphological and molecular studies of pathogenicity, virulence and resistance in clubroot caused by *Plasmodiophora brassicae* (Doctoral dissertation, RMIT University).

**Chroston EC, Hielscher A, Strieker M, Wittstock U**. 2022. The impact of nitrile-specifier proteins on Indolic carbinol and nitrile formation in homogenates of *Arabidopsis thaliana*. Molecules **27**, 8042. doi:10.3390/molecules27228042

**Cao T, Manolii VP, Zhou Q, Hwang SF, Strelkov SE**. 2020. Effect of canola (*Brassica napus*) cultivar rotation on *Plasmodiophora brassicae* pathotype composition. Canadian Journal of Plant Science **100**, 218–225. doi: 10.1139/cjps-2019-0126

**Carlson DG, Daxenbichler ME, VanEtten CH, Tookey HL, Williams PH**. 1981. Glucosinolates in Crucifer Vegetables: Turnips and rutabagas. Journal of Agricultural and Food Chemistry **29**, 1235–1239. doi: 10.1021/jf00108a034

**Calderón-Villalobos LI, Lee S, De Oliveira C, *et al.***. 2012. A combinatorial Tir1/AFB–Aux/IAA co-receptor system for differential sensing of Auxin. Nature Chemical Biology **8**, 477–485. doi: 10.1038/nchembio.926

**Chevolleau S, Gasc N, Rollin P, Tulliez J**. 1997. Enzymatic, chemical, and thermal breakdown of 3H-labeled glucobrassicin, the parent indole glucosinolate. Journal of Agricultural and Food Chemistry **45**, 4290–4296. doi: 10.1021/jf970449k

**Chhajed S, Mostafa I, He Y, Abou-Hashem M, El-Domiaty M, Chen S**. 2020. Glucosinolate biosynthesis and the glucosinolate–myrosinase system in plant defense. Agronomy **10**, 1786. doi:10.3390/agronomy10111786

**Chhajed S, Misra BB, Tello N, Chen S**. 2019. Chemodiversity of the glucosinolate-myrosinase system at the Single Cell Type Resolution. Frontiers in Plant Science **10**. doi: 10.3389/fpls.2019.00618

**Clemens S**. 2006. Evolution and function of phytochelatin synthases. Journal of Plant Physiology **163**, 319–332. doi: 10.1016/j.jplph.2005.11.010

**Czerniawski P, Bednarek P**. 2018. Glutathione S-transferases in the biosynthesis of sulfur-containing secondary metabolites in Brassicaceae plants. Frontiers in Plant Science **9**. doi: 10.3389/fpls.2018.01639

**Czubatka-Bieńkowska A, Kaczmarek J, Marzec-Schmidt K, Nieróbca A, Czajka A, Jędryczka M**. 2020. Country-wide qPCR-based assessment of *Plasmodiophora brassicae* spread in agricultural soils and recommendations for the cultivation of Brassicaceae crops in Poland. Pathogens **9**, 1070. doi: 10.3390/pathogens9121070

**Canola Council of Canada**. 2019. List of Clubroot-resistant canola varieties. Available at: https://www.canolacouncil.org/canola-watch/2019/01/10/list-of-clubroot-resistant-canola-varieties/ [Accessed November 20, 2022]

**Canola Council of Canada.** 2021. Updated clubroot maps and survey results. Available at: https://www.canolacouncil.org/canola-watch/2021/01/14/updated-clubroot-maps-and-survey-results/ [Accessed July 25, 2022]

**Canola Council of Canada**. 2022. Grown on Canadian farms, consumed around the world. Available online at: https://www.canolacouncil.org/about-canola/industry/ [accessed November 9, 2022]

**Chong C, Chiang MS, Crête R**. 1981. Thiocyanate ion content in relation to clubroot disease severity in CABBAGES1. HortScience **16**, 663–664. doi: 10.21273/hortsci.16.5.663

**Chong C, Chiang MS, Crete R**. 1985. Studies on glucosinolates in clubroot resistant selections and susceptible commercial cultivars of cabbages. Euphytica **34**, 65–73. doi: 10.1007/bf00022864

**Caldana C, Scheible WR, Mueller-Roeber B, Ruzicic S**. 2007. A quantitative RT-PCR platform for high-throughput expression profiling of 2500 rice transcription factors. Plant Methods **3**. doi: 10.1186/1746-4811-3-7

**Chen J, Pang W, Chen B, Zhang C, Piao Z**. 2016a. Transcriptome analysis of *Brassica rapa* near-isogenic lines carrying clubroot-resistant and –susceptible alleles in response to *Plasmodiophora brassicae* during early infection. Frontiers in Plant Science **6**. doi: 10.3389/fpls.2015.01183

**Chen SW, Liu T, Gao Y, Zhang C, Peng SD, Bai MB, Li SJ, Xu L, Zhou XY, Lin LB**. 2016b. Discovery of clubroot-resistant genes in *Brassica napus* by transcriptome sequencing. Genetics and Molecular Research **15**. doi: 10.4238/gmr.15038243

**Chu M, Song T, Falk KC, *et al.***. 2014. Fine mapping of RCR1 and analyses of its effect on transcriptome patterns during infection by *Plasmodiophora Brassicae*. BMC Genomics **15**. doi: 10.1186/1471-2164-15-1166

**Choe HT, Cosgrove DJ**. 2010. Expansins as agents in Hormone Action. Plant Hormones, 262–281. doi: 10.1007/978-1-4020-2686-7_13

**Ciaghi S, Schwelm A, Neuhauser S**. 2019. Transcriptomic response in symptomless roots of clubroot infected kohlrabi (*Brassica oleracea* var. Gongylodes) mirrors resistant plants. BMC Plant Biology **19**. doi: 10.1186/s12870-019-1902-z

**Chapman EJ, Estelle M**. 2009. Cytokinin and auxin intersection in Root Meristems. Genome Biology **10**, 210. doi: 10.1186/gb-2009-10-2-210

**Dharmasiri N, Dharmasiri S, Estelle M**. 2005a. The F-box protein tir1 is an auxin receptor. Nature **435**, 441–445. doi: 10.1038/nature03543

**Dharmasiri N, Dharmasiri S, Weijers D, Lechner E, Yamada M, Hobbie L, Ehrismann JS, Jürgens G, Estelle M**. 2005b. Plant development is regulated by a family of auxin receptor F Box Proteins. Developmental Cell **9**, 109–119. doi: 10.1016/j.devcel.2005.05.014

**dos Santos Maraschin F, Memelink J, Offringa R**. 2009. Auxin-induced, SCFtir1-mediated poly-ubiquitination marks aux/IAA proteins for degradation. The Plant Journal **59**, 100–109. doi: 10.1111/j.1365-313x.2009.03854.x

**Duca D, Lorv J, Patten CL, Rose D, Glick BR**. 2014. Indole-3-acetic acid in plant–microbe interactions. Antonie van Leeuwenhoek **106**, 85–125. doi: 10.1007/s10482-013-0095-y

**Davies PJ**. 2010. Regulatory factors in hormone action: Level, location and signal transduction. Plant Hormones, 16–35. doi: 10.1007/978-1-4020-2686-7_2

**Diederichsen E, Frauen M, Ludwig-Müller J**. 2014. Clubroot disease management challenges from a German perspective. Canadian Journal of Plant Pathology **36**, 85–98. doi: 10.1080/07060661.2013.861871

**Dixon GR**. 2009. The occurrence and economic impact of *Plasmodiophora brassicae* and Clubroot disease. Journal of Plant Growth Regulation **28**, 194–202. doi: 10.1007/s00344-009-9090-y

**Devos S, Vissenberg K, Verbelen JP, Prinsen E**. 2005. Infection of Chinese cabbage by *Plasmodiophora brassicae* leads to a stimulation of plant growth: Impacts on cell wall metabolism and hormone balance. New Phytologist **166**, 241–250. doi: 10.1111/j.1469-8137.2004.01304.x

**Devos S, Laukens K, Deckers P, Van Der Straeten D, Beeckman T, Inzé D, Van Onckelen H, Witters E, Prinsen E**. 2006. A hormone and proteome approach to picturing the initial metabolic events during *Plasmodiophora brassicae* infection on Arabidopsis. Molecular Plant-Microbe Interactions® **19**, 1431–1443. doi: 10.1094/mpmi-19-1431

**Douglas Grubb C, Zipp BJ, Ludwig-Müller J, Masuno MN, Molinski TF, Abel S**. 2004. Arabidopsis glucosyltransferase UGT74B1 functions in glucosinolate biosynthesis and auxin homeostasis. The Plant Journal **40**, 893–908. doi: 10.1111/j.1365-313x.2004.02261.x

**Ding X, Cao Y, Huang L, Zhao J, Xu C, Li X, Wang S**. 2008. Activation of the indole-3-acetic acid–amido synthetase GH3-8 suppresses Expansin expression and promotes salicylate- and jasmonate-independent basal immunity in Rice. The Plant Cell **20**, 228–240. doi: 10.1105/tpc.107.055657

**Estey RH**. 1994. *Essays on the early history of Plant Pathology and Mycology in Canada*. Montreal, Quebec: McGull-Queen's University Press.

**Fahey JW, Zalcmann AT, Talalay P**. 2001. The chemical diversity and distribution of glucosinolates and isothiocyanates among plants. Phytochemistry **56**, 5–51. doi: 10.1016/s0031-9422(00)00316-2

**Fu J, Wang S**. 2011. Insights into auxin signaling in Plant-Pathogen interactions. Frontiers in Plant Science **2**. doi: 10.3389/fpls.2011.00074

**Frandsen HB, Sørensen JC, Jensen SK, Markedal KE, Joehnke MS, Maribo H, Sørensen S, Sørensen H**. 2019. Non-enzymatic transformations of dietary 2-hydroxyalkenyl and aromatic glucosinolates in the stomach of monogastrics. Food Chemistry **291**, 77–86. doi: 10.1016/j.foodchem.2019.03.136

**Friberg H, Lagerlöf J, Rämert B**. 2006. Usefulness of nonhost plants in managing *Plasmodiophora brassicae*. Plant Pathology **55**, 690–695. doi: 10.1111/j.1365-3059.2006.01408.x

**Fredua-Agyeman R, Hwang SF, Strelkov SE, Zhou Q, Feindel D**. 2018. Potential loss of clubroot resistance genes from donor parent *Brassica rapa* subsp. *rapifera* (ECD 04) during doubled haploid production. Plant Pathology **67**, 892–901. doi: 10.1111/ppa.12816

**Fredua-Agyeman R, Hwang SF, Strelkov SE, Zhou Q, Manolii VP, Feindel D**. 2019. Identification of Brassica accessions resistant to 'old' and 'new' pathotypes of *Plasmodiophora brassicae* from Canada. Plant Pathology **68**, 708–718. doi: 10.1111/ppa.12980

**Fredua-Agyeman R, Yu Z, Hwang SF, Strelkov SE**. 2020. Genome-wide mapping of loci associated with resistance to Clubroot in *Brassica napus ssp. napobrassica* (rutabaga) accessions from Nordic countries. Frontiers in Plant Science **11**. doi: 10.3389/fpls.2020.00742

**Foo HL, Grønning LM, Goodenough L, Bones AM, Danielsen B-E, Whiting DA, Rossiter JT**. 2000. Purification and characterisation of epithiospecifier protein from *Brassica napus*: Enzymic intramolecular sulphur addition within alkenyl thiohydroximates derived from alkenyl glucosinolate hydrolysis. FEBS Letters **468**, 243–246. doi: 10.1016/s0014-5793(00)01176-5

**Gunnaiah R, Kushalappa AC, Duggavathi R, Fox S, Somers DJ**. 2012. Integrated Metabolo-proteomic approach to decipher the mechanisms by which wheat QTL (FHB1) contributes to resistance against *Fusarium graminearum*. PLoS ONE **7**. doi: 10.1371/journal.pone.0040695

**Gachon CM, Langlois-Meurinne M, Henry Y, Saindrenan P**. 2005. Transcriptional co-regulation of secondary metabolism enzymes in Arabidopsis: Functional and evolutionary implications. Plant Molecular Biology **58**. doi: 10.1007/s11103-005-5346-5

**Geu-Flores F, Møldrup ME, Böttcher C, Olsen CE, Scheel D, Halkier BA**. 2011. Cytosolic γ-glutamyl peptidases process glutathione conjugates in the biosynthesis of glucosinolates and Camalexin in Arabidopsis. The Plant Cell **23**, 2456–2469. doi: 10.1105/tpc.111.083998

**Grogan J, DeVito SC, Pearlman RS, Korzekwa KR**. 1992. Modeling cyanide release from nitriles: Prediction of cytochrome p 450-mediated acute nitrile toxicity. Chemical Research in Toxicology **5**, 548–552. doi: 10.1021/tx00028a014

**Grsic-Rausch S, Kobelt P, Siemens JM, Bischoff M, Ludwig-Müller J**. 2000. Expression and localization of nitrilase during symptom development of the Clubroot disease in Arabidopsis. Plant Physiology **122**, 369–378. doi: 10.1104/pp.122.2.369

**Galletti S, Bernardi R, Leoni O, Rollin P, Palmieri S**. 2001 Preparation and biological activity of four epiprogoitrin myrosinase-derived products. Journal of Agricultural and Food Chemistry **49**, 471–476. doi: 10.1021/jf000736f

**Grsic S, Kirchheim B, Pieper K, Fritsch M, Hilgenberg W, Ludwig-Müller J**. 1999. Induction of auxin biosynthetic enzymes by jasmonic acid and in clubroot diseased Chinese cabbage plants. Physiologia Plantarum **105**, 521–531. doi: 10.1034/j.1399-3054.1999.105318.x

**Gowers S**. 2010. Swedes and turnips. Root and Tuber Crops, 245–289. doi: 10.1007/978-0-387-92765-7_8

**Grosser K, van Dam NM**. 2017. A straightforward method for glucosinolate extraction and analysis with high-pressure liquid chromatography (HPLC). Journal of Visualized Experiments. doi: 10.3791/55425

**He Q, Yang L, Hu W, Zhang J, Xing Y**. 2018. Overexpression of an auxin receptor OSAFB6 significantly enhanced grain yield by increasing cytokinin and decreasing auxin concentrations in rice panicle. Scientific Reports **8**. doi: 10.1038/s41598-018-32450-x

**Harun S, Abdullah-Zawawi MR, Goh HH, Mohamed-Hussein ZA**. 2020. A comprehensive gene inventory for glucosinolate biosynthetic pathway in *Arabidopsis thaliana*. Journal of Agricultural and Food Chemistry **68**, 7281–7297. doi: 10.1021/acs.jafc.0c01916

**Halkier BA, Gershenzon J**. 2006. Biology and biochemistry of glucosinolates. Annual Review of Plant Biology **57**, 303–333. doi: 10.1146/annurev.arplant.57.032905.105228

**Hirai M**. 2006. Genetic analysis of Clubroot resistance in brassica crops. Breeding Science **56**, 223–229. doi: 10.1270/jsbbs.56.223

**Hossain MS, Ye W, Hossain MA, Okuma E, Uraji M, Nakamura Y, Mori IC, Murata Y**. 2013. Glucosinolate degradation products, isothiocyanates, nitriles, and thiocyanates, induce stomatal closure accompanied by peroxidase-mediated reactive oxygen species production in *Arabidopsis thaliana*. Bioscience, Biotechnology, and Biochemistry **77**, 977–983. doi: 10.1271/bbb.120928

**Howard RJ, Strelkov SE, Harding MW**. 2010. Clubroot of cruciferous crops – new perspectives on an old disease. Canadian Journal of Plant Pathology **32**, 43–57. doi: 10.1080/07060661003621761

**Hull AK, Vij R, Celenza JL**. 2000. Arabidopsis cytochrome p450s that catalyze the first step of tryptophan-dependent indole-3-acetic acid biosynthesis. Proceedings of the National Academy of Sciences **97**, 2379–2384. doi: 10.1073/pnas.040569997

**Hwang SF, Howard RJ, Strelkov SE, Gossen BD, Peng G**. 2014. Management of clubroot (*Plasmodiophora brassicae*) on canola (*Brassica napus*) in Western Canada. Canadian Journal of Plant Pathology **36**, 49–65. doi: 10.1080/07060661.2013.863806

**Hasan MJ, Strelkov SE, Howard RJ, Rahman H**. 2012. Screening of Brassica germplasm for resistance to *Plasmodiophora brassicae* pathotypes prevalent in Canada for broadening

diversity in Clubroot Resistance. Canadian Journal of Plant Science **92**, 501–515. doi: 10.4141/cjps2010-006

**Hasan MJ, Rahman H**. 2016. Genetics and molecular mapping of resistance to *Plasmodiophora brassicae* pathotypes 2, 3, 5, 6, and 8 in rutabaga (*Brassica napus* var. *napobrassica*). Genome **59**, 805–815. doi: 10.1139/gen-2016-0034

**Hansen BG, Halkier BA**. 2005. New insight into the biosynthesis and regulation of indole compounds in *Arabidopsis thaliana*. Planta **221**, 603–606. doi:10.1007/s00425-005-1553-1

**Horiuchi S, Hori M** (1980) A simple greenhouse technique for obtaining high levels of clubroot incidence. Bulletin of the Chugoku National Agricultural Experiment Station. **17**, 33–35. doi:10.1002/pmic.201500224.

**Hanschen FS, Schreiner M**. 2017. Isothiocyanates, nitriles, and epithionitriles from glucosinolates are affected by genotype and developmental stage in brassica oleracea varieties. Frontiers in Plant Science **8**. doi: 10.3389/fpls.2017.01095

**Ingram DS, Tommerup IC**. 1972. The life history of *Plasmodiophora brassicae* Woron. Proceedings of the Royal Society of London. Series B. Biological Sciences **180**, 103–112. doi: 10.1098/rspb.1972.0008

**Ishida M, Hara M, Fukino N, Kakizaki T, Morimitsu Y**. 2014. Glucosinolate metabolism, functionality and breeding for the improvement of Brassicaceae Vegetables. Breeding Science **64**, 48–59. doi: 10.1270/jsbbs.64.48

**Ishikawa T, Okazaki K, Kuroda H, Itoh K, Mitsui T, Hori H**. 2007. Molecular cloning of *Brassica rapa* nitrilases and their expression during clubroot development. Molecular Plant Pathology **8**, 623–637. doi: 10.1111/j.1364-3703.2007.00414.x

**Ikegami H, Imuro Y, Naiki T**. 1981. Growth of *Plasmodiophora brassicae* in the root and callus of Chinese cabbage (No. RESEARCH). AVRDC. doi: 10.3186/jjphytopath.44.456

**Irani S, Trost B, Waldner M, Nayidu N, Tu J, Kusalik AJ, Todd CD, Wei Y, Bonham-Smith PC**. 2018. Transcriptome analysis of response to *Plasmodiophora brassicae* infection in the Arabidopsis shoot and root. BMC Genomics **19**. doi: 10.1186/s12864-017-4426-7

**Jayasinghege CP, Ozga JA, Waduthanthri KD, Reinecke DM**. 2017. Regulation of ethylene-related gene expression by indole-3-acetic acid and 4-chloroindole-3-acetic acid in relation to pea fruit and seed development. Journal of Experimental Botany **68**, 4137–4151. doi: 10.1093/jxb/erx217

**Jayasinghege CPA**. 2017. Characterization of Auxin Receptors and Auxin-Ethylene Interaction During Pea Fruit Development.

**Jayasinghege CP, Ozga JA, Nadeau CD, Kaur H, Reinecke DM**. 2019. TIR1 auxin receptors are implicated in the differential response to 4-CL-IAA and IAA in developing Pea Fruit. Journal of Experimental Botany **70**, 1239–1253. doi: 10.1093/jxb/ery456

**Jakubowska A, Kowalczyk S, Leźnicki AJ**. 1993. Enzymatic hydrolysis of 4-O and 6-o-Indol-3-ylacetyl-β-d-glucose in plant tissues. Journal of Plant Physiology **142**, 61–66. doi: 10.1016/s0176-1617(11)80108-2

**Ju HY, Chong C, Mullin WJ, Bible BB**. 1982. Volatile isothiocyanates and nitriles from glucosinolates in rutabaga and Turnip1. Journal of the American Society for Horticultural Science **107**, 1050–1054. doi: 10.21273/jashs.107.6.1050

**Johansson ON, Fantozzi E, Fahlberg P, Nilsson AK, Buhot N, Tör M, Andersson MX**. 2014. Role of the penetration-resistance genes *PEN1, pen2* and *pen3* in the hypersensitive response and race-specific resistance in *Arabidopsis thaliana*. The Plant Journal **79**, 466–476. doi: 10.1111/tpj.12571

**Jacobs T**. 1997. Why Do Plant Cells Divide? The Plant Cell, 1021–1029. doi: 10.1105/tpc.9.7.1021

**Juen A, Traugott M**. 2006. Amplification facilitators and multiplex PCR: Tools to overcome PCR-inhibition in DNA-gut-content analysis of soil-living invertebrates. Soil Biology and Biochemistry **38**, 1872–1879. doi: 10.1016/j.soilbio.2005.11.034

**Ji R, Zhao L, Xing M, Shen X, Bi Q, Peng S, Feng H**. 2014. Infection of *Plasmodiophora brassicae* in Chinese cabbage. Genetics and Molecular Research **13**, 10976–10982. doi: 10.4238/2014.december.19.20

**Kyndt T, Goverse A, Haegeman A, Warmerdam S, Wanjau C, Jahani M, Engler G, de Almeida Engler J, Gheysen G**. 2016. Redirection of auxin flow in *Arabidopsis thaliana* roots after infection by root-knot nematodes. Journal of Experimental Botany **67**, 4559–4570. doi: 10.1093/jxb/erw230

**Kobae Y, Sekino T, Yoshioka H, Nakagawa T, Martinoia E, Maeshima M**. 2006. Loss of ATPDR8, a plasma membrane ABC transporter of *Arabidopsis thaliana*, causes hypersensitive cell death upon pathogen infection. Plant and Cell Physiology **47**, 309–318. doi: 10.1093/pcp/pcj001

**Katz E, Nisani S, Yadav BS, Woldemariam MG, Shai B, Obolski U, Ehrlich M, Shani E, Jander G, Chamovitz DA**. 2015. The glucosinolate breakdown product indole-3-carbinol acts as an auxin antagonist in roots of *Arabidopsis thaliana*. The Plant Journal **82**, 547–555. doi: 10.1111/tpj.12824

**Kim J, Harter K, Theologis A**. 1997. Protein–protein interactions among the aux/IAA proteins. Proceedings of the National Academy of Sciences **94**, 11786–11791. doi: 10.1073/pnas.94.22.11786

**Kim JH, Lee BW, Schroeder FC, Jander G**. 2008. Identification of indole glucosinolate breakdown products with antifeedant effects on *Myzus Persicae* (green peach aphid). The Plant Journal **54**, 1015–1026. doi: 10.1111/j.1365-313x.2008.03476.x

**Kissen R, Bones AM**. 2009. Nitrile-specifier proteins involved in glucosinolate hydrolysis in *Arabidopsis thaliana*. Journal of Biological Chemistry **284**, 12057–12070. doi: 10.1074/jbc.m807500200

**Klein M, Papenbrock J**. 2009. Kinetics and substrate specificities of desulfo-glucosinolate sulfotransferases in *Arabidopsis thaliana*. Physiologia Plantarum **135**, 140–149. doi: 10.1111/j.1399-3054.2008.01182.x

**Korasick DA, Enders TA, Strader LC**. 2013. Auxin biosynthesis and storage forms. Journal of Experimental Botany **64**, 2541–2555. doi: 10.1093/jxb/ert080

**Kowalczyk S, Bandurski RS**. 1990. Isomerization of 1-*o*-indol-3-ylacetyl-β-d-glucose: enzymatic hydrolysis of 1-O, 4-O, and 6-O-indol-3-ylacetyl-β-D-glucose and the enzymatic synthesis of indole-3-acetyl glycerol by a hormone metabolizing complex. Plant Physiology **94**, 4–12. doi: 10.1104/pp.94.1.4

**Karling JS**. 1968. *The Plasmodiophorales*. New York city, New York: Hafner Publishing.

**Kaur H, Ozga JA, Reinecke DM**. 2020. Balancing of hormonal biosynthesis and catabolism pathways, a strategy to ameliorate the negative effects of heat stress on reproductive growth. Plant, Cell & Environment **44**, 1486–1503. doi: 10.1111/pce.13820

**Klopsch R, Witzel K, Börner A, Schreiner M, Hanschen FS**. 2017. Metabolic profiling of glucosinolates and their hydrolysis products in a germplasm collection of *Brassica Rapa* Turnips. Food Research International **100**, 392–403. doi: 10.1016/j.foodres.2017.04.016

**Köppel R, Ruf J, Rentsch J**. 2010. Multiplex real-time PCR for the detection and quantification of DNA from beef, pork, horse and sheep. European Food Research and Technology **232**, 151–155. doi: 10.1007/s00217-010-1371-y

**Kou E, Huang X, Zhu Y, Su W, Liu H, Sun G, Chen R, Hao Y, Song S**. 2021. Crosstalk between auxin and gibberellin during stalk elongation in flowering Chinese cabbage. Scientific Reports **11**. doi: 10.1038/s41598-021-83519-z

**Kepinski S, Leyser O**. 2005. The Arabidopsis F-box protein TIR1 is an auxin receptor. Nature **435**, 446–451. doi: 10.1038/nature03542

**Lipka U, Fuchs R, Kuhns C, Petutschnig E, Lipka V**. 2010. Live and let die – Arabidopsis nonhost resistance to powdery mildews. European Journal of Cell Biology **89**, 194–199. doi: 10.1016/j.ejcb.2009.11.011

**Lammerink J**. 1967. The inheritance of clubroot resistance in *Brassica napus* L. New Zealand Journal of Agricultural Research **10**, 109–115. doi: 10.1080/00288233.1967.10423081

**Lemarié S, Robert-Seilaniantz A, Lariagon C, Lemoine J, Marnet N, Levrel A, Jubault M, Manzanares-Dauleux MJ, Gravot A**. 2015. Camalexin contributes to the partial resistance of *Arabidopsis thaliana* to the biotrophic soilborne protist *Plasmodiophora Brassicae*. Frontiers in Plant Science **6**. doi: 10.3389/fpls.2015.00539

**Ludwig-Müller J, Auer S, Jülke S, Marschollek S**. 2017. Manipulation of auxin and cytokinin balance during the *Plasmodiophora brassicae–Arabidopsis thaliana* interaction. Methods in Molecular Biology, 41–60. doi: 10.1007/978-1-4939-6831-2_3

**Ludwig-Müller J**. 2011. Auxin conjugates: Their role for plant development and in the evolution of Land Plants. Journal of Experimental Botany **62**, 1757–1773. doi: 10.1093/jxb/erq412

**Ludwig-Müller J, Prinsen E, Rolfe SA, Scholes JD**. 2009. Metabolism and plant hormone action during Clubroot disease. Journal of Plant Growth Regulation **28**, 229–244. doi: 10.1007/s00344-009-9089-4

**Ludwig-Müller J, Schuller A**. 2007. What can we learn from clubroots: Alterations in host roots and hormone homeostasis caused by *Plasmodiophora brassicae*? European Journal of Plant Pathology **121**, 291–302. doi: 10.1007/s10658-007-9237-2

**Ludwig-Müller J, Pieper K, Ruppel M, Cohen JD, Epstein E, Kiddle G, Bennett R**. 1999. Indole glucosinolate and auxin biosynthesis in *Arabidopsis thaliana* (L.) heynh. Glucosinolate Mutants and the development of Clubroot Disease. Planta **208**, 409–419. doi: 10.1007/s004250050576

**Ludwig-Müller J, Schubert B, Pieper K, Ihmig S, Hilgenberg W**. 1997. Glucosinolate content in susceptible and resistant Chinese cabbage varieties during development of Clubroot Disease. Phytochemistry **44**, 407–414. doi: 10.1016/s0031-9422(96)00498-0

**Ludwig-Muller J, Epstein E, Hilgenberg W**. 1996. Auxin-conjugate hydrolysis in Chinese cabbage: Characterization of an amidohydrolase and its role during infection with Clubroot disease. Physiologia Plantarum **97**, 627–634. doi: 10.1034/j.1399-3054.1996.970401.x

**Ludwig-Müller J, Bendel U, Thermann P, Ruppel M, Epstein E, Hilgenberg W**. 1993. Concentrations of indole-3-acetic acid in plants of tolerant and susceptible varieties of Chinese cabbage infected with *Plasmodiophora brassicae* Woron. New Phytologist **125**, 763–769. doi: 10.1111/j.1469-8137.1993.tb03926.x

**Livak KJ, Schmittgen TD**. 2001. Analysis of relative gene expression data using real-time quantitative PCR and the $2^{-\Delta\Delta CT}$ method. Methods **25**, 402–408. doi: 10.1006/meth.2001.1262

**Li X, Nair A, Wang S, Wang L**. 2014. Quality control of RNA-seq experiments. Methods in Molecular Biology, 137–146. doi: 10.1007/978-1-4939-2291-8_8

**Li Y, Zhang X, Cai X and Li C.** 2007. Effect of different nutrient solutions on three foliage-ornamental plants in water culture. Journal of Anhui Agricultural Sciences **23**, 7065-7067.

**Ligerot Y, de Saint Germain A, Waldie T, *et al.***. 2017. The pea branching RMS2 gene encodes the PSAFB4/5 auxin receptor and is involved in an auxin-strigolactone regulation loop. PLOS Genetics **13**. doi: 10.1371/journal.pgen.1007089

**Lam HK, McAdam SAM, McAdam EL, Ross JJ**. 2015. Evidence that chlorinated auxin is restricted to the Fabaceae but not to the Fabeae. Plant Physiology **168**, 798–803. doi: 10.1104/pp.15.00410

**Malinowski R, Truman W, Blicharz S**. 2019. Genius architect or clever thief—how *Plasmodiophora brassicae* reprograms host development to establish a pathogen-oriented physiological sink. Molecular Plant-Microbe Interactions® **32**, 1259–1266. doi: 10.1094/mpmi-03-19-0069-cr

**Mithen RF, Lewis BG, Fenwick GR**. 1986. In vitro activity of glucosinolates and their products against *Leptosphaeria maculans*. Transactions of the British Mycological Society **87**, 433–440. doi: 10.1016/s0007-1536(86)80219-4

**Mullin WJ, Collins MJ, Proudfoot KG**. 1980. Glucosinolate content and CLUBROOT of rutabaga and turnip. Canadian Journal of Plant Science **60**, 605–612. doi: 10.4141/cjps80-087

**Macleod AJ, Rossiter JT**. 1987. Degradation of 2-hydroxybut-3-enylglucosinolate (progoitrin). Phytochemistry **26**, 669–673. doi: 10.1016/s0031-9422(00)84763-9

**Matusheski NV, Swarup R, Juvik JA, Mithen R, Bennett M, Jeffery EH**. 2006. Epithiospecifier protein from broccoli (*Brassica oleracea* l. ssp. *italica*) inhibits formation of the anticancer agent sulforaphane. Journal of Agricultural and Food Chemistry **54**, 2069–2076. doi: 10.1021/jf0525277

**Myers DF**. 1985. Lime and the control of Clubroot of crucifers: Effects of pH, calcium, magnesium, and their interactions. Phytopathology **75**, 670. doi: 10.1094/phyto-75-670

**Ma KW, Ma W**. 2016. Phytohormone pathways as targets of pathogens to facilitate infection. Plant Molecular Biology **91**, 713–725. doi: 10.1007/s11103-016-0452-0

**Murakami H, Tsushima S, Kuroyanagi Y, Shishido Y**. 2002. Reduction of resting spore density of *Plasmodiophora brassicae* and clubroot disease severity by liming. Soil Science and Plant Nutrition **48**, 685–691. doi: 10.1080/00380768.2002.10409258

**Mousdale DM**. 1981. Endogenous indolyl-3-acetic acid and pathogen-induced plant growth disorders: Distinction between hyperplasia and neoplastic development. Experientia **37**, 972–973. doi: 10.1007/bf01971786

**Morasse I, Pageau D, Lafond, J.** 1997. Attention à la hernie des crucifères dans le canola. Grandes cultures, **7**, 22-23.

**Mashiguchi K, Hisano H, Takeda-Kamiya N, *et al.***. 2019.*Aagrobacterium tumefaciens* enhances biosynthesis of two distinct auxins in the formation of Crown Galls. Plant and Cell Physiology **60**, 29–37. doi: 10.1787/9789264009998-8-fr

**Miao Y, Zentgraf U**. 2007. The antagonist function of Arabidopsis WRKY53 and ESR/ESP in leaf senescence is modulated by the jasmonic and salicylic acid equilibrium. The Plant Cell **19**, 819–830. doi: 10.1105/tpc.106.042705

**Mikkelsen MD, Naur P, Halkier BA**. 2004. Arabidopsis mutants in the C-s lyase of glucosinolate biosynthesis establish a critical role for indole-3-acetaldoxime in auxin homeostasis. The Plant Journal **37**, 770–777. doi: 10.1111/j.1365-313x.2004.02002.x

**Mikkelsen MD, Hansen CH, Wittstock U, Halkier BA**. 2000. Cytochrome P450 CYP79B2 from Arabidopsis catalyzes the conversion of tryptophan to indole-3-acetaldoxime, a precursor of indole glucosinolates and indole-3-acetic acid. Journal of Biological Chemistry **275**, 33712–33717. doi: 10.1074/jbc.m001667200

**Malka SK, Cheng Y**. 2017. Possible interactions between the biosynthetic pathways of indole glucosinolate and Auxin. Frontiers in Plant Science **8** 2131. doi: 10.3389/fpls.2017.02131

**Mei C, Qi M, Sheng G, Yang Y**. 2006. Inducible overexpression of a rice allene oxide synthase gene increases the endogenous jasmonic acid level, *pr* gene expression, and host resistance to fungal infection. Molecular Plant-Microbe Interactions® **19**, 1127–1137. doi: 10.1094/mpmi-19-1127

**Mulelu AE, Kirykowicz AM, Woodward JD**. 2019. Cryo-Em and directed evolution reveal how Arabidopsis nitrilase specificity is influenced by its quaternary structure. Communications Biology **2**.

**Nafisi M, Goregaoker S, Botanga CJ, Glawischnig E, Olsen CE, Halkier BA, Glazebrook J**. 2007. Arabidopsis cytochrome P450 monooxygenase 71A13 catalyzes the conversion of indole-3-acetaldoxime in Camalexin Synthesis. The Plant Cell **19**, 2039–2052. doi: 10.1105/tpc.107.051383

**Nakano RT, Piślewska-Bednarek M, Yamada K, *et al.***. 2017. PYK10 myrosinase reveals a functional coordination between endoplasmic reticulum bodies and glucosinolates in *Arabidopsis thaliana*. The Plant Journal **89**, 204–220. doi: 10.1111/tpj.13377

**Naur P, Petersen BL, Mikkelsen MD, Bak S, Rasmussen H, Olsen CE, Halkier BA**. 2003. CYP83A1 and CYP83B1, two nonredundant cytochrome P450 enzymes metabolizing oximes in the biosynthesis of glucosinolates in Arabidopsis. Plant Physiology **133**, 63–72. doi: 10.1104/pp.102.019240

**Neuhaus K, Grsic-Rausch S, Sauerteig S, Ludwig-Müller J**. 2000. Arabidopsis plants transformed with nitrilase 1 or 2 in antisense direction are delayed in Clubroot development. Journal of Plant Physiology **156**, 756–761. doi: 10.1016/s0176-1617(00)80243-6

**Normanly J, Grisafi P, Fink GR, Bartel B**. 1997. Arabidopsis mutants resistant to the auxin effects of indole-3-acetonitrile are defective in the nitrilase encoded by the NIT1 gene. The Plant Cell **9**, 1781. doi: 10.2307/3870524

**Nadeau CD, Ozga JA, Kurepin LV, Jin A, Pharis RP, Reinecke DM**. 2011. Tissue-specific regulation of gibberellin biosynthesis in developing pea seeds. Plant Physiology **156**, 897–912. doi: 10.1104/pp.111.172577

**Overvoorde PJ, Okushima Y, Alonso José M., *et al.***. 2005. Functional genomic analysis of the *auxin/indole-3-acetic acid* gene family members in *Arabidopsis thaliana* [w]. The Plant Cell **17**, 3282–3300. doi: 10.1105/tpc.105.036723

**Ockendon JG, Buczacki ST**. 1979. Indole glucosinolate incidence and clubroot susceptibility of three cruciferous weeds. Transactions of the British Mycological Society **72**, 156–157. doi: 10.1016/s0007-1536(79)80020-0

**Ozga JA, Reinecke DM, Nadeau CD.** 2010. Auxin receptors. US Patent No. US9441237B2. Patent application 2010; granted September 13, 2016.

**Ozga JA, Yu J, Reinecke DM**. 2003. Pollination-, development-, and auxin-specific regulation of gibberellin 3β-hydroxylase gene expression in pea fruit and seeds. Plant Physiology **131**, 1137–1146. doi: 10.1104/pp.102.015974

**Paciorek T, Friml Jiří**. 2006. Auxin signaling. Journal of Cell Science **119**, 1199–1202. doi: 10.1242/jcs.02910

**Patten CL, Blakney AJ, Coulson TJ**. 2013. Activity, distribution and function of indole-3-acetic acid biosynthetic pathways in bacteria. Critical Reviews in Microbiology **39**, 395–415. doi: 10.3109/1040841x.2012.716819

**Patten CL, Glick BR**. 1996. Bacterial biosynthesis of indole-3-acetic acid. Canadian Journal of Microbiology **42**, 207–220. doi: 10.1139/m96-032

**Park S, Ozga JA, Cohen JD, Reinecke DM**. 2010. Evidence of 4-CL-IAA and IAA bound to proteins in pea fruit and seeds. Journal of Plant Growth Regulation **29**, 184–193. doi: 10.1007/s00344-009-9123-6

**Parry G, Calderón-Villalobos LI, Prigge M, Peret B, Dharmasiri S, Itoh H, Lechner E, Gray WM, Bennett M, Estelle M**. 2009. Complex regulation of the TIR1/AFB family of auxin receptors. Proceedings of the National Academy of Sciences **106**, 22540–22545. doi: 10.1073/pnas.0911967106

**Pfalz M, Mukhaimar M, Perreau F, Kirk J, Hansen CI, Olsen CE, Agerbirk N, Kroymann J**. 2016. Methyl transfer in glucosinolate biosynthesis mediated by indole glucosinolate *o*-methyltransferase 5. Plant Physiology **172**, 2190–2203. doi: 10.1104/pp.16.01402

**Pfalz M, Mikkelsen MD, Bednarek P, Olsen CE, Halkier BA, Kroymann J**. 2011. Metabolic Engineering in *Nicotiana benthamiana* reveals key enzyme functions in Arabidopsis indole glucosinolate modification. The Plant Cell **23**, 716–729. doi: 10.1105/tpc.110.081711

**Piotrowski M**. 2008. Primary or secondary? versatile nitrilases in plant metabolism. Phytochemistry **69**, 2655–2667. doi: 10.1016/j.phytochem.2008.08.020

**Piotrowski M, Schönfelder S, Weiler EW**. 2001. The *Arabidopsis thaliana* Isogene NIT4 and its orthologs in tobacco encode β-cyano-L-alanine hydratase/nitrilase. Journal of Biological Chemistry **276**, 2616–2621. doi: 10.1074/jbc.m007890200

**Piślewska-Bednarek M, Nakano RT, Hiruma K, *et al.***. 2018. Glutathione transferase U13 functions in pathogen-triggered glucosinolate metabolism. Plant Physiology **176**, 538–551. doi: 10.1104/pp.17.01455

**Pollmann S, Neu D, Weiler EW**. 2003. Molecular cloning and characterization of an amidase from *Arabidopsis thaliana* capable of converting indole-3-acetamide into the plant growth hormone, indole-3-acetic acid. Phytochemistry **62**, 293–300. doi: 10.1016/s0031-9422(02)00563-0

**Pollmann S, Müller A, Piotrowski M, Weiler E**. 2002. Occurrence and formation of indole-3-acetamide in *Arabidopsis thaliana*. Planta **216**, 155–161. doi: 10.1007/s00425-002-0868-4

**Quint M, Gray WM**. 2006. Auxin signaling. Current Opinion in Plant Biology **9**, 448–453. doi: 10.1016/j.pbi.2006.07.006

**Qi L, Yan J, Li Y, *et al.***. 2012. *Arabidopsis thaliana* plants differentially modulate auxin biosynthesis and transport during defense responses to the necrotrophic pathogen *Alternaria brassicicola*. New Phytologist **195**, 872–882. doi: 10.1111/j.1469-8137.2012.04208.x

**R Core Team**. 2020. R: A language and environment for statistical computing. R Foundation for Statistical Computing, Vienna, Austria. URL https://www.R-project.org/.

**Rogato A, Valkov VT, Nadzieja M, Stougaard J, Chiurazzi M**. 2021. The *Lotus japonicus* AFB6 gene is involved in the Auxin Dependent Root Developmental program. International Journal of Molecular Sciences **22**, 8495. doi: 10.3390/ijms22168495

**Rayle DL, Evans ML, Hertel R**. 1970. Action of auxin on cell elongation. Proceedings of the National Academy of Sciences **65**, 184–191. doi: 10.1073/pnas.65.1.184

**Růžička K, Šimášková M, Duclercq J, Petrášek J, Zažímalová E, Simon S, Friml J, Van Montagu MC, Benková E**. 2009. Cytokinin regulates root meristem activity via modulation of the Polar Auxin Transport. Proceedings of the National Academy of Sciences **106**, 4284–4289. doi: 10.1073/pnas.0900060106

**Robin AH, Yi G-E, Laila R, Hossain MR, Park J-I, Kim HR, Nou I-S**. 2017. *Leptosphaeria maculans* alters glucosinolate profiles in blackleg disease-resistant and -susceptible cabbage lines. Frontiers in Plant Science **8**. doi: 10.3389/fpls.2017.01769

**Radojčić Redovniković I, Glivetić T, Delonga K, Vorkapić-Furač J** 2008. Glucosinolates and their potential role in plant. Periodicum biologorum, **110**, 297-309

**Raa JAN**. 1971. Indole-3-acetic acid levels and the role of indole-3-acetic acid oxidase in the normal root and club-root of cabbage. Physiologia Plantarum **25**, 130–134. doi: 10.1111/j.1399-3054.1971.tb01101.x

**Rahman H, Peng G, Yu F, Falk KC, Kulkarni M, Selvaraj G**. 2014. Genetics and breeding for Clubroot Resistance in Canadian Spring Canola (*Brassica napus* L.). Canadian Journal of Plant Pathology **36**, 122–134. doi: 10.1080/07060661.2013.862571

**Rask L, Andréasson E, Ekbom B, Eriksson S, Pontoppidan B, Meijer J**. 2000. Myrosinase: Gene family evolution and herbivore defense in Brassicaceae. Plant Molecular Evolution **42**, 93–113. doi: 10.1007/978-94-011-4221-2_5

**Revelou P-K, Kokotou MG, Constantinou-Kokotou V**. 2018. Determination of indole-type phytonutrients in cruciferous vegetables. Natural Product Research **34**, 2554–2557. doi: 10.1080/14786419.2018.1543680

**Rahikainen M, Trotta A, Alegre S, Pascual J, Vuorinen K, Overmyer K, Moffatt B, Ravanel S, Glawischnig E, Kangasjärvi S**. 2016. PP2A-B′γ modulates foliar *trans*-methylation capacity and the formation of 4-methoxy-Indol-3-yl-methyl glucosinolate in Arabidopsis leaves. The Plant Journal **89**, 112–127. doi: 10.1111/tpj.13326

**Sade D, Shriki O, Cuadros-Inostroza A, Tohge T, Semel Y, Haviv Y, Willmitzer L, Fernie AR, Czosnek H, Brotman Y**. 2015. Comparative metabolomics and transcriptomics of plant response to tomato yellow leaf curl virus infection in resistant and susceptible tomato cultivars. Metabolomics **11**, 81–97. doi: 10.1007/s11306-014-0670-x

**St. Clair DA**. 2010. Quantitative disease resistance and quantitative resistance loci in breeding. Annual Review of Phytopathology **48**, 247–268. doi: 10.1146/annurev-phyto-080508-081904

**Somé A, Manzanares MJ, Laurens F, Baron F, Thomas G, Rouxel F**. 1996. variation for virulence on *Brassica napus* L. amongst *Plasmodiophora brassicae* collections from France and derived single-spore isolates**.** Plant Pathology **45**, 432–439. doi: 10.1046/j.1365-3059.1996.d01-155.x

**Siemens J, Glawischnig E, Ludwig-Müller J**. 2008. Indole glucosinolates and Camalexin do not influence the development of the clubroot disease in *Arabidopsis thaliana*. Journal of Phytopathology **156**, 332–337. doi: 10.1111/j.1439-0434.2007.01359.x

**Siemens J, Keller I, Sarx J, Kunz S, Schuller A, Nagel W, Schmülling T, Parniske M, Ludwig-Müller J**. 2006. Transcriptome analysis of Arabidopsis clubroots indicate a key role for cytokinins in disease development. Molecular Plant-Microbe Interactions® **19**, 480–494. doi: 10.1094/mpmi-19-0480

**Stein M, Dittgen J, Sánchez-Rodríguez C, Hou BH, Molina A, Schulze-Lefert P, Lipka V, Somerville S**. 2006. Arabidopsi*s* pen3/PDR8, an ATP binding cassette transporter, contributes to Nonhost resistance to inappropriate pathogens that enter by direct penetration. The Plant Cell **18**, 731–746. doi: 10.1105/tpc.105.038372

**Strelkov SE, Tewari JP, Smith-Degenhardt E**. 2006. Characterization of *Plasmodiophora brassicae* populations from Alberta, Canada. Canadian Journal of Plant Pathology **28**, 467–474. doi: 10.1080/07060660609507321

**Strelkov SE, Hwang S-F, Manolii VP, Cao T, Fredua-Agyeman R, Harding MW, Peng G, Gossen BD, Mcdonald MR, Feindel D**. 2018. Virulence and pathotype classification of *Plasmodiophora brassicae* populations collected from clubroot resistant canola (*Brassica napus*) in Canada. Canadian Journal of Plant Pathology **40**, 284–298. doi: 10.1080/07060661.2018.1459851

**Strelkov SE, Hwang SF, Manolii VP, Cao T, Feindel D**. 2016. Emergence of new virulence phenotypes of *Plasmodiophora brassicae* on canola (*Brassica napus*) in Alberta, Canada. European Journal of Plant Pathology **145**, 517–529. doi: 10.1007/s10658-016-0888-8

**Strelkov SE, Hwang SF, Manolii VP, Cao T, Fredua-Agyeman R, Harding MW, Peng G, Gossen BD, Mcdonald MR, Feindel D**. 2018. Virulence and pathotype classification of *Plasmodiophora brassicae* populations collected from clubroot resistant canola (*Brassica napus*) in Canada. Canadian Journal of Plant Pathology **40**, 284–298. doi: 10.1080/07060661.2018.1459851

**Strelkov SE, Manolii VP, Harding MW, Daniels GC, Nuffer P, Aigu Y, Hwang, SF**. 2020. The occurrence and spread of clubroot on canola in Alberta in 2019. Canadian Journal of Plant Pathology, **42**, 117-120.

**Sugawara S, Hishiyama S, Jikumaru Y, Hanada A, Nishimura T, Koshiba T, Zhao Y, Kamiya Y, Kasahara H**. 2009. Biochemical analyses of indole-3-acetaldoxime-dependent

auxin biosynthesis in Arabidopsis. Proceedings of the National Academy of Sciences **106**, 5430–5435. doi: 10.1073/pnas.0811226106

**Spaner D**. 2002. Agronomic and horticultural characters of rutabaga in Eastern Canada. Canadian Journal of Plant Science **82**, 221–224. doi: 10.4141/p01-086

**Sugiyama R, Hirai MY**. 2019. Atypical myrosinase as a mediator of glucosinolate functions in plants. Frontiers in Plant Science **10**. doi: 10.3389/fpls.2019.01008

**Szerszen JB, Szczyglowski K, Bandurski RS**. 1994. *IAGLU*, a gene from *Zea mays* involved in conjugation of growth hormone indole-3-acetic acid. Science **265**, 1699–1701. doi: 10.1126/science.8085154

**Salehin M, Bagchi R, Estelle M**. 2015. SCFTIR1/AFB -based auxin perception: Mechanism and role in plant growth and development. The Plant Cell **27**, 9–19. doi: 10.1105/tpc.114.133744

**Sticher L, Mauch-Mani B, Métraux and JP**. 1997. Systemic acquired resistance. Annual Review of Phytopathology **35**, 235–270. doi: 10.1146/annurev.phyto.35.1.235

**Stone JD, Storchova H**. 2014. The application of RNA-seq to the comprehensive analysis of plant mitochondrial transcriptomes. Molecular Genetics and Genomics **290**, 1–9. doi: 10.1007/s00438-014-0905-6

**Shi H, Zhou Y, Jia E, Pan M, Bai Y, Ge Q**. 2021. Bias in RNA-seq library preparation: Current challenges and solutions. BioMed Research International **2021**, 1–11. doi: 10.1155/2021/6647597

**Sakai Y, Kotoura S, Yano T, Kurihara T, Uchida K, Miake K, Akiyama H, Tanabe S.** 2011**.** Quantification of pork, chicken and beef by using a novel reference molecule. Bioscience, Biotechnology, and Biochemistry **75**, 1639–1643. doi: 10.1271/bbb.110024

**Su YH, Liu YB, Zhang X-S**. 2011. Auxin–cytokinin interaction regulates meristem development. Molecular Plant **4**, 616–625. doi: 10.1093/mp/ssr007

**Tewari JP, Strelkov SE, Orchard D, Hartman M, Lange RM, Turkington TK**. 2005. Identification of Clubroot of crucifers on canola (*Brassica napus*) in Alberta. Canadian Journal of Plant Pathology **27**, 143–144. doi: 10.1080/07060660509507206

**Tookey HL**. 1973. Crambe thioglucoside glucohydrolase (EC 3.2. 3.1): separation of a protein required for epithiobutane formation. Canadian Journal of Biochemistry **51**,1654-1660. doi: 10.1139/o73-222

**Tan X, Calderon-Villalobos LI, Sharon M, Zheng C, Robinson CV, Estelle M, Zheng N**. 2007. Mechanism of auxin perception by the TIR1 ubiquitin ligase. Nature **446**, 640–645. doi: 10.1038/nature05731

**Ting HM, Cheah BH, Chen YC, *et al.***. 2020. The role of a glucosinolate-derived nitrile in plant immune responses. Frontiers in Plant Science **11**. doi: 10.3389/fpls.2020.00257

**Toufighi K, Brady SM, Austin R, Ly E, Provart NJ**. 2005. The Botany Array Resource: E-Northerns, expression angling, and promoter analyses. The Plant Journal **43**, 153–163. doi: 10.1111/j.1365-313x.2005.02437.x

**Tivendale ND, Davidson SE, Davies NW, *et al.***. 2012. Biosynthesis of the halogenated auxin, 4-chloroindole-3-acetic acid. Plant Physiology **159**, 1055–1063. doi: 10.1104/pp.112.198457

**Torsvik V, Øvreås L**. 2002. Microbial diversity and function in soil: From genes to ecosystems. Current Opinion in Microbiology **5**, 240–245.

**Ugajin T, Takita K, Takahashi H, Muraoka S, Tada T, Mitsui T, Hayakawa T, Ohyama T, Hori H**. 2003. Increase in indole-3-acetic acid (iaa) level and nitrilase activity in turnips induced by *Plasmodiophora brassicae* infection. Plant Biotechnology **20**, 215–220. doi: 10.5511/plantbiotechnology.20.215

**Ulmasov T, Murfett J, Hagen G, Guilfoyle TJ**. 1997. Aux/IAA proteins repress expression of reporter genes containing natural and highly active synthetic auxin response elements. The Plant Cell **9**, 1963. doi: 10.2307/3870557

**Villalobos C, Caballero E, Sanz-Blasco S, Núñez L**. 2012. Study of neurotoxic intracellular calcium signalling triggered by amyloids. Methods in Molecular Biology, 289–302. doi: 10.1007/978-1-61779-551-0_20

**Vaughn SF, Berhow MA**. 2005. Glucosinolate hydrolysis products from various plant sources: Ph effects, isolation, and purification. Industrial Crops and Products **21**, 193–202. doi: 10.1016/j.indcrop.2004.03.004

**Velasquez SM, Barbez E, Kleine-Vehn J, Estevez JM**. 2016. Auxin and cellular elongation. Plant Physiology **170**, 1206–1215. doi: 10.1104/pp.15.01863

**Vasav AP, Barvkar VT**. 2019. Phylogenomic analysis of cytochrome P450 multigene family and their differential expression analysis in *Solanum lycopersicum* L. suggested tissue specific promoters. BMC Genomics **20**.

**Van Rossum G, Drake FL**. 2009. Python 3 Reference Manual:(Python Documentation Manual Part 2). Scotts Valley, CA: CreateSpace.

**Wretblad S, Dixelius C**. 2000. B-genome derived resistance to *Leptosphaeria maculans* in near isogenic *Brassica napus* lines is independent of glucosinolate profile. Physiologia Plantarum **110**, 461–468. doi:10.1111/j.1399-3054.2000.1100406.x

**Wittstock U, Kurzbach E, Herfurth AM, Stauber EJ**. 2016. Glucosinolate breakdown. Advances in Botanical Research, 125–169. doi: 10.1016/bs.abr.2016.06.006

**Wang Z, Gerstein M, Snyder M**. 2009. RNA-seq: A revolutionary tool for transcriptomics. Nature Reviews Genetics **10**, 57–63. doi: 10.1038/nrg2484

**Wang J, Yu H, Zhao Z, Sheng X, Shen Y, Gu H**. 2019. Natural variation of glucosinolates and their breakdown products in broccoli (*Brassica oleracea* var. *Italica*) seeds. Journal of Agricultural and Food Chemistry **67**, 12528–12537. doi: 10.1021/acs.jafc.9b06533

**Wang J, Huang Y, Li XL, Li HZ**. 2011. Research progress in clubroot of crucifers. Plant Protection, **37**, 153-158.

**Wang R, Estelle M**. 2014. Diversity and specificity: Auxin perception and signaling through the TIR1/AFB pathway. Current Opinion in Plant Biology **21**, 51–58. doi: 10.1016/j.pbi.2014.06.006

**Wagner G, Laperche A, Lariagon C, Marnet N, Renault D, Guitton Y, Bouchereau A, Delourme R, Manzanares-Dauleux MJ, Gravot A**. 2019. Resolution of quantitative resistance to Clubroot into QTL-specific metabolic modules. Journal of Experimental Botany **70**, 5375–5390. doi: 10.1093/jxb/erz265

**Woodward AW, Bartel B**. 2005. Auxin: Regulation, action, and interaction. Annals of Botany **95**, 707–735. doi: 10.1093/aob/mci083

**Williams, PH**. 1966. A system for the determination of races of *Plasmodiophora brassicae* that infect cabbage and rutabaga. Phytopathology, **56**, 624-626.

**Wallenhammar AC**. 1996. prevalence of *Plasmodiophora brassicae* in a spring oilseed rape growing area in central Sweden and factors influencing soil infestation levels. Plant Pathology **45**, 710–719. doi: 10.1046/j.1365-3059.1996.d01-173.x

**Wentzell AM, Rowe HC, Hansen BG, Ticconi C, Halkier BA, Kliebenstein DJ**. 2007. Linking metabolic qtls with network and CIS-eqtls controlling biosynthetic pathways. PLoS Genetics **3** 162. doi: 10.1371/journal.pgen.0030162

**Wittstock U, Kurzbach E, Herfurth A-M, Stauber EJ**. 2016. Glucosinolate breakdown. Advances in Botanical Research, 125–169. doi: 10.1016/bs.abr.2016.06.006

**Wittstock U, Burow M**. 2010. Glucosinolate breakdown in Arabidopsis: Mechanism, regulation, and biological significance. The Arabidopsis Book **8**. doi: 10.1199/tab.0134

**Wittstock U, Burow M**. 2007. Tipping the scales - specifier proteins in glucosinolate hydrolysis. IUBMB Life **59**, 744–751. doi: 10.1080/15216540701736277

**Wittstock U, Kliebenstein DJ, Lambrix V, Reichelt M, Gershenzon J**. 2003. Chapter five glucosinolate hydrolysis and its impact on generalist and specialist insect herbivores. Recent Advances in Phytochemistry, 101–125. doi: 10.1016/s0079-9920(03)80020-5

**Wittstock U, Halkier BA**. 2002. Glucosinolate Research in the Arabidopsis era. Trends in Plant Science **7**, 263–270. doi: 10.1016/s1360-1385(02)02273-2

**Wa S. K. K. 2009.** Discovering clubroot resistance genes in Brassica vegetable crops (Doctoral dissertation, RMIT University).

**Xu L, Ren L, Chen K, Liu F, Fang X**. 2016. Putative role of IAA during the early response of *Brassica napus* l. to *Plasmodiophora brassicae*. European Journal of Plant Pathology **145**, 601–613. doi: 10.1007/s10658-016-0877-y

**Xu L, Yang H, Ren L, Chen W, Liu L, Liu F, Zeng L, Yan R, Chen K, Fang X**. 2018. Jasmonic acid-mediated aliphatic glucosinolate metabolism is involved in clubroot disease development in *Brassica napus* L. Frontiers in Plant Science **9**. doi: 10.3389/fpls.2018.00750

**Xie Q, Wei X, Liu Y, Han F, Li Z**. 2022. Germplasm enhancement and identification of loci conferring resistance against *Plasmodiophora brassicae* in Broccoli. Genes **13**, 1600. doi: 10.3390/genes13091600

**Yan X, Chen S**. 2007. Regulation of plant glucosinolate metabolism. Planta **226**, 1343–1352. doi: 10.1007/s00425-007-0627-7

**Yogendra KN, Kushalappa AC, Sarmiento F, Rodriguez E, Mosquera T**. 2014. Metabolomics deciphers quantitative resistance mechanisms in diploid potato clones against late blight. Functional Plant Biology **42**, 284. doi: 10.1071/fp14177

**Yang B, Rahman MH, Liang Y, Shah S, Kav NN**. 2009. Characterization of defense signaling pathways of *Brassica napus* and *Brassica carinata* in response to *Sclerotinia sclerotiorum* Challenge. Plant Molecular Biology Reporter **28**, 253–263. doi: 10.1007/s11105-009-0149-5

**Yang T, Davies PJ, Reid JB**. 1996. Genetic dissection of the relative roles of auxin and gibberellin in the regulation of STEM elongation in intact light-grown peas. Plant Physiology **110**, 1029–1034. doi: 10.1104/pp.110.3.1029

**Yi GE, Robin A, Yang K, Park JI, Hwang B, Nou IS**. 2016. Exogenous methyl jasmonate and salicylic acid induce subspecies-specific patterns of glucosinolate accumulation and gene expression in *Brassica oleracea* L. Molecules **21**, 1417. doi: 10.3390/molecules21101417

**Zamani-Noor N**. 2017. Variation in pathotypes and virulence of *Plasmodiophora brassicae* populations in Germany. Plant Pathology **66**, 316–324. doi: 10.1111/ppa.12573

**Zamani-Noor N, Hornbacher J, Comel CJ, Papenbrock J**. 2021. Variation of glucosinolate contents in clubroot-resistant and -susceptible *Brassica napus* cultivars in response to virulence of *Plasmodiophora Brassicae*. Pathogens **10**, 563. doi: 10.3390/pathogens10050563

**Zhang L, Zhang F, Melotto M, Yao J, He SY**. 2017. Jasmonate signaling and manipulation by pathogens and insects. Journal of Experimental Botany. doi: 10.1093/jxb/erw478

**Zhang L, Kawaguchi R, Morikawa-Ichinose T, Allahham A, Kim SJ, Maruyama-Nakashita A**. 2020. Sulfur deficiency-induced glucosinolate catabolism attributed to two β-glucosidases, BGLU28 and BGLU30, is required for plant growth maintenance under sulfur deficiency. Plant and Cell Physiology **61**, 803–813. doi: 10.1093/pcp/pcaa006

**Zhang H, Tan X, Li L, *et al.***. 2019. Suppression of auxin signalling promotes rice susceptibility to rice black streaked dwarf virus infection. Molecular Plant Pathology **20**, 1093–1104. doi: 10.1111/mpp.12814

**Zhang H, Li L, He Y, *et al.***. 2020. Distinct modes of manipulation of rice auxin response factor OSARF17 by different plant RNA viruses for infection. Proceedings of the National Academy of Sciences **117**, 9112–9121. doi: 10.1073/pnas.1918254117

**Zhang H, Feng J, Hwang SF, Strelkov SE, Falak I, Huang X, Sun R**. 2015. Mapping of clubroot (*Plasmodiophora brassicae*) resistance in canola (*Brassica napus*). Plant Pathology **65**, 435–440. doi: 10.1111/ppa.12422

**Zhang J, Pontoppidan B, Xue J, Rask L, Meijer J**. 2002. The third myrosinase gene TGG3 in *Arabidopsis thaliana* is a pseudogene specifically expressed in stamen and Petal. Physiologia Plantarum **115**, 25–34. doi: 10.1034/j.1399-3054.2002.1150103.x

**Zhang X, Liu Y, Fang Z, Li Z, Yang L, Zhuang M, Zhang Y, Lv H**. 2016. Comparative transcriptome analysis between broccoli (*Brassica oleracea* var. *Italica*) and wild cabbage (*Brassica macrocarpa* guss.) in response to *Plasmodiophora brassicae* during different infection stages. Frontiers in Plant Science **7**. doi: 10.3389/fpls.2016.01929

**Zhao Y**. 2012. Auxin biosynthesis: A simple two-step pathway converts tryptophan to indole-3-acetic acid in plants. Molecular Plant **5**, 334–338. doi: 10.1093/mp/ssr104

**Zhao Y**. 2014. Auxin biosynthesis. The Arabidopsis Book **12**. doi: 10.1199/tab.0173

**Zhao Y**. 2010. Auxin biosynthesis and its role in plant development. Annual Review of Plant Biology **61**, 49–64. doi: 10.1146/annurev-arplant-042809-112308

**Zhao Y, Hull AK, Gupta NR, Goss KA, Alonso J, Ecker JR, Normanly J, Chory J, Celenza JL**. 2002. Trp-dependent auxin biosynthesis in Arabidopsis: Involvement of cytochrome p450s CYP79B2 and CYP79B3. Genes & Development **16**, 3100–3112. doi: 10.1101/gad.1035402

**Zhao S, Fung-Leung W-P, Bittner A, Ngo K, Liu X**. 2014. Comparison of RNA-seq and microarray in transcriptome profiling of activated T cells. PLoS ONE **9**. doi: 10.1371/journal.pone.0078644

**Zhao L, Mao D, Lin Z, Yang X, et al.** 2007. Effects of different nutrient solution on pigment content and photosynthesis of *Coleus blumei*. Guangdong Academy of Agricultural Sciences. **6**, 30-3.

**Zhou Q, Galindo-González L, Manolii V, Hwang SF, Strelkov SE**. 2020. Comparative transcriptome analysis of rutabaga (*Brassica napus*) cultivars indicates activation of salicylic acid and ethylene-mediated defenses in response to *Plasmodiophora Brassicae.* International Journal of Molecular Sciences **21**, 8381. doi: 10.3390/ijms21218381

**Zubieta C, He X-Z, Dixon RA, Noel JP**. 2001. Nature Structural Biology **8**, 271–279. doi: 10.1038/85029

# Appendix-A

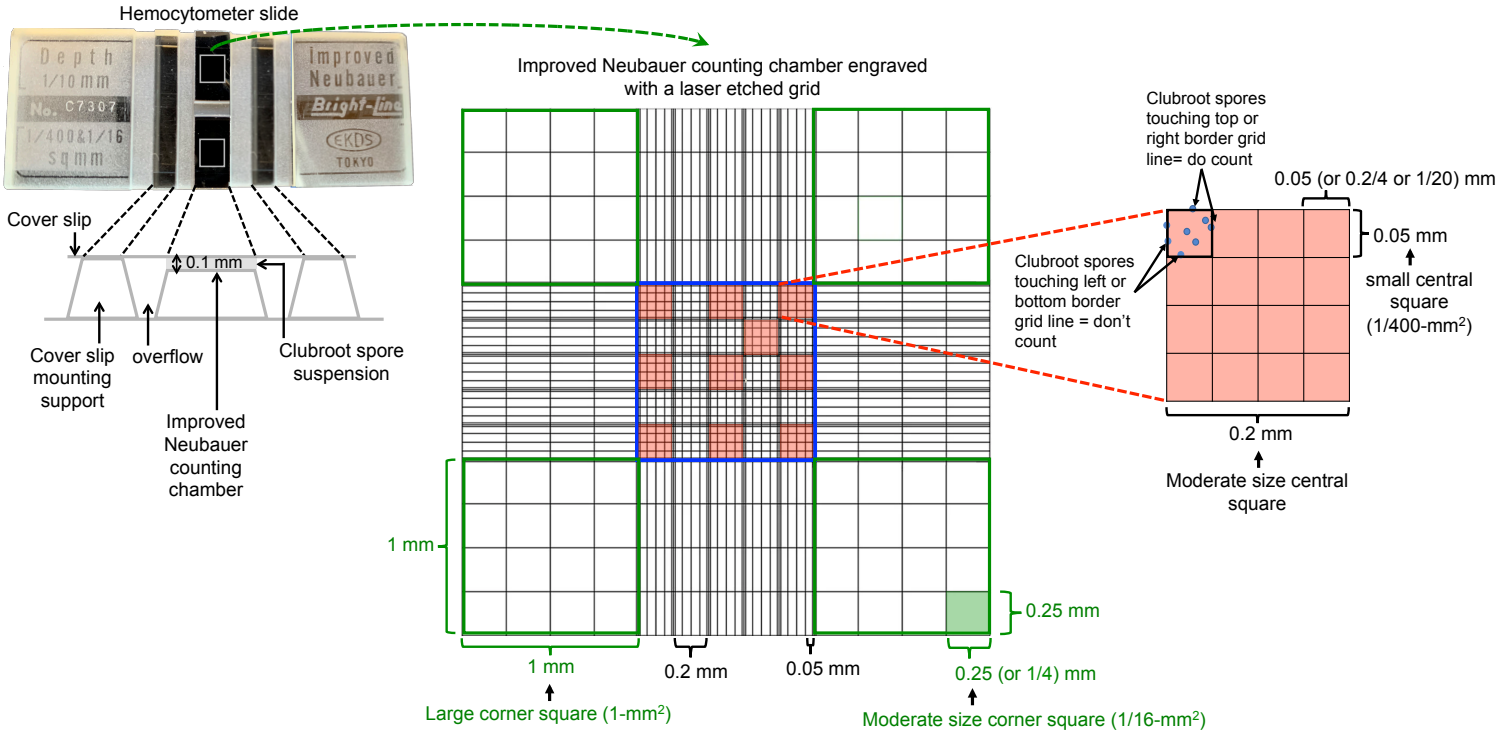


**Appendix Figure A1. Schematic representation of the improved Neubauer counting chamber of the hemocytometer used for estimating the clubroot resting spore concentration.** A hemocytometer is a thick rectangular microscopic glass slide (30 mm width, 70 mm length and 4 mm thick) with a H-shaped indentation at the center of the slide that separates the two counting chambers. Each counting chamber consists of a laser-etched square grid of perpendicular lines which measures 3 mm x 3 mm and is subdivided into 9 large squares each with a 1-mm$^2$ (1 x 1 mm) area. Each large corner square outlined in green thick border is further divided into 16 moderate size squares each with a 0.0625-mm$^2$ or 1/16-mm$^2$ (0.25 x 0.25 mm) area (a square shaded in green). The central square outlined in blue thick border is divided into 25 moderate size squares each with a 0.004-mm$^2$ (0.20 x0.20 mm) area. Each moderate size central square is subdivided into 16 small squares. The central square is therefore composed of 400 small squares each with a 0.0025-mm$^2$ or 1/400-mm$^2$ (0.05 x 0.05 mm) area. The central square of the improved Neubauer counting chamber was used to estimate the clubroot resting spore concentration. In detail, within the central square, of 25 moderate size squares only ten squares shaded in red were selected, and within each of the selected moderate size central square

only the top-left small square outlined in black thick border was used for counting clubroot spores. Altogether, the spore count across 10 small squares was averaged. Under the microscope at 40x magnification, the resting spore of clubroot is spherical shaped moderate-size structure with a distinct hyaline thick cell wall. When counting spores that touch the top and right grid borders were included while those touching the bottom and the left grid border were excluded. Each of the 9 large squares in the improved Neubauer counting chamber has the space to accommodate 0.1-µL or 0.1 $mm^3$ volume of the suspension. The average number of spores per small square was then multiplied by 400 to calculate the number of resting spores in one of the nine squares of the improved Neubauer grid. This average number of spores per 0.1-µL was multiplied by the multiplication factor of $10^4$, to get the average number of spores per mL.

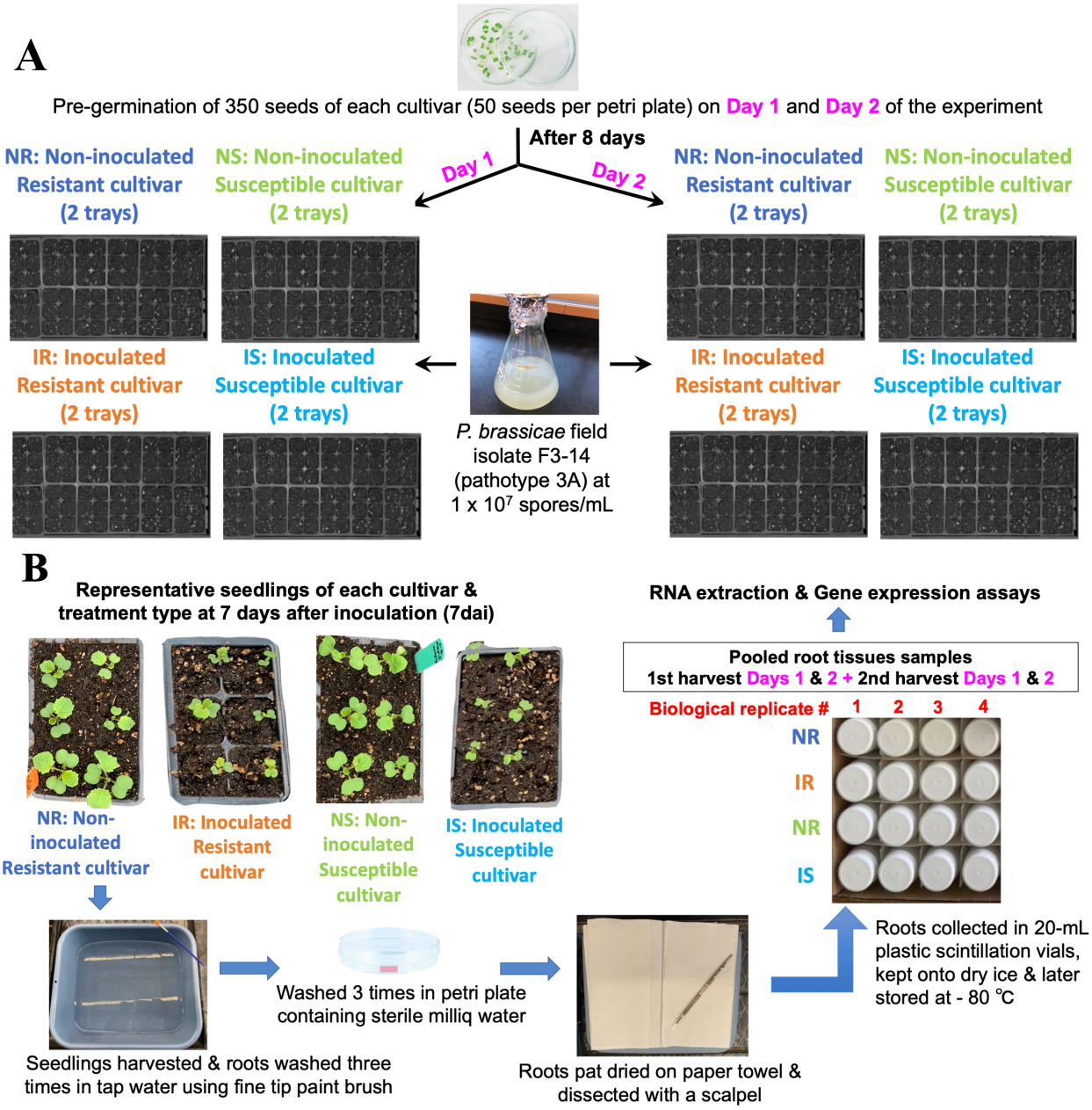


**Appendix Figure A2. The procedure followed for growing rutabaga seedlings and harvesting root samples for PCR and Taqman qRT-PCR studies.** [A]: This growth experiment was planted on two consecutive days and consisted of a total of 16 trays, 4 trays each of non-inoculated control and clubroot-inoculated plants for resistant and susceptible cultivars, labeled as non-inoculated resistant (NR), non-inoculated susceptible (NS), inoculated resistant (IR), and inoculated susceptible (IS) cultivars. For inoculation, 8-d old petri plate pre-germinated seedlings were first dipped for 10-s in the freshly prepared resting spore suspension of *P.*

*brassicae* pathotype 3A field isolate F3-14 at 1 x $10^7$ spores/mL and then transferred to 72 cell insert-trays (insert size is 3.8 x 3.8 x 5.7 cm; one seedling per insert) filled with water-saturated Sunshine #4 peat-based medium. An additional 1 mL of spore suspension was added to the base of each seedling with micropipette to ensure enough disease pressure. The non-inoculated seedlings were moved directly from petri plates to the trays with water-saturated peat-based medium and were kept separated from the inoculated plants to avoid cross-contamination. [B]: After 7 days of growth, first the non-inoculated control seedlings of both cultivars were harvested. Seedlings were washed three times in tap water with fine tip painting brush followed by three washes in petri dishes containing milliq water. Clean washed seedlings were then pat dried using paper towels; roots were dissected with a scalpel, and collected in 20 mL plastic scintillation vials, placed onto dry ice, and stored at -80 ºC until further processed for PCR and taqman qRT-PCR assays. For performing PCR assays, this growth experiment was repeated three times and three independent biological replicates of roots from non-inoculated control and 7-d clubroot-inoculated seedlings of resistant cultivar were harvested. Each biological replicate is a pool of roots obtained from 115 seedlings for non-inoculated resistant cultivar and 101 seedlings for inoculated resistant cultivars. For taqman qRT-PCR assays, this growth experiment was repeated two times and four independent biological replicates of roots for each treatment and cultivar were collected. Each biological replicate is a pool of roots obtained from 75 seedlings for non-inoculated sensitive cultivar, 77 seedlings for non-inoculated resistant cultivar, and 78 seedlings for inoculated sensitive and resistant cultivars.

```
   1 ATGGATTACA TTTTGCTCTT ATTGCCACTC GTATTGTTTC TACTAGCTTA CAAATTCTTA
  61 TTCTCATCTA AGAGTTTCAA TCTTCCACCA GGACCAACTC CCTTTCCCAT CGTCGGCAAC
 121 CTCCACCTCG TGAAACCACC GGTGCACCGT CTCTTCCGTC GTTTCGCGGA CAAGTACGGT
 181 GACATCTTCT CCCTCCGTTA CGGCTCTCGC CAAGTCGTCG TGATCTCTTC CTTGCCCCTC
 241 GTCAGAGAAT GCTTTACTGG TCAGAACGAC GTTATTTTAA CGAACCGACC GCATTTTCTG
 301 ACCGCAAAGT ACGTTGCTTA CGACTACACC ACGGTTGGAA CCGCCGCATA TGGCGACCAC
 361 TGGCGTAATC TCCGCCGTAT TTGCTCTCTT GAGATCCTTT CCTCTAACCG TCTCACTGGA
 421 TTCCTCTCCG TTCGTAAAGA CGAGATCCGA CGGTTGCTCA CGAAACTCTC ACGTGACTAT
 481 AATGGCCAAG TCGTTGAGCT TGAGCCTCTT CTTGCAGATT TGACGTTCAA TAATATTGTC
 541 CGTATGGTCA CTGGGAGACG TTACTACGGA GACCAGGTTC ACAACAAGGA AGAAGCGAAC
 601 CTATTCAAGA AGCTAGTGAC GCAGATCAAC GACAATAGTG GTGCGAGCCA TCCAGGAGAT
 661 TATTTACCAA TTCTCAAAGT TTTCGGACAC GGCTACGAGA AGAAAGTGAA AGCACTCGGC
 721 GAAGCCATGG ACACTTTCTT GCAGCGACTG CTCGACGATT GCCGTAGAGA TGGAGAGAGC
 781 AACACAATGC TTAGTCATCT GTTGTCTTTA CAAGTAGACC AACCCAAGTA TTACAGTGAC
 841 GTCATCATCA AAGGCCTCAT GCTCAGTATG ATGCTTGCGG GGACGGATAC TGCAGCCGTG
 901 ACACTAGAAT GGGCGATGGC GAGTTTGTTG AAAAGTCCTG AAGTGTTGAA GAAGGCGAAA
 961 GCCGAGATAG ATGATAAGAT TGGACATGAA CGTTTGGTCG ACGAACCGGA CATTTTGAAT
1021 CTCCCTTATC TCCAAAACAT AGTTTCACAG ATTCTTATTC TCATCTAA
```

**Appendix Figure A3: The complete coding sequence of gene encoding cytochrome P450 monooxygenase, family 81, subfamily F, polypeptide 2 (*BnCYP81F2*: BnaA10g11280D) retrieved from *Brassica napus* genome (AST_PRJEB5043_v1; http://plants.ensembl.org/Brassica_napus/Info/Index).** Forward and reverse PCR primers are highlighted in grey. Forward and reverse qPCR primers and probe binding sites are colored and underlined in green, red, and orange respectively.

```
   1 ATGTTTTACT ATGTGATACT CCCTCTGGCT CTCCTTCTCA TTGCTTACAA ATTCACCTCC
  61 AAGACGAAGC GTCTCAACCT CCCTCCCTCT CCGCCTCACT CTCTCCCCAT TATTGGCCAC
 121 CATCGCCTCA TCAAACCGCC TGTCCACCGT CTCTTCCACA GACTCGCCAA AGCACACGGC
 181 CCAATATTCT ACCTCCGACT CGGTACCCGC CGTGCCGTCG TCATCTCTTC CTCCGCACTC
 241 GCAAAAGAAT GCTTCACGGG TCACAACGAC GTCGTAGTAT CAAACCGCCC TCGTTTCCTA
 301 ACCTCCAAAT ACATCGCTTA CAACTACACC ACCATAGCAA CCACACCTTA CGGTGACCAC
 361 TGGCGCAACC TCCGCAAGAT CTGCTCCCTC GAAATCGTCT CCTCGAAACG TCTCGCCAAC
 421 TTTCTCCACA TCCGCAAAGA GGAAATCCAC CGCATGCTCA CGAGACTCTC ACGTGACGCG
 481 CTCATCAACA ACGAGGTCGA GCTCGAGTCA CTTTTTTACG ATCTAACGTT CAACAACATA
 541 GTGAGGATGG TTACAGGGAA GATCTACTAC GGAGAAGATG CTAGTGACAA AGCAGAAGCA
 601 GATACGTTCA AGAAACTAAT TGCTTATATT ACTAGTACTA GTGGCGCGAG GCACCCTGGA
 661 GAATACTTAC CATTCCTGAA AATATTTGGA AGGAGTTTTG AAAAGAAAGT GAAAGCTGTT
 721 GGAGAAGCCA TGGATGCAAT CTTGCAGCGT CTGCTTGATG AGTGTAGGGG AAATAAAGAT
 781 GGTAACACAA TGGTTAATCA CTTGCTCTCT TTGCAACAAC AAGATCCAGA GTATTACAGT
 841 GAGGTCATCA TCAAAGGCCT AATGCTGGGC ATCATGTTTG CGGCATCAGA GACATCAGCT
 901 GTGACAATAG AGTGGGCGAT GGCGAGTTTG TTGAATCATC CAGAGTTGTT AGAAAAATTA
 961 AAATTAGAAA TTGATGAGAA AATCGGACAA GGCCGTTTGA TTGAGGAAAC AGACATACCA
1021 AACCTACCTT ACCTTCAAAA CGTAGTGTCC GAAACGTTCC GGCTATACCC AGCTGCGCCG
1081 CTTCTTGTGC CAAGATTAAC GGTAGAGGAC ATCAAAGTCG GAGGATACGA CGTGCCACGT
1141 GAAACGATGG TGATGGTGAA CGCATGGACT ATCCACAGGG ATCCAGAACT TTGGACCGAA
1201 CCAGAGAGGT TTAACCCAGA TAGGTTTAAT GGTGAAAGAG GGGAAGGAGA CAAAGACGAT
1261 GTCCGTACGC TGATAACGTT TGGAAGTGGA CGAAGAATGT GTCCCGGTGC AGGGTTAGCG
1321 AATAAGATTG TGACCTTGGC GTTAGGTTCA TTGATTCAGT GCTTTGATTG GGGAAGAGTC
1381 AATGGCGAAG AGATTGATAT GACTGAAGGT CCAGAGATGG CAATGCGTAA GGTGGTGCCG
1441 TTACGAGCCA TGTGTCACCT TCGACCCGTT ATGAATAAGC TTGTTACGGA CTCAAAGGTT
1501 TAA
```

**Appendix Figure A4: The complete coding sequence of gene encoding cytochrome P450 monooxygenase, family 81, subfamily F, polypeptide 4 (*BnCYP81F4*: BnaCnng68210D) retrieved from *Brassica napus* genome (AST_PRJEB5043_v1; http://plants.ensembl.org/Brassica_napus/Info/Index).** Forward and reverse PCR primers are highlighted in grey. Forward and reverse qPCR primers and probe binding sites are colored and underlined in green, red, and orange respectively.

```
   1 ATGGGACACC TTGTAGACCC TAAAACCATG AATGAGATTA ATGGAGATGA TGAGACCGAG
  61 CTTGGTTTGA GGGCAGTGAG GCTAGCCAAT TACATTACCT TCCCCATGGT TTTCAAAGCC
 121 GCCATTGAGC TCGGTGTCAT CGACGCTCTC TACTTAGCTG CTCGTGATGA CGTCAATGGA
 181 TCTGGATCGT TCCTCAAACC GTCTGAGATA GCTACTCGGC TTCCCACACC GCCTAGTAAC
 241 CCTGAAGCAC CGGTTTTACT GGACCGTATG CTTCGTTTAC TCGCCAGTTA CTCAATGGTC
 301 AAGTGTCAGA TAGTAGACGG CGAGAGGGTG TACAAAGCTG AGCCCATTTG TAAGTATTTC
 361 TTGAGATACA ATATTGAAGA AATGGGGACA CTTGCTTCTC AGTTCATTCT TGAACTTGAT
 421 AGTGTCTTCC TCAACACATG GGCACAGTTG AAAGATGTGG TGCTAGAGGG AGGAGATGCA
 481 TTTGCTCGTG CCAATGGTGG GTTGAAGCTC TTTGATTACA TGGGCACAGA TGAAAGACTA
 541 AGCAAACTCT TTAACCGGAC TGGATTCAGC GTTGGAGTTA TGCAGAAGTT TCTTGAAGTT
 601 TATAAAGGTT TCGAAGGAAT CAATGTGTTG GTTGATGTAG GAGGAGGAGT TGGAAACACA
 661 CTAGGTTTTG TTACTTCAAA GTATCCAAAC ATTAAGGGTA TTAATTTTGA TCTAACTTGT
 721 GCTTTGGCAC AAGCACCTTC TTATCCTAAT GTGGAACATG TGGCTGGAGA TATGTTTGTA
 781 GAAATCCCAA GAGGAGATGC TATCATCTTG AAACGTATGC TTCATGATTG GAATGATGAA
 841 GACTGTGCAA AGATTCTCAA GAACTGCTGG AAGGCATTAC CGGAGAATGG GAAAGTGATA
 901 ATCATGGAGC TAGTTATTCC AGATGAGGCA GAGAGTAAAG ATGTGCAGGC CAACATTGCA
 961 TTTGATATGG ATTTGTTGAT GCTCACACAA CTCTCTGGAG GAAAAGAGAG AACAAAAGCT
1021 GAGTATGAAG CTATGGCTGC TAATTCAGGT TTTGCAAGTT GCAAATTTGT GTGCCCTGCA
1081 TATCATTTAT GGGTCATTGA GTTCTCTAAA TAG

   1 ATGGGACACC TTTTAGACCC TAAAACCATG AATGAGATTA ATGGAGATGA TGAGACCGAG
  61 CTTGGTTTGA GGGCAGTGAG GCTAGCCAAT TACATTACCT TCCCCATGGT TTTCAAAGCC
 121 GCCATTGAGC TCGGTGTCAT CGACGCTCTC TACTTAGCTG CTCGTGATGA CGTCAATGGA
 181 TCTGGATCGT TCCTCAAACC GTCTGAGATA GCTACTCGGC TTCCCACACC GCCTAGTAAC
 241 CCTGAAGCAC CGGTTTTGCT GGACCGTATG CTTCGTTTAC TCGCCAGTTA CTCAATGGTC
 301 AAGTGTCAGA TAGTAGACGG TGAGAGGGTG TACAAAGCTG AGCCCATTTG TAAGTATTTC
 361 TTGAGATACA ATATCGAAGA AATGGGGACA CTTGCTTCTC AGTTCATTCT TGAACTTGAT
 421 AGTGTCTTCC TCAACACATG GGCACAGTTG AAAGATGTGG TGCTAGAAGG AGGAGATGCA
 481 TTTGCTCGTG CCAATGGTGG GTTGAAGCTC TTTGACTACA TGGGCACAGA TGAAAGACTA
 541 AGCAAACTCT TTAACCGGAC TGGATTCAGC GTTGGAGTTA TGCAGAAGTT TCTTGAAGTT
 601 TATAAAGGTT TTGAAGGAAT CAATGTGTTG GTTGATGTAG GAGGAGGAGT TGGAAACACA
 661 CTAGGTTTTG TTACTTCAAA GTACCCGAAC ATTAAGGGTA TTAATTTTGA TCTAACTTGT
 721 GCTTTGGCAC AAGCACCTTC TTATCCTAAT GTGGAGCATG TGGCTGGAGA TATGTTTGTA
 781 GAAATCCCAA GAGGAGATGC TATCATCTTG AAACGTATGC TTCATGATTG GAATGATGAG
 841 GACTGTGCAA AGATTCTCAA GAACTGCTGG AAGGCATTAC CGGAGAATGG GAAAGTGATA
 901 ATCATGGAGC TAGTTATTCC AGATGAGGCA GAGAGTAAAG ATGTGCAGGC CAACATTGCA
 961 TTTGATATGG ATTTGTTGAT GCTCACACAA CTCTCTGGAG GAAAAGAGAG AACAAAAGCT
1021 GAGTATGAAG CTATGGCTGC TAATTCAGGT TTTGCAAGTT GCAAATTTGT ATGCCCTGCA
1081 TATCATTTAC GGGTCATTGA GTTCTCTAAA TAG
```

**Appendix Figure A5: The complete coding sequence of gene encoding indole glucosinolate *O*-methyltransferase 5 (*BnIGMT5a*: BnaC06g37610D, Top; *BnIGMT5b*: BnaA07g33060D, Bottom) retrieved from *Brassica napus* genome (AST_PRJEB5043_v1; http://plants.ensembl.org/Brassica_napus/Info/Index).** Forward and reverse PCR primers are highlighted in grey. Forward and reverse qPCR primers and probe binding sites are colored and underlined in green, red, and orange respectively.

```
   1 ATGGCTAGGG GATCTCGTTT TTTCATCATC CTTTCGATAA TCTCATTGTT TGCAAACACA
  61 ATCGATTCTA GAACATTAGA TCGACATAGT TTCCCGGATG GATTCGTTTT TGGAACGGCT
 121 GCGTCTGCGT ATCAGTACGA AGGAGCAACA GATGAAGGTG GCAAGTCTCC AGCTATATGG
 181 GACCACTTCA GCCGCACTTA CCCAGAACGG ACGAAGATGC ATAACGCACA TGTAGCGATT
 241 GATTTTTATC ACCGTTATAA GGATGACATA AAATTGATGA AGGAGCTAAA CATGGACGCT
 301 TTCAGATTTT CAATCTCGTG GGCCAGACTA ATTCCAAGTG GAAAGCTAAA GGATGGAGTA
 361 AACAAAGAAG GTGTACAATT CTACAAGGAT CTTATCGACG AACTTCTTGC TAATGACATA
 421 CAACCATCAA TGACACTATA TCATTGGGAC CATCCACAAT CTTTGGAGGA CGAATATGGT
 481 GGCTTTTTGA GCACTAAAAT TGTAGAAGAC TTTCGAGATT TTGCAAGAAT TTGTTTCGAA
 541 GAGTTTGGAG ATAAAGTTAA GATGTGGACA ACGATCAATG AACCGTACAT CATGACTATT
 601 GCGGGTTACG ACCAAGGTAA CAAGGCGGCT GGTCGATGCT CATCATGGGT AAACGAAAAG
 661 TGTCATGCGG GCGATTCGAG TACCGAGCCT TACATTGTTT CACATAACGT TCTTCTTGCT
 721 CATGCCGCTG CGGTAGACGA GTTCAGAAAG TCTAAACAAA TATCGCATGA TAGCCAAATT
 781 GGGATAGTTT TATCACCAAG ATGGTTCGAG CCTTTTCATT CCGACTCTAC TGATGATAAA
 841 GAAGCAGCTG AAAGAGCTCT TGCTTATGAA ATTGAATGGC ATCTTGATCC AGTGATTCAT
 901 GGAGATTATC CAGAGATTGT GAAAAAATAC GCGGGAGATA AGTTACCTTC ATTTACTGAG
 961 GAGGAATCAA ACATGTTAAA AAATTCATCA GATTTTGTGG GAATAAACTA CTATACAGCA
1021 CGCTTCGCTA CTCATATTCC TGAGATCGAC CCAGCAAAGC CTCGGTTCAA GACTGATCAT
1081 CACGTCGAAT GGAAACTGAC TAACCACAGT GGCCACATTA TCGGACCCGG GGATGAGAGA
1141 GGTTTAATAT TGTCTCATCC ACAAGGCTTG AGAAAAGTTC TAAACTATAT CAAAGATAGA
1201 TACAATAACA TCCCAGTCTA CATCAAAGAA AATGGAATCA ACGATAATGA CGATGGTACA
1261 AAACCAAGAG AAGAGATTCT TAAGGACACA TTTAGGATTG AGTACCATGA CACACATATC
1321 CAACAACTTC ACAAAGCTAT AGTTGAAGAT GGTTGTGACG TAAGAGGATA TTATGCATGG
1381 TCAATGATGG ACAACTTTGA ATGGGAACAT GGGTACACTG CTAGATTTGG TCTTTACTAT
1441 GTTGACTTTG TCAACGGTCT AAAACGTTAC CCAAAAGACT CGGTGAAGTG GTTTAAGCAG
1501 TTCCTCAAGA GATCGATCGG TCAGGCTAAA GAAGAGGAAG TGAGGGAGAT GTTACGTGTG
1561 GATGGGAATA AGACTCTGCA TGAGCAAGTG GGTTTTGGTG AATCGTCAGG ATTTTTTGTA
1621 TCTTTCATGG CGACGTACCA ATCGAAGAGA GAGGAGGAGA ATCGTTGCTC GTCTGATTTA
1681 TTTTATGGCC GTTTCGATGT TTTGAAGAAG ATAGAGGATT CATCATCATT TTATTGA
```

```
   1 ATGGCTAGGG GATCTCGTTT TTTCATCATC CTTTCGATAA TCTCATTGTT TGCAAACACA
  61 ATCGATTCTA GAACATTAGA TCGACATAGT TTCCCTGATG GATTCGTTTT TGGAACGGCT
 121 GCGTCTGCGT ATCAGTACGA AGGAGCAACA GATGAAGGTG GCAAGTCTCC AGCTATATGG
 181 GACCACTTCA GCCGCACTTA CCCAGAACGG ACGAAGATGC ATAATGCAGA TGTAGCGATT
 241 GATTTTTATC ACCGTTATAA GGATGACATA AAATTGATGA AGGAGCTAAA CATGGACGCT
 301 TTCAGATTTT CAATCTCGTG GGCCAGACTA ATTCCAAGTG GAAAGCTAAA GGATGGAGTA
 361 AACAAAGAAG GTGTACAATT CTACAAGGAT CTTATCGACG AACTTCTTGC TAATGACATA
 421 CAACCATCAA TGACACTATA TCATTGGGAC CATCCACAAT CTTTGGAGGA CGAATATGGT
 481 GGCTTTTTGA GCACTAAAAT TGTAGAAGAC TTTCGAGATT TTGCAAGAAT TTGTTTCGAA
 541 GAGTTTGGAG ATAAAGTTAA GATGTGGACA ACGATCAATG AACCGTACAT CATGACTATT
 601 GCGGGTTACG ACCAAGGTAA CAAGGCGGCT GGTCGATGCT CATCATGGGT AAACGAAAAG
 661 TGTCATGCGG GCGATTCGAG TACCGAGCCT TACATTGTTT CACATAACGT TCTTCTTGCT
 721 CATGCCGCTG CGGTAGACGA GTTCAGAAAG TCTAAACAAA TATCGCATGA TAGCCAAATT
 781 GGGATAGTTT TATCACCAAG ATGGTTCGAG CCTTTTCATT CCGACTCTAC TGATGATAAA
 841 GAAGCAGCTG AAAGAGCTCT TGCTTATGAA ATTGAATGGC ATCTTGATCC AGTGATTCAT
 901 GGAGATTATC CAGAGATTGT GAAAAAATAC GCGGGAGATA AGTTACCTTC ATTTACTGAG
 961 GAAGAATCAA ACATGTTAAA AAATTCATCA GATTTTGTCG GAATAAACTA CTATACAGCA
1021 CGCTTCGCTA CTCATATTCC TGAGATCGAC CCAGCAAAGC CTCGGTTCAA GACTGATCAT
1081 CACGTCGAAT GGAAACTGAC TAACCACAGT GGCCACATTA TCGGACCCGG GGATGAGAGG
1141 GGTTTAATAT TGTCTCATCC AGAAGGCTTG AGAAAAGTTC TAAACTATAT CAAAGATAGA
1201 TACAATAACA TTCCAGTCTA CATCAAAGAA AATGGAATCA ACGATAATGA CGATGGTACA
1261 AAACCAAGAG AAGAGATTCT TAAGGACACC TTTAGGATTG AGTACCATGA CACGCATATC
1321 CAACAACTTC ACAAAGCTAT AGTTGAAGAT GGTTGTGACG TAAGAGGATA TTATGCATGG
1381 TCAATGATGG ACAACTTTGA ATGGGAACAT GGGTACACTG CTAGATTTGG TCTTTACTAT
1441 GTTGACTTTG TCAACGGTCT AAAACGTTAC CCAAAAGACT CGGTGAAGTG GTTTAAGCAG
1501 TTCCTCAAGA GATCGATCGG TCAGGCTAAA GAAGAGGAAG TGAGGGAGAT GTTACGTGTG
1561 GATGGGAATA AGACTCTGCA TGAGCAAGTG GGTTTTGGTG AATCGTCAGG ATTTTTTGTA
1621 TCTTTCATGG CGACGTACCA ATCGAAGAGA GAGGAGGAGA ATCGTTGCTC GTCTGATTTA
1681 TTTTATGGCC GTTTCGATGT TTTGAAGAAG ATAGAGGATT CATCATCATT TTATTGA
```

**Appendix Figure A6: The complete coding sequence of gene encoding *β*-Glucosidase 30 (*BnBGLU30a*: BnaC04g22390D, Top; *BnBGLU30b*: BnaA04g01360D, Bottom) retrieved from *Brassica napus* genome (AST_PRJEB5043_v1; http://plants.ensembl.org/Brassica_napus/Info/Index).** Forward and reverse PCR primers are highlighted in grey. Forward and reverse qPCR primers and probe binding sites are colored and underlined in green, red, and orange respectively.

```
  1 ATGAGTCCTG TGGCTGAGAA CAAATGGGTC AAGGTGGGTC AGAAAGGATC AGGTCCTGGA
 61 CCAAGAAGCT CACATGCACT TACCGTCGTG GGCAACAAAG TCTACTGCTT TGGCGGGGAG
121 CTTAAACCAA CGATCCACAT CGACAACGAT CTCTACGTCT TCGATCTCGA GACTCAAGAA
181 TGGTCCATAG CCCCAGCAAC AGGGGACGCT CCGTTCCCCT GTTTCGGTGT CTCAATGGTC
241 CCTATCGGCA CCACCATCTA CGTCTACGGT GGCCGCGACG ACACTCGCAG ATACAACGGC
301 CTTTACTCTT ACGACACTCT CACAAACAAG TGGGAGATGC TGTCTCCCGT TGAGGAAGGG
361 CTTCCCGGTC GTAGCTACCA CTCTATGGCA TGTGATGATC GTAACGTTTA CGTCTTTGGT
421 GGTGTTACGG CCAAAGGACG TGTAAACACG TTGCATGGCT ATGACGTGGT TGGTCGGAAG
481 TGGGTTGAGT ATCCGGCGGG TGGTGAAGCT TGTAAAGGGA GAGGAGGACC AGGGCTTGTG
541 GTTGTGGAAG GGAAGGTTTG GGTTTTGTTT GGGTTTGACG GTAATGAATT GGGTGATATT
601 CATTGCTTTG ATTTGGGTAC ATGTAAATGG ACCGCTGTGG AGACCACCGG GGATGTACCG
661 CCGGCGAGAA GTGTGTTTCC GGCGGTTCGT TCGGGGAAAG AGATTGTGGT ATATGGTGGT
721 GAGGAGGAGC CGCATGAGCT GATGCATATG GGAGCTGGGA AGTTGTCTGG AGAGGTTTAT
781 AGGCTTGATA CGGAGACGTT GGTTTGGGAG AAGGTTGTGG ATGGTACTGA GGAAGGGAAG
841 AAGCCGAGTC CACGTGGGTG GTGCGCGTTT GCGGTTGCGG TTAAGGATGG TGAGGAAGGT
901 TTGCTGGTTC ACGGTGGGAA TAGTCCGACC AACGAGCGTC TTGATGATAT GGTGTTTTGG
961 CGTTTCTAG
```

**Appendix Figure A7: The complete coding sequence of gene encoding nitrile specifier protein 5 (*BnNSP5*: BnaA02g29990D) retrieved from *Brassica napus* genome (AST_PRJEB5043_v1; http://plants.ensembl.org/Brassica_napus/Info/Index).** Forward and reverse PCR primers are highlighted in grey. Forward and reverse qPCR primers and probe binding sites are colored and underlined in green, red, and orange respectively.

```
   1 ATGTCGACTC CCAAAAACAC AACTCAAGCT AACGGCGATT CCTCATCATC CATCGTTCGA
  61 GCTACAATCG TCCAGGCCTC CACCGTCTAT AACGATACTC CTAAAACTAT AGAAAAGGCG
 121 GAGAAGTTAA TTGCGGAGGC GGCAAGCAAC GGGTCCGAGC TTGTGGTGTT CCCGGAGGGG
 181 TTTATCGGTG GTTATCCTCG TGGGTTTAGG TTCGGTATAG CTGTTGGAAT TCACAACGAA
 241 GATGGTCGTG ATGACTTCCG CAAATATCAT GATTCTGCCA TTCATGTTCC TGGGCCTGAA
 301 GTAGATAAAC TGGCTGAACT AGCTAGGAAA AACAATGTGT ACTTGGTAAT GGGGGCTATA
 361 GAGAAGGATG GCTATACACT CTACTGCACA GCCCTTTTCT TCAATTCTGA GGGTCGATAC
 421 TTGGGTAAGC ACCGTAAGGT CATGCCAACA AGTCTCGAAC GTTGCATCTG GGGTTTCGGG
 481 GACGGATCAA CCATCCCTGT TTACGACACA CCCATTGGCA AACTCGGTGC TGCTATTTGC
 541 TGGGAAAATA GAATGCCCCT CTACAGAACT GCCCTGTACG GAAAGGGAGT TGAATTATAT
 601 TGTGCACCTA CTGCCGATGG TTCCAAGGAA TGGCAATCGT CGATGATGCA CATTGCCATG
 661 GAGGGTGGAT GTTTCGTATT GTCGGCTTGC CAGTTCTGCC AGCGTAAAGA TTTCCCTGCG
 721 CATGTTGATC ACCTTTTTAC CGACTGGTAC GATGACCAAC ACGATGAAGC CATAGTCTCC
 781 CAAGGTGGTA GTGTCATTAT TTCACCATTG GGAAAGGTTC TCGCTGGACC AAACTTTGAA
 841 TCAGAGGGTC TCATCACAGC TGATCTTGAT CTTGGTGACA TAGCAAGAGC TAAGTTATAC
 901 TTTGATGTGG TGGGACATTA CTCGAAACCA GATGTTTTTA ACTTGACCGT AAATGAGCAC
 961 CCGAAGAAAC CAGTTACATT CGTCTCGAAG ACGGTGAAAG CTGAGGATGG CTCAGAGTCT
1021 AAGGAGAAAT AA

   1 ATGTCGACTC TCAAAAACAC AACTCAAGTT AACGGCGATG CCTCATCATC CATCGTTCGA
  61 GCTACAATCG TCCAGGCCTC CACCGTCTAT AACGATACTC CCAAAACTAT AGAAAAGGCG
 121 GAGAAGTTAA TTGCGGAGGC GGCAAGCAAC GGGTCCGAGC TTGTGGTGTT CCCGGAGGGG
 181 TTTATCGGTG GATATCCTCG TGGATTTAGG TTTGGTATAG CGGTTGGTAT TCACAACGAA
 241 GAAGGTCGTG ATGACTTCCG CAAATATCAT GCTTCTGCCA TTCATGTTCC TGGGCCTGAA
 301 GTAGATAAAC TGGCGGAACT AGCTAGGAAA AACAATGTGT ACTTGGTAAT GGGGGCAATA
 361 GAGAAGGATG GCTATACACT CTACTGCACA GCCCTTTTCT TCAATTCTGA GGGTCGATTC
 421 TTGGGTAAGC ACCGTAAGGT CATGCCAACA AGTCTCGAAC GTTGCATATG GGGTTTTGGA
 481 GACGGATCAA CCATCCCTGT TTACGACACA CCCATTGGCA AACTCGGTGC TGCTATTTGC
 541 TGGGAAAATA GAATGCCCCT CTACAGAACT GCCCTGTACG GAAAGGGAGT TGAATTATAT
 601 TGTGCACCTA CTGCCGATGG TTCCAAGGAA TGGCAATCGT CAATGATGCA CATTGCCATG
 661 GAGGGTGGAT GTTTCGTATT GTCGGCTTGC CAGTTCTGCC AGCGTAAAGA TTTCCCTGCG
 721 CATGTTGATC ACCTTTTTAC CGACTGGTAC GATGACCAAC ACGATGAAGC CATTGTCTCC
 781 CAAGGTGGTA GTGTCATTAT TTCACCATTG GGAAAAGTTC TCGCTGGACC AAACTTTGAA
 841 TCAGAGGGTC TCATCACAGC TGATCTTGAT CTTGGTGACA TAGCAAGAGC TAAGTTATAC
 901 TTTGATGTGG TGGGACATTA CTCGAAACCA GATGTTTTTA ACTTGACCGT AAATGAGCAC
 961 CCGAAGAAAC CAGTGACATT CGTCTCGAAG ACGGTGAAAG CTGAGGATGA CACAGAGGCT
1021 AAGGAGAAAT AA
```

**Appendix Figure A8: The complete coding sequence of gene encoding nitrilase 2 (*BnNIT2a*: BnaC03g13560D, Top; *BnNIT2b*: BnaA03g10890D, Bottom) retrieved from *Brassica napus* genome (AST_PRJEB5043_v1; http://plants.ensembl.org/Brassica_napus/Info/Index).** Forward and reverse PCR primers are highlighted in grey. Forward and reverse qPCR primers and probe binding sites are colored and underlined in green, red, and orange respectively.

```
   1 ATGTCCACTC ACCAACAAGA TATGTCTCTC GTCACGTCCA CTCCTCCGAT CAACAACGGC
  61 AATCAAATCT TCCCAGAGAT CGAGATGTCC GGACACTCCT CCTCCATCGT ACGAGCAACC
 121 GTCGTCCAGG CATGCACCAT CTTCTACGAT ACTCCCGCCA CGCTAGACAA GGCTGAGAGG
 181 TTACTTGCCG AGGCGGCGGA TAACGGGTCA CAGCTCGTTG TGTTCCCGGA GGCGTTCATC
 241 GGCGGATATC CTCGCGGCTC CAGCTTCGAG TTGGCCATTG GTGCTCGAAC GGCTAAAGGA
 301 AGAGACGACT TTCGCAAGTA TCTTGCTTCT GCTATTGATG TTCCCGGCCC TGAGGTGGAA
 361 CGTATGGCGG AGATGGCTAG GAAGTACAAA GTGTTCTTGG TTATGGGTGT GATTGAGAGG
 421 GAAGGTTATA CGTTATACTG CTCTGTCCTT TTCTTTGACT CGCATGGTCA GTTCTTGGGT
 481 AAGCACCGGA AACTCATGCC TACGGCTCTT GAACGTTGCA TTTGGGGGTT CGGAGATGGA
 541 TCAACCATCC CTGTTTTCGA TACTCCGATT GGGAAAATCG GTGCTGCTAT TTGTTGGGAG
 601 AATAGGATGC CATCTTTAAG AACCGCAATG TATGCCAAAG GCATTGAGAT ATATTGTGCA
 661 CCTACTGCTG ATGCTAGAGA AACTTGGCTA GCATCAATGA CCCACATCGC TCTTGAAGGA
 721 GGCTGTTTTG TTTTGTCAGC TAACCAATTC TGTCGCCGTA AAGACTATCC TCCACCACCG
 781 GAATACACGT TTTCCGGTTC AGAAGAGAGC CTCACACCGG ACTCTGTTGT CTGTGCTGGT
 841 GGAAGCTCTA TCATTTCGCC TTTGGGGATT GTTCTAGCTG GACCAAACTA TGAAGGAGAG
 901 GGTCTTATCT CAGCTGATCT AGATCTTGGG GACATAGCAC GAGCTAAGTT TGACTTTGAT
 961 GTGGTCGGTC ATTACTCGAG GCCTGAAGTT TTTAGCTTGA ACATAAAGGA GCACCCGAGG
1021 AAAGCGGTTA GCTTCACGTC CAAGGTAACC AAAGATGAGA CCGTCAAAAA CTGA
```

```
   1 ATGTCCACTC ACCAACAAGA TATGTCTCTC GTCACGTCCA CTCCGATCAA CAACGGCAAT
  61 CAAATCTTCC CAGAGATCGA GATGTCCGGC GACTCCTCCT CCATCGTACG AGCAACCGTC
 121 GTCCAGGCAT GCACCATCTT CTACGATACT CCCGCCACGC TAGACAAGGC TGAGAGGTTA
 181 CTTGCCGAGG CGGCGGATAA CGGGTCACAG CTCGTGGTGT TCCCGGAGGC GTTCATCGGC
 241 GGATATCCTC GCGGCTCCAG CTTCGAGTTG GCCATCGGTG CTCGGACGGC TAAAGGAAGA
 301 GACGACTTTC GCAAGTATCT TGCTTCTGCT ATTGATGTTC CCGGCCCTGA AGTGGAACGT
 361 ATGGCGGAGA TGGCTAGGAA GTACAAAGTG TTCTTGGTTA TGGGTGTGAT TGAGAGGGAA
 421 GGTTATACGT TATACTGCTC TGTCCTTTTC TTTGACTCAC AAGGTCAGTT CTTGGGTAAG
 481 CACCGGAAAC TCATGCCTAC GGCTCTTGAA CGTTGCATTT GGGGGTTCGG AGATGGATCA
 541 ACCATCCCTG TTTTCGATAC TCCGATTGGG AAAATCGGTG CTGCTATTTG TTGGGAGAAT
 601 AGGATGCCGT CTTTAAGAAC CGCTATGTAT GCCAAAGGCA TTGAGATATA TTGTGCACCT
 661 ACTGCTGATG CTAGAGAAAC TTGGCTAGCG TCAATGACTC ACATCGCTCT TGAAGGAGGC
 721 TGTTTTGTTT TGTCAGCTAA CCAGTTCTGT CGCCGTAAAG ACTATCCTCC ACCACCGGAA
 781 TACACGTTTT CCGGTTCAGA AGAGAGCCTC ACACCGGACT CTGTTGTCTG TGCCGGTGGA
 841 AGCTCTATCA TTTCGCCTTT GGGGATTGTT CTAGCTGGAC CAAACTATGA AGGAGAGGCT
 901 CTTATCTCAG CTGATCTAGA TCTTGGGGAC ATAGCACGAG CTAAGTTTGA CTTTGATGTG
 961 GTCGGTCATT ACTCGAGGCC TGAAGTTTTT AGCTTGAACA TAAAGGAGCA TCCGAGGAAA
1021 GCGGCCAGCT TCACGTCCAA GGTAACCAAA GATGAGACCG TCAAAATGTG A
```

**Appendix Figure A9: The complete coding sequence of gene encoding nitrilase 4 (*BnNIT4a*: BnaA02g05560D, Top; *BnNIT4b*: BnaC02g09450D, Bottom) retrieved from *Brassica napus* genome (AST_PRJEB5043_v1; http://plants.ensembl.org/Brassica_napus/Info/Index).** Forward and reverse PCR primers are highlighted in grey. Forward and reverse qPCR primers and probe binding sites are colored and underlined in green, red, and orange respectively.

```
  1 ATGGCTCAGA ACGATACAGT CAAGCTCATA GGTTCTTGGG CGAGCCCTTT TTCCATCAGG
 61 GCTCGAGCGG CTCTACACTT GAAGTCTGTC AAGTACGAGT ACTCGGACGA ACCTGATGTT
121 CTCAGGTCAA AGAGTGAACT CCTTCTCAAG TCCAACCCCA TCTTCAAGAA AGTCCCAGTT
181 CTCATCCATG GTGATGTTTC CATCTGTGAG TCACTCAACA TTGTTCAGTA CATTGATGAA
241 GCTTGGTCCT CAGGTCCTTC CATCCTTCCT TCTCATCCGG TGGAACGTGC CAACGCTCGG
301 TTCTGGGCTC TCTTCATCGA TGAAAAGATC TTTGGATCTT TGGAAGCCGT GGGCGGAGCA
361 AAAGACGACG AAGGGAGAAT GGCTGCGGCT GGAAAGCTGA TGGAGAATTT GGCGATACTT
421 GAAGAGGCGT TTCAGAAGAG CAGCAAAGGA TTAGGGTTCT TTGGAGGAGA AAACATAGGC
481 TTCCTCGACC TTGCATGTGG GACTCTTTTG GGTCCAGTGT CTGTGATCGA GGCGTTTTCT
541 GGCGTCAAGT TTCTCCGGCA AGAAACAACA CCTGGACTGA TCCAATGGGC GGAGAAGTTT
601 AGGGCTCATG AAGCTGTCAA GCCTTACATG CCTACCCCCG AAGAGTTCGT TGCATTCGCA
661 AAGAAGAAGT TCAATGTTGA GTGA
```

**Appendix Figure A10: The complete coding sequence of gene encoding glutathione S-transferase TAU type 13 (*BnGSTU13*: BnaA07g09120D) retrieved from *Brassica napus* genome (AST_PRJEB5043_v1; http://plants.ensembl.org/Brassica_napus/Info/Index).** Forward and reverse PCR primers are highlighted in grey. Forward and reverse qPCR primers and probe binding sites are colored and underlined in green, red, and orange respectively.

```
   1 ATGAAGAATA ACGATAATGA TCCATCGAAG TCACTCATCG GACCACACTT TCTGTTCGTG
  61 ACATTTGGAG CACATGGCCA CATCAACCCA TCTCTCGAGC TCGCCAAACG CCTAGCCGTA
 121 ACCATCACCG GAGCTAGAGT CACCTTCGCC GCCCCAATCT CCGCCTACAA CCGCGGTATG
 181 TTCTCCAAAG AAAACTCCCC CGAAACCCTA ATCTTCGCCA CTTACTCAGA TGGCCACGAC
 241 GACGGCATCA AATCCTCTAC TTCCTCCGAC AAATCTCGCC AAGACGCATC CGGACAATAC
 301 ATGTCTGAGA TGAGACGACG TGGCATTGAA ACCCTAACCG AACTAATCGA AGATAACCGG
 361 CGTCAAAACC GGCCTTTCAC CTGCGTGGTT TACACCATGA TCCTCCTCAC TTGGGTCGCT
 421 GAGCTGGCGC GTGAGTTCCA CATCCCTTCT GCTCTTCTAT GGATCCAGCC AGTAACCATA
 481 TTCTCCATCT TCTACCACTA CTTCAACGGC TACGCAGATG CAATCTCAGA GATGGTTATT
 541 AATAACAACC CTTCCGGTTC TATTAAATTA CCGTCTCTGC CACTGTTCCG TCTCCGTGAT
 601 CTTCCTACGT TCCTCGTCCC TACAAACGCA TATTCGTTTC TTCTTCCCGC GTTTCGAGAG
 661 CAGATAGAGT TACTGAAGCA AGAGGAAAAC CCTATGATCC TCGTCAATAG TTTCCAAGAG
 721 CTTGAACAAG AAGCTCTAAG TATGGTTCTT GATAATATCA AGATCGTCCC CGTCGGTCCG
 781 TTGATAACTT CAAGGACCGA CTCCGGGGCT GACGGTGAAT ATGACAAGTG GTTGGATACG
 841 AAAATAGATT CATCTGTGGT TTATATCTCG TTCGGGACGG TTGCCGTGTT GAGCAAGAAA
 901 CAGCTCGTGG AGATCTGTAA GGCGTTGATA CAGAGTCGGA GACCGTTTCT GTGGGTGATT
 961 ACGGATAAGT CTTACAGAAG CAAAGAAGAC GGGGAAGAGA AAGAGGACGA GATCATAAGG
1021 ACGGTGGTTT CTTGGTGCGA TCAGTTTAGG TGGACTGATC AGATGACAAA TGCGAAGCTT
1081 TTGGAGGAGT GTTGGAGGAC GGGTGTGAGG GTGGTGGAGA AGAAGGAAGG GGAAGAAGTT
1141 GTGGTGGAGA GTGGGGAGAT ACGGCGGTGC ATTGAGGAAG TGATGGAGGA GAAAGGGGAG
1201 GAGTATAGAA GAAACGCGGC GAGGTGGAGA GATTTAGCGG CGGAGACGTG GGCACTACAA
1261 GCATTAGGAG GATGGGAGAA TGAGCTTGAC GAGCTCCTTG AATCTGGGCA GAGGCATTAC
1321 GTTATTACTA GACCTCCTTC TAAGCTACAC ACAACCAAGG CCATTTTAGC CAACCCTGGG
1381 AACGAGAGCT CGTGGAGATA CCAGAAAGTT CTTTACAAAG ACGACGCAGC GTCTTGGATT
1441 AGTGATCCAA GTGTTTCTTC GGTCTGTTTG AGAGTTCTTT CGCGTACGGA TTGCTTCCAT
1501 GGATTCGCTC TGAGCACCCT TTTGGATCTT CTATGCGTTG GATTGAGACC AACGAGCGAG
1561 CATAGAGACT CGGTGAAAGC TCTAACTAAT GAAGAGGCAG ATACGAACTT GGCCGGTTTG
1621 GTGTGTACAT TTGAATTAGT TATTGATTAT CGTGAATCAT ATGAACATGT TTTCATACAT
1681 CAAAGGTTCA AAACAAATCC TGATTTCTTG GCTTCTTGTG TTTATTGA
```

**Appendix Figure A11: The complete coding sequence of gene encoding indole-3-acetate *β*-D-glucosyltransferase (*BnIAGLU*: BnaA03g41970D) retrieved from *Brassica napus* genome (AST_PRJEB5043_v1; http://plants.ensembl.org/Brassica_napus/Info/Index).** Forward and reverse PCR primers are highlighted in grey. Forward and reverse qPCR primers and probe binding sites are colored and underlined in green, red, and orange respectively.

```
  1 ATGAGGGAGA TCATAAGCAT TCATATAGGA CAGGCAGGGA TCCAAGTTGG AAACTCGTGC
 61 TGGGAGCTTT ACTGCCTCGA ACATGGGATC CAGCCCGACG GCATGATGCC CAGTGATACA
121 ACGGTTGGTG TTGCGCACGA CGCTTTCAAC ACTTTCTTCA GCGAGACTGG TGCTGGAAAG
181 CATGTTCCCA GAGCCGTCTT CGTTGATCTG GAGCCTACTG TTATCGATGA AGTCCGTACC
241 GGAACGTACC GTCAGCTTTT CCATCCGGAG CAGCTTATCT CTGGGAAAGA GGACGCTGCT
301 AACAACTTCG CAAGAGGACA TTACACTGTT GGTAAGGAGA TTGTGGACCT TTGTCTTGAC
361 CGTGTGAGGA AGCTTGCCGA TAACTGTACC GGCTTGCAGG GCGACCATTG TGAGTTACAC
421 CAGAGTTCAT CATCAAAAGC TTTTGTTGTA CAAAACTTTC TTCTTAATCT TCTTGCAAGT
481 GTAAAATATT ATCCATCGGA AATATGTTAT ACGGCCATGT AG
```

**Appendix Figure A12: The complete coding sequence of tubulin gene (*BnTubulin*: BnaA03g41970D) retrieved from *Brassica napus* genome (AST_PRJEB5043_v1; http://plants.ensembl.org/Brassica_napus/Info/Index).** Forward and reverse qPCR primers and probe binding sites are colored and underlined in green, red, and orange respectively.

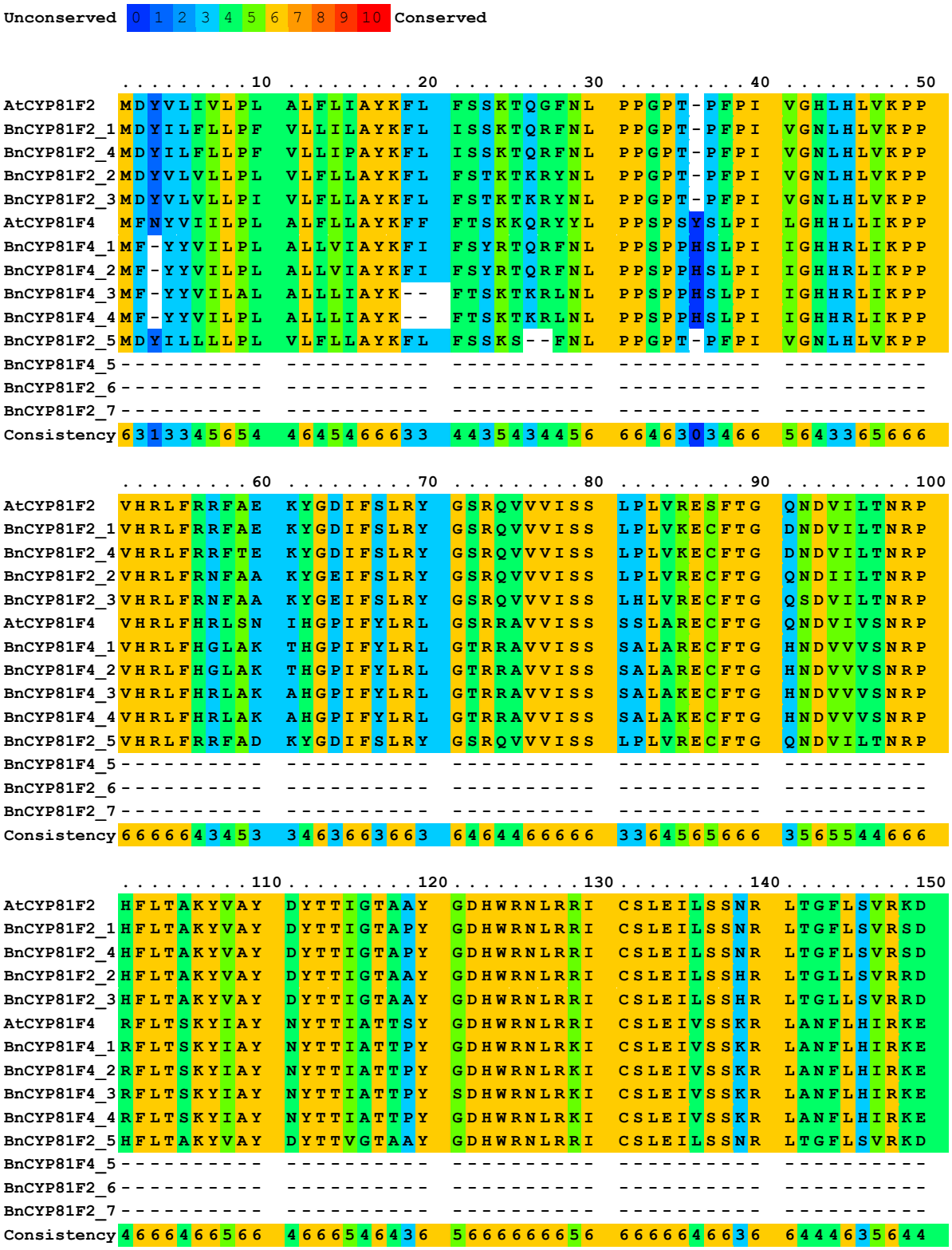
Unconserved 0 1 2 3 4 5 6 7 8 9 10 Conserved
AtCYP81F2
BnCYP81F2_1
BnCYP81F2_4
BnCYP81F2_2
BnCYP81F2_3
AtCYP81F4
BnCYP81F4_1
BnCYP81F4_2
BnCYP81F4_3
BnCYP81F4_4
BnCYP81F2_5
BnCYP81F4_5
BnCYP81F2_6
BnCYP81F2_7
Consistency

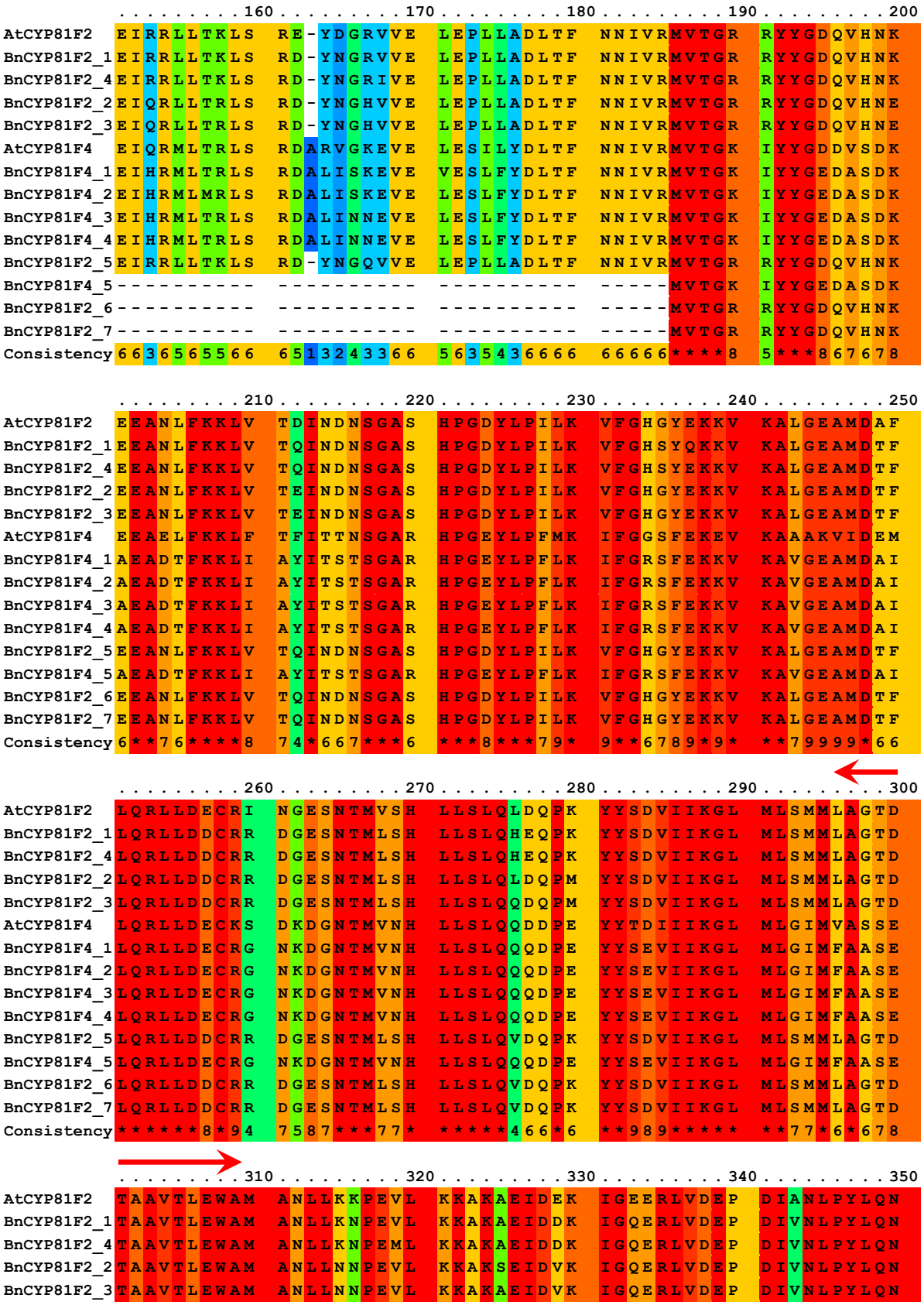
160 170 180 190 200
AtCYP81F2 EIRRLLTKLS RE-YDGRVVE LEPLLADLTF NNIVRMVTGR RYYGDQVHNK
BnCYP81F2_1 EIRRLLTKLS RD-YNGRVVE LEPLLADLTF NNIVRMVTGR RYYGDQVHNK
BnCYP81F2_4 EIRRLLTKLS RD-YNGRIVE LEPLLADLTF NNIVRMVTGR RYYGDQVHNK
BnCYP81F2_2 EIQRLLTRLS RD-YNGHVVE LEPLLADLTF NNIVRMVTGR RYYGDQVHNE
BnCYP81F2_3 EIQRLLTRLS RD-YNGHVVE LEPLLADLTF NNIVRMVTGR RYYGDQVHNE
AtCYP81F4 EIQRMLTRLS RDARVGKEVE LESILYDLTF NNIVRMVTGK IYYGDDVSDK
BnCYP81F4_1 EIHRMLTRLS RDALISKEVE VESLFYDLTF NNIVRMVTGK IYYGEDASDK
BnCYP81F4_2 EIHRMLMRLS RDALISKEVE LESLFYDLTF NNIVRMVTGK IYYGEDASDK
BnCYP81F4_3 EIHRMLTRLS RDALINNEVE LESLFYDLTF NNIVRMVTGK IYYGEDASDK
BnCYP81F4_4 EIHRMLTRLS RDALINNEVE LESLFYDLTF NNIVRMVTGK IYYGEDASDK
BnCYP81F2_5 EIRRLLTKLS RD-YNGQVVE LEPLLADLTF NNIVRMVTGR RYYGDQVHNK
BnCYP81F4_5 ---------- ---------- ---------- -----MVTGK IYYGEDASDK
BnCYP81F2_6 ---------- ---------- ---------- -----MVTGR RYYGDQVHNK
BnCYP81F2_7 ---------- ---------- ---------- -----MVTGR RYYGDQVHNK
Consistency 6636565566 651324336 6 5635436666 66666****8 5***867678
210 220 230 240 250
AtCYP81F2 EEANLFKKLV TDINDNSGAS HPGDYLPILK VFGHGYEKKV KALGEAMDAF
BnCYP81F2_1 EEANLFKKLV TQINDNSGAS HPGDYLPILK VFGHSYQKKV KALGEAMDTF
BnCYP81F2_4 EEANLFKKLV TQINDNSGAS HPGDYLPILK VFGHSYEKKV KALGEAMDTF
BnCYP81F2_2 EEANLFKKLV TEINDNSGAS HPGDYLPILK VFGHGYEKKV KALGEAMDTF
BnCYP81F2_3 EEANLFKKLV TEINDNSGAS HPGDYLPILK VFGHGYEKKV KALGEAMDTF
AtCYP81F4 EEAELFKKLF TFITTNSGAR HPGEYLPFMK IFGGSFEKEV KAAAKVIDEM
BnCYP81F4_1 AEADTFKKLI AYITSTSGAR HPGEYLPFLK IFGRSFEKKV KAVGEAMDAI
BnCYP81F4_2 AEADTFKKLI AYITSTSGAR HPGEYLPFLK IFGRSFEKKV KAVGEAMDAI
BnCYP81F4_3 AEADTFKKLI AYITSTSGAR HPGEYLPFLK IFGRSFEKKV KAVGEAMDAI
BnCYP81F4_4 AEADTFKKLI AYITSTSGAR HPGEYLPFLK IFGRSFEKKV KAVGEAMDAI
BnCYP81F2_5 EEANLFKKLV TQINDNSGAS HPGDYLPILK VFGHGYEKKV KALGEAMDTF
BnCYP81F4_5 AEADTFKKLI AYITSTSGAR HPGEYLPFLK IFGRSFEKKV KAVGEAMDAI
BnCYP81F2_6 EEANLFKKLV TQINDNSGAS HPGDYLPILK VFGHGYEKKV KALGEAMDTF
BnCYP81F2_7 EEANLFKKLV TQINDNSGAS HPGDYLPILK VFGHGYEKKV KALGEAMDTF
Consistency 6**76****8 74*667***6 ***8***79* 9**6789*9* **79999*66
260 270 280 290 300
AtCYP81F2 LQRLLDECRI NGESNTMVSH LLSLQLDQPK YYSDVIIKGL MLSMMLAGTD
BnCYP81F2_1 LQRLLDDCRR DGESNTMLSH LLSLQHEQPK YYSDVIIKGL MLSMMLAGTD
BnCYP81F2_4 LQRLLDDCRR DGESNTMLSH LLSLQHEQPK YYSDVIIKGL MLSMMLAGTD
BnCYP81F2_2 LQRLLDDCRR DGESNTMLSH LLSLQLDQPM YYSDVIIKGL MLSMMLAGTD
BnCYP81F2_3 LQRLLDDCRR DGESNTMLSH LLSLQQDQPM YYSDVIIKGL MLSMMLAGTD
AtCYP81F4 LQRLLDECKS DKDGNTMVNH LLSLQQDDPE YYTDIIIKGL MLGIMVASSE
BnCYP81F4_1 LQRLLDECRG NKDGNTMVNH LLSLQQQDPE YYSEVIIKGL MLGIMFAASE
BnCYP81F4_2 LQRLLDECRG NKDGNTMVNH LLSLQQQDPE YYSEVIIKGL MLGIMFAASE
BnCYP81F4_3 LQRLLDECRG NKDGNTMVNH LLSLQQQDPE YYSEVIIKGL MLGIMFAASE
BnCYP81F4_4 LQRLLDECRG NKDGNTMVNH LLSLQQQDPE YYSEVIIKGL MLGIMFAASE
BnCYP81F2_5 LQRLLDDCRR DGESNTMLSH LLSLQVDQPK YYSDVIIKGL MLSMMLAGTD
BnCYP81F4_5 LQRLLDECRG NKDGNTMVNH LLSLQQQDPE YYSEVIIKGL MLGIMFAASE
BnCYP81F2_6 LQRLLDDCRR DGESNTMLSH LLSLQVDQPK YYSDVIIKGL MLSMMLAGTD
BnCYP81F2_7 LQRLLDDCRR DGESNTMLSH LLSLQVDQPK YYSDVIIKGL MLSMMLAGTD
Consistency ******8*94 7587***77* *****466*6 **989***** **77*6*678
310 320 330 340 350
AtCYP81F2 TAAVTLEWAM ANLLKKPEVL KKAKAEIDEK IGEERLVDEP DIANLPYLQN
BnCYP81F2_1 TAAVTLEWAM ANLLKNPEVL KKAKAEIDDK IGQERLVDEP DIVNLPYLQN
BnCYP81F2_4 TAAVTLEWAM ANLLKNPEML KKAKAEIDDK IGQERLVDEP DIVNLPYLQN
BnCYP81F2_2 TAAVTLEWAM ANLLNNPEVL KKAKSEIDVK IGQERLVDEP DIVNLPYLQN
BnCYP81F2_3 TAAVTLEWAM ANLLNNPEVL KKAKAEIDVK IGQERLVDEP DIVNLPYLQN

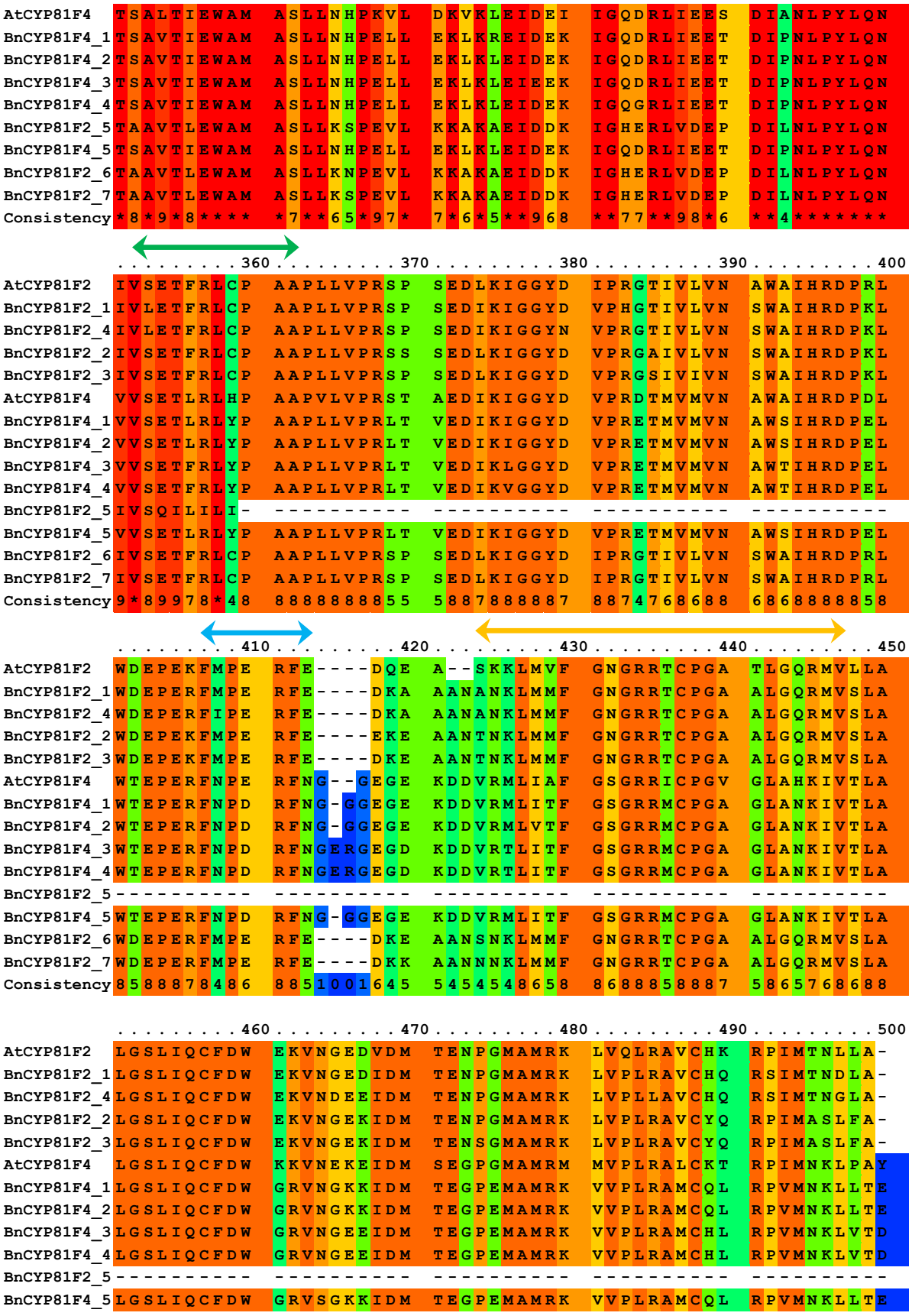
AtCYP81F4
BnCYP81F4_1
BnCYP81F4_2
BnCYP81F4_3
BnCYP81F4_4
BnCYP81F2_5
BnCYP81F4_5
BnCYP81F2_6
BnCYP81F2_7
Consistency
360
370
380
390
400
AtCYP81F2
BnCYP81F2_1
BnCYP81F2_4
BnCYP81F2_2
BnCYP81F2_3
AtCYP81F4
BnCYP81F4_1
BnCYP81F4_2
BnCYP81F4_3
BnCYP81F4_4
BnCYP81F2_5
BnCYP81F4_5
BnCYP81F2_6
BnCYP81F2_7
Consistency
410
420
430
440
450
AtCYP81F2
BnCYP81F2_1
BnCYP81F2_4
BnCYP81F2_2
BnCYP81F2_3
AtCYP81F4
BnCYP81F4_1
BnCYP81F4_2
BnCYP81F4_3
BnCYP81F4_4
BnCYP81F2_5
BnCYP81F4_5
BnCYP81F2_6
BnCYP81F2_7
Consistency
460
470
480
490
500
AtCYP81F2
BnCYP81F2_1
BnCYP81F2_4
BnCYP81F2_2
BnCYP81F2_3
AtCYP81F4
BnCYP81F4_1
BnCYP81F4_2
BnCYP81F4_3
BnCYP81F4_4
BnCYP81F2_5
BnCYP81F4_5

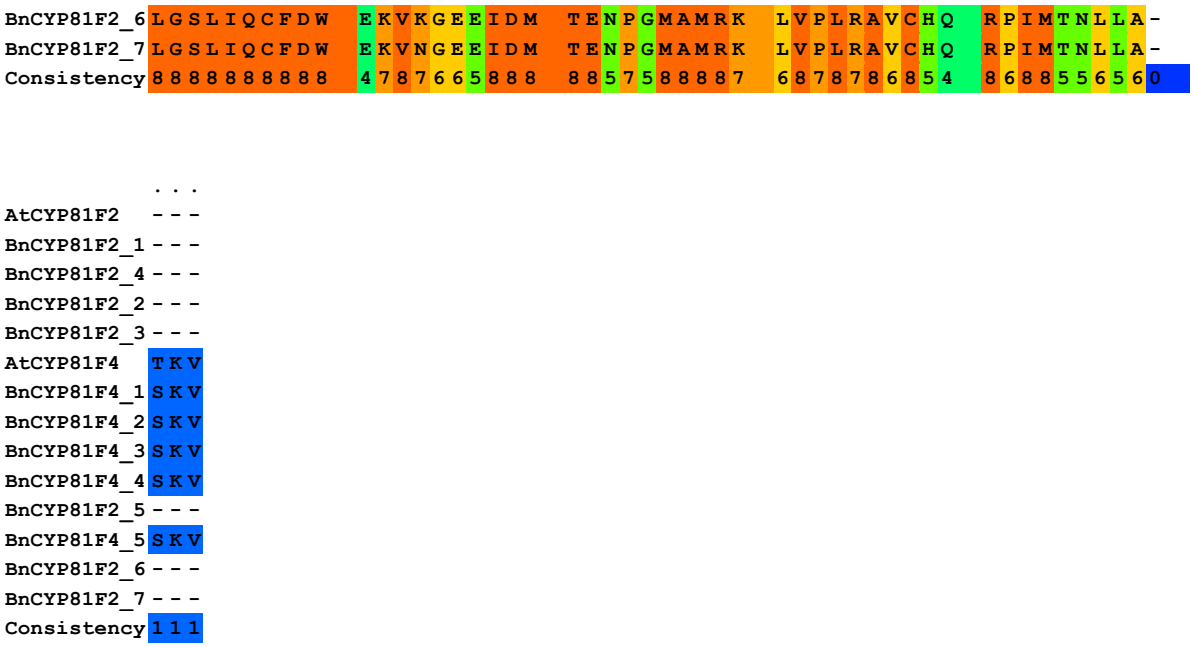


**Appendix Figure A13: Amino acid sequence alignment of cytochrome P450 monooxygenase, family 81, subfamily F polypeptide 2 and 4, the enzymes that participate in indole GSL modification.** These sequences from *Arabidopsis* (AtCYP81F2: AT5G57220.1, AtCYP81F4: AT4G37410.1) and *Brassica napus* (BnCYP81F2_1: BnaA02g08270D, BnCYP81F2_2: BnaA03g10380D, BnCYP81F2_3: BnaC03g13070D, BnCYP81F2_4: BnaC02g11750D, BnCYP81F2_5: BnaA10g11280D, BnCYP81F2_6: BnaC09g32980D, BnCYP81F2_7: BnaA10g11290D, BnCYP81F4_1: BnaC03g61420D, BnCYP81F4_2: BnaA08g15660D, BnCYP81F4_3: BnaC01g01530D, BnCYP81F4_4: BnaCnng68210D, BnCYP81F4_5: BnaCnng74800D) were aligned using the PSI-PRALINE multiple sequence alignment tool under default parameters. The CYP81F amino acid sequences contain four conserved motifs, including AGxDT (I-helix) marked with a red arrow, heme binding motif marked with an orange arrow, KETLR (K-helix) marked with a green arrow, and PERF/W motif marked with a cyan arrow (Vasav and Barvkar, 2019). Note that, the gaps have been introduced to maximize matching, the amino acid numbers refer to position only and not to actual number in the sequence.

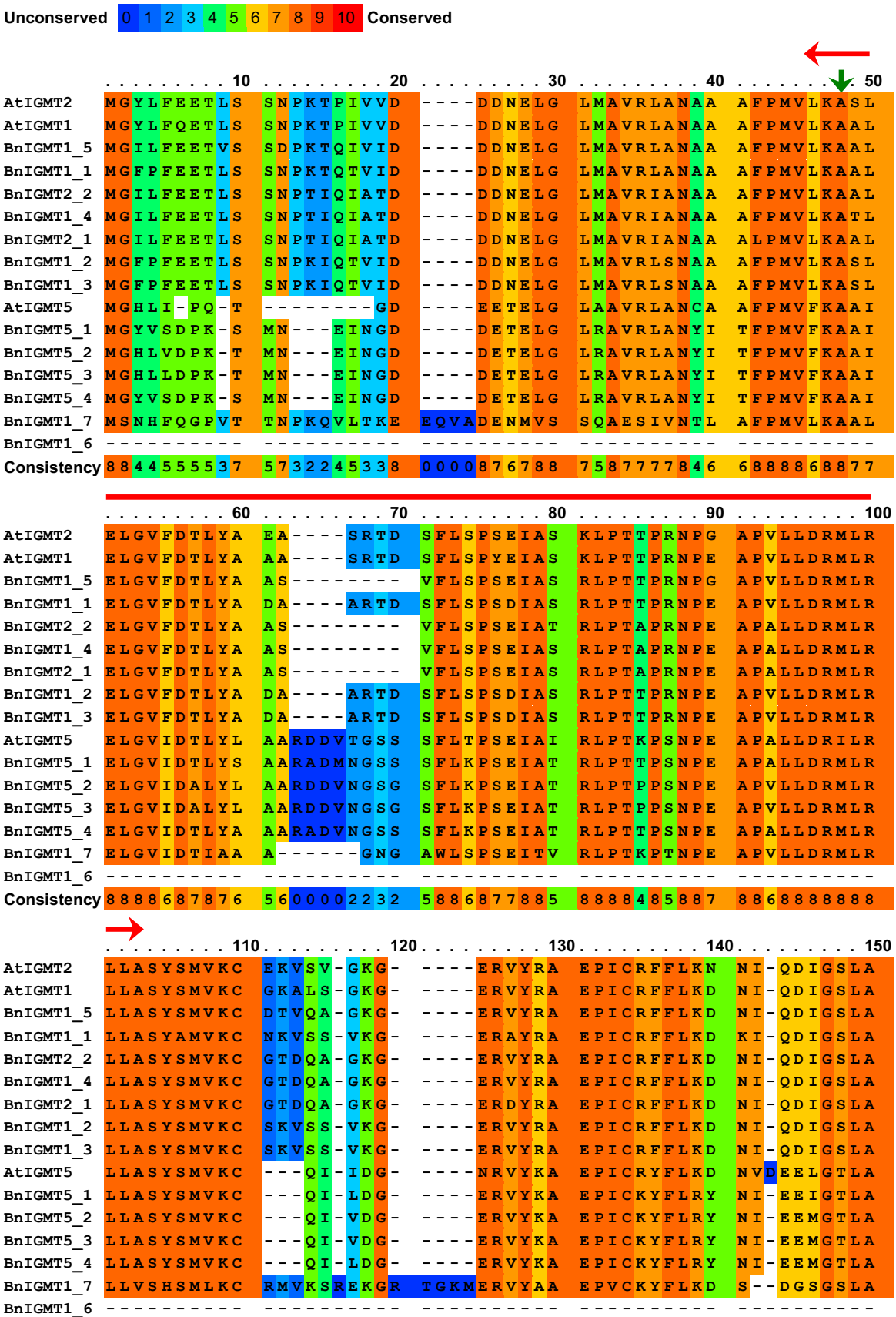
Unconserved 0 1 2 3 4 5 6 7 8 9 10 Conserved
10 20 30 40 50
AtIGMT2 MGYLFEETLS SNPKTPIVVD ----DDNELG LMAVRLANAA AFPMVLKASL
AtIGMT1 MGYLFQETLS SNPKTPIVVD ----DDNELG LMAVRLANAA AFPMVLKAAL
BnIGMT1_5 MGILFEETVS SDPKTQIVID ----DDNELG LMAVRLANAA AFPMVLKAAL
BnIGMT1_1 MGFPFEETLS SNPKTQTVID ----DDNELG LMAVRLANAA AFPMVLKAAL
BnIGMT2_2 MGILFEETLS SNPTIQIATD ----DDNELG LMAVRIANAA AFPMVLKAAL
BnIGMT1_4 MGILFEETLS SNPTIQIATD ----DDNELG LMAVRIANAA AFPMVLKATL
BnIGMT2_1 MGILFEETLS SNPTIQIATD ----DDNELG LMAVRIANAA ALPMVLKAAL
BnIGMT1_2 MGFPFEETLS SNPKIQTVID ----DDNELG LMAVRLSNAA AFPMVLKASL
BnIGMT1_3 MGFPFEETLS SNPKIQTVID ----DDNELG LMAVRLSNAA AFPMVLKASL
AtIGMT5 MGHLI-PQ-T ---------GD ----EETELG LAAVRLANCA AFPMVFKAAI
BnIGMT5_1 MGYVSDPK-S MN---EINGD ----DETELG LRAVRLANYI TFPMVFKAAI
BnIGMT5_2 MGHLVDPK-T MN---EINGD ----DETELG LRAVRLANYI TFPMVFKAAI
BnIGMT5_3 MGHLLDPK-T MN---EINGD ----DETELG LRAVRLANYI TFPMVFKAAI
BnIGMT5_4 MGYVSDPK-S MN---EINGD ----DETELG LRAVRLANYI TFPMVFKAAI
BnIGMT1_7 MSNHFQGPVT TNPKQVLTKE EQVADENMVS SQAESIVNTL AFPMVLKAAL
BnIGMT1_6 ---------- ---------- ---------- ---------- ----------
Consistency 8844555537 5732245338 0000876788 7587777846 6888868877
60 70 80 90 100
AtIGMT2 ELGVFDTLYA EA----SRTD SFLSPSEIAS KLPTTPRNPG APVLLDRMLR
AtIGMT1 ELGVFDTLYA AA----SRTD SFLSPYEIAS KLPTTPRNPE APVLLDRMLR
BnIGMT1_5 ELGVFDTLYA AS--------- VFLSPSEIAS RLPTTPRNPG APVLLDRMLR
BnIGMT1_1 ELGVFDTLYA DA----ARTD SFLSPSDIAS RLPTTPRNPE APVLLDRMLR
BnIGMT2_2 ELGVFDTLYA AS--------- VFLSPSEIAT RLPTAPRNPE APALLDRMLR
BnIGMT1_4 ELGVFDTLYA AS--------- VFLSPSEIAS RLPTAPRNPE APALLDRMLR
BnIGMT2_1 ELGVFDTLYA AS--------- VFLSPSEIAS RLPTAPRNPE APALLDRMLR
BnIGMT1_2 ELGVFDTLYA DA----ARTD SFLSPSDIAS RLPTTPRNPE APVLLDRMLR
BnIGMT1_3 ELGVFDTLYA DA----ARTD SFLSPSDIAS RLPTTPRNPE APVLLDRMLR
AtIGMT5 ELGVIDTLYL AARDDVTGSS SFLTPSEIAI RLPTKPSNPE APALLDRILR
BnIGMT5_1 ELGVIDTLYS AARADMNGSS SFLKPSEIAT RLPTTPSNPE APALLDRMLR
BnIGMT5_2 ELGVIDALYL AARDDVNGSG SFLKPSEIAT RLPTPPSNPE APVLLDRMLR
BnIGMT5_3 ELGVIDALYL AARDDVNGSG SFLKPSEIAT RLPTPPSNPE APVLLDRMLR
BnIGMT5_4 ELGVIDTLYA AARADVNGSS SFLKPSEIAT RLPTTPSNPE APALLDRMLR
BnIGMT1_7 ELGVIDTIAA A------GNG AWLSPSEITV RLPTKPTNPE APVLLDRMLR
BnIGMT1_6 ---------- ---------- ---------- ---------- ----------
Consistency 8888687876 5600002232 5886877885 8888485887 8868888888
110 120 130 140 150
AtIGMT2 LLASYSMVKC EKVSV-GKG- ----ERVYRA EPICRFFLKN NI-QDIGSLA
AtIGMT1 LLASYSMVKC GKALS-GKG- ----ERVYRA EPICRFFLKD NI-QDIGSLA
BnIGMT1_5 LLASYSMVKC DTVQA-GKG- ----ERVYRA EPICRFFLKD NI-QDIGSLA
BnIGMT1_1 LLASYAMVKC NKVSS-VKG- ----ERAYRA EPICRFFLKD KI-QDIGSLA
BnIGMT2_2 LLASYSMVKC GTDQA-GKG- ----ERVYRA EPICRFFLKD NI-QDIGSLA
BnIGMT1_4 LLASYSMVKC GTDQA-GKG- ----ERVYRA EPICRFFLKD NI-QDIGSLA
BnIGMT2_1 LLASYSMVKC GTDQA-GKG- ----ERDYRA EPICRFFLKD NI-QDIGSLA
BnIGMT1_2 LLASYSMVKC SKVSS-VKG- ----ERVYRA EPICRFFLKD NI-QDIGSLA
BnIGMT1_3 LLASYSMVKC SKVSS-VKG- ----ERVYRA EPICRFFLKD NI-QDIGSLA
AtIGMT5 LLASYSMVKC ---QI-IDG- ----NRVYKA EPICRYFLKD NVDEELGTLA
BnIGMT5_1 LLASYSMVKC ---QI-LDG- ----ERVYKA EPICKYFLRY NI-EEIGTLA
BnIGMT5_2 LLASYSMVKC ---QI-VDG- ----ERVYKA EPICKYFLRY NI-EEMGTLA
BnIGMT5_3 LLASYSMVKC ---QI-VDG- ----ERVYKA EPICKYFLRY NI-EEMGTLA
BnIGMT5_4 LLASYSMVKC ---QI-LDG- ----ERVYKA EPICKYFLRY NI-EEMGTLA
BnIGMT1_7 LLVSHSMLKC RMVKSREKGR TGKMERVYAA EPVCKYFLKD S--DGSGSLA
BnIGMT1_6 ---------- ---------- ---------- ---------- ----------

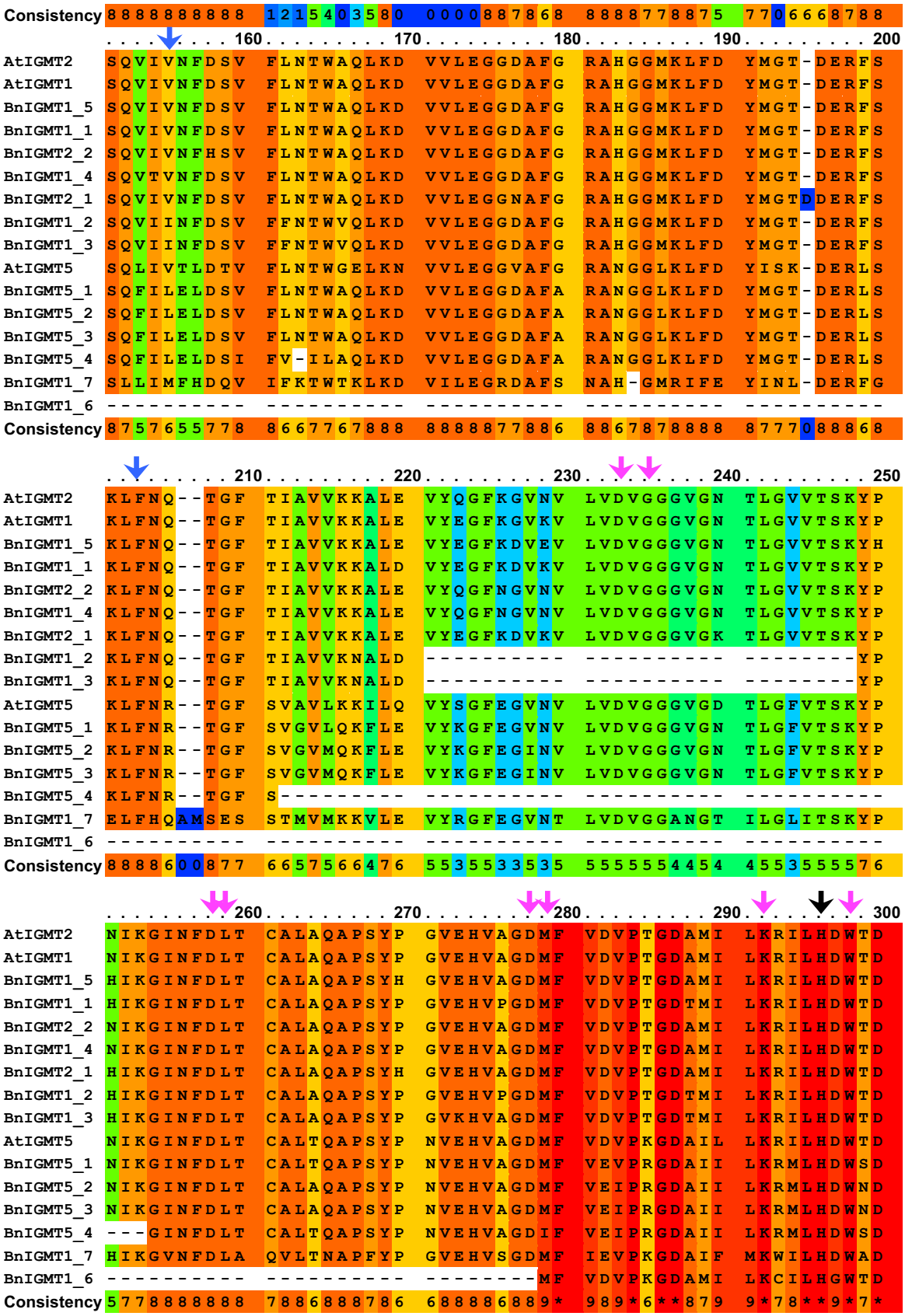
Consistency
AtIGMT2
AtIGMT1
BnIGMT1_5
BnIGMT1_1
BnIGMT2_2
BnIGMT1_4
BnIGMT2_1
BnIGMT1_2
BnIGMT1_3
AtIGMT5
BnIGMT5_1
BnIGMT5_2
BnIGMT5_3
BnIGMT5_4
BnIGMT1_7
BnIGMT1_6
160
170
180
190
200
210
220
230
240
250
260
270
280
290
300

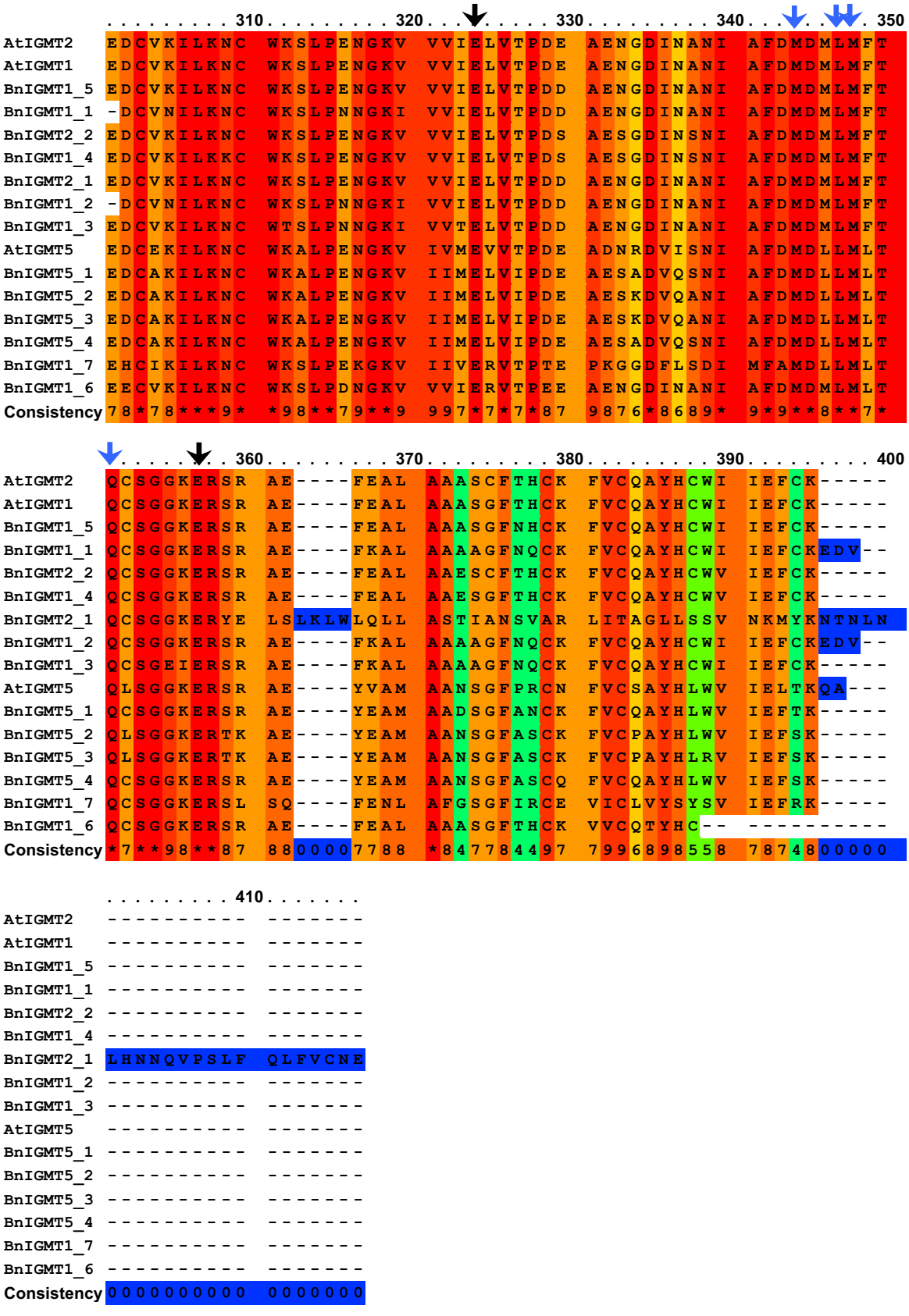
310 320 330 340 350
AtIGMT2 EDCVKILKNC WKSLPENGKV VVIELVTPDE AENGDINANI AFDMDMLMFT
AtIGMT1 EDCVKILKNC WKSLPENGKV VVIELVTPDE AENGDINANI AFDMDMLMFT
BnIGMT1_5 EDCVKILKNC WKSLPENGKV VVIELVTPDD AENGDINANI AFDMDMLMFT
BnIGMT1_1 -DCVNILKNC WKSLPNNGKI VVIELVTPDD AENGDINANI AFDMDMLMFT
BnIGMT2_2 EDCVKILKNC WKSLPENGKV VVIELVTPDS AESGDINSNI AFDMDMLMFT
BnIGMT1_4 EDCVKILKKC WKSLPENGKV VVIELVTPDS AESGDINSNI AFDMDMLMFT
BnIGMT2_1 EDCVKILKNC WKSLPENGKV VVIELVTPDD AENGDINANI AFDMDMLMFT
BnIGMT1_2 -DCVNILKNC WKSLPNNGKI VVIELVTPDD AENGDINANI AFDMDMLMFT
BnIGMT1_3 EDCVKILKNC WTSLPNNGKI VVTELVTPDD AENGDINANI AFDMDMLMFT
AtIGMT5 EDCEKILKNC WKALPENGKV IVMEVVTPDE ADNRDVISNI AFDMDLLMLT
BnIGMT5_1 EDCAKILKNC WKALPENGKV IIMELVIPDE AESADVQSNI AFDMDLLMLT
BnIGMT5_2 EDCAKILKNC WKALPENGKV IIMELVIPDE AESKDVQANI AFDMDLLMLT
BnIGMT5_3 EDCAKILKNC WKALPENGKV IIMELVIPDE AESKDVQANI AFDMDLLMLT
BnIGMT5_4 EDCAKILKNC WKALPENGKV IIMELVIPDE AESADVQSNI AFDMDLLMLT
BnIGMT1_7 EHCIKILKNC WKSLPEKGKV IIVERVTPTE PKGGDFLSDI MFAMDLLMLT
BnIGMT1_6 EECVKILKNC WKSLPDNGKV VVIERVTPEE AENGDINANI AFDMDMLMLT
Consistency 78*78***9* *98**79**9 997*7*7*87 9876*8689* 9*9**8**7*
360 370 380 390 400
AtIGMT2 QCSGGKERSR AE----FEAL AAAASCFTHCK FVCQAYHCWI IEFCK-----
AtIGMT1 QCSGGKERSR AE----FEAL AAAASGFTHCK FVCQAYHCWI IEFCK-----
BnIGMT1_5 QCSGGKERSR AE----FEAL AAAASGFNHCK FVCQAYHCWI IEFCK-----
BnIGMT1_1 QCSGGKERSR AE----FKAL AAAAAGFNQCK FVCQAYHCWI IEFCKEDV--
BnIGMT2_2 QCSGGKERSR AE----FEAL AAAESCFTHCK FVCQAYHCWV IEFCK-----
BnIGMT1_4 QCSGGKERSR AE----FEAL AAAESGFTHCK FVCQAYHCWV IEFCK-----
BnIGMT2_1 QCSGGKERYE LSLKLWLQLL ASTIANSVAR LITAGLLSSV NKMYKNTNLN
BnIGMT1_2 QCSGGKERSR AE----FKAL AAAAAGFNQCK FVCQAYHCWI IEFCKEDV--
BnIGMT1_3 QCSGEIERSR AE----FKAL AAAAAGFNQCK FVCQAYHCWI IEFCK-----
AtIGMT5 QLSGGKERSR AE----YVAM AANSGFPRCN FVCSAYHLWV IELTKQA---
BnIGMT5_1 QCSGGKERSR AE----YEAM AADSGFANCK FVCQAYHLWV IEFTK-----
BnIGMT5_2 QLSGGKERTK AE----YEAM AANSGFASCK FVCPAYHLWV IEFSK-----
BnIGMT5_3 QLSGGKERTK AE----YEAM AANSGFASCK FVCPAYHLRV IEFSK-----
BnIGMT5_4 QCSGGKERSR AE----YEAM AANSGFASCQ FVCQAYHLWV IEFSK-----
BnIGMT1_7 QCSGGKERSL SQ----FENL AFGSGFIRCE VICLVYSYSV IEFRK-----
BnIGMT1_6 QCSGGKERSR AE----FEAL AAASGFTHCK VVCQTYHC-- ----------
Consistency *7**98**87 880000778 8*8477844 97 799689855 8 787480000
410
AtIGMT2 ---------- -------
AtIGMT1 ---------- -------
BnIGMT1_5 ---------- -------
BnIGMT1_1 ---------- -------
BnIGMT2_2 ---------- -------
BnIGMT1_4 ---------- -------
BnIGMT2_1 LHNNQVPSLF QLFVCNE
BnIGMT1_2 ---------- -------
BnIGMT1_3 ---------- -------
AtIGMT5 ---------- -------
BnIGMT5_1 ---------- -------
BnIGMT5_2 ---------- -------
BnIGMT5_3 ---------- -------
BnIGMT5_4 ---------- -------
BnIGMT1_7 ---------- -------
BnIGMT1_6 ---------- -------
Consistency 0000000000 0000000

**Appendix Figure A14: Amino acid sequence alignment of indole glucosinolate *O*-Methyltransferase, the enzyme that participates in indole GSL side-chain modification.** These sequences from *Arabidopsis* (AtIGMT1: AT1G21100.1, AtIGMT2: AT1G21120.1, AtIGMT5: AT1G76790.1) and *Brassica napus* (BnIGMT1_1: BnaA07g11060D, BnIGMT1_2: BnaA02g19270D, BnIGMT1_3: BnaC07g14620D, BnIGMT1_4: BnaC07g14640D, BnIGMT1_5: BnaA07g11080D, BnIGMT1_6: BnaA06g14960D, BnIGMT1_7: BnaA07g20960D, BnIGMT2_1: BnaC07g14650D, BnIGMT2_2: BnaA07g11070D, BnIGMT5_1: BnaC06g21620D, BnIGMT5_2: BnaC06g37610D, BnIGMT5_3: BnaA07g33060D, BnIGMT5_4: BnaA07g21250D) were aligned using the PSI-PRALINE multiple sequence alignment tool under default parameters. The dimerization domain is present at the *N*-terminus of all the amino acid sequences of IGMT indicated with a red horizontal arrow, mediates dimer formation, and contributes the dimer interphase to the substrate binding site (Rahikainen et al., 2017). The highly conserved residues involved in S-adenosyl-L-methionine (SAM, as a methyl source)/ S-adenosyl-L-homocysteine (SAH, the methyl ether derivative as product) binding (pink) are the glycine-rich sequence E/DXGXGXG in the SAM-binding *N*-terminal region of the protein, which interacts with the amino acid portion of SAM. The substrate-binding domain is present at the *C*-terminus of all the amino acid sequences of IGMT. The amino acid residues of IGMT protein sequences involved in substrate binding, substrate binding to the dyad related monomer, and catalysis are indicated with blue, green, and black vertical arrows, respectively (Zubieta et al., 2001). Note that, the gaps have been introduced to maximize matching, the amino acid numbers refer to position only and not to actual number in the sequence.

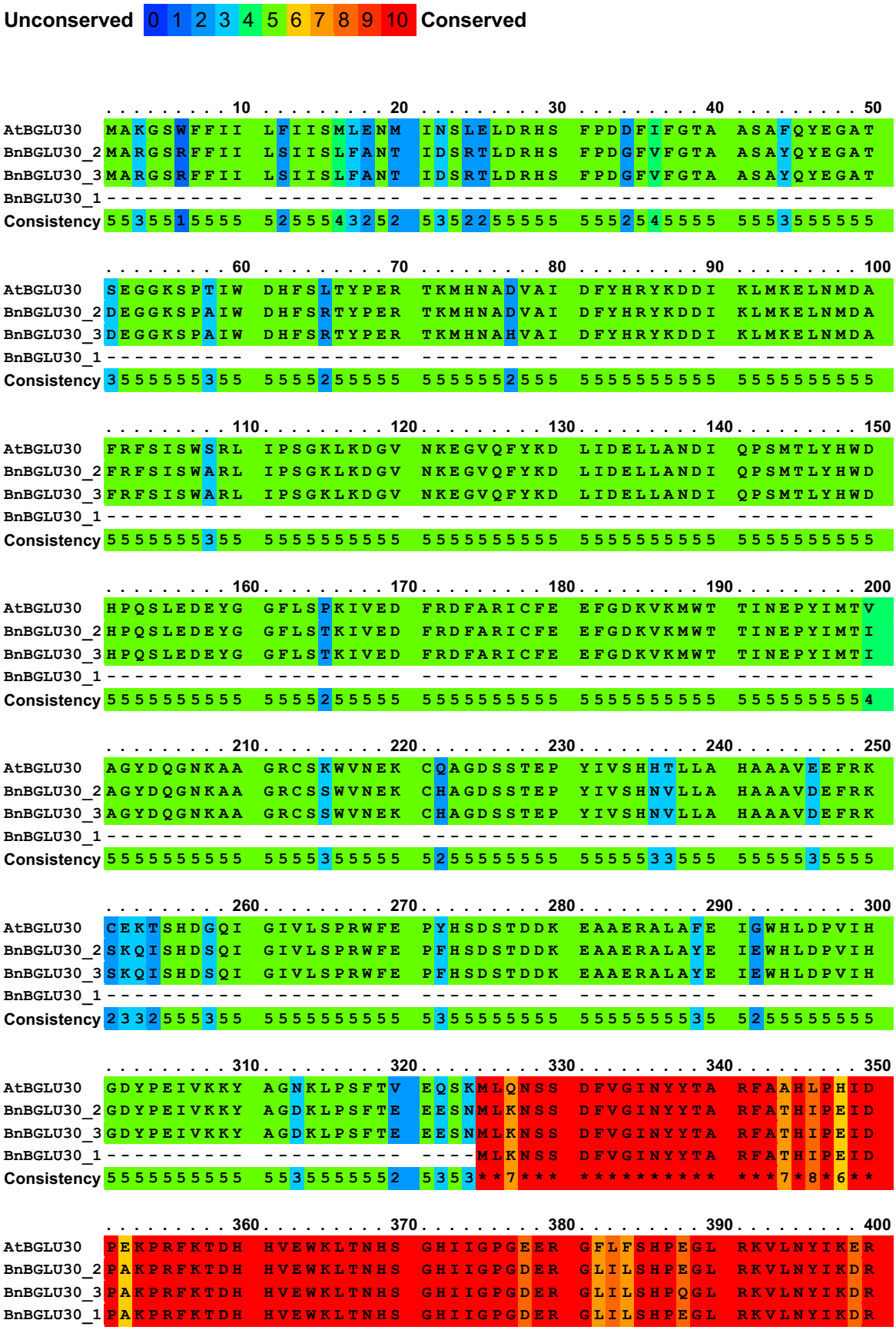
Unconserved 0 1 2 3 4 5 6 7 8 9 10 Conserved
10 20 30 40 50
AtBGLU30 MAKGSWFFII LFIISMLENM INSLELDRHS FPDDFIFGTA ASAFQYEGAT
BnBGLU30_2 MARGSRFFII LSIISLFANT IDSRTLDRHS FPDGFVFGTA ASAYQYEGAT
BnBGLU30_3 MARGSRFFII LSIISLFANT IDSRTLDRHS FPDGFVFGTA ASAYQYEGAT
BnBGLU30_1 ---------- ---------- ---------- ---------- ----------
Consistency 5535515555 5255543252 5352255555 5552545555 5553555555
60 70 80 90 100
AtBGLU30 SEGGKSPTIW DHFSLTYPER TKMHNADVAI DFYHRYKDDI KLMKELNMDA
BnBGLU30_2 DEGGKSPAIW DHFSRTYPER TKMHNADVAI DFYHRYKDDI KLMKELNMDA
BnBGLU30_3 DEGGKSPAIW DHFSRTYPER TKMHNAHVAI DFYHRYKDDI KLMKELNMDA
BnBGLU30_1 ---------- ---------- ---------- ---------- ----------
Consistency 3555555355 5555255555 5555552555 5555555555 5555555555
110 120 130 140 150
AtBGLU30 FRFSISWSRL IPSGKLKDGV NKEGVQFYKD LIDELLANDI QPSMTLYHWD
BnBGLU30_2 FRFSISWARL IPSGKLKDGV NKEGVQFYKD LIDELLANDI QPSMTLYHWD
BnBGLU30_3 FRFSISWARL IPSGKLKDGV NKEGVQFYKD LIDELLANDI QPSMTLYHWD
BnBGLU30_1 ---------- ---------- ---------- ---------- ----------
Consistency 5555555355 5555555555 5555555555 5555555555 5555555555
160 170 180 190 200
AtBGLU30 HPQSLEDEYG GFLSPKIVED FRDFARICFE EFGDKVKMWT TINEPYIMTV
BnBGLU30_2 HPQSLEDEYG GFLSTKIVED FRDFARICFE EFGDKVKMWT TINEPYIMTI
BnBGLU30_3 HPQSLEDEYG GFLSTKIVED FRDFARICFE EFGDKVKMWT TINEPYIMTI
BnBGLU30_1 ---------- ---------- ---------- ---------- ----------
Consistency 5555555555 5555255555 5555555555 5555555555 5555555554
210 220 230 240 250
AtBGLU30 AGYDQGNKAA GRCSKWVNEK CQAGDSSTEP YIVSHHTLLA HAAAVEEFRK
BnBGLU30_2 AGYDQGNKAA GRCSSWVNEK CHAGDSSTEP YIVSHNVLLA HAAAVDEFRK
BnBGLU30_3 AGYDQGNKAA GRCSSWVNEK CHAGDSSTEP YIVSHNVLLA HAAAVDEFRK
BnBGLU30_1 ---------- ---------- ---------- ---------- ----------
Consistency 5555555555 5555355555 5255555555 5555533555 5555535555
260 270 280 290 300
AtBGLU30 CEKTSHDGQI GIVLSPRWFE PYHSDSTDDK EAAERALAFE IGWHLDPVIH
BnBGLU30_2 SKQISHDSQI GIVLSPRWFE PFHSDSTDDK EAAERALAYE IEWHLDPVIH
BnBGLU30_3 SKQISHDSQI GIVLSPRWFE PFHSDSTDDK EAAERALAYE IEWHLDPVIH
BnBGLU30_1 ---------- ---------- ---------- ---------- ----------
Consistency 2332555355 5555555555 5355555555 5555555535 5255555555
310 320 330 340 350
AtBGLU30 GDYPEIVKKY AGNKLPSFTV EQSKMLQNSS DFVGINYYTA RFAAHLPHID
BnBGLU30_2 GDYPEIVKKY AGDKLPSFTE EESNMLKNSS DFVGINYYTA RFATHIPEID
BnBGLU30_3 GDYPEIVKKY AGDKLPSFTE EESNMLKNSS DFVGINYYTA RFATHIPEID
BnBGLU30_1 ---------- ---------- ----MLKNSS DFVGINYYTA RFATHIPEID
Consistency 5555555555 5535555555 5353**7*** ********** ***7*8*6**
360 370 380 390 400
AtBGLU30 PEKPRFKTDH HVEWKLTNHS GHIIGPGEER GFLFSHPEGL RKVLNYIKER
BnBGLU30_2 PAKPRFKTDH HVEWKLTNHS GHIIGPGDER GLILSHPEGL RKVLNYIKDR
BnBGLU30_3 PAKPRFKTDH HVEWKLTNHS GHIIGPGDER GLILSHPQGL RKVLNYIKDR
BnBGLU30_1 PAKPRFKTDH HVEWKLTNHS GHIIGPGDER GLILSHPEGL RKVLNYIKDR

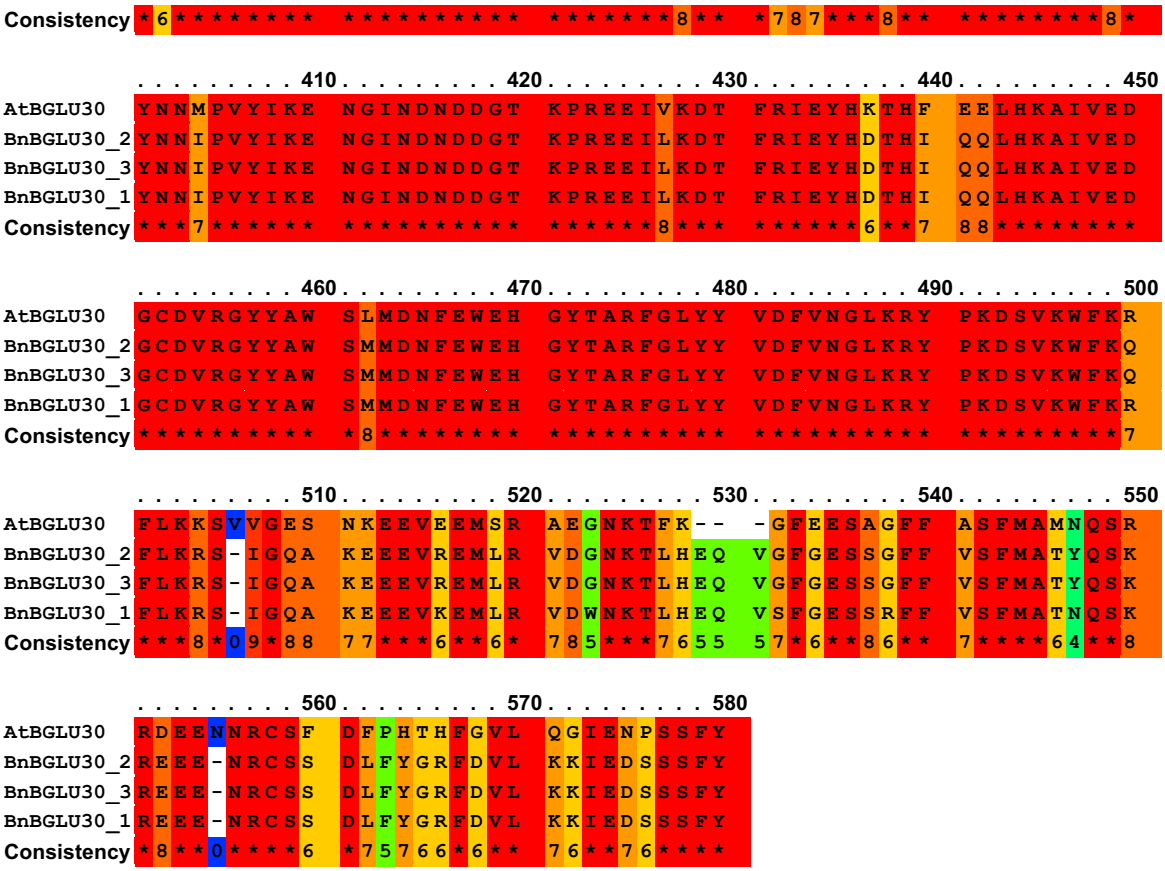


**Appendix Figure A15: Amino acid sequence alignment of *β*-glucosidase 30, the enzymes that participate in indole GSL degradation pathway.** These sequences from *Arabidopsis* (AtBGLU30: AT3G60140.1) and *Brassica napus* (BnBGLU30_1: BnaA04g27530D, BnBGLU30_2: BnaA04g01360D, BnBGLU30_3: BnaC04g22390D) were aligned using the PSI-PRALINE multiple sequence alignment tool under default parameters. Note that, the gaps have been introduced to maximize matching, the amino acid numbers refer to position only and not to actual number in the sequence.

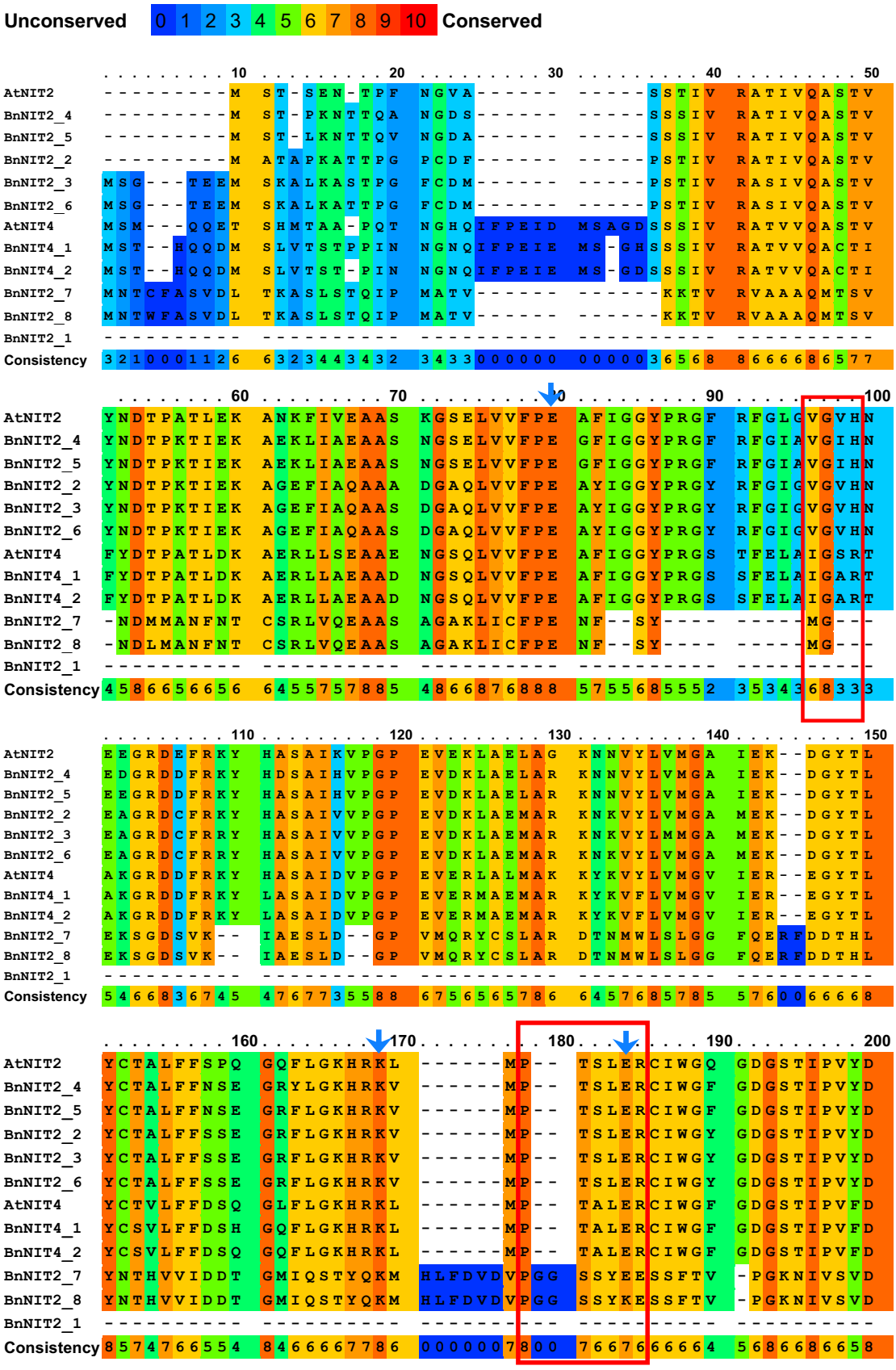
Unconserved
0 1 2 3 4 5 6 7 8 9 10
Conserved
AtNIT2
BnNIT2_4
BnNIT2_5
BnNIT2_2
BnNIT2_3
BnNIT2_6
AtNIT4
BnNIT4_1
BnNIT4_2
BnNIT2_7
BnNIT2_8
BnNIT2_1
Consistency

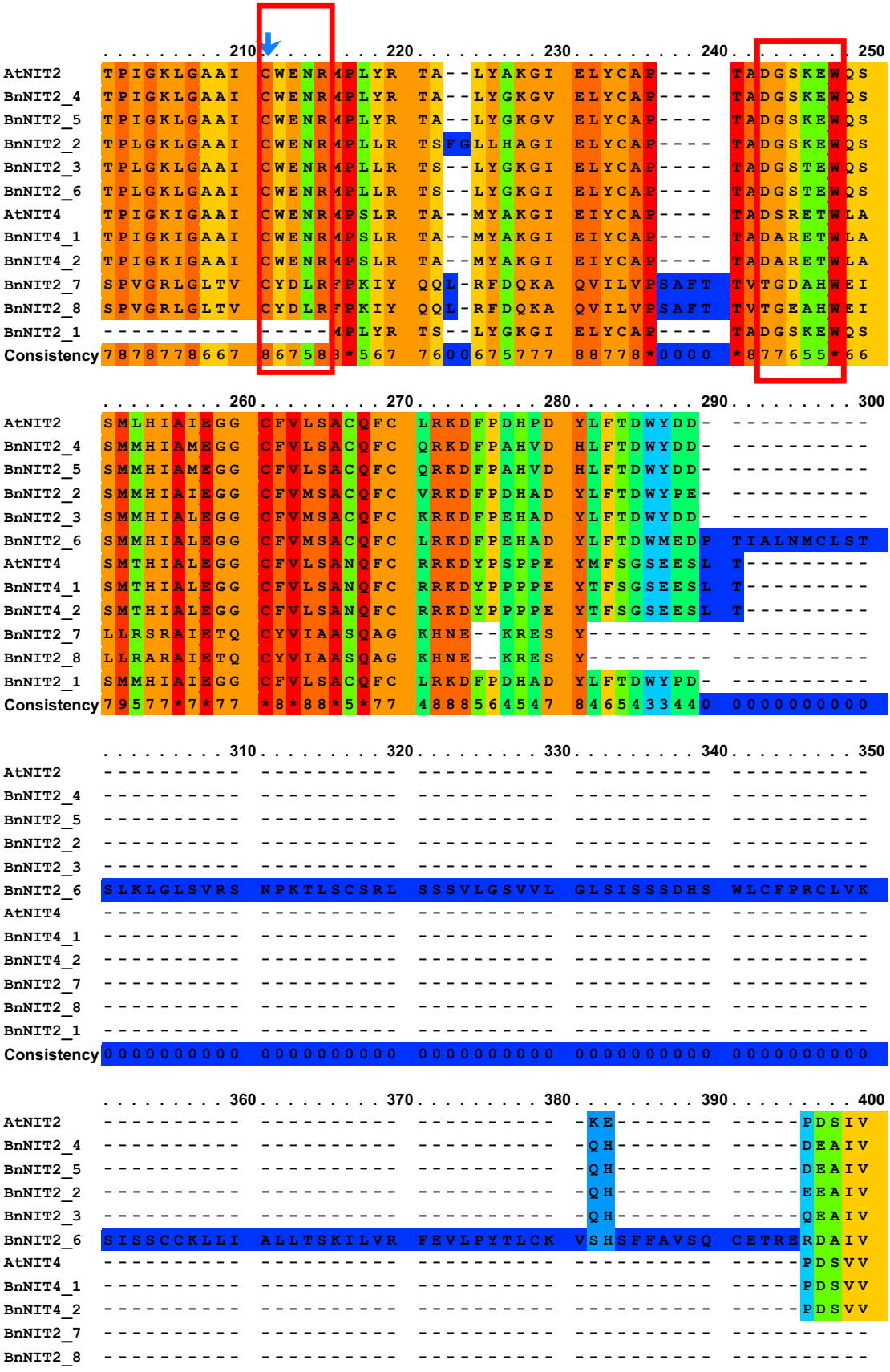
210 220 230 240 250
AtNIT2 TPIGKLGAAI CWENRMPLYR TA--LYAKGI ELYCAP---- TADGSKEWQS
BnNIT2_4 TPIGKLGAAI CWENRMPLYR TA--LYGKGV ELYCAP---- TADGSKEWQS
BnNIT2_5 TPIGKLGAAI CWENRMPLYR TA--LYGKGV ELYCAP---- TADGSKEWQS
BnNIT2_2 TPLGKLGAAI CWENRMPLLR TSFGLLHAGI ELYCAP---- TADGSKEWQS
BnNIT2_3 TPLGKLGAAI CWENRMPLLR TS--LYGKGI ELYCAP---- TADGSTEWQS
BnNIT2_6 TPLGKLGAAI CWENRMPLLR TS--LYGKGI ELYCAP---- TADGSTEWQS
AtNIT4 TPIGKIGAAI CWENRMPSLR TA--MYAKGI EIYCAP---- TADSRETWLA
BnNIT4_1 TPIGKIGAAI CWENRMPSLR TA--MYAKGI EIYCAP---- TADARETWLA
BnNIT4_2 TPIGKIGAAI CWENRMPSLR TA--MYAKGI EIYCAP---- TADARETWLA
BnNIT2_7 SPVGRLGLTV CYDLRFPKIY QQL-RFDQKA QVILVPSAFT TVTGDAHWEI
BnNIT2_8 SPVGRLGLTV CYDLRFPKIY QQL-RFDQKA QVILVPSAFT TVTGEAHWEI
BnNIT2_1 ---------- -----MPLYR TS--LYGKGI ELYCAP---- TADGSKEWQS
Consistency 7878778667 867583*567 760067577 88778*0000 *877655*66
260 270 280 290 300
AtNIT2 SMLHIAIEGG CFVLSACQFC LRKDFPDHPD YLFTDWYDD- ----------
BnNIT2_4 SMMHIAMEGG CFVLSACQFC QRKDFPAHVD HLFTDWYDD- ----------
BnNIT2_5 SMMHIAMEGG CFVLSACQFC QRKDFPAHVD HLFTDWYDD- ----------
BnNIT2_2 SMMHIAIEGG CFVMSACQFC VRKDFPDHAD YLFTDWYPE- ----------
BnNIT2_3 SMMHIALEGG CFVMSACQFC KRKDFPEHAD YLFTDWYDD- ----------
BnNIT2_6 SMMHIALEGG CFVMSACQFC LRKDFPEHAD YLFTDWMEDP TIALNMCLST
AtNIT4 SMTHIALEGG CFVLSANQFC RRKDYPSPPE YMFSGSEESL T---------
BnNIT4_1 SMTHIALEGG CFVLSANQFC RRKDYPPPPE YTFSGSEESL T---------
BnNIT4_2 SMTHIALEGG CFVLSANQFC RRKDYPPPPE YTFSGSEESL T---------
BnNIT2_7 LLRSRAIETQ CYVIAASQAG KHNE--KRES Y---------- ----------
BnNIT2_8 LLRARAIETQ CYVIAASQAG KHNE--KRES Y---------- ----------
BnNIT2_1 SMMHIAIEGG CFVLSACQFC LRKDFPDHAD YLFTDWYPD- ----------
Consistency 795774*7*77 *8*88*5*77 4888564547 8465433440 0000000000
310 320 330 340 350
AtNIT2 ---------- ---------- ---------- ---------- ----------
BnNIT2_4 ---------- ---------- ---------- ---------- ----------
BnNIT2_5 ---------- ---------- ---------- ---------- ----------
BnNIT2_2 ---------- ---------- ---------- ---------- ----------
BnNIT2_3 ---------- ---------- ---------- ---------- ----------
BnNIT2_6 SLKLGLSVRS NPKTLSCSRL SSSVLGSVVL GLSISSSDHS WLCFPRCLVK
AtNIT4 ---------- ---------- ---------- ---------- ----------
BnNIT4_1 ---------- ---------- ---------- ---------- ----------
BnNIT4_2 ---------- ---------- ---------- ---------- ----------
BnNIT2_7 ---------- ---------- ---------- ---------- ----------
BnNIT2_8 ---------- ---------- ---------- ---------- ----------
BnNIT2_1 ---------- ---------- ---------- ---------- ----------
Consistency 0000000000 0000000000 0000000000 0000000000 0000000000
360 370 380 390 400
AtNIT2 ---------- ---------- ---------- -KE------- -----PDSIV
BnNIT2_4 ---------- ---------- ---------- -QH------- -----DEAIV
BnNIT2_5 ---------- ---------- ---------- -QH------- -----DEAIV
BnNIT2_2 ---------- ---------- ---------- -QH------- -----EEAIV
BnNIT2_3 ---------- ---------- ---------- -QH------- -----QEAIV
BnNIT2_6 SISSCCKLLI ALLTSKILVR FEVLPYTLCK VSHSFFAVSQ CETRERDAIV
AtNIT4 ---------- ---------- ---------- ---------- -----PDSVV
BnNIT4_1 ---------- ---------- ---------- ---------- -----PDSVV
BnNIT4_2 ---------- ---------- ---------- ---------- -----PDSVV
BnNIT2_7 ---------- ---------- ---------- ---------- ----------
BnNIT2_8 ---------- ---------- ---------- ---------- ----------

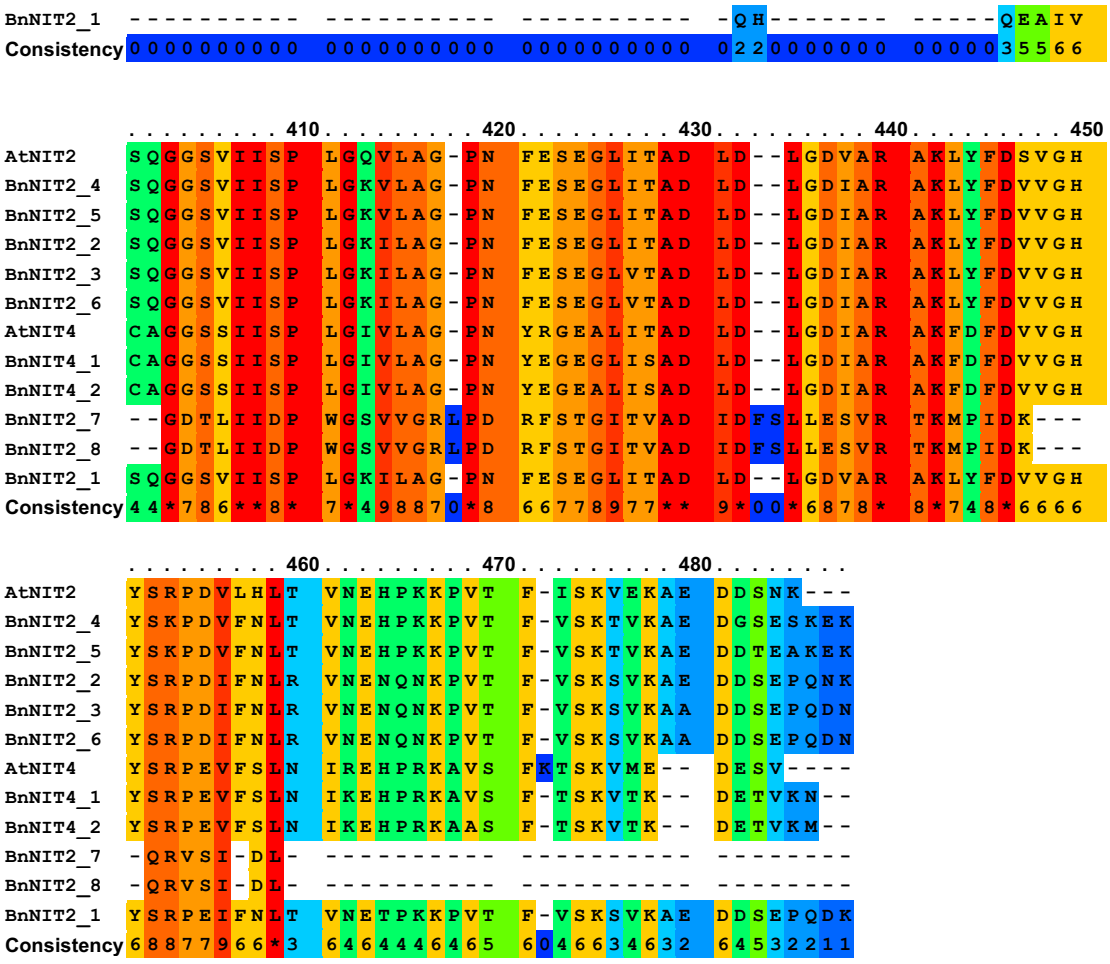


**Appendix Figure A16: Amino acid sequence alignment of Nitrilases, the enzymes that participate in indole GSL degradation pathways.** The sequences from *Arabidopsis* (AtNIT2: AT3G44300.1, AtNIT4: AT5G22300.1) and *Brassica napus* (BnNIT2_1: BnaCnng75490D, BnNIT2_2: BnaC02g07040D, BnNIT2_3: BnaA06g38980D, BnNIT2_4: BnaC03g13560D, BnNIT2_5: BnaA03g10890D, BnNIT2_6: BnaC03g54910D, BnNIT2_7: BnaC09g25430D, BnNIT2_8: BnaAnng32700D, BnNIT4_1: BnaA02g05560D, BnNIT4_2: BnaC02g09450D were aligned using the PSI-PRALINE multiple sequence alignment tool under default parameters. The amino acid residues that contribute to the catalytic tetrad in the coding sequences of NITs are indicated with blue vertical arrows and regions that form the substrate-binding pocket are outlined in red (Mulelu et al., 2019). Note that, the gaps have been introduced to maximize matching, the amino acid numbers refer to position only and not to actual number in the sequence.

**Appendix Table A1.** PCR primer sequences used for amplification of gene of interest in root tissues of non-inoculated control and 7d-*P. brassicae*-inoculated rutabaga resistant 'Wilhelmsburger' cultivar.

| Enzyme/Protein | Gene name | *Brassica napus* Gene Accession ID | Primer Sequence |
|---|---|---|---|
| Indole glucosinolate modification genes | | | |
| Cytochrome P450 monooxygenase, family 81, subfamily F | ***BnCYP81F2*** | BnaA10g11280D | F: 5'-GAGTTTCAATCTTCCACCAGG-3'<br>R: 5'-ATCCAGTGAGACGGTTAGAGG-3' |
| | ***BnCYP81F4*** | BnaCnng68210D | F: 5'-AATTGATGAGAAAATCGGACAAGGC-3'<br>R: 5'-CCGTAACAAGCTTATTCATAACGGG-3' |
| Indole glucosinolate *O*-methyltransferase | ***BnIGMT5a*** [a] | BnaC06g37610D | F: 5'-GTCTTCCTCAACACATGGGCACAGT-3' |
| | ***BnIGMT5b*** [a] | BnaA07g33060D | R: 5'-GCAACTTGCAAAACCTGAATTAGCAGCC-3' |
| | ***BnIGMT1*** [a] | BnaC07g14640D | F: 5'-CCGGATTTACCATCGCTGTCGTA-3' |
| | ***BnIGMT1/2*** [a] | BnaA07g11070D | R: 5'-AGTTGATATCTCCACTCTCAGCACTAT-3' |
| Indole glucosinolate degradation genes | | | |
| $\beta$-glucosidase | ***BnBGLU30a*** [a] | BnaC04g22390D | F: 5'-GTGGCAAGTCTCCAGCTATATG-3' |
| | ***BnBGLU30b*** [a] | BnaA04g01360D | R: 5'-GACTTTCTGAACTCGTCTACCG-3' |
| Nitrile specifier protein | ***BnNSP5*** | BnaA02g29990D | F: 5'-ACTTACCGTCGTGGGCAA-3'<br>R: 5'-AGCGGTCCATTTACATGTAC-3' |
| Nitrilase | ***BnNIT2a*** [a] | BnaC03g13560D | F: 5'-CTCAAGCTAACGGCGATT-3' |
| | ***BnNIT2 b*** [a] | BnaA03g10890D | R: 5'-GGCTTCATCGTGTTGGTCATC-3' |
| | ***BnNIT4a*** [a] | BnaA02g05560D | F: 5'-CAGGCATGCACCATCTTCTAC-3' |
| | ***BnNIT4b*** [a] | BnaC02g09450D | R: 5'-GTGTGAGGCTCTCTTCTGAAC-3' |
| Glutathione S-transferase TAU type | ***BnGSTU13*** | BnaA07g09120D | F: 5'-CCTGATGTTCTCAGGTCAAAGAGTG-3'<br>R: 5'-TTCGGGGGTAGGCATGTAAGGCTTG-3' |
| Auxin conjugation gene | | | |

| | | | |
|---|---|---|---|
| Indole-3-acetate *β*-D-glucosyltransferase | ***BnIAGLU*** | BnaA03g41970D | F: 5'-CGAAGTCACTCATCGGACCACAC-3'<br>R: 5'-CTCGAAACGCGGGAAGAAGAAA-3' |

[a] Due to very high homology at the nucleotide sequence level, primers were designed to homologous sequences among the genes to produce a common amplicon across the genes.

**Appendix Table A2.** Two-way ANOVA analysis followed by mean separation using Tukey HSD post-hoc test was performed on the relative transcript abundance of genes in the root tissues of non-inoculated control and 7d-*P. brassicae*-inoculated rutabaga resistant 'Wilhelmsburger' and susceptible 'Laurentian' cultivars, degrees of freedom, F value, and probability for treatments (non-inoculated vs. 7d-*P. brassicae*-inoculated), cultivars, and treatments x cultivars interaction presented in Figures 3-9.

| | Treatments | | Cultivars | | Treatments x Cultivars | | Tukey HSD post-hoc test (p values) | | | |
|---|---|---|---|---|---|---|---|---|---|---|
| **Gene name** | **F value** | **Pr(>F)** | **F value** | **Pr(>F)** | **F value** | **Pr(>F)** | **CRR vs IRR** | **CSR vs ISR** | **CRR vs CSR** | **IRR vs ISR** |
| ***BnCYP81F2*** | 214.698 | 5.08E-09 | 46.982 | 1.76E-05 | 5.049 | 4.42E-02 | 7.50E-06 | 3.00E-07 | 3.03E-02 | 1.64E-04 |
| Degrees of freedom | 1 | | 1 | | 1 | | | | | |
| | | | | | | | | | | |
| ***BnCYP81F4*** | 32.62 | 9.73E-05 | 1111.91 | 3.36E-13 | 43.66 | 2.51E-05 | 9.19E-01 | 8.10E-06 | 0.00E+00 | 0.00E+00 |
| Degrees of freedom | 1 | | 1 | | 1 | | | | | |
| | | | | | | | | | | |
| ***BnIGMT5*** | 0.198 | 6.64E-01 | 0.127 | 7.28E-01 | 5.745 | 3.37E-02 | 5.34E-01 | 2.38E-01 | 2.60E-01 | 4.994-01 |
| Degrees of freedom | 1 | | 1 | | 1 | | | | | |
| | | | | | | | | | | |
| ***BnBGLU30*** | 545.286 | 2.27E-11 | 0.317 | 5.84E-01 | 12.408 | 4.20E-03 | 0.00E+00 | 0.00E+00 | 2.10E-01 | 5.74E-02 |
| Degrees of freedom | 1 | | 1 | | 1 | | | | | |
| | | | | | | | | | | |
| ***BnNSP5*** | 39.02 | 4.28E0-5 | 61.042 | 4.79E-06 | 0.018 | 0.896 | 4.74E-03 | 3.43E-03 | 5.64E-04 | 7.59E-04 |
| Degrees of freedom | 1 | | 1 | | 1 | | | | | |
| | | | | | | | | | | |
| ***BnNIT2*** | 16.783 | 1.48E-02 | 99.887 | 3.60E-07 | 0.032 | 8.61E-01 | 4.55E-02 | 7.02E-02 | 7.98E-05 | 5.64E-05 |
| Degrees of freedom | 1 | | 1 | | 1 | | | | | |
| | | | | | | | | | | |
| ***BnNIT4*** | 84.699 | 8.72E-07 | 21.477 | 5.76E-04 | 4.437 | 5.69E-02 | 1.47E-03 | 1.96E-05 | 3.25E-01 | 2.23E-03 |
| Degrees of freedom | 1 | | 1 | | 1 | | | | | |
| | | | | | | | | | | |
| ***BnGSTU13*** | 3.275 | 9.55E-02 | 37.168 | 5.36E-05 | 5.253 | 4.08E-02 | 9.86E-01 | 5.63E-02 | 8.04E-02 | 3.48E-04 |
| Degrees of freedom | 1 | | 1 | | 1 | | | | | |
| | | | | | | | | | | |
| ***BnIAGLU*** | 6.045 | 4.92E-02 | | | | | | | | |
| Degrees of freedom | 1 | | | | | | | | | |

# Appendix-B

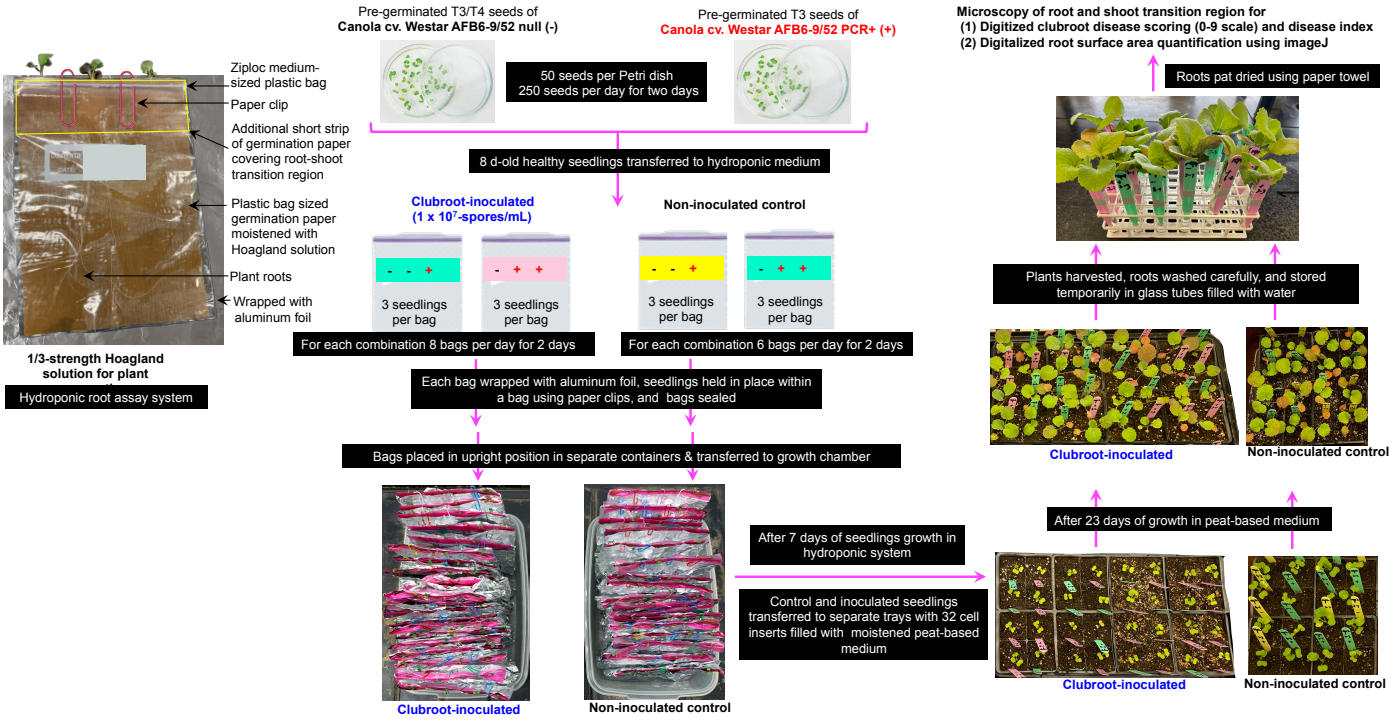


**Appendix Figure B1. Plastic bag used for hydroponic root assay system.** Two independently transformed Canola cv. Westar lines expressing the pea auxin receptor AFB6 and their respective null controls (AFB6-9 and AFB6-52 lines) were used for performing clubroot inoculation assays, for digitalized clubroot disease scoring, and for root surface area quantification. Eight-day-old pre-germinated seedlings were transferred to pre-labelled Ziploc medium-sized plastic bags measuring 17.7 x 18.8 cm. Each bag was lined with a sterile brown germination paper measuring 17 x 18 cm pre-soaked in 50 mL of sterile 1/3 strength Hoagland solution. An additional 150 mL of Hoagland solution was added to each bag to provide adequate nutrients for the growing seedlings. The plastic bags were then covered with aluminum foil to create a dark environment that facilitated root growth. For the non-inoculated control seedlings, three seedlings were directly transferred from the Petri dishes to each plastic bag, with a combination of two Null and a PCR+ seedling or a Null and two PCR+ seedlings in each bag. In the case of the clubroot pathogen-inoculated seedlings, the roots were dipped into a suspension of clubroot resting spores with a concentration of 1 x $10^7$ spores/mL before being transferred to the plastic bags. To ensure sufficient disease pressure, an additional 1 mL spore suspension (*P. brassicae* at 1 x $10^7$

spores/mL) was added onto the roots of each seedling using a micropipette. Finally, three seedlings were held in place between two layers of Hoagland-moistened paper (a 17 x 18 cm brown paper that fits the bag and an additional short strip of 17 x 4 cm brown paper that covers the root shoot transition region) in each bag using paper clips. Following a growth period of 7 days in the hydroponic system, the seedlings were transferred to trays with 32 cell inserts. Each cell insert (5.89 x 4.54 x 7.04 cm) was filled with moistened peat-based medium. After a period of 30 days following the inoculation with *P. brassicae*, the plant roots were washed two times carefully and subsequently transferred to pre-labelled glass tubes filled with water. Finally, the microscopic images of the root-shoot transition zone were captured and assessed for clubroot disease symptoms on a scale of 0-9 for calculating clubroot disease index and quantifying the surface area of the root using imageJ.

**Appendix Table B1.** Two-way ANOVA analysis followed by mean separation using Tukey HSD post-hoc test was performed on the root surface area of non-inoculated and 30d-*P. brassicae*-inoculated canola cv. Westar *AFB6-9* PCR+ and *AFB6-9* Null, degrees of freedom, F value, and probability for treatments (non-inoculated vs. 30d-*P. brassicae*-inoculated), lines (*AFB6-9* PCR+ vs. *AFB6-9* Null), and treatments x lines interaction presented in Figure 3.10.

| | Treatments | | Lines | | Treatments x Lines | |
|---|---|---|---|---|---|---|
| | **F value** | **Pr(>F)** | **F value** | **Pr(>F)** | **F value** | **Pr(>F)** |
| **Root surface area** | 165.654 | 2.00E-16 | 21.457 | 5.48E-06 | 3.338 | 6.87E-02 |
| Degrees of freedom | 1 | | 1 | | 1 | |

| **Pairwise comparisons** | **Tukey HSD post-hoc test (p values)** |
|---|---|
| Clubroot-inoculated *AFB6-9* Null vs Non-inoculated *AFB6-9* Null | 0.00E-07 |
| | |
| Clubroot-inoculated *AFB6-9* PCR+ vs Non-inoculated *AFB6-9* PCR+ | 0.00E-07 |
| | |
| Non-inoculated *AFB6-9* PCR+ vs Non-inoculated *AFB6-9* Null | 9.96E-01 |
| | |
| Clubroot-inoculated *AFB6-9* PCR+ vs Clubroot-inoculated *AFB6-9* Null | 6.70E-06 |

**Appendix Table B2.** Two-way ANOVA analysis followed by mean separation using Tukey HSD post-hoc test was performed on the root surface area of non-inoculated and 30d-*P. brassicae*-inoculated canola cv. Westar *AFB6-52* PCR+ and *AFB6-52* Null, degrees of freedom, F value, and probability for treatments (non-inoculated vs. 30d-*P. brassicae*-inoculated), lines (*AFB6-52* PCR+ vs. *AFB6-52* Null), and treatments x lines interaction presented in Figure 3.13.

| | Treatments | | Lines | | Treatments x Lines | |
|---|---|---|---|---|---|---|
| | **F value** | **Pr(>F)** | **F value** | **Pr(>F)** | **F value** | **Pr(>F)** |
| **Root surface area** | 80.813 | 9.17E-15 | 4.866 | 2.95E-02 | 2.174 | 1.43E-01 |
| Degrees of freedom | 1 | | 1 | | 1 | |

| **Pairwise comparisons** | **Tukey HSD post-hoc test (p values)** |
|---|---|
| Clubroot-inoculated *AFB6-52* Null vs Non-inoculated *AFB6-52* Null | 0.00E-07 |
| | |
| Clubroot-inoculated *AFB6-52* PCR+ vs Non-inoculated *AFB6-52* PCR+ | 5.00E-06 |
| | |
| Non-inoculated *AFB6-52* PCR+ vs Non-inoculated *AFB6-52* Null | 1.00E+01 |
| | |
| Clubroot-inoculated *AFB6-52* PCR+ vs Clubroot-inoculated *AFB6-52* Null | 4.49E-01 |